Influence of nano-particles of alumina (Al2O3) and titanium di-boride (TiB2) on the microstructure and properties of the alloy Al-Cu 3-Fe1-Si9 for foundry applications to high pressure

Iban Vicario Gomez

▶ To cite this version:

Iban Vicario Gomez. Influence of nano-particles of alumina (Al2O3) and titanium di-boride (TiB2) on the microstructure and properties of the alloy Al-Cu 3-Fe1-Si9 for foundry applications to high pressure. Material chemistry. Université Sciences et Technologies - Bordeaux I, 2011. English. NNT : 2011BOR14420 . tel-00670402

HAL Id: tel-00670402
https://theses.hal.science/tel-00670402

Submitted on 15 Feb 2012

N° d'ordre : 4420

THÈSE

PRÉSENTÉE A

L'UNIVERSITÉ BORDEAUX 1

ÉCOLE DOCTORALE DES SCIENCES CHIMIQUES

Par Iban Vicario Gomez

POUR OBTENIR LE GRADE DE

DOCTEUR

SPÉCIALITÉ : Physico-Chimie de la Matière Condensée

Influence des nano-particules d'alumine (Al$_2$O$_3$) et de di-borure de titane (TiB$_2$) sur la microstructure et les propriétés de l'alliage Al-Si9-Cu3-Fe1 pour des applications de fonderie à haute pression

Directeurs de recherche : M. J.-F. Silvain, Mme A. Poulon

Soutenue le : 19 décembre 2011

Après avis de :

M. Felix Peñalba	Docteur – TECNALIA, Espagne	Rapporteur
M. Joël Douin	Directeur de Recherche – CEMES, Toulouse	Rapporteur

Devant la commission d'examen formée de :

Mme Angeline Poulon	Maître de Conférence – ICMCB, Bordeaux	Examinateur
M. Claude Delmas	Directeur de Recherche – ICMCB, Bordeaux	Président
M. Jean-François Silvain	Directeur de Recherche – ICMCB, Bordeaux	Examinateur
M. Pedro Egizabal	Docteur – TECNALIA, Espagne	Examinateur

Université Bordeaux 1
Les Sciences et les Technologies au service de l'Homme et de l'environnement

PhD Thesis document. Université Bordeaux I. "Influence of Alumina (Al$_2$O$_3$) and Titanium Diboride (TiB$_2$) nanoparticulates on the microstructure and properties of Al Si9 Cu3 Fe1 alloys for high pressure die casting applications".

December 2011

Influence of Alumina (Al$_2$O$_3$) and Titanium Diboride (TiB$_2$) nanoparticulates on the microstructure and properties of Al Si9 Cu3 Fe1 alloys for high pressure die casting applications.

OCTOBER 2011

Influence of Alumina (Al_2O_3) and Titanium Diboride (TiB_2) nanoparticulates on the microstructure and properties of Al Si9 Cu3 Fe1 alloys for high pressure die casting applications

ACKNOWLEDGEMENTS

Influence of Alumina (Al_2O_3) and Titanium Diboride (TiB_2) nanoparticulates on the microstructure and properties of Al Si9 Cu3 Fe1 alloys for high pressure die casting applications

LIST OF ACRONYMS

AES: Auger Electron Spectroscopy.

AFM: Atomic Force Microscopy.

Al_2O_3: Alumina.

AMC: Aluminium Matrix Composite.

APS: Average Particle Size.

ASTM: American Society for Testing Materials (standards).

B: Boron.

CTE: Coefficient of Thermal Expansion.

DC: Die casting.

DTA: Differential Thermal Analysis.

DSC: Differential scanning calorimetry.

EDM: Electrical Discharge Machine.

EDS: Energy Dispersive X-Ray Spectroscopy (mapping).

HPDC: High Pressure Die Casting.

IACS: International Annealed Copper Standard.

KBF_4: Potassium Tetrafluoroborate.

K_2TiF_6: Potassium Hexafluorotitanate.

LPDC: Low Pressure Die Casting.

MALS: Multi Angle Light Scattering.

MMC: Metal Matrix Composites.

OM: Optical Microscopy.

PMMC: Powder metallurgy Matrix Composites.

RHP: Reactive hot pressing.

SDAS: Secondary Dendrite Arm Spacing.

SEI: Secondary Electron Image.

SPS: Spark Plasma Synthesis.

SHS: Self-propagating High temperature Synthesis.

TiB_2: Titanium Diboride.

TP1: Grain Refining test of Aluminium Association.

UTS: Ultimate Tensile Strength.

WDS: Wavelength Dispersive X-ray Microanalysis.

XRD: X- Ray Diffraction.

YS: Yield Strength.

Influence of Alumina (Al_2O_3) and Titanium Diboride (TiB_2) nanoparticulates on the microstructure and properties of Al Si9 Cu3 Fe1 alloys for high pressure die casting applications

INDEX   **PAGE**

ACKNOWLEDGEMENTS   ii

LIST OF ACRONYMS   iii

INDEX   iv

Influence of Alumina (Al$_2$O$_3$) and Titanium Diboride (TiB$_2$) nanoparticulates on the microstructure and properties of Al Si9 Cu3 Fe1 alloys for high pressure die casting applications

Influence of Alumina (Al$_2$O$_3$) and Titanium Diboride (TiB$_2$) nanoparticles on the microstructure and properties of Al-Si9 Cu3 alloys for high pressure die casting applications.

CHAPTER 1:   INTRODUCTION. OBJECTIVES OF THE THESIS.

CHAPTER 1: INTRODUCTION. OBJECTIVES OF THE THESIS

Influence of Alumina (Al$_2$O$_3$) and Titanium Diboride (TiB$_2$) nanoparticles on the microstructure and properties of Al-Si9 Cu3 alloys for high pressure die casting applications.

CHAPTER 1:   INTRODUCTION. OBJECTIVES OF THE THESIS.

1.1 Introduction

The process of high pressure die casting (HPDC) is one of the most productive processes in the field of light alloys as aluminium and magnesium. Thin profiles, complex geometries, high load capacities and concepts of lightweight construction are good arguments for this kind of production. The very good ratio between the properties and weight of aluminium has permitted the use of aluminium in a large number of applications in near all the sectors, especially in construction, transport and energy. About 70% of total aluminium castings are produced by high pressure die casting.

As the pure aluminium has low mechanical properties and is not possible to be die casted because its tendency to get stuck in the die, it's alloyed by the addition of elements such as Si, Cu, Fe and Zn. The most common alloy in our days for HPDC is the Al Si9 Cu3 Fe1, which shows a very good mechanical and flow properties, with low tendency to get stuck. Many alloys have been developed in order to increase some properties, by limiting or increasing the percentage of same elements as Mn, Cr, Ni, and Fe. Each component has an effect to improve or decrease alloy properties.

The present work is based on the study of the Al Si9 Cu3 Fe1 alloyed with nanoparticles. Samples of two different reinforcement nanoparticles (Al$_2$O$_3$ and TiB$_2$) has been made in a high pressure die casting machine, in which the metal is casted into a metallic die under big speeds and pressures. It's also very important to determinate the possibility to employ nanoparticles as refining and reinforcement agents of Al Si9 Cu3 Fe1, due to the lack of general industrial employment and the difficulties to develop a specific grain refiner for Al Si9 Cu3 Fe1 alloys. Also because the addition of very little particles has been related to increase mechanical properties [Egi 07]. In the case of the TiB$_2$, if the measure of the added particles is less than 2 µm, the average grain size of the alloy is strongly reduced [Que 04-02], increasing the mechanical properties of the aluminium up to a 14.7% in UTS and a Elongation of 5.5% [Han 02].

The election of the reinforced alloys have been designed to overcome the new designs of aluminium cast parts, including better mechanical properties at higher temperatures (up to 200ºC) and higher service pressures (up to 400 bar), with lowers total weights due to the reduction of the width of parts. The percentage of particles is very low (less than 1%), due to the processing difficulties to obtain high concentrations. The particle size is from 15 to 40 nanometers in alumina powders and around 200 nanometers in the titanium diboride. In order to get this very small titanium diboride, we have bought TiB$_2$ powders with a particle seizure of mesh 325, and an analogue material made at Tecnalia by dry ball milling of SHS TiB$_2$.

Influence of Alumina (Al$_2$O$_3$) and Titanium Diboride (TiB$_2$) nanoparticles on the microstructure and properties of Al-Si9 Cu3 alloys for high pressure die casting applications.

CHAPTER 1:   INTRODUCTION. OBJECTIVES OF THE THESIS.

1.2 Objectives

The main objective of the work is to study the influence of TiB$_2$ and Al$_2$O$_3$ nano-particles (up to 1 wt. %) on the properties and physical features of aluminium casting alloys processed through an under pressure process known as high pressure die casting.

One base alloy was selected for the study, the Al-Si9Cu3Fe1 alloy, an Al-Si alloy containing around 9 wt. % of Silicon and the 3 wt. % of Copper. It's extensively used in casting applications due to its excellent castability, good balance of properties and its large use in the industry (more than 70% of total HPDC aluminium casted parts). The main tasks of the work have been the selection of two reinforced nano-materials, the preparation of the nanosize TiB$_2$ from SHS bricks and mesh 325 powders, the homogeneous distribution of the particles in the matrix, the production of castings via DC and HPDC for characterization purposes, the physical, thermal and mechanical characterization, the comparison of their properties with those of the corresponding unreinforced alloy, and the analysis of the differences between the reinforced and unreinforced alloys.

1.2.1   Analysis of the influence of the TiB$_2$ and Al$_2$O$_3$ nano-particles on the solidification and microstructure of the Al Si9 Cu3 Fe1 alloy

TiB$_2$ particles have a great influence in the solidification and in the obtained microstructure of the aluminium alloys. Normally it's added to liquid aluminium in rods containing a 3-5% of Titanium and a 1% of boron. The amount of refining rod changes with the alloy, being about the 0.3 – 0.6 wt. % for the Al Si9 Cu3 Fe1 alloy. In this master alloy, TiB$_2$ particles are over the nanoscale.

TiB$_2$ particles are practicable insoluble in aluminium, due to the low wetting angle between the TiB$_2$ and the aluminium. Employing the differential thermal analysis (DTA), we can observe that they change the solidification curve of the alloy, with an earlier start of the solidification due to the decrease of the undercooling temperature, reducing the solidification time [Egi 07].

Influence of Alumina (Al$_2$O$_3$) and Titanium Diboride (TiB$_2$) nanoparticles on the microstructure and properties of Al-Si9 Cu3 alloys for high pressure die casting applications.

CHAPTER 1:   INTRODUCTION. OBJECTIVES OF THE THESIS.

In this type of alloys, it's remarkable the poisoning effect and the decrease of the refining action with time, argumented by the settle down of particles bigger than 2-5 microns. As the particles are practically insoluble in the liquid aluminium, the particles that don't became a nucleation site trend to get pushed from the solidification front to the grain boundaries. The addition of grain refiners in the Al Si9 Cu3 Fe1 as Al Ti5 B1, Al Ti3 B1 and Al Ti C have been reported [Boo 02] to decrease the internal porosity, with an average lower porosity size and with a better distribution of porosity in the part.

The reinforced and refined alloys studied in this work have been charged with different percentages, from 0.001% to around 1 wt. % of nano-particles. This amount exceeds the level necessary for grain refining in same cases, but it's to determinate, as one part of the work, the refining effect at low concentrations (percentage of 0.15% of Ti at least in commercial refining rods), in order to get the crystallization of Al$_3$Ti around the TiB$_2$ particles [Bac74]. It has been impossible by the moment to increase this percentage up to the 5% or 10%, because increasing the percentage of nano-particles promotes dross formation. The aim was to test if the nano-particles improved the properties of the alloys following the patterns shown by other particle reinforced aluminium matrix composites (AMC) or if they have a special behavior. At the same time, the increase of the amount of particles has an influence on other features of the alloys such as the solidification pattern, microstructure and thermal properties. All of these aspects have been studied in the present work.

Al$_2$O$_3$ particles have traditionally in situ studied as non desirable particles in the alloys, been related to the formation of oxides and their related problems as hard points, corrosion problems and failures in parts. Even though the main effect of the presence of Al$_2$O$_3$ particles into aluminium alloys is the reinforcement of the aluminium alloy, there are other additional microstructural changes that can also be explained by the presence of these Al$_2$O$_3$ particles. Al$_2$O$_3$ particles promote also the refinement of the grain size, and the particles that don't participate in nucleation events tend to be pushed by the solidification front and lie at grain boundaries. Porosity of the samples decreases. The average size of the pores is smaller and the remaining porosity is more evenly distributed through the addition of grain refiners. Al$_2$O$_3$ particles are substantially insoluble in aluminium with high contact angles [She 05] and they change the solidification characteristics of the alloy. Solidification events start earlier due to the lower undercooling required and solidification time is reduced.

Influence of Alumina (Al$_2$O$_3$) and Titanium Diboride (TiB$_2$) nanoparticles on the microstructure and properties of Al-Si9 Cu3 alloys for high pressure die casting applications.

CHAPTER 1: INTRODUCTION. OBJECTIVES OF THE THESIS.

The solidification curves of the reinforced and unreinforced materials have been studied and the effect of the presence of nano-particles on the main solidification parameters, such as the maximum temperature of primary α-Aluminium growth, temperature and time difference between the maximum and minimum of the liquidus recalescence determined. TP1 grain refining normalized essays have been developed in order to determinate the ASTM grain size and the microstructure of the aluminium. Also, we have done tests in order to have a comparison with the Al Ti5 B1 standard refining master alloy, because it´s the more employed aluminium grain refiner in the industry. The microstructure and composition of the reinforced alloys has been thoroughly studied through Optical Microscopy, Scanning Electronic Microscopy (SEM), Transmission Electronic Microscopy (TEM) and Atomic Force microscopy (AFM). Image analysis and the identification of the elements of the different phases have also been carried out in order to study the influence of the presence of the TiB$_2$ and Al$_2$O$_3$ nano particles on the microstructure of the alloy. The main objective of the microstructural analysis was to analyze the interaction of TiB$_2$ and Al$_2$O$_3$ particles with the matrices (See Chapter 4 on Solidification and Microstructure).

Better properties related to the decrease in the grain size, reinforcement of the alloy and the decrease of porosity permit to expect a good behavior of nano-particles at very low particle concentration.

1.2.2 Analysis of the influence of the Al$_2$O$_3$ and TiB$_2$ nano-particles on the mechanical and thermal properties of the Al-Si9 Cu3 Fe 1 alloy.

The thermal and mechanical characterization has been carried out with samples obtained with the DC and HPDC process. The production route was previously optimized in order to obtain sound samples with a correct and homogeneous distribution of TiB$_2$ and Al$_2$O$_3$ particles. The mechanical characterization has consisted on tensile tests at room temperature and at 200ºC. Cast samples have been tested and results have been compared to those obtained with the corresponding unreinforced materials. The obtained samples have not being thermally treated, due to the difficulty of treating HPDC samples with entrapped air. Thermal conductivity has been determinate in the reinforced alloys and compared with the base alloy.

The experimental results have been compared with the models employed for calculating mechanical and thermal properties of materials reinforced with ceramic particles and to check the expected improvement in the alloy properties.

Influence of Alumina (Al$_2$O$_3$) and Titanium Diboride (TiB$_2$) nanoparticles on the microstructure and properties of Al-Si9 Cu3 alloys for high pressure die casting applications.

CHAPTER 2:   LITERATURE REVIEW

CHAPTER 2: LITERATURE REVIEW

Influence of Alumina (Al$_2$O$_3$) and Titanium Diboride (TiB$_2$) nanoparticles on the microstructure and properties of Al-Si9 Cu3 alloys for high pressure die casting applications.

CHAPTER 2:   LITERATURE REVIEW

2.1 Introduction

Aluminium is the third most abundant element, after oxygen and silicon, and the most abundant metal in the Earth's crust. As is very reactive, Aluminium is not in nature as a free metal. The chief source of aluminium is the bauxite ore (an aluminium oxide). It begins its extraction in the XVIII century, but it was industrialized thanks to the Sainte-Claire Deville and Hall – Héroult methods in the second part of the XIX century.

It's very interesting for many applications because it depends on the alloy it has low density, excellent corrosion resistance, is ductile and malleable, with a good finish surface. It is no magnetic and no sparking, with a very good conductivity of electricity and heat. Corrosion resistance can be excellent due to a thin surface layer that prevents further oxidation. The corrosion resistance is reduced when is alloyed with copper, where salts are present, and in the presence of dissimilar metals. Aluminium has approximately one-third the density and properties of steel. It can be machined, cast, drawn and extruded. It can be also recycled with little energy consumption. However, the pure aluminium has low mechanical properties. The yield strength (YS) of pure aluminium is about 7 to 11 MPa, commercially pure aluminium has a YS of about 70 Mpa, and aluminium alloys have YS ranging up to 600 MPa. The additions of alloying elements allowed aluminium to become a very competitive material in many fields due to the different properties that can be performed in function of the composition of the alloy. The industrial application of aluminium is wide, from packaging to transport, including other areas as electricity and electronics.

The alloying elements can develop three main roles: 1) As basic alloying elements, 2) as ancillary additions (dopants) or 3) as impurities. The four more employed elements are silicon, copper, zinc and magnesium. They are several elements employed in same alloys, as Mn, Ti, Cr, Ni, Sn and Sr. Silicon enhances castability and tensile properties, Copper strengthens the alloy, Zinc increase machinability and Magnesium increase the mechanical properties after thermal treatments. Manganese modifies the β-iron intermetallic to a skeleton structure, Titanium refines the grain and the Strontium modifies the eutectic structure. They are also inoculants that can modify the microstructure of aluminium, by reducing the grain size (TiB$_2$, TiC) or modifying the eutectic structure (Sr, Na, P). Mechanical properties can be increased and porosity can be reduced, giving alloys with improved mechanical and more stable properties. Normally the percentage of addition of those particles is less than 1wt.%. The use of refining elements has been developed over the last sixty years. The refining effect of master alloys, as the more employed Al Ti5 B1, provide the increase of mechanical properties, grains are more equiaxed and they are more uniformly distributed and smaller, decreasing porosity and as a consecuence it's harmful effect.

Influence of Alumina (Al$_2$O$_3$) and Titanium Diboride (TiB$_2$) nanoparticles on the microstructure and properties of Al-Si9 Cu3 alloys for high pressure die casting applications.

CHAPTER 2: LITERATURE REVIEW

Another way of increasing the mechanical properties of aluminium are metal matrix composites (MMCs). They are fabricated by additioning ceramic components to the aluminium alloy, increasing the properties that can be obtained by combination of different alloying elements. They are many types of sizes (from nano to millimeters), shapes (particulates, fibers, pre-forms…) and materials (Al$_2$O$_3$, SiC, B$_4$C, TiB$_2$…) that are employed as reinforcements. They are very interesting because of the possibility of tailoring different properties in different locations of a part. The reinforcement volume, composition, size, type and way of producing permits the development of parts with application in the aeronautics, electronics and transport industry. Metal nanoparticles are being investigated for several applications, due to the new properties obtained in the nano-reinforced materials:

- Health protection: Silver (antibacterial) and other noble metals.

- Magnetic applications: Iron based alloys to reduce loses in energy transmission, due to small size of the grains compared to the magnetic domain size and also by interface effects on magnetic properties.

- Structural applications: Light metals with superior mechanical properties: Al and Mg alloys, Ti and Ti alloys with a radical improvement of various kinds of mechanical properties, caused by a change in their deformation mechanism comparing to conventional materials.

- Coatings: Radically improved tribological properties, higher wear resistance, less friction, better corrosion resistance, sustainable production process, etc. The improved properties are connected with the uniformity of the micro-structure.

- Hydrogen storage: Mg and its alloys. Properties are connected with high diffusion rates for hydrogen, and increased solubility limits in the nanoscale material.

The most rapid increase of patents concerns nano-powders, mainly of noble metals, as well as aluminium. Powders are suspended in a fluid or another material. In this case, the most important property is the high contribution of surfaces of the particle to the properties or function of the material they are embedded in. This results in a high material activity, which could be used as catalyst or as source of ions for antibacterial properties, etc. The second rapidly developing field concerns light metals with improved mechanical properties. Here the specific mechanical properties of nanostructure materials are concerned: High strength combined by special processing methods with ductility, high fatigue limits, elevated temperature strength, corrosion or wear resistance, etc.

Influence of Alumina (Al_2O_3) and Titanium Diboride (TiB_2) nanoparticles on the microstructure and properties of Al-Si9 Cu3 alloys for high pressure die casting applications.

CHAPTER 2: LITERATURE REVIEW

In the case of the nano-ceramics, nanocrystalline materials exhibit increased strength/hardness, enhanced diffusivity, improved ductility/toughness, reduced density, reduced elastic modulus, increased electrical resistance, increased specific heat, optimized thermal expansion coefficient, lower thermal conductivity, and finally superior soft magnetic properties in comparison to conventional coarse grained materials. Since nanocrystalline materials contain a very large fraction of atoms at its surface, the numerous interfaces provide a high density of short-circuit diffusion paths. The enhanced diffusivity can have a significant effect on mechanical properties such as creep and superplasticity, and ability to efficiently dope nanocrystalline materials with impurities at relatively low temperatures. The increased diffusivity leads to increased solid solubility limits and increased sinterability of nanocrystalline powders [Loe 01].

It's expected to increase the properties of aluminium alloys due to 1) the introduction of nano-particles, and 2) to the high surface area in comparison with the weight of particles.

The materials (TiB_2 and Al_2O_3) that have being chosen for the study have application as reinforcement of aluminium alloys, because they don't react with the molten aluminium and because they can be introduced in the alloy by in situ and *ex-situ* processes. TiB_2 and Al_2O_3 nanoparticles are always added in small concentrations to avoid problems in the filling of the moulds, due to the increased viscosity of the resultant MMC. In this chapter, a review of the main properties of TiB_2 and Al_2O_3, as well as a description of them use in the aluminium industry as grain refiner and as reinforcement for MMCs are described.

2.2 High pressure die casting process

In high pressure die casting [Bro 99], usually known as pressure die casting, molten alloy is injected under pressure into a highly accurate split metal mould. It is the most widely used casting process for aluminium alloys. Production rates are fast, process can be highly automated, and dimensional accuracy and surface finish are excellent. Thin-walled components are possible and little or no machining is needed on the cast component, since holes, grooves and recesses can be finish cast. Doehler was among the first to patent die casting-related technology in 1910 [Que 04-02]. The initial machines produced aluminium castings in reusable metal moulds, where a manually powered pull bar transmitted the force required to fill the mould. In 1927, the horizontal cold chamber die casting machine was developed, which represents the basis of today's technology.

Influence of Alumina (Al$_2$O$_3$) and Titanium Diboride (TiB$_2$) nanoparticles on the microstructure and properties of Al-Si9 Cu3 alloys for high pressure die casting applications.

CHAPTER 2: LITERATURE REVIEW

The transportation industry, and in particular the automotive industry, is imposed to seek light materials in the development of robust parts. The global production of aluminium and magnesium alloys has therefore increased, and the consumption of aluminium concurrently exceeds the existing production capacity of primary metal.

It's therefore necessary to exploit, or invent, economically sustainable processes that can give light weight products with integrated functions that fulfil the requirements for recycling and fuel consumption regulations. High pressure die casting (HPDC) is a method well suited for those demands. HPDC is a fully automatic, large volume, high productivity process for the production of complex, thin walled near net shape castings, with part weights ranging from a few grams to more than 25 kg. It has traditionally been utilised in the production of housing or not complicated parts, but this has changed. Presently, feasible products are automotive front end structures and instrument panels in magnesium alloys and B-pillars in aluminium alloys. However, for HPDC to be competitive for extended automotive applications and attractive for new market segments, the crash worthiness and fatigue properties must be improved and a scientific comprehension of the process and metal behaviour is required.

The four principal metals, with different alloy compositions, that are commonly hot or cold chamber die cast are aluminium, zinc, magnesium and copper-base alloys. The injection system in the hot chamber machines is immersed into the melt and the pressure is therefore limited. The system also degrades quickly if exposed to aluminium. In the cold chamber process, the metal reservoir is separated from the injection system. The metal is filled into a steel shot sleeve, as shown in Fig. 2.1. The shot sleeve is typically 200-300ºC.
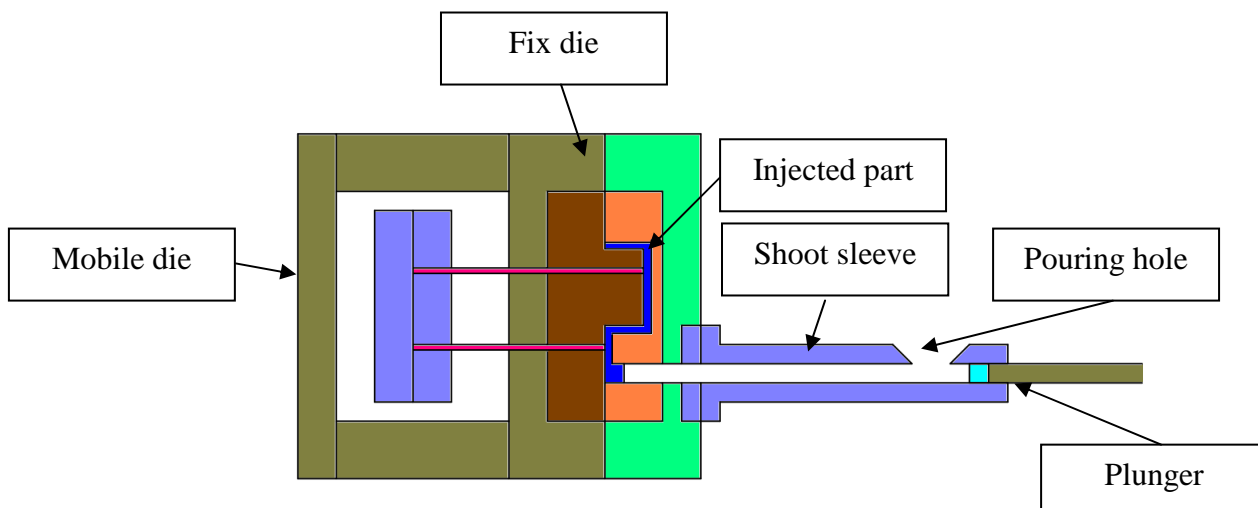
Fig.2.1: Illustration of cold chamber high pressure die casting.

Influence of Alumina (Al$_2$O$_3$) and Titanium Diboride (TiB$_2$) nanoparticles on the microstructure and properties of Al-Si9 Cu3 alloys for high pressure die casting applications.

CHAPTER 2:   LITERATURE REVIEW

A <u>production cycle in HPDC</u> consists on:

  1) Pouring of metal into the shot sleeve;

  2) Plunger movement.

  3) Rapid die filling.

  4) High hydraulic pressure during solidification by the plunger to feed the solidification shrinkage.

  5) The die is opened.

  6) The casting is ejected.

The hydraulic energy is provided by a computerized system that permits control metal position, velocity and plunger acceleration to optimize the flow and the pressure during filling and solidification. The specific pressure applied in the die cavity variates normally from 600 to1200 Bar. Die cavity air may be evacuated to reduce air entrapment during die filling, and high integrity die castings can therefore be produced by utilizing vacuum systems. Alternatively semi-solid metalworking (SSM) can be used to reduce turbulence. A short die filling time and thin walls results in high cooling rates (Typically 100 to 1000ºC.s^{-1}).This promotes a fine grain size which provides decent mechanical properties. However, the properties can be improved by intimate interrelationship between product and process design through amended metal handling, accurate process control, and optimized runner and die design.

The capacity of the injection system is described by the so called P-Q^2 diagram which is supplied with the HPDC machine. It has been deduced that the pressure, P, is proportional to the square of the flow rate, Q. The working conditions are determined from the intersection of the die line with the machine line in the P-Q^2 diagram. Furthermore, suitable timing, good dimensional stability and correct assessment of the fluid and heat flow are prerequisites for better castings. Cycle times depend on size and section thickness of the component, being typically 40 shots per hour for a component of 5 kg. Machines are described by their "locking force", which determines the cross-sectional area of the casting which can be made, which is in turn related to the overall size and weight of casting. Machines can have locking forces from 100 to over 4000 tonnes. Dies are expensive but can have a life of more than 100000 shots.

Influence of Alumina (Al$_2$O$_3$) and Titanium Diboride (TiB$_2$) nanoparticles on the microstructure and properties of Al-Si9 Cu3 alloys for high pressure die casting applications.

CHAPTER 2:   LITERATURE REVIEW

This process is therefore most suitable for long runs of castings. One drawback of the process is that almost inevitably some air is trapped in the die with the liquid metal, so that the casting contains gas porosity, although it is frequently internal, so that the component may be leak-tight. The presence of internal gas prevents subsequent heat treatment (the residual gas expands and distorts the casting) and also places a limit on the mechanical properties attained by the casting, as we can see in Fig. 2.2. In artificial ageing temperaratures of 150ºC, blistering appears. For this reason, the process has mainly been used for castings which do not require the highest strength. Another disadvantage is that standard sand cores cannot be used, since the high pressure liquid metal would penetrate the core. Coring is thus limited to straight "draws" which can be formed with retractable steel "pulls".
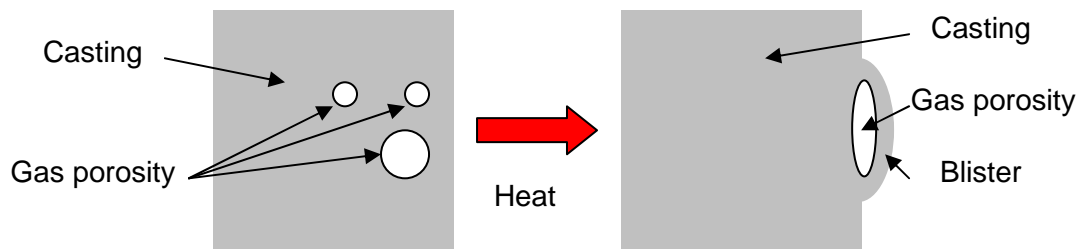
Fig.2.2: Blistering process with entrapped gas porosity.

Apparently minor factors such as amount of lubrication, its composition and application procedures can turn out to be very important for the final casting characteristics. Whilst several process parameters can affect the properties of the castings, the alloy itself is important. The alloy characteristics must fulfil the necessary requirements in castability which involves i.e. higher fluidity, good feeding and low hot tearing tendency. The most common HPDC aluminium alloy is the A380 (AlSi9Cu3) alloy, but a generally more utilized foundry alloy for other casting processes is the A356 Al-Si alloy which has good fluidity.

One of the main features of recent researches have been the development of special machines and processes which improve the hydraulic integrity and mechanical properties of pressure die cast components.

In our case, we have chosen HPDC process because as we have seen it's possible to incorporate the process in the industry with low modifications employing the liquid route, and providing an economical viable process with enough quality.

Influence of Alumina (Al_2O_3) and Titanium Diboride (TiB_2) nanoparticles on the microstructure and properties of Al-Si9 Cu3 alloys for high pressure die casting applications.

CHAPTER 2:   LITERATURE REVIEW

2.2.1   Aluminium alloys.

As the pure aluminium has low mechanical properties, they have been developed many different aluminium alloys, by the addition of several different elements to give different properties to pure aluminium. They are also several ways of classifying the Aluminium alloys. One is by separating casting and forging alloys. Another is by the nature of the alloying elements, where they are classified by the main alloying element in the wrought aluminium alloys.

The most employed classification for wrought alloys is a four digits classification, where the first of the four digits in the designation indicates the alloy group as follows in Table 2.1.:

Alloying elements	Designation
Aluminium, 99.00 percent and greater	1xxx

Aluminium alloys grouped by major alloying elements:

Copper	2xxx
Manganese	3xxx
Silicon	4xxx
Magnesium	5xxx
Magnesium and Silicon	6xxx
Zinc	7xxx
Other elements	8xxx
Unused series	9xxx

Table 2.1: Aluminium Wrought Alloys Classification.

2.2.2   Aluminium based die casting alloys

Between the different aluminium alloys, the Al-Si-Cu family is the most employed in HPDC (near a 90% of total), with a composition of 7-12% Si, 0,7-2% Fe, 0-4% Cu and lot of elements that have a great influence in the properties of the alloy. Some new alloys (Silafont, Magsimal…) are employed for special applications.

Influence of Alumina (Al_2O_3) and Titanium Diboride (TiB_2) nanoparticles on the microstructure and properties of Al-Si9 Cu3 alloys for high pressure die casting applications.

CHAPTER 2:   LITERATURE REVIEW

2.2.2.1 Aluminium-Silicon-Copper alloys

They have an excellent castability, fluidity and corrosion resistance. Silicon gives good castability, copper strengthening and machinability, and iron percentage must be enough to avoid die soldering. They have low density (2.76 g/cm^3). Machinability is good, corrosion resistance fair, good anti-soldering, fair polishing and anodizing appearance with good pressure tightness.

As they include a percentage of iron >0.7% they are ideal for HPDC, decreasing the soldering effect and primary melting metals are not necessary, so they are produced by recycling aluminium scraps. The high percentage of silicon, near to the eutectic point (12.6 wt.% of Si), gives an excellent fluidity and castability, making possible to create very complex parts with very small cast walls (up to 0.5 mm approximately) and reducing the solidification temperature from 660ºC to about 577ºC.

Changing the rest of elements of the alloy, it's possible to increase properties (UTS, YS, Elongation), but, normally, other properties can decrease. If we increase the UTS and the YS, the tendency of the Elongation is to decrease, and if we increase the Elongation normally the UTS decreases.

One of the most popular Al-Si-Cu alloys is the Al-Si9-Cu3-Fe1 alloy. Following we resume some of as cast properties of DIN EN 1706:2010-06 for injection processing of EN AC- 46000 to EN AC- 46500 alloys: Density of about 2.76 g/ cm^3, YS 0.2% (MPa): 140, UTS (MPa): 240, Elongation (%): <1, Hardness (HBW): 80, Coefficient of thermal expansion (10-6. ºC^{-1}): 20-21 and Thermal Conductivity (W/m ºK): 110-150.

2.3 Aluminium grain refining

The addition of elements such as Ti, Zr, B, N and C to the aluminium alloys promotes the grain refinement of the aluminium, and can control the growth parameter of crystals of aluminium in the solidification. The added elements act as nucleation nuclei at small undercoolings of the α-Al grains. The refining effect modifies the columnar solidification to an equiaxed one, with a minor grain diameter and more uniform distribution. The diminution of grain size improves the alloy behavior, with less blistering and hot tearing, higher and quickly deformation processes, less internal porosity and cracks, improve also the elongation and ductility [Tam 08].

Influence of Alumina (Al_2O_3) and Titanium Diboride (TiB_2) nanoparticles on the microstructure and properties of Al-Si9 Cu3 alloys for high pressure die casting applications.

CHAPTER 2:   LITERATURE REVIEW

The most employed grain refiner is the Al-5Ti-1B and the rest of the Al-Ti-B compositions. They are also special applications where other refiners are employed, as the Al-Ti-C, Al-B, Al-Ti and modifiers as Al-Sr. The refiners have a tendency to loss it efficiency in the time (Fading). The reason is not clear yet, but the more accepted theory is the agglomeration of ceramic particles and the poisoning effect of different elements (Si, Zr, V, Ta and Cu). Nevertheless, because the similar chemical properties of the surrounding elements of the periodic table, a partial substitution of Ti can be made with V,Zr,Cd,Hf or Ta, and the same with the substitution of boron by C,Si,N,P,Be and Mg [Guz 86],[Ram 08]. The master alloys are normally added in rods or ingots. The Al- Ti -B master alloy is the most common used for aluminium alloys, and they are a mixture of two interdispersed crystals in a matrix of solified aluminium. Titanium diboride (TiB_2) and titanium aluminide ($TiAl_3$) are the two phases.

They are different theories for the explanation of the refining effect, but two are the most employed: the peritectic and the boride-carbide theory. Nowadays, the boride-carbide theory is more accepted [Ask 03]. However, new theories are being proposed in order to explain the exact way of the refining of aluminium alloys.

The peritectic theory started in 1951. This theory proposed that the interface of $TiAl_3$ and the liquid aluminium is the place for the nucleation of α grains and for grain growth. It was based in the observation of $TiAl_3$ particles in the center of α grains and that there was no nucleation below or at the melting temperature. This theory has not an explanation for the boron effect. The boride-carbide theory is based on the idea that the nucleation starts at the TiB_2 or TiC particles, which have very little solubility in the melt, but can't explain why is necessary an extra percentaje of Ti in the melt to have a positive action [Iva 04].

The nucleation is the physical process by which a new phase is produced in the aluminium. There is a critical radius that must be formed by atoms clustering together in the liquid before the solid particle is stable and begins to grow. The undercooling is the temperature to which the aluminium must be cool below the equilibrium freezing temperature before nucleation occurs. The nucleation can be homogeneous or heterogeneous. In the homogeneous nucleation, the formation of a critically sized solid from the liquid by clustering together of a large number of atoms at a high undercooling promote the nucleation, without an external surface. In the heterogeneous, the nucleation is formed due to the formation of a critically sized solid from the liquid on an impurity surface [Ask 03].

Influence of Alumina (Al$_2$O$_3$) and Titanium Diboride (TiB$_2$) nanoparticles on the microstructure and properties of Al-Si9 Cu3 alloys for high pressure die casting applications.

CHAPTER 2: LITERATURE REVIEW

When a metal is not refined, there is a necessary undercooling to start the nucleation, and as much as the nucleation releases the latent heat of fusion, the liquid temperature increases (Recalescence), as in Fig.2.3.(a). After this, the metal solidifies at constant temperature. If the metal is refined, it's no necessary to have an undercooling, so no recalescence is observed, beginning the solidification at the melting temperature (See Fig. 2.3. (b)). We can conclude that the lowest the undercooling, the more equiaxed the grains.
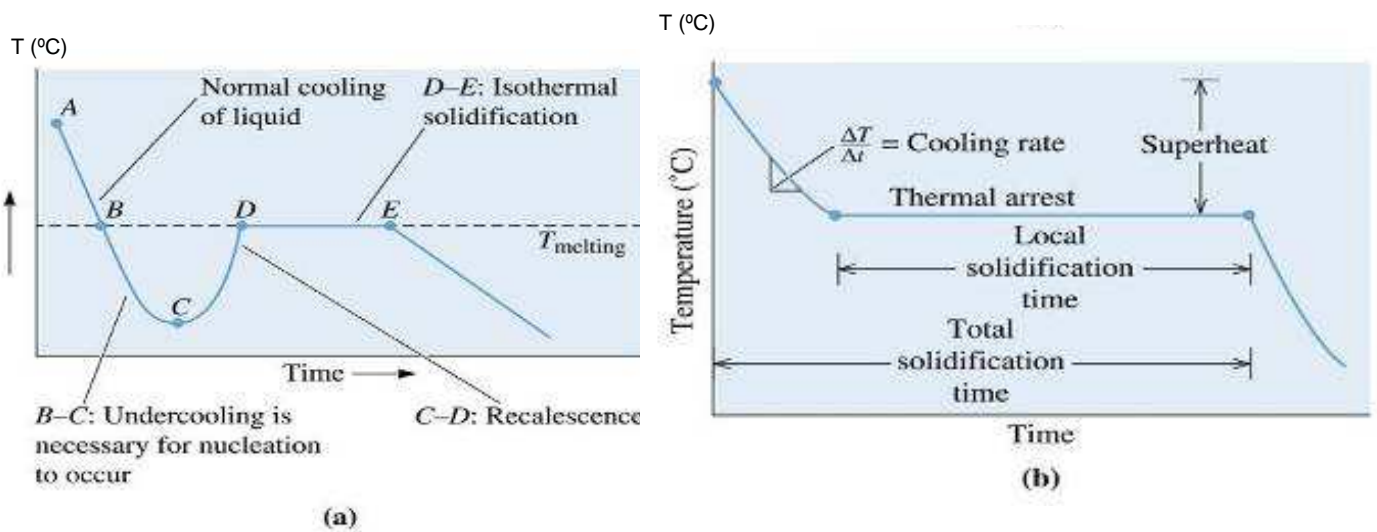
Fig.2.3. (a) and Fig.2.3. (b): Solidification diagrams of Temperature / Time [Ask 03].

In our samples we expect to have a lower recalescence, due to the refining effect of Al$_2$O$_3$ and TiB$_2$, promoting smaller grain size.

Solidification of aluminium alloys

One metal should evacuate the heat to solidify. When the liquid aluminium is under cooled, a protuberance on the solid-liquid interface can grow fast, creating a dendrite. Latent heat of fusion is removed by raising the temperature of the liquid back to the freezing temperature. The mechanism of solidification begins with the formation of the nucleus in the liquid state, those nucleus increase their size from the liquid (Homogeneous) or from the inoculants (Heterogeneous). Then those nuclei increase their size, and finally the liquid is totally transformed to solid.

Influence of Alumina (Al_2O_3) and Titanium Diboride (TiB_2) nanoparticles on the microstructure and properties of Al-Si9 Cu3 alloys for high pressure die casting applications.

CHAPTER 2:   LITERATURE REVIEW

Homogeneous nucleation models of α-Al grains

The homogeneous solidification is generated by a local variation in one element concentration (Undercooling). It is characterized by low number of nuclei and a high undercooling. The nuclei are randomly distributed in all over the liquid, and the solidification starts in this points. In the experiments, the undercooling is not bigger than a dozen of degrees. This low value is explained by the presence of external nuclei that provokes the solidification.

The homogeneous nucleation develops columnar grains, but equiaxed grains have better YS and UTS. The solute affects the morphology and size of dendrites. The total free energy of the solid-liquid system changes with the size of the solid. The solid is an embryo if its radius size is less than the critical radius size, and is a nucleus if its radius is greater than the critical radius. As we can observe in Fig. 2.4., the bigger is the radius of the embryo, the bigger is the possibility of acting as a nucleus.
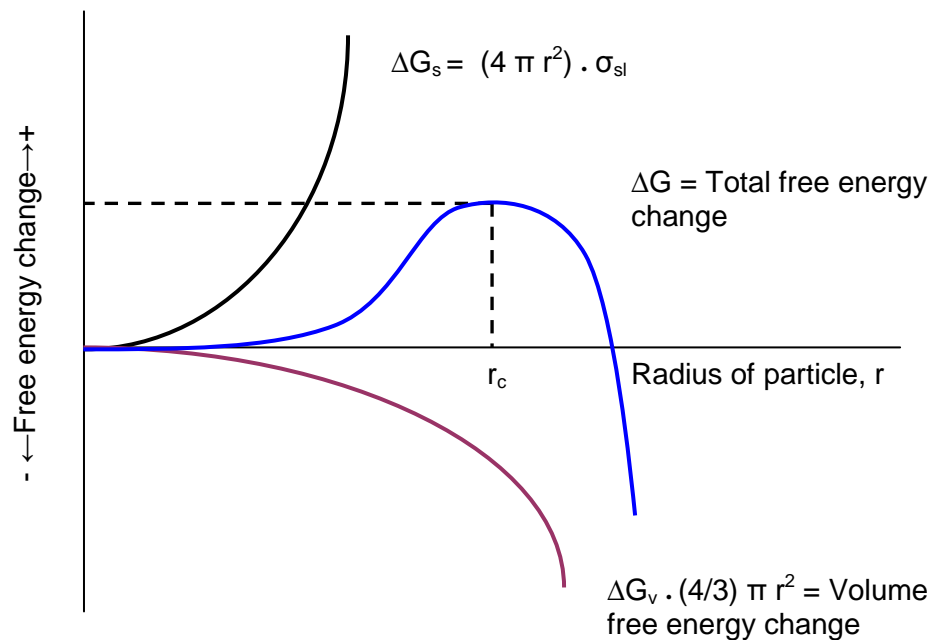
Fig.2.4: Determination of critical radius [Ask 03].

Influence of Alumina (Al_2O_3) and Titanium Diboride (TiB_2) nanoparticles on the microstructure and properties of Al-Si9 Cu3 alloys for high pressure die casting applications.

CHAPTER 2:   LITERATURE REVIEW

The critical radius calculation is based on the thermodynamic properties. At one temperature, the thermodynamically more stable state has the lowest free energy (G). For a given undercooling ΔT, we have that $\Delta G = G_s - G_l$, where G_s is the free energy in the solid state and G_l in the liquid state. If g_α and g_γ are the free enthalpies of every phase per volume unity, and γ is the interface energy value per surface unit between the two surfaces, we can obtain the free enthalpy of a nucleus with a radius R as:

$$\Delta G = 4\pi R^2 (1/3 R (g_\alpha - g_\gamma) + \gamma) = 4/3 \pi R^3 (g_\alpha - g_\gamma) + 4 \pi R^2 \gamma$$

Derivating respect the temperature the equation we obtain the critical radius:

$$R_c = 2 \gamma / (g_\alpha - g_\gamma)$$

As $(g_\alpha - g_\gamma) = \Delta H - T \Delta S$; where $T = T_c$ (Critic temperature of nucleus formation), and $\Delta H = T_c . \Delta S$, we obtain the critical radius:

$$R_c = 2 \gamma / (g_\alpha - g_\gamma) = 2 \gamma T_c / (\Delta H . \Delta T)$$

The critical radius decreases when the undercooling increases its value. In the heterogeneous solidification there is only a little variation, having a lower ΔG [Cti 01]. In Fig. 2.5. we observe how changes the radius, with a decrease in the heterogeneous (green line) undercooling. As in our case, particles will be added to obtain a heterogeneous nucleation, and we expect a better nucleation. Also the HPDC process has very high cooling rates, which can therefore promote a decrease of the critical radius.

Fig.2.5: Undercooling variation between homogeneous and heterogeneous nucleation.

Influence of Alumina (Al_2O_3) and Titanium Diboride (TiB_2) nanoparticles on the microstructure and properties of Al-Si9 Cu3 alloys for high pressure die casting applications.

CHAPTER 2:   LITERATURE REVIEW

Heterogeneous nucleation models of α-Al grains

In this type of nucleation, the nucleation begins in an impurity surface, as carbides or oxides for example. In order to act as a nucleating agent, the impurity must have a low contact angle with the aluminium, so that the solid formed on the impurity surface can be bigger than the critical radius, with a smaller increase in the surface energy. This is the reason why the heterogeneous nucleation can occur with low undercoolings.

As they act as nuclei, they are employed to refine the grain. In order to be efficient, inoculants must be in crystallographic concordance with the aluminium matrix, be uniformly dispersed in the melt and have an atomic radius bigger than the critical radius. Indeed if the nucleus has a smaller radius it tends to dissolve and if we have a bigger one, it has smaller system energy and it will therefore increase in siz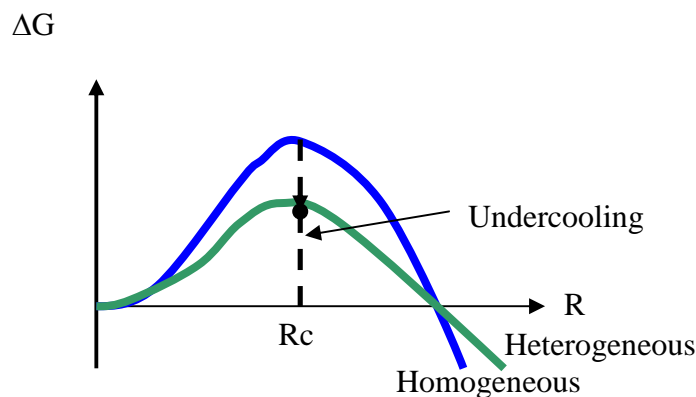e. The efficiency of the nucleus in the heterogeneous solidification depends on the contact angle; so it depends on the interface energy between the solid and the liquid.

The grain size is easier to control in the heterogeneous solidification. They are several inoculants that can be employed: $TiAl_3$, TiB_2, TiC, ZrB_2, TiN, and AlB_3 [Guz 86]. We will focus on TiB_2 because is considered the most potent nucleator agent and Al_2O_3, because of its disponibility in very small sizes, the possibility of manufacturing from aluminium recovery salts and its stability and wettability.

AL-TI-B systems as grain refiners

The first theory to explain the refining effect was the peritectic theory. Particles of $TiAl_3$ were found by Davis and Maxwell in the center of α-aluminium grains, not nucleation below or at the melting point, and nucleation took place around the peritectic temperature (665°C). This theory has not an explanation for the refining effect of boron. Maxwell and Hellawell take the contact angle as an adjustable parameter in the classical heterogeneous nucleation theory. Greer found that experimental data could be better explained by the free-growth criterion to describe the initiation of grains [Gre 00], applicable where the formation of the first solid (α-Al) on inoculants particles occurs above the liquidus or at very small undercoolings. [Que 04-01]

The most important barrier to the formation of a freely growing grain involves the shape of the α-Al/Liquid interface on the inoculants particle. The TiB_2 particles in the Al-Ti-B master alloys are hexagonal platelets, with their main faces being {0 0 0 1}, on which the nucleation of α-Al occurs [Sch 98]. Those phases can be approximated to a circle (Diameter d). As a thin layer of α-Al on a {0 0 0 1} face on an inoculants particle grows outwards, the radius of curvature of the α-Al/Liquid interface first decrease; that is energetically unfavorable unless the undercooling is increased. When the α-Al cap on the inoculants particle has grown outward to form a hemisphere, the radius of curvature of the α-Al/Liquid interface is minimum, and more growth is energetically favorable.

Influence of Alumina (Al$_2$O$_3$) and Titanium Diboride (TiB$_2$) nanoparticles on the microstructure and properties of Al-Si9 Cu3 alloys for high pressure die casting applications.

CHAPTER 2:   LITERATURE REVIEW

The undercooling for which the hemispheric α-Al/liquid interface is in equilibrium marks the onset of the free growth and the effective initiation of the grain [Que 04-02]. The critical undercooling, ΔT_{fg} is calculated by:

$$\Delta T_{fg} = 4\gamma/\Delta S_v.d$$

Where γ is the interface energy value per surface unit between the two surfaces (solid / liquid interfacial energy), ΔS_v is the entropy of fusion per unit of volume and "d" is the particle diameter. Large particles become active nuclei at smaller undercoolings, and smaller inoculate particles remain inactive if the maximum undercooling reached in the melt does not exceed their critical ΔT_{fg}. For the aluminium alloys containing more than a 1% of silicon, the ratio Ti:B is increased to 1, with an Al Ti3 B3 composition.

In order to determinate the grain refinement of various aluminium-based alloys, we can use the grain growth index (GGI), represented as [Bac 00]:

$$GGI = \sum m_i C_i (k_i - 1) = m_1 C_1 (k_1 - 1) + m_2 C_2 (k_2 - 1) + ...$$

Where m_i is the slope of the liquidus in the binary (Al-i) system, C_i is the concentration of its dissolved solute in the alloy and k_i is the distribution coefficient of solute i between solid and liquid. m_1, C_1, K_1, etc. represents the corresponding values for each alloy constituent.

The amount of Ti results in a GGI value in refined alloy which corresponds to grain size less than equal to desired grain size (GGI$_d$), it can be calculated with the formula [Bac 00]:

$$Amount_{Ti} = \frac{GGI_d - GGI_b}{(K_{Ti} - 1)m_{Ti}}$$

Where "amount$_{Ti}$" is the percentage by weight of Ti to be added to the melt, "GGI$_d$" is the grain growth index resulting in aluminium castings having a minimal grain size, "GGI$_b$" is the grain growth index of the original aluminium base material, "m$_{Ti}$" is the slope of the liquidus in the binary (Al-Ti) system, "K$_{Ti}$" is the distribution coefficient of Ti between solid and liquid. Calculations can be made also with multinary systems. It exists a relationship between grain size and the dendrite coherency point (f$_s$*) which can be used to optimise nucleation. The dendrite coherency point is the moment when a solid phase network is established throughout the entire volume of a casting, and from the moment phenomenas like macro segregation, shrinkage, porosities and hot tearing start to develop. To establish the coherency point, the fraction solid is determined as function of the solidification rate (df$_s$/dt), by thermal analytical technique or by measuring the viscosity [Bac 00]. The grain size decreases (as the number of grain boundaries increases) when we increase the % of Ti [Que 04-02].

Influence of Alumina (Al$_2$O$_3$) and Titanium Diboride (TiB$_2$) nanoparticles on the microstructure and properties of Al-Si9 Cu3 alloys for high pressure die casting applications.

CHAPTER 2:   LITERATURE REVIEW

We can also see the relationship between the particle diameter and the undercooling needed for grain initiation. We can observe at Fig.2.6., that as the particle measure increases, the undercooling decreases, so the potential of been active as a nucleation site is increased. We can determinate that TiB$_2$ particles of about 1 micron can be active with only a 1ºC of undercooling. However, very fine particles need a very high undercooling in order to be activated.
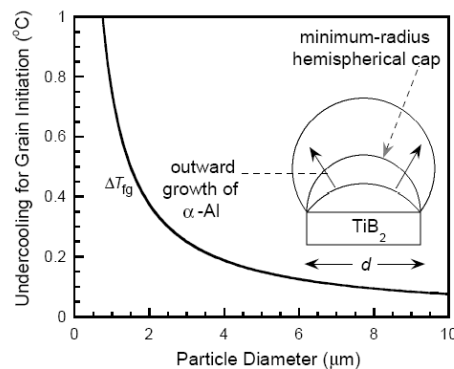
Fig.2.6.: Necessary undercooling in function of particle diameter [Que 04-02]

Maxwell-Hellawell theory (Heterogeneous nucleation) don't match the reality, being much more adequate then the isothermal-melt model. The grain refinement of aluminium silicon alloys is more difficult than with other alloys; the quantity of Si in the alloy has a great influence on it. As the silicon percentage is increased over 3 wt%, the grain refining loose their action, leading to an increase of the grain size [Que 04-02]. In the case of commercial grain refiners, there is a poisoning effect (Lost of the refiner characteristics with time), due to the interaction of silicon with refiners. This is also related with the time of effect of refiners. Refiners loose their properties in time (fading effect). As we increase the undercooling temperature, the minimum particle diameter working as a nucleus decrease, and as we increase the particle diameter, the required undercooling for nucleation decreases.

In our case the use of nano-particles should demand a higher undercooling, due to the small size, but in the other hand the fading effect should be eliminated, remaining the nucleation effect during the time. Also as they have a very high specific area and a tendency to agglomerate, clustering of particles acting as nucleation sizes could be detected.

Influence of Alumina (Al$_2$O$_3$) and Titanium Diboride (TiB$_2$) nanoparticles on the microstructure and properties of Al-Si9 Cu3 alloys for high pressure die casting applications.

CHAPTER 2:   LITERATURE REVIEW

2.4 Aluminium reinforcement

Aluminium metal matrix composites has been developed from the 1950´s. A composite is a heterogeneous mixture of two or more materials, which have been bonded together at a fine scale that can be considered a material with properties of its own. An aluminium metal matrix composite (AMC) contains the aluminium as the continuous matrix and a reinforcement which represents at least a few percent of the material. The two materials are originated from separate original components and which remain distinct in processing the material. The reinforcement is mostly added as particulates, but they are also for example continuous fibres, whiskers, short fibres and 3D performs. They are several materials that are used as reinforcements as C, SiC, SiO$_2$, B$_4$C, Al$_2$O$_3$, TiB$_2$ [Tjo 03].

The creep performance, toughness, wear resistance and the thermal stress are increased in those materials. Thermal and electrical conductivities can be high and tailorable. The biggest disadvantage of those materials is the high price, but also the galvanic corrosion, low ductility and anisotropy [Mor 01]. They are many ways to obtain AMC, but they are 3 main routes, the liquid, the solid and the deposition process as we can observe in Fig.2.7. [Mor1] :
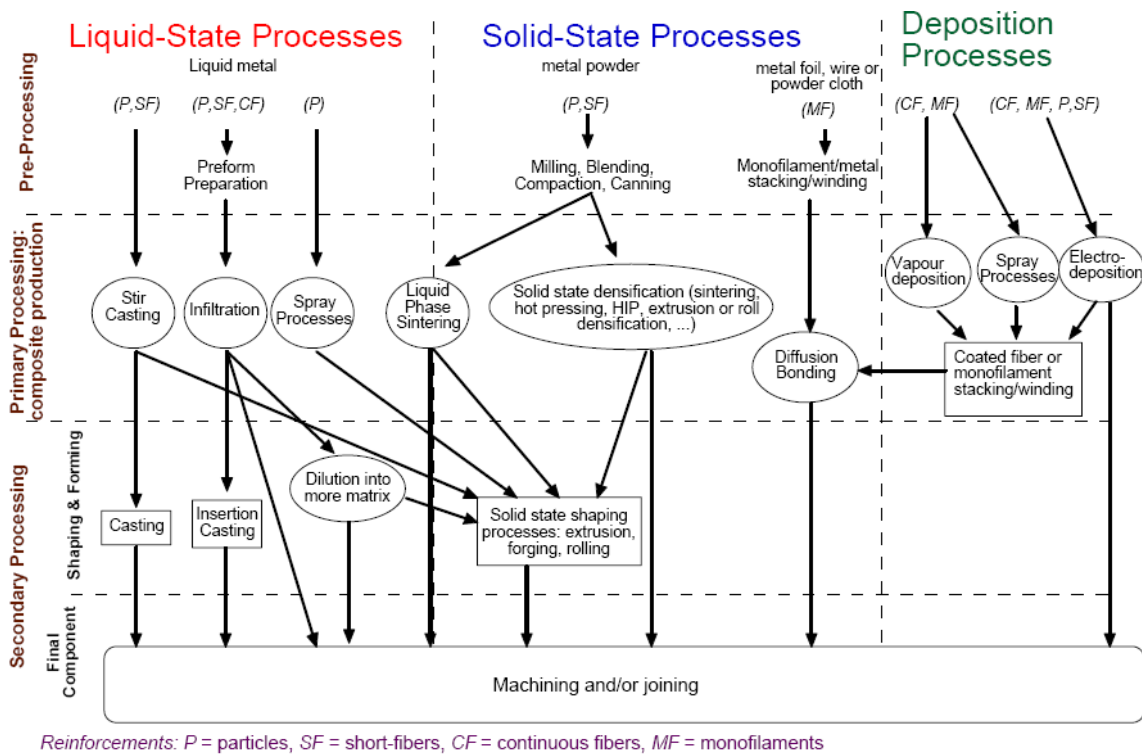

Fig.2.7: AMC processing routes [Mor 01]

Influence of Alumina (Al$_2$O$_3$) and Titanium Diboride (TiB$_2$) nanoparticles on the microstructure and properties of Al-Si9 Cu3 alloys for high pressure die casting applications.

CHAPTER 2:   LITERATURE REVIEW

AMCs are mostly fabricated by liquid ingot casting and powder metallurgy (PM) routes. Ingot casting process offers substantial cost reduction advantages in terms of mass production over PM route. However, many structural defects such as gas porosity, oxide inclusions, agglomeration of the reinforcements and an interfacial product are often produced in cast AMCs. Such defects affect the mechanical performances of AMCs. From this aspect, squeeze casting can be used to eliminate gas porosity and shrinkage.

AMCs generally are difficult to machine due to the high hardness and abrasive nature of the ceramic reinforcing phase. Accordingly, PM route with near net shape capability is more attractive than the casting technique. Furthermore, PM processing of AMCs results in better mechanical properties with homogeneous microstructure, i.e. more uniform distribution of ceramic particles. Thus, the microstructures of AMCs are sensitively determined by process conditions. Another promising method is infiltration. The ceramic reinforcement is formed previously, and placed in the die. Then aluminium is introduced in the die, covering the ceramic. Ceramic parts can be denses or have open or close porosity.

The incorporation of ceramic reinforcements to AMCs generates the residual stresses during cooling from the material processing temperature. This is due to a large difference between the coefficient of thermal expansion (CTE) of the reinforcement and matrix. The thermal properties can be tailored through proper control of the reinforcement and matrix. TiB$_2$ particles increases in general the UTS and YS, and depending on the studies the elongation can increase or decrease [Tee 01] [Mis 04]. Among the reinforcing particulates, titanium diboride (TiB$_2$) is particularly attractive because it exhibits high elastic modulus and hardness, high melting point, superior wear resistance and good thermal stability. Moreover, TiB$_2$ particles do not react with aluminium, thereby avoiding the formation of brittle reaction products at the reinforcement – matrix interface.

In AMCs reducing grain size (D) has also an impact on strengthening precipitates or disperser size (δ), and increasing volume fraction (d) on strengthening in metallic alloys. The nanoscale structures can have a significant impact on the strength of metals, increasing mechanical properties [Dav 07]. Mechanical properties are optimal for reinforcement size ranging from 10 to 40 nm. However, the particles must been desagglomerated. In our case, the nano-particles can produce a decrease of grain size and a strengthening of precipitates. Also, an increase in volume fraction by the high specific area can produce an increase of the mechanical properties.

Influence of Alumina (Al$_2$O$_3$) and Titanium Diboride (TiB$_2$) nanoparticles on the microstructure and properties of Al-Si9 Cu3 alloys for high pressure die casting applications.

CHAPTER 2:   LITERATURE REVIEW

Types of AMC materials

As metallic matrix, near all the most employed aluminium alloys have been reinforced with particles, but the most commonly used are the aluminium, magnesium and titanium, in spite of others like copper and iron. The AMC are classified according to the reinforcement shape and the name of the matrix, as we observe in Fig.2.8:

Monofilaments   Whiskers/ Short fibers   Particles
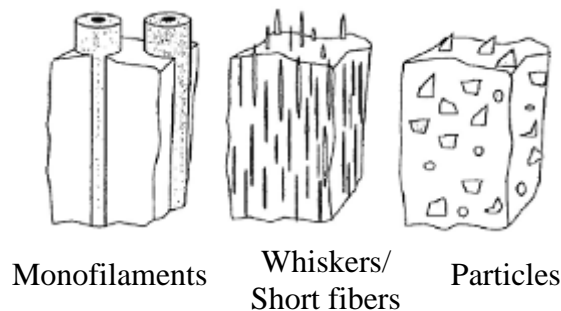
Fig.2.8: Reinforcement shape classification of AMC [Mor 01].

* *__Continuously reinforced AMCs:__* The metal is reinforced with a continuous reinforcement (monofilaments or fibre tows). The main problem is the chemical attack, because it can produce sometimes a galvanic corrosion, so if there is an interaction between the two materials, fibres are coated to avoid the galvanic par. The properties are anisotropic.

* *__Discontinuously reinforced AMCs:__* The metal is reinforced with a discontinuous reinforcement, and the reinforcement has not a chemical reaction with the matrix. The properties in this case are generally isotropic and can be tailored.

* *__Interpenetrating phase composites:__* The metal is reinforced with a three-dimensionally percolating phase, for example ceramic foam.

* *__Liquid phase sintered metallic materials:__* Include the cemented carbides, in which carbide particles are bonded together by a metal such as cobalt, or the tungsten heavy alloys.

Influence of Alumina (Al$_2$O$_3$) and Titanium Diboride (TiB$_2$) nanoparticles on the microstructure and properties of Al-Si9 Cu3 alloys for high pressure die casting applications.

CHAPTER 2: LITERATURE REVIEW

Applications of aluminium metal matrix composites

The metal matrix composites have had a small penetration in general in fields like automotive, due to the high price of those products. The combination of good mechanical properties at high temperatures with a light weight has been employed in a wide range of products of different sectors. They are currently being used in applications such as components for aeronautics, sports, racings, etc.

Light weight automotive components: Engine components (Connecting rods, Cylinder liners, bearing stiffeners, blocks and heads), Transmission parts (Synchronizer rings, valves, covers), Suspension components (Struts, hubs, CVJ), Brake parts (Calliper bodies, brake disk, calliper pistons).

Light weight aerospace components: Aerofoils, leading edges, blades, landing gear parts, brake parts, spacecraft structural parts, mirror parts, satellite parts.

Sports: Golf puts, tennis racquets…

The most employed materials for reinforced metals by number are listed in fig.2.9. [Mor 01], where we can observe how the Al$_2$O$_3$ and TiB$_2$ are one of the most commons:

Fig.2.9.: Materials employed in MMCs by number of companies [Mor 01]

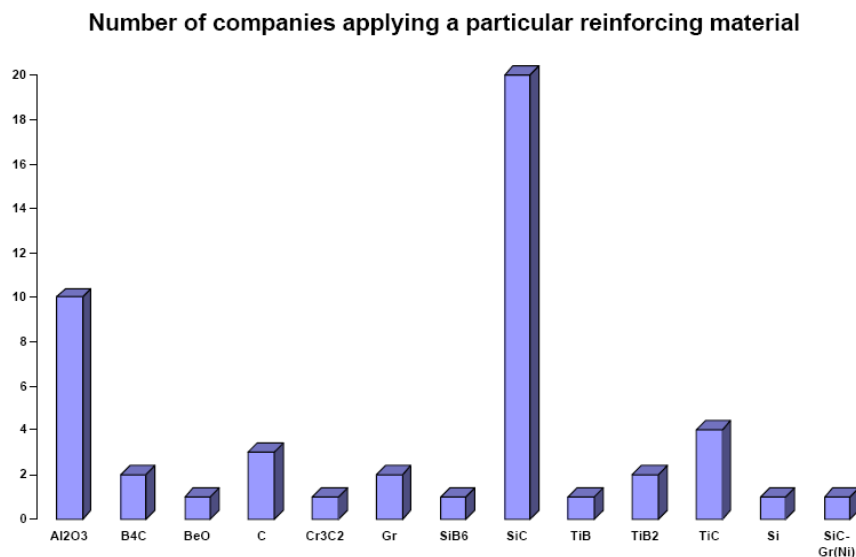There are commercial aluminium alloys as Duralcan^{TM} of Alcan, which can be employed by the HPDC casting process. However, there is no mass application for those materials and the developments have being employed in aeronautics, automotive and sports.

Influence of Alumina (Al$_2$O$_3$) and Titanium Diboride (TiB$_2$) nanoparticles on the microstructure and properties of Al-Si9 Cu3 alloys for high pressure die casting applications.

CHAPTER 2:   LITERATURE REVIEW

They are same problems in order to introduce AMCs in a mass production process. Normally those problems are related with the product price, the necessity of stirring the melt at the holding furnace, the recyclability, the cleanness of the melt, the employment of an inert gas and finally the machinability.

The porosity problems decrease, because ceramic particles tend to get around the porosity, and they decrease their volume. However, the higher viscosity promotes more incomplete filling, cold laps and inclusions. It's expected to employ the developed alloys in new automotive applications, with higher requirements than nowadays products, especially at high service temperatures.

In situ produced Al/TiB$_2$-Al$_2$O$_3$ composites

The TiB$_2$ particles are reported to form from reactive hot pressing of either Al–Ti–B, Al–TiO$_2$–B or Al–TiO$_2$–B$_2$O$_3$ systems. However, Al$_2$O$_3$ particles are also in situ formed simultaneously in such systems. It is difficult to assess independently the reinforcing effect of in situ TiB$_2$ particles. Moreover, intermetallic compound (Al$_3$Ti) with plate-like structure is also induced in the above-mentioned systems. The formation of brittle Al$_3$Ti phase could lead to premature failure of in situ TiB$_2$ +Al$_2$O$_3$/Al composites. To eliminate intermetallic compound, the Al–TiB$_2$ composite can be fabricated via PM process followed by hipping, in which the TiB$_2$ particulates are blended with Al powders. Pure Al is selected as the matrix material instead of the Al-alloy in order to exclude the precipitation hardening effect.

The interfaces of *in-situ* particle/matrix are clean and free of impurities or contaminants. The size of *in-situ* formed ceramic particles is in the order of 0.3 µm. They are thermodynamically stable and compatible with the matrix. *In-situ* particles formed in the aluminium alloys are typically of TiC and TiB$_2$ or combination of both TiC and TiB$_2$ phases. TiB$_2$ particulate is particularly attractive because it exhibits high hardness, superior wear resistance, high melting point, good thermal stability, high stiffness and high strength at elevated temperatures. In contrast to SiC, TiB$_2$ particles do not react with aluminium, thereby avoiding the formation of brittle reaction products at the reaction–matrix interface. Al$_3$Ti block particles with several tens of micrometers in size are formed in the Ti–Al–B system. The yield strength of (TiB$_2$+Al$_2$O$_3$)/Al composites tends to increase with increasing TiB$_2$ content. A strong interfacial bonding exists between the TiB$_2$ reinforcing phase and the matrix, and this contributes to superior creep resistance [Dho 11],[Mit 95],[Tjo 03].

Influence of Alumina (Al_2O_3) and Titanium Diboride (TiB_2) nanoparticles on the microstructure and properties of Al-Si9 Cu3 alloys for high pressure die casting applications.

CHAPTER 2: LITERATURE REVIEW

It is generally known that the particle sizes of the matrix and reinforcing ceramic powders play an important role in the distribution of reinforcing particles in the matrices of PMMCs. Fine reinforcing particles often tend to agglomerate into clusters during PM processing. The degree of homogeneity of the particle dispersion is determined by the relative particle size (RPS) ratio between the matrix and reinforcing particles. Higher RPS ratios (40:1; 25:1; 18:1) favour particle clustering, thereby yielding poor tensile strength and ductility. Lower RPS ratios (e.g. 5:1 and 3:1) promote a more uniform distribution of the reinforcement (SiC) in the 2124 Al matrix, leading to a higher strength in the composites. Increasing the RPS ratio results in a less-uniform reinforcement distribution [Tam 05], which in turn leads to a decrease in the material manufacture and the mechanical properties of Al–6% Cu–0.4% Mn/15% SiCp composites. It is noted that RPS ratio can be varied by changing the particle size of either the reinforcement or the matrix, separately or simultaneously. Young's modulus and ultimate tensile strength of the Al–TiB_2p MMCs tend to increase with increasing TiB_2 volume content at the expense of tensile ductility. Also reduces the coefficient of thermal expansion (CTE) of the Al–TiB_2 composites.

In situ Al/TiB_2 composites can be prepared using powder metallurgical technique and casting process. Exothermic dispersion reactions (XD process) between the elemental powders of composites i.e. Al, Ti and B under either ingot casting or PM route are commonly adopted to prepare in situ Al/TiB_2 composites. Gotman et al. used the SHS technique to fabricate in situ Al/TiB_2 composites. In this process, elemental powders of the composites were compacted and synthesized by utilizing the heat released during the exothermic reactions of their formation. The ignition of compacted powder mixtures by an electric current initiates a combustion wave that propagates through the blend, leaving behind the reaction products. Reactive spontaneous infiltration refers to the process in which in situ TiB_2 particles are formed by simultaneous infiltration of molten aluminium into ceramic fillers (TiN + B) under a protective nitrogen or argon atmosphere.

Other casting approach involves adding mixed Ti and B bearing salts (i.e. K_2TiF_6 and KBF_4) to molten aluminium, being the most employed for the refining master alloy production. The reaction is:
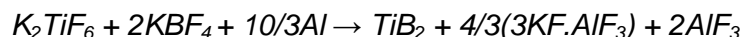
$$K_2TiF_6 + 2KBF_4 + 10/3Al \rightarrow TiB_2 + 4/3(3KF.AlF_3) + 2AlF_3$$

CHAPTER 2:   LITERATURE REVIEW

K_2TiF_6 and KBF_4 react with molten aluminium to produce $TiAl_3$ and AlB_2. After, there is a reaction between them, and Ti and B ions are released and diffused into liquid Al. When they reach saturation, they will be separated out as the intermetallic compounds TiB_2, $TiAl_3$ and AlB_2. A K_3AlF_6 and KF mixture are formed due to excessive KF. Consequently, elements Ti and B from the salts tend to react with Al exothermically, giving rise to the dispersion of TiB_2 particles in the Al matrix. Among these processes, RHP is attractive due to their simplicity and flexibility. RHP encompasses both the exothermic conversion of reactants to in situ reinforcements and the subsequent hot compaction of the porous powder mixture. They have being synthesized in situ TiB_2 particulates from the Al–TiO_2–B and Al–TiO_2–B_2O_3 systems via reactive hot pressing of the elemental powders. For the Al–TiO_2–B system, three types of in situ reinforcements, i.e. Al_2O_3, TiB_2 and Al_3Ti can be created during reactive hot pressing process. The synthesized reactions can be summarized as:

$$3TiO_2 + 13Al \rightarrow 2Al_2O_3 + 3Al_3Ti \text{ (1)}$$

$$3TiO_2 + 6B + 4Al \rightarrow 2Al_2O_3 + 3TiB_2 \text{ (2)}$$
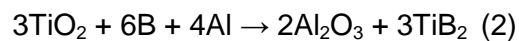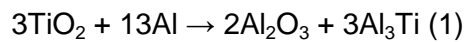
In the absence of boron, only TiO_2 reacts with Al, leading to the formation of Al_2O_3 and Al_3Ti phases (Reaction (1)). Al_3Ti is an intermetallic compound having low density, high melting point, high hardness, and high Young's modulus. Also it's very brittle, due to its tetragonal structure and platelet morphology.

Effort has been expended to eliminate the Al_3Ti compound in the RHP process via the incorporation of B into the TiO_2–Al system (reaction (2)). In this case, in situ TiB_2 and Al_2O_3 particles are created at the expense of Al_3Ti. Thus the amounts of Al_2O_3, TiB_2 and Al_3Ti phases can be controlled by varying the boron content. For the synthesis of in situ Al composites using Al–TiO_2–B_2O_3 system, excess B from B_2O_3 can react with Ti from TiO_2 to produce Al_2O_3 and TiB_2 reinforcement in the Al composite. The following reactions are expected:

$$B_2O_3 + 2Al \rightarrow Al_2O_3 + 2B \text{ (3)}$$

$$3TiO_2 + 4Al \rightarrow 2Al_2O_3 + 3Ti: \text{ (4)}$$

The Ti reduced from the reaction (4) then reacts with B to form TiB_2 or with Al to form Al_3Ti according to reaction:
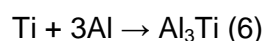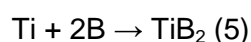
$$Ti + 2B \rightarrow TiB_2 \text{ (5)}$$

$$Ti + 3Al \rightarrow Al_3Ti \text{ (6)}$$

Influence of Alumina (Al_2O_3) and Titanium Diboride (TiB_2) nanoparticles on the microstructure and properties of Al-Si9 Cu3 alloys for high pressure die casting applications.
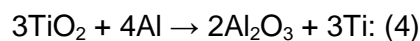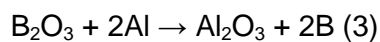
CHAPTER 2:   LITERATURE REVIEW

It is suggested that Ti can also react with Al and B to form titanium aluminium borides $(Ti,Al)_xB_y$ via the following reaction:

$$xTi + xAl + yB \rightarrow (Ti,Al)_xB_y$$

The main disadvantage of in situ composites is that TiB_2 particles are pushed to the grain boundaries and they get agglomerated [Sch 07], having a reduced effect in the nucleating process, to reduce the interfacial energy.

Ex situ produced Al/TiB$_2$ – Al$_2$O$_3$ composites

Generally, the ceramic reinforcements are prepared independently and incorporated into the matrix alloy during conventional liquid casting and PM routes. Such composites fabricated are termed as ex situ composites. The ex situ MMCs fabricated by those methods are still not economically favourable due to the high cost of reinforcing particles. Moreover, ex situ ceramic particulates generally have a size ranging from a few micrometers to several hundred micrometers. Large ceramic particulates often act as micro concentrators of stress and give rise to particle fracture during mechanical loading.

Recently, novel in situ processing such as exothermic dispersion (XD), reactive hot pressing (RHP), self-propagating high temperature synthesis (SHS) and reactive infiltration have attracted considerable attention. In these processes, ceramic reinforcing particles are formed in situ in the matrix melt from the chemical reactions or from the exothermic reactions between the elemental powders of composites under hot pressing conditions. Ultrafine in situ ceramic particulates are thermodynamically stable, free of surface contamination and disperse more uniformly within the matrices of MMCs, leading to stronger particle-matrix bonding. Such unique properties make in situ MMCs possess excellent mechanical properties and economical viability vs. their ex situ counterparts. TiB_2 particulates with the average size of about 1 µm reinforcement phase can be synthesized via self-propagating high-temperature synthesis (SHS) reaction of 50 wt.% Al–Ti–B systems, with the molar ratio of Ti to B= 1:2. Al (99.0 purity, 29 µm), Ti (99.5 purity, 15 µm), and B (98.0 purity, 3 µm) are mixed by ball milling for 8 h and are mechanically pressed into a cylindrical perform. The cylindrical perform with about 70% theoretical density is heated in a closed electronic resistance furnace filled with high purity Ar gas. At about 680–720 ◦C, a SHS reaction of Al–Ti–B system takes place and TiB_2–Al master alloy is then formed. Composite specimens with 7.5 wt.% TiB_2 can be prepared by adding the desired amount of TiB_2–Al master alloy to molten metal and using the semisolid slurry stirring technique. The composite melt is stirred in the semisolid temperature range for 20 min, and the composite slurry is heated to 700 ºC and poured into a steel mould.

Influence of Alumina (Al_2O_3) and Titanium Diboride (TiB_2) nanoparticles on the microstructure and properties of Al-Si9 Cu3 alloys for high pressure die casting applications.

CHAPTER 2:   LITERATURE REVIEW

The cyclic responses of Al-based MMCs reinforced with ex situ ceramic particles are known to be very sensitive to the matrix microstructures or aging heat-treatment. Under aged and naturally aged composites with very fine precipitates display cyclic hardening behaviour fatigued at various applied strain amplitudes, due the interactions among dislocations. Peak aged composites exhibit cyclic hardening cycled at higher applied strain amplitudes, but the hardening is less pronounced when compared with naturally aged MMCs. Composites prepared from the TiO_2–Al–B system exhibit higher yield and tensile strengths than composites fabricated from the Al–TiO_2–B_2O_3 system. This is due to a complete elimination of brittle Al_3Ti phase in the composite 1 by proper adjusting of the molecular ratios of B/TiO_2 to 6/3. The size of in situ TiB_2 particles formed in the matrix of Al-based composites varies from 0.5 to 1.5 µm.

For the first trials, commercial TiB_2 have been chosen, with a measure of about 3 – 6 µm (-325 Mesh). This material should be reduced (by ball milling) to a measure below 0.5 µm. TiB_2 is produced by using a continuous chemical process that controls stoichiometry and particle size to create high purity powder. The shapes of the processed crystals are flat, hexagonal platelets. When solidified into shapes, the resultant ceramic is electrically conductive, a property very rare among ceramic materials. This makes it valuable in electrical applications and also enables it to be formed into complex shapes using electrical discharge machining (EDM).

Applications

• Electrically conductive composites such as aluminium evaporation boats. As an excellent conductor of both electricity and heat, TiB_2 is valuable in electronic and special applications.

• Refractory material and antioxidant additive that is no reactive to most molten non ferrous metals and alloys. Also for thermal management materials, because TiB_2 enhances thermal conductivity when used as filler in polymeric matrices.

• Military armour because it's tough enough, and also improves fracture toughness of ceramic cutting tools and other components.

• Additives for producing special ceramic composite materials. Titanium Diboride will not react with molten non ferrous metals including Cu, Zn and Al. TiB_2 is used as crucibles, vacuum metallization components and electrodes for processing these materials.

Influence of Alumina (Al_2O_3) and Titanium Diboride (TiB_2) nanoparticles on the microstructure and properties of Al-Si9 Cu3 alloys for high pressure die casting applications.

CHAPTER 2:   LITERATURE REVIEW

As we have observed before, the alumina is greatly employed to obtain aluminium metal matrix composites. In Table 2.2. we can see some applications of nanoalumina:

Application	Market segment	Examples
Transparent improvement of scratch resistance in various coating systems	Lacquers & coatings. Cosmetics	Scratch-proof automotive topcoats, parquet lacquers, furniture lacquers, lacquers for electronic devices. Scratch-proof nail polish.
Controlled adjustment of translucence and transparency	Lacquers & coatings. Cosmetics. Plastics	Use as matting agent for lacquers and coatings. Controlled adjustment of translucence in creams. Use as matting agent.
Transparent control of rheological properties in liquids and pastes	Inks & paints. Ceramics	Reduction of structural viscosity in ink jet formulations. Production of ceramic slurries with high solid content.
Transparent improvement of mechanical properties	Dental materials. Plastics. Fibres & textiles	Improvement of the mechanical properties of dental nanocomposites, of plastics in general, of fibres in general and of the converting of master batches filled with particles in fibre spinning plants.

Table 2.2: Applications of nanoalumina [Nan 11], [Buh 11].

In automotive brake discs, drums, callipers or back-plate applications are employed. Partially reinforced piston for use in diesel engines AlSi12CuMgNi (KS 1275; 3.4032) reinforced with Saffil (α-Al_2O_3) short fibre 10, 15 and 20 vol.%. Other suitable applications are found in engine and gearbox parts. Bike and golf components are also developing rapidly. In our case, we'll investigate the reinforcement with nano-particles of AMCs, expecting better isotropic properties with a good particle distribution, due to the nano-particle size of the particles.

2.4.1   Influence of reinforcements in aluminium alloys properties.

The reinforcements in aluminium promote the increase of creep performance, toughness, wear resistance and the thermal distortion, with a combination of good mechanical properties at high temperatures and a light weight. Tensile measurements [Mah 08] show that Young's modulus and ultimate tensile strength tend to increase with increasing reinforcement volume, but with a decrease of tensile ductility. In order to determinate the most important mechanical properties in materials that are working at traction forces, the tensile test are employed. Test bars are tested in equipments where the relation between the stress and the deformation are registered, giving a stress-strain diagram as shows simplified in Fig. 2.10. From this diagram we can determinate the yield stress, the ultimate tensile stress, the elastic modulus and the elongation, that are employed in the design of parts. The yield stress (YS) represents the stress at which plastic deformation becomes noticeable. It's chosen when a 0,2% plastic deformation has taken place. In the yield stress area the material deforms without an increase in applied load. In the stress hardening there is an increase in the material resistance, due to the change in the atomic and crystalline structure.

Influence of Alumina (Al$_2$O$_3$) and Titanium Diboride (TiB$_2$) nanoparticles on the microstructure and properties of Al-Si9 Cu3 alloys for high pressure die casting applications.

CHAPTER 2:   LITERATURE REVIEW

We can observe a decrease in the stress after the ultimate stress point, but is promoted by the decrease in the lateral area of the sample. From the diagram we can obtain also the elastic modulus (E) that is defined as the slope in the linear region and the elongation (ε), which corresponds with the plastic deformation in the broken test bar. UTS gives the stress before necking.
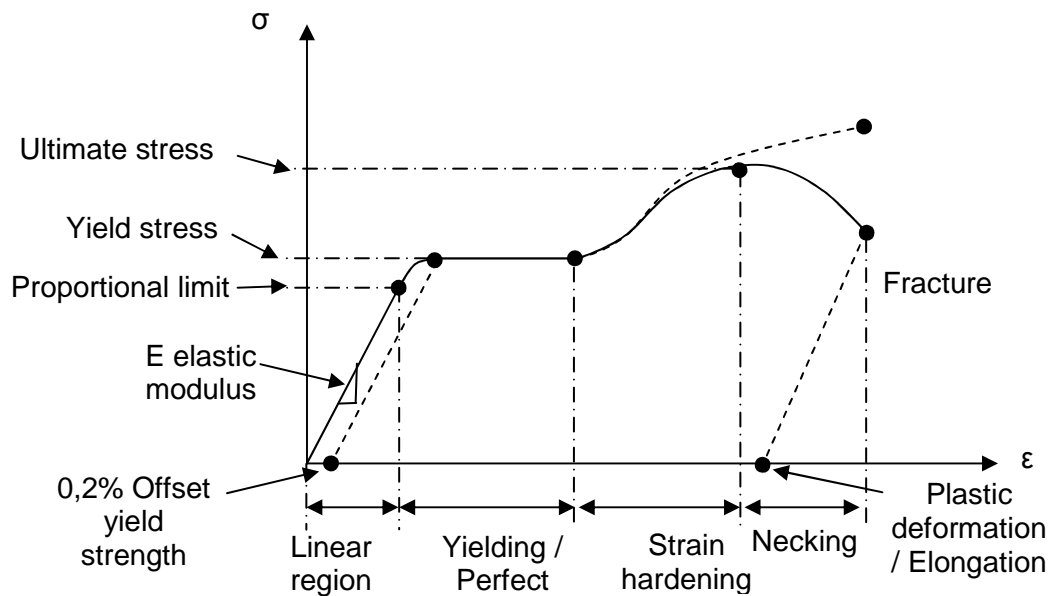
Fig.2.10.: Stress – strain diagram

In order to design a part that must support a charge during use, we must assure that the part doesn't plastically deform. In this case we should select a material with high YS. In the case of ductile material with an important plastic deformation, the UTS is not very important, but it can give us the hardness and the soundness of the part. In our case, both properties and the elongation are important parameters to determinate, due to the behaviour as not very plastic materials of the Al Si9 Cu3 alloys.

In order to determinate the mechanical properties in function of the composition of the alloy, experimental formulas have been [Mac 98], employing an experiment design employing an L16 and a modified L8 Taguchi orthogonal array in the limits of concentration of the allowing elements of Al Si hypoeutectic alloys. We can observe the equations for YS, UTS and Elongation:

Yield Strength:

P1= (9.81 + 0.49 Si + 1.44 Cu + 1.48 Fe +13.07 Mg + 1.01 Mn + 1.45 Ni + 3.84 Cr + 0.34 Zn + 5.81 Ti + 12.72 Sr)x6.89512.

Influence of Alumina (Al_2O_3) and Titanium Diboride (TiB_2) nanoparticles on the microstructure and properties of Al-Si9 Cu3 alloys for high pressure die casting applications.

CHAPTER 2:   LITERATURE REVIEW

Ultimate Tensile Strength:

P2= (44.93 - 0.46 Si + 0.67 Cu - 0.18 Fe + 0.76 Mg - 0.13 Mn + 0.23 Ni + 0.16 Cr + 0.32 Zn + 0.20 Ti + 0.35 Sr)x6.89512.

Elongation:

P3 = (10.62 - 0.61 Si - 0.50 Cu - 0.46 Fe - 0.57 Mg - 0.21 Mn -0.07 Ni + 0.06 Cr + 0.25 Zn +0.08 Ti + 0.07 Sr)x6.89512.

In order to increase alloys properties and specially the YS we should study what are the parameters that can increase the YS. The increase in YS can be attributed to the coupled effects of:

(a) Orowan strengthening;

(b) Grain refinement;

(c) Formation of internal thermal stress due to different CTE values between the matrix and the reinforcement particles;

(d) Effective load transfer between the matrix and the reinforcement;

(e) Hardening due to the strain misfit between the reinforcing particulates and the matrix.

The contributions to the increase in the YS of the composites by the various strengthening mechanisms could be taken as a simple summation of the root of the sum of squares of the different mechanisms, and have been discussed in several recent studies. Owing to the presence of the dispersed nano-size particles in the matrix, dislocation loops form as dislocation lines bow and bypass the particles.

There is a general formula (generalized Hall Pech equation) to calculate the YS, taking into account more variables than the medium diameter of the nucleus, as the microstructures and dislocations. In general it has being assumed that a decrease of nucleus diameter promotes an increase of YS. YS can be calculated with the general formula [Lem 81], [Cly 93], [Han 05], [Arp 03], [Alu 11]:

$$\sigma = \sigma_i + \sigma_s + \sigma_p + \sigma_d + \sigma_{ss} + \sigma_t + \sigma_{hp}$$

Influence of Alumina (Al$_2$O$_3$) and Titanium Diboride (TiB$_2$) nanoparticles on the microstructure and properties of Al-Si9 Cu3 alloys for high pressure die casting applications.

CHAPTER 2:   LITERATURE REVIEW

Where:

$\underline{\sigma_i}$: Stress induced resistance because the friction generated by the opposition to the dislocations movement.

$\underline{\sigma_s}$: Stress induced resistance by the solid solution elements (Function of the concentration of elements and the difference between the atomic radius of solute and solvent).

$\underline{\sigma_p}$: Stress induced resistance by the precipitates (Function of precipitates concentration and the average distance).

$\underline{\sigma_d}$: Stress induced resistance by dislocations (Function of shear modulus, Burgers vector and the dislocation density).

$\underline{\sigma_{ss}}$: Stress induced resistance by the sub-grains or by the sub- structure (Relation very similar to Hall-Petch).

$\underline{\sigma_t}$: Stress induced resistance by the texture or isotropy (Function of preferential crystallographic directions)

$\underline{\sigma_{hp}}$: Stress deduced from Hall-Petch relation for grain size. The refinement in grain size arises as a result of the presence of reinforcing particles which act as nucleation sites during recrystallization, and the pinning of grain boundaries. The contribution to the increase in YS due to grain size strengthening can be described by the Hall–Petch equation [Zha 08]:

$$\sigma_{hp} = K.d^{-\frac{1}{2}}$$

where K is the Hall–Petch coefficient, and d is the grain diameter.

It may be noted that, based on the contributions by the above-mentioned strengthening mechanisms, the YS of the composites should increase with increasing volume fraction of reinforcement. However, when the volume fraction of nano-particulates is increased, the strength and ductility of the composites drops but remains higher than compared pure metal one [Hum 91]. This may be due to the agglomeration of nanoparticulates with increasing volume fraction, which reduces the Orowan strengthening effect. The increment in ductility of the aluminium by reinforcement particulates may be attributed [Mah 08] to a more uniform microstructure where stress concentration is reduced, a uniform distribution of reinforcements and very short distances between nanoparticles that prevent crack growth and their interconnection. Ultra-fine ceramic particles inhibits stress concentration and crack growth. If the SDAS decreases [Gro 09], UTS and elongation are increased.

In our case, we have chosen very low percentages of reinforcement particles in order to avoid the drop in the mechanical properties by increasing the volume fraction.

Influence of Alumina (Al_2O_3) and Titanium Diboride (TiB_2) nanoparticles on the microstructure and properties of Al-Si9 Cu3 alloys for high pressure die casting applications.

CHAPTER 2:   LITERATURE REVIEW

2.4.2 TiB_2 Generalities

Titanium diboride, TiB_2, is a ceramic compound from the combination of titanium and boron, with hexagonal crystal structure and space group P6/mmm. It has a high melting point (around 3225ºC), hardness, strength to density ratio and wear resistance. It can't be found in the nature, and can be prepared by many different methods as direct reaction, carbothermal reduction, SHS reaction…

It is resistant to oxidation at high temperatures and to HF and HCl acids, but not to alkalis, H_2SO_4 and HNO_3. It don't reacts with many melted metallic alloys, so is employed in aluminium melting as thermocouples, cathodes for aluminium smelting, chemical applications and as a reinforcement for composites. It's a ceramic with high thermal and electrical conductivity. It can be shaped to a desired shape with high or low densification porosity, and can be also machined by electrical discharge. In order to produce near dense TiB_2, several methods have been employed, including sintering, hot pressing, hot isostatic pressing, microwave sintering, dynamic compactness, vacuum arc melting, spark plasma sintering and SHS [Mor1].

The production of **<u>in situ Al-TiB₂</u>** metal-matrix composites (MMC) is based on a process in which titanium (K_2TiF_6) and boron (KBF_4) containing salts are reacted with molten aluminium to generate *in-situ* TiB_2 particulates. Cryolite salts react with the molten Al alloy such that the titanium and boron enter the aluminium and combine to form in situ TiB_2 particles of about 1µm size. The remaining cryolite slag is decanted from the furnace and the Al-TiB_2 master alloy is alloyed to its final composition and cast to billet or waffle plate [Mor 01].

Influence of Alumina (Al$_2$O$_3$) and Titanium Diboride (TiB$_2$) nanoparticles on the microstructure and properties of Al-Si9 Cu3 alloys for high pressure die casting applications.

CHAPTER 2: LITERATURE REVIEW

They are also new techniques to prepare *ex-situ* nanocrystalline TiB$_2$, by SHS, mechanical alloying, solvothermal reaction [Gu 02] and solution phase reaction. In the next chapters we will explain a new method developed in the project for the nano TiB$_2$ production. The process has been optimised to achieve a 20 wt.% reinforcement on laboratory scale. Superior material properties are strongly dependent on the homogeneous distribution of fine TiB$_2$ particles in the Al matrix. The average particle size is 1 to 2 µm, giving additional mechanical strength due to dispersion hardening [MMC 01]. In our case, we have employed two different *ex-situ* TiB$_2$ particles, with the same high energy ball milling process, in order to obtain TiB$_2$ nano-particles with an average size of 500 nm. The 2 employed TiB$_2$ particles are:

1) **SHS TiB$_2$ produced at Tecnalia** from Ti and B with a TiB$_2$ grain size from 1 to 6 microns.

2) **Solvothermal processed commercial TiB$_2$** produced by the with a mesh 325 grain size.

Structure

The TiB$_2$ has a prevalent covalently bounded and hexagonal close-packed crystal structure of the AlB$_2$ type, designated C32, with space group P6/mmm. The lattice parameters have slight quadratic dependence, and a = b =302.9, c = 322.9, α = β =90⁰, γ = 120⁰, as we can observe in Fig.2.11. The prevalent covalent bonding determinates the low ductility, high hardness and high melting point.
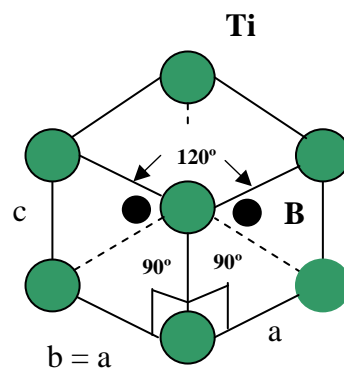
Fig.2.11.: Scheme of the crystal structure of TiB$_2$.

Properties

TiB$_2$ has a high hardness and stiffness, in combination with high electrical and thermal conductivity. The thermal and electrical conductivity is not a normal characteristic of most conventional ceramics. It offers a combination of attractive properties, with high hardness, high strength, high specific modulus, high melting point, excellent wearing and oxidation resistance at high temperatures (Up to 1400 ⁰C).

Influence of Alumina (Al₂O₃) and Titanium Diboride (TiB₂) nanoparticles on the microstructure

and properties of Al-Si9 Cu3 alloys for high pressure die casting applications.

CHAPTER 2:   LITERATURE REVIEW

In the Table 2.3. we can resume the TiB_2 properties for a material with a density of 4.5 $\pm$ 0.1 g/cm^3 and a grain size of 9$\pm$1 µm [Mun 00]. We can observe TiB_2 properties, and specially the maintenance of the elastic modulus and flexural strength at high temperatures, that can provide the increase of mechanical properties at higher temperatures for the elected alloy. We will test how TiB_2 particles modify alloy properties and if we get the expected improvements.

Property	20ºC	500ºC	1000ºC	1200ºC	1500ºC	2000ºC
Bulk modulus (GPa)	240	234	228			
Compressive strength (GPa)	1.8					
Creep rate[c] (10^{-9} s^{-1})					0,005	3,1
Density[d] (g/cm^3)	4.500	4.449	4.389	4.363	4.322	4.248
Elastic modulus (GPa)	565	550	534			
Flexural strength (MPa)	400	429	459	471	489	
Fracture toughness (MPa m$^{1/2}$)	6,2					
Friction coefficient[e]	0.9	0.9	0.6			
Hardness (GPa)[f]	25	11	4.6			
Lattice parameter[d] a /Å	3.029	3.039	3.052	3.057	3.066	3.082
Lattice parameter[d] c /Å	3.229	3.244	3.262	3.269	3.281	3.303
Poisson's ratio	0.108	0.108	0.108			
Shear modulus (GPa)	255	248	241			
Sound Velocity, longitudinal[g] (Km/s)	11.4	11.3	11.2			
Sound velocity, shear[g] (km/s)	7.53	7.47	7.40			
Specific heat (J kg^{-1} K^{-1})	617	1073	1186	1228	1291	1396
Thermal conductivity (W m^{-1} K^{-1})	96	81	78.1	77.8		
Thermal diffusivity (cm^2/s)	0.30	0.17	0.149	0.147		
Thermal expansion[d,h] αa (10^{-6} K^{-1})	6.4	7.0	7.7	7.9	8.3	8.9
Thermal expansion[d,h] αc (10^{-6} K^{-1})	9.2	9.8	10.4	10.6	11.0	11.6
Thermal expansion[h] αm (10^{-6} K^{-1})	7.4	7.9	8.6	8.8	9.2	9.8
Wear coefficient[e] (10^{-3})	1.7					
Weibull modulus	11					

Table 2.3: properties of TiB₂ [Mun 00]

[a] Density 4.32 g/cm^3, grain size 2 µm, V_{slide} /P_{load} = 0.2 ms^{-1} MPa^{-1}

[b] Vickers indentation, load = 5 N

[c] Single crystal, hexagonal unit cell.

[d] Single crystal.

[e] ρ = 4.32 g/cm3, g = 2 µm, vs/Pc = 0.2 m s^{-1} MPa^{-1}.

[f] Vickers hardness, load = 5 N.

[g] vshear = (G/ρ)$^{1/2}$; vlongitudinal = [(4/3) G/ ρ +B/ ρ]$^{1/2}$.

[h] Coefficient of thermal expansion $\alpha_x = (1/x_0)(x-x_0)/(T-T_0)$, x = a or c , cumulative from the reference state at 20 ºC(Corresponding to T_0 = 293 K); $\alpha_m = (2\alpha_a+\alpha_c)/3$.

Influence of Alumina (Al$_2$O$_3$) and Titanium Diboride (TiB$_2$) nanoparticles on the microstructure and properties of Al-Si9 Cu3 alloys for high pressure die casting applications.

CHAPTER 2:   LITERATURE REVIEW

Applications

TiB$_2$ applications have been limited to very specific applications, due to the processing cost of the material and the variability in the material properties. It has been employed in aluminium melting, impact resistant armors, cutting tools, crucibles and resistant coatings.

2.4.3   Alumina (Al$_2$O$_3$). Generalities.

Aluminium oxide is an amphoteric oxide of aluminium with the chemical formula Al$_2$O$_3$. It is also commonly referred to as alumina or aloxite in the mining, ceramic and materials science communities. It is produced by the Bayer process from bauxite. Its most significant use is in the production of aluminium metal, although it is also used as abrasive, due to its hardness, and as a refractory material due to its high melting point.

Corundum is the most common naturally-occurring crystalline form of aluminium oxide. Much less-common rubies and sapphires are gem-quality forms of corundum with their characteristic colours due to trace impurities in the corundum structure. Rubies are given their characteristic deep red colour and their laser qualities by traces of the metallic element chromium. Sapphires are in different colours given by various other impurities, such as iron and titanium.

Properties

Aluminium oxide is an electrical insulator but has a relatively high thermal conductivity (40 W/m K). In its most commonly occurring crystalline form, called corundum or α-aluminium oxide, its hardness makes it suitable for use as an abrasive and as a component in cutting tools. Aluminium oxide is responsible for metallic aluminium's resistance to wearing. Metallic aluminium is very reactive with atmospheric oxygen, and a thin passivation layer of alumina quickly forms on any exposed aluminium surface. This layer protects the metal from further oxidation. The thickness and properties of this oxide layer can be enhanced using a process called anodising. A number of alloys, such as aluminium bronzes, exploit this property by including a proportion of aluminium in the alloy to enhance corrosion resistance. The alumina generated by anodising is typically amorphous, but discharge assisted oxidation processes such as plasma electrolytic oxidation result in a significant proportion of crystalline alumina in the coating, enhancing its hardness. Aluminium oxide was taken off the United States Environmental Protection Agency's chemicals lists in 1988. Aluminium oxide is in the Toxics Release Inventory (TRI) list of the Environmental Protection Agency (EPA) if it is in a fibrous form.

Influence of Alumina (Al$_2$O$_3$) and Titanium Diboride (TiB$_2$) nanoparticles on the microstructure and properties of Al-Si9 Cu3 alloys for high pressure die casting applications.

CHAPTER 2: LITERATURE REVIEW

Aluminium oxide, also known as alumina, is the main component of bauxite, the principal ore of aluminium. The largest manufacturers in the world of alumina are Alcoa, Alcan and Rusal. Companies which are specialized in the production of special aluminium oxides and aluminium hydroxides. The bauxite ore is made up of impure Al$_2$O$_3$, Fe$_2$O$_3$, and SiO$_2$. Bauxite is purified by the Bayer process [Hid 99]:

$$Al_2O_3 + 3\ H_2O + 2\ NaOH \rightarrow 2\ NaAl(OH)_4$$
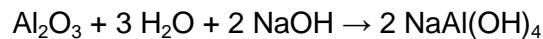
The Fe$_2$O$_3$ does not dissolve in the base. The SiO$_2$ dissolves as silicate Si(OH)$_6^{2-}$. Upon filtering, Fe$_2$O$_3$ is removed. When the Bayer liquor is cooled, Al(OH)$_3$ precipitates, leaving the silicates in solution. The mixture is then calcined (heated strongly) to give aluminium oxide:

$$2\ Al(OH)_3 + Heat \rightarrow Al_2O_3 + 3H_2O$$
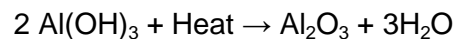
The alumina formed tends to be multi-phase, i.e. constituting several of the alumina phases rather than solely corundum. The production process can therefore be optimized to produce a tailored product. The type of phases present affects, for example, the solubility and pore structure of the alumina product which, in turn, affects the cost of aluminium production and pollution control.

Structure

The crystal system of corundum (α-Alumina) is a trigonal Bravais lattice with a space group R-3c, 2 formula units per unit cell of aluminium oxide, but is most commonly referred to a slightly distorted hexagonal close-packing of oxygen ions, or a larger hexagonal cell with 6 formula units, as we can observe in the Fig.2.12. Alumina has also other phases (γ,δ,ε,η,θ,χ,…), all corresponding to the Al$_2$O$_3$ formula, but the only one that its thermo stable is the α-Alumina. The electro negativity of alumina is 2, with a 63% of ionic character and 37% of covalent.
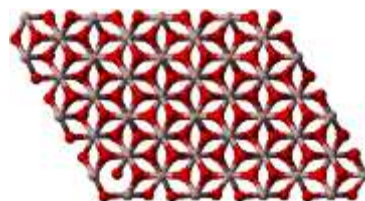

Fig.2.12.: Scheme of the crystal structure of Al$_2$O$_3$ [Wik 11].

Influence of Alumina (Al$_2$O$_3$) and Titanium Diboride (TiB$_2$) nanoparticles on the microstructure and properties of Al-Si9 Cu3 alloys for high pressure die casting applications.

CHAPTER 2: LITERATURE REVIEW

Properties

Alumina has a very interesting combination of mechanical, electrical and chemical properties. Mechanically is very hard, resistant to abrasive wear and dimensional stable. Electrically it has high resistivity, good dielectric strength and low dielectric loss factor at high frequencies. It is inert against from chemicals, maintaining characteristics at high temperature [Jac 77]. The melting temperature is 2030 – 2050 ºC, boiling temperature: 3500 ºC, thermal conductivity "k" is 30.1 W/m.K, the lineal dilatation coefficient is 8.3 - 9 x 10^{-6} ºC, thermal conductivity 10^{-10} – 10^{-12} (Ω.m)$^{-1}$, the tensile strength is 380 GPa, Poison coefficient of 0.26, hardness of 18-23 HV (GPa), ultimate strength of 200 - 345 MPa and a density of 3.97 g/cm^3. In the table 2.4., we can resume the Alumina properties for a high purity (99.5 % or higher) and nearly fully densified (98 % of the theoretical density, or higher) sintered alpha-alumina materials with a nominal grain size of 5 µm. The good properties of the elastic modulus and flexural strength at high temperatures can provide the increase of mechanical properties at higher temperatures for the elected alloy. Because of that we want to explore the potential application of Al$_2$O$_3$ in the reinforced alloys.

Property	20ºC	500ºC	1000ºC	1200ºC	1400ºC	1500ºC
Bulk modulus (GPa)	257	247	237	233	229	227
Compressive strength (GPa)	3.0	1.6	0.7	0.4	0.3	0.28
Creep rate (10^{-9} s^{-1}) at 150 MPa	0	0	4	280	6600	24600
Density (g/cm^3)	3.984	3.943	3.891	3.868	3.845	3.834
Elastic modulus (GPa)	416	390	364	354	343	338
Flexural strength (MPa)	380	375	345	300	210	130
Fracture toughness (Mpa m$^{1/2}$) for crack length of 300 µm	3.5	3.0	2.7	2.6	2.5	2.5
Friction coefficient [] at 2 GPa	0.40	0.8	0.4			
Hardness (GPa) (Vickers, 1 kg) [GPa]	15	8.5	4.6	3.7	2.9	2.5
Lattice parameter a /Å	4.761	4.777	4.797	4.806	4.815	4.820
Lattice parameter c /Å	12.991	13.040	13.102	13.129	13.156	13.169
Poisson's ratio	0.231	0.237	0.244	0.247	0.250	0.252
Shear modulus (GPa)	169	158	146	142	137	135
Sound Velocity, longitudinal (Km/s)	11.00	10.77	10.54	10.44	10.35	10.30
Sound velocity, shear (km/s)	6.51	6.33	6.14	6.06	5.97	5.93
Specific heat (J kg^{-1} K^{-1})	755	1165	1255	1285	1315	1330
Tensile strength (MPa)	267	267	243	140	22	13
Thermal conductivity (W m^{-1} K^{-1})	33	11.4	7.22	6.67	6.34	6.23
Thermal diffusivity (cm^2/s)	0.111	0.0251	0.0150	0.0136	0.0127	0.0124
Thermal expansion from 0ºC αm (10^{-6} K^{-1})	4.6	7.1	8.1	8.3	8.5	8.6
Wear coefficient (10^{-3})	-4	-6				
Weibull Modulus	11	11	11	11	11	11
Weibull modulus	395	390	360	310	210	125

Table 2.4.: properties of AL$_2$O$_3$ [MUN 97] [MMC 01-2].

Influence of Alumina (Al_2O_3) and Titanium Diboride (TiB_2) nanoparticles on the microstructure and properties of Al-Si9 Cu3 alloys for high pressure die casting applications.

CHAPTER 2: LITERATURE REVIEW

Applications

Annual world production in 2005 of alumina is approximately 45 million tones, over 90% of which are used in the manufacture of aluminium metal. The major uses of special aluminium oxides are in refractories, ceramics, polishing and abrasive applications. Large tonnages are also used in the manufacture of zeolites, coating titania pigments, and as fire retardant /smoke suppressants.

Alumina is a medium for chemical chromatography, available in basic (pH 9.5), acidic (pH 4.5 when in water) and neutral formulations. In lighting, GE developed "Lucalox" in 1961, a transparent alumina used in sodium vapor lamps. Aluminium oxide is also used in preparation of coating suspensions in compact fluorescent lamps.

Health and medical applications include it as a material in hip replacements. It is used in water filters (derived water treatment chemicals such as aluminium sulfate, aluminium chlorohydrate and sodium aluminate, are one of the few methods available to filter water-soluble fluorides out of water). It is also used in toothpaste formulations.

Most pre-finished wood flooring now uses aluminium oxide as a hard protective coating. In 2004, 3M developed a technique for making a ceramic composed of aluminium oxide and rare earth elements to produce a strong glass called transparent alumina. Alumina can be grown as a coating on aluminium by anodizing or by plasma electrolytic oxidation (see the "Properties" section, Table 2.3.). Its strength and abrasive characteristics are due to aluminium oxide's great hardness (position 9 on the Mohs scale of mineral hardness).

It is widely used as a coarse or fine abrasive, including as a much less expensive substitute for industrial diamond. Many types of sandpaper use aluminium oxide crystals. In addition, its low heat retention and low specific heat make it widely used in grinding operations, particularly cutoff tools. As the powdery abrasive mineral aloxite, it is a major component, along with silica, of the cue tip "chalk" used in billiards.

Aluminium oxide powder is used in some CD/DVD polishing and scratch-repair kits. Its polishing qualities are also behind its use in toothpaste. Is also widely used in the fabrication of superconducting devices, particularly single electron transistors and superconducting quantum interference devices (SQUID), where it is used to form highly resistive quantum tunneling barriers.

Influence of Alumina (Al$_2$O$_3$) and Titanium Diboride (TiB$_2$) nanoparticles on the microstructure and properties of Al-Si9 Cu3 alloys for high pressure die casting applications.

CHAPTER 2:   LITERATURE REVIEW

2.5 Processing of aluminium matrix reinforced alloys

2.5.1   Introduction.

As we have seen before, there are several ways to produce aluminium reinforced alloys. In our case, we have elected the reinforcement with externally produced particles in the liquid state because is a cheap process that generates the same properties in all the directions. However, in order to get the better properties, a good process must be employed. Ceramic particles must have for our project the smallest possible size, and we have chosen SHS as the process for the production on TiB$_2$ particles because it produces small TiB$_2$ particles about 1-5 microns at a good processing cost. As we decrease particle size, particles tends to agglomerate, promoting a decrease in properties and a more inhomogeneous structure. Also the introduction of ceramic particles in liquid aluminium is very complicated, due to the tendency to get indissolved in the dross. In order to produce parts in an economic and industrial way, HPDC process has been elected. In the next points we'll review all the process aspects that have to be studied in order to get the best properties for an industrial process.

2.5.2   Formation and particle degglomeration

2.5.2.1 In Situ formation of reinforcement particles

In the case of producing TiB$_2$, in order to introduce the borides particles in the melting, the most employed process is by reacting borides particles with the aluminium in the melt, by means of a salt which reacts with aluminium to produce boron, and one or more salts which reacts with aluminium to produce a boride-forming metal or metals. In situ production of the boride particles produces particles with less than 1 micron in size.

2.5.2.2 Ex Situ formation of reinforcement particles

However, AMC have been fabricated by the dispersion of very fine (Less than 0.1 micron) oxide or carbide particles throughout the metal or alloy matrix, by mechanical mixing of metal powders of 5 micron diameter or less with the oxide or carbide powder (Preferably 0.01 micron to 0.1 micron). Presence of oxygen can result in oxide formation at the interface of the ceramic, and the metal desinhibit interfacial binding between the ceramic phase and the matrix, adversely effecting ductility, reducing strength, loss of elongation and crack propagation. It's important that the metal is capable of dissolving or sparingly dissolving the constituents of the ceramic phase, and having a lesser capability for dissolving the ceramic precipitate. Metal matrix component must act as a solvent for the reaction species, but not for ceramic precipitate. In the case of Al$_2$O$_3$ lot of commercial types of nanosized particles are available, because it's one of the most employed nano-particles.

Influence of Alumina (Al$_2$O$_3$) and Titanium Diboride (TiB$_2$) nanoparticles on the microstructure and properties of Al-Si9 Cu3 alloys for high pressure die casting applications.

CHAPTER 2:   LITERATURE REVIEW

For our project, we have elected the composition and size of commercial Al$_2$O$_3$ nano-powders to be introduced in liquid aluminium, avoiding liquid dissolutions that should promote an explosion, and we have developed the reduction of SHS formed TiB$_2$ from the micron size to the nano-size, because no commercial nano-TiB$_2$ was available at the beginning of the project.

2.5.3   Mixture and wetting of particles

2.5.3.1 Solid state mixture of particles

The mixture of aluminium and reinforced particles can be made in the solid or liquid state. In the case of solid state, nanocrystalines powders made by milling process must be consolidated in a bulk form. Powder consolidation lead to significant grain growth, because traditional consolidation involves high temperatures (at least 0.8 T$_m$, with T$_m$ the melting temperature). Nanometric surface modification of the nanometric powders consisting on zincating and further on, electroless plating of copper in nanoparticulate form on nanostructured makes the conventional powder metallurgy consolidation possible at much lower temperatures. This is a result of the Gibbs-Thompson effect under which nanoparticles freely coalesce into agglomerates until the energy of the agglomerates equals the surface energy. An increase in temperature reactive the nanoparticle coalescent mechanism, which finally results in complete compact at lower temperatures. Atomic-scale computer simulations have previously identified a deformation mechanism, which becomes important in nanocrystalline metals with grain sizes below 10–15 nm. Instead of proceeding through dislocation activity in the grains, the deformation occurs by slip events in the grain boundaries, leading to a reverse Hall–Petch effect, i.e. a decrease in hardness with decreasing grain size.

In most coarse-grained metals, severe plastic deformation leads to grain refinement. Indeed, severe plastic deformation is often used to generate nanocrystalline metals with grain sizes down to hundred nanometres. Simulations indicate that those processes are suppressed in sufficiently small grains, and instead the sliding events in the grain boundaries dramatically enhance diffusion processes, and lead to grain coarsening as the deformation proceeds [Sch 04]. Grain boundaries are found to participate directly in the deformation process of nanocrystalline metals, and at sufficiently small grain sizes they appear to be carrying the majority of the deformation.

A systematic variation of the mechanical properties with grain size is seen. The metal becomes harder as the grain size is decreased, but if the grains reached a small enough size, the critical grain size which is typically less than 100 nm (3.9 ×10−6 in), the yield strength would either remain constant or decrease with decreasing grains size [Con 00]. This is called the reverse Hall-Petch effect, since the opposite behaviour is usually seen in metals with larger grain sizes.

Influence of Alumina (Al$_2$O$_3$) and Titanium Diboride (TiB$_2$) nanoparticles on the microstructure and properties of Al-Si9 Cu3 alloys for high pressure die casting applications.

CHAPTER 2:   LITERATURE REVIEW

In coarse-grained metals, the plastic deformation is carried by dislocations, and the grain boundaries act as barriers to the dislocations. Reducing the grain size thus reduces the mobility of the dislocations, and leads to a harder metal. In nanocrystalline metals with sufficiently small grain sizes, the major part of the plastic deformation is carried by the grain boundaries at least according to the computer simulations. It is, therefore, not surprising that decreasing the grain size leads to a softening of the metal, as the volume fraction of the grain boundaries increases.

Based on the simulations, one can therefore predict that there should be an "optimal" grain size, where the hardness of a metal is maximal [Sch 01], as we can observe in fig.2.13. We can note that grain sizes about 20 nm has the highest hardness, with a reduction in hardness in case we reduce more the grain size
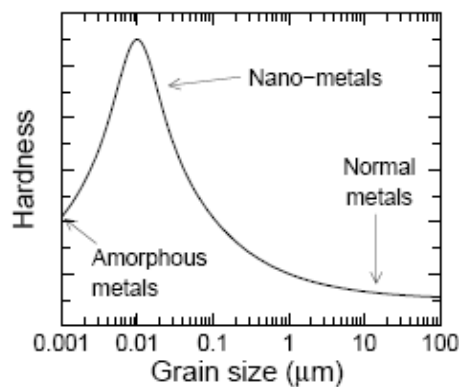
Fig.2.13.: Relation between grain size and hardness [Sch 01]

2.5.3.2 Liquid state mixture of particles

The liquid mixture is made as its name indicates the mixing of ceramic particles in the aluminium matrix by different methods. One of the ways of dispersing the materials in the liquid aluminium is to wrap them into an aluminium film. After pouring the metal over the film, powders are reduced and correctly dispersed in the aluminium matrix [Miy 73]. The particles that are hard, insoluble and with pin shape are not adequate to be dispersed in the liquid aluminium, due to their tendency to create defects as pin holes and tears [Sig 86]. It's beneficial to introduce the powder over an extended period of time, wrapped in a foil of aluminium [Ban 88].

The reasonably uniform distribution of reinforcement particulates can be attributed to suitable blending parameters and the high extrusion ratio used in secondary processing. In theory, homogeneous distribution of reinforcements can be obtained, irrespective of the size difference between the matrix powder and the reinforcement particulates, provided a large deformation load is applied during secondary processing.

Influence of Alumina (Al$_2$O$_3$) and Titanium Diboride (TiB$_2$) nanoparticles on the microstructure and properties of Al-Si9 Cu3 alloys for high pressure die casting applications.

CHAPTER 2:   LITERATURE REVIEW

However, a limited amount of clustering of reinforcement is unavoidable in this case, owing to the high surface energy associated with the nanoparticles. Minimal standard deviation in density measurement results also reflects the uniform distribution of reinforcement in the synthesized materials. Marginal grain refinement in composite samples as a result of the presence of particulates can be attributed to:

(a) The ability of nano-size particulates to nucleate grains during recrystallization;

(b) The restricted growth of grains due to grain boundary pinning. There is also an ideal percentage of nano-reinforce.

Results are better for nano than micro reinforcing particles. Nanoclusters are formed in the initial stage of the phase decomposition and play very important roles in producing nanoprecipitates. Micro alloying elements are also expected to modify the nanostructures of aluminium alloys. Nanoclusters act as useful nucleation sites for precipitates inside the grain and near the grain boundaries [Sat 06].

TiB$_2$ and Al$_2$O$_3$ crystals are insoluble in aluminium. Rapid cooling must be got for avoiding crystal to increase its size. If TiB$_2$ crystal have a measure < of 1 μm, it don't increase their size, maintaining their dimensions at high temperatures in long periods of time [All 74]. If matrix grains are smaller than 30 μm, TiB$_2$ crystals are very well dispersed, due to the abundance of grain borders and also by the dispersion of same TIB$_2$ particles inside the grains.

In our case we have elected the stirring method. Aluminium and reinforcement particles are ball milled and cold pressed. In order to get a better distribution of nanoparticles in the liquid aluminium a vigorous stirring process is employed.

Al$_2$O$_3$ crystals are excellent insulators. They have large band gap energies (Eg), i.e., Eg(Al$_2$O$_3$) =8,8 eV. Electrons in these oxides are strongly localized and the production and diffusion of ionic defects in the oxides are limited. Therefore, long-range charge transfer and ion transport do not occur in those oxides at relatively low temperature (e.g., <1.000 °C). Metal interactions with these insulating oxides are often confined to the interfaces, which only involve oxide surface atoms and metal atoms in contact with the substrate surface. The interactions are strongly dependent on the surface properties of oxide substrates. Surface stoichiometry, surface finishing, and surface defects are the most important factors influencing the metal–oxide interactions.

Influence of Alumina (Al$_2$O$_3$) and Titanium Diboride (TiB$_2$) nanoparticles on the microstructure and properties of Al-Si9 Cu3 alloys for high pressure die casting applications.

CHAPTER 2:   LITERATURE REVIEW

Among the various polymorphs of alumina, corundum, α-Al$_2$O$_3$, is the most stable phase and has been subjected to extensive studies. In particular, the crystallographically simple and energetically stable α-Al$_2$O$_3$(0001) surface offers a good playground for understanding of insulating oxide surfaces and metal–Al$_2$O$_3$ interactions. Alumina surfaces are often prepared by mechanical polishing, ion sputtering, and annealing. Naturally, different surface preparation processes result in various surface properties, which, in turn, may cause different behaviours of metal growth on these surfaces. The most stable structure of Al/Al$_2$O$_3$ interfaces is reached for metals on the oxygen terminated surface as long as the oxygen chemical potential is above a critical value. Many theoretical results show that hydroxylation of the clean α-Al$_2$O$_3$(0001) surfaces may result in a further lowering of the energy of those surfaces. The above mentioned O$^-$ and Al terminated surfaces are expected to be reactive to water.

The theoretical results of metal interactions on alumina surfaces rely on the choice of the surface termination (Al-terminated or O-terminated), calculation models (cluster or slab) and metal coverage (isolated atom or metal film). The bonding between the metals with small Pauling electro negativity and Al$_2$O$_3$ is mainly ionic. Abs initio calculations of bonding at Al(111)/α-Al$_2$O$_3$(0001) interface also indicate that Al–O bonds constitute the primary interfacial interaction. The bonds are very similar to the cation–anion bonds found in Al$_2$O$_3$ bulk and are mainly ionic. Various surface science studies have confirmed that oxidation reactions can happen between metals and α-Al$_2$O$_3$(0001) surfaces near room temperature. In the oxidation, reactions are strictly limited to the interfaces. Subsequently, metallic over layers will develop with metal coverage above 1 monolayer. The results clearly show that all of the interfaces are atomically sharp and no interface reaction phases thicker than a monolayer have been observed.

The results indicate that only those metal and atoms right at the interface, which are in contact with surface oxygen, became oxidized. Alumina has a high thermodynamic stability (ΔH^{o}f ~ –600 kJ mol^{-1}) and oxygen diffusion in the crystal is highly limited. The oxidation of metal multilayer may be either thermodynamically impossible or/and kinetically limited [Fu 07].

Aluminium oxide nanoparticles have important applications in ceramic industry and can be used as an abrasive material, in heterogeneous catalysis, as an absorbent, a biomaterial and as reinforcements of metal–matrix composites (MMCs). In order to be used for effective discontinuous reinforcements in a continuous metal–matrix, Al$_2$O$_3$ particles have to fulfil certain structural and morphological requirements: small particle size and narrow size distribution, large surface area, spherical morphology and the absence of agglomerates. As far as the hot wall aerosol synthesis method (Spray Pyrolysis), as basic chemical route for obtaining advanced materials, is concerned, it offers several advantages in the preparation of well-defined oxide powders over conventional synthesis [Mar 08].

Influence of Alumina (Al$_2$O$_3$) and Titanium Diboride (TiB$_2$) nanoparticles on the microstructure and properties of Al-Si9 Cu3 alloys for high pressure die casting applications.

CHAPTER 2:   LITERATURE REVIEW

Reducing the sizes of low dimensional materials leads to dramatic increase in the portion of surface/interface atoms. The properties of a solid are essentially controlled by related surface/interface energies. Although such changes are believed to dominate behaviours of nanoscale structures, little experience or intuition for the expected phenomena, especially for the size-dependence of the energies and their practical implications, are modelled analytically. The classic thermodynamics as a powerful traditional theoretical tool is used to model different bulk interface energies and the corresponding size dependences. During the modelling, an emphasis on size dependences of the interface energies is given, which is induced by size dependence of coherent energy of atoms within nanocrystals. It is found that solid–vapour interface energy, liquid–vapour interface energy, solid–liquid interface energy, and solid–solid interface energy of nanoparticles and thin films fall as their diameters or thickness decrease to several nanometres while the solid–vapour interface energy ratio between different facets is size-independent and equals to the corresponding bulk value. Predictions of the established analytic models without any free parameters, such as size and temperature, dependences of these four kinds of interface energies and related surface stress, correspond to experimental or other theoretical results. The established models are suitable for low dimensional materials with different dimensions and different chemical bond natures. Moreover, several related applications in the fields of nanophase transitions, nanocrystal growth, and self-diffusion of liquids are known [Jia 08].

In our case, the election of Al$_2$O$_3$ has been done in order to have as we have note before a small particle size and narrow size distribution, large surface area, spherical morphology and the absence of agglomerates in order to have an effective reinforcement. All these aspects are cover with the 15 nm γ Al$_2$O$_3$ and 40 nm α Al$_2$O$_3$, because they have a spherical morphology and a very narrow size distribution. In the case of TiB$_2$, we have not so rounded particles, with 3 different dispersion curves, but the most important distribution if about 500 nm. However, the particle size is smaller, due to the differences in size measure due to agglomeration.

Influence of Alumina (Al$_2$O$_3$) and Titanium Diboride (TiB$_2$) nanoparticles on the microstructure and properties of Al-Si9 Cu3 alloys for high pressure die casting applications.

CHAPTER 3:   EXPERIMENTAL PROCEDURE

CHAPTER 3: EXPERIMENTAL PROCEDURE

Influence of Alumina (Al$_2$O$_3$) and Titanium Diboride (TiB$_2$) nanoparticles on the microstructure and properties of Al-Si9 Cu3 alloys for high pressure die casting applications.

CHAPTER 3:   EXPERIMENTAL PROCEDURE

3.1 Introduction

High pressure die casting (HPDC) is a foundry process that belongs to the family of metallic die casting technologies, in which a metallic die (Normally H11 or H13 steel) are used to produce complex parts. The metal is feeded inside the cavity, and during the solidification, a pressure is applied in order to decrease the porosity, to feed all the part and to decrease the lineal contraction (From 1.5% to 0.7%). Dies are submitted to thermal cycles, due to the heat transferred from injected metal to the die. In order to avoid the metal to get stuck in the die, lubricants and cooling lines are employed, and finally thermo-regulating the temperature of the die. The HPDC has been selected to carry out the study of the influence of TiB$_2$ or Al$_2$O$_3$ reinforced metals as it's a very attractive way of mass production of MMC components. On the one hand, it's possible to cast near shape components that reduce machining operations (Very important to avoid the wear of toolings when they work with ceramic reinforcements). On the other hand, it's also a very suitable foundry technology to produce high quality automated mass productions with a very quick and inexpensive process. The final cost may be compensated by the production of big series (Due to the very expensive dies employed in the process) and by replacing materials more expensive or with higher density.

The industrialization of MMC by HPDC has in the other hand the problem of getting a good distribution and wettability of reinforcement particles. Same intents to get MMC´s by HPDC infiltration of performs are being investigated, but some problems as the good infiltration and the fixation of performs to die must be overcome [Kau 07]. The number of publications dealing with MMCs processed through HPDC is low, in comparison with semisolid or molten metal injected by HPDC. The literature is based in Die casting of MMC by the liquid metallurgy and by mechanical alloying and sintering.

3.2 Selection and acquisition of materials

3.2.1   Introduction. Selection of materials

The reinforced materials employed for this work are not all commercially available and are produced at lab scale for research related projects or industrial casting trials. They are based on the Al Si9 Cu3 Fe1 aluminium alloys to which up to 1 wt. % TiB$_2$ or Al$_2$O$_3$ nanoparticles were incorporated to improve their performance. The Al Si9 Cu3 Fe1 is a hypoeutectic aluminium-silicon alloy. The castability of the alloy for die casting is quite good, but alloys with increased Si have more fluidity.

Influence of Alumina (Al$_2$O$_3$) and Titanium Diboride (TiB$_2$) nanoparticles on the microstructure and properties of Al-Si9 Cu3 alloys for high pressure die casting applications.

CHAPTER 3:   EXPERIMENTAL PROCEDURE

In order to have a common nomenclature in the next sections, we define the different reinforced alloys as:

1) 0.2 wt.% SHS TiB$_2$ reinforced alloy. 500 nm of average size.

2) 0.2 wt.% Commercial TiB$_2$ reinforced alloy. 500 nm of average size.

3) 0.17 wt.% α alumina reinforced alloy. 40 nm of average size.

4) 0.1 wt.% γ Alumina reinforced alloy. 15 nm of average size.

3.2.1.1 TiB$_2$

TiB$_2$ particles are commercially available and have been produced by the Momentive performance materials company, by using a continuous chemical process that controls the stoichiometry and particle size to create high purity powders. The product is named HCT-F. The shapes of the processed crystals are flat, hexagonal platelets. They have a size in the range of 3-6 μm (Mesh -325). The surface area is 1.0 (m^2/g). Also SHS produced TiB$_2$ has been produced at Tecnalia, with a TiB$_2$ grain smaller than 5 μm. As the minimum particle size is of 0.5 μm, and the desired shape is not the platelets, a dry ball milling process with stainless steel balls and a wet high energy ball milling has being made in order to decrease to a nanometric size and to round the TiB$_2$ particles, with SHS and commercial TiB$_2$ particles. There was not any nano TiB$_2$ commercially available at the beginning of this work.

Selection of materials and processing method for SHS TiB$_2$

The employed equipment for SHS reaction is composed by a mixer, a briquetting tool, an SHS reactor and generator, and a ball milling device, as we can observe in Fig. 3.1. We can see the process: 1) Aluminium and TiB$_2$ particles are mixed in a mixer machine, 2) they are cold pressed, obtaining a briquette that is placed in reaction base, 3) Vacuum is made in the reactor, 4) the electric generator gives the necessary electrical discharge for start the SHS reaction, 5) a master alloy is obtained and 6) finally is milled to reduce its size.

Influence of Alumina (Al$_2$O$_3$) and Titanium Diboride (TiB$_2$) nanoparticles on the microstructure and properties of Al-Si9 Cu3 alloys for high pressure die casting applications.

CHAPTER 3:   EXPERIMENTAL PROCEDURE

Mixer	Cold Press
Briquette	**SHS Preparation**
Reactor	**Generator**
Master Alloy	**Ball Milling**

Table 3.1: SHS process.

Influence of Alumina (Al_2O_3) and Titanium Diboride (TiB_2) nanoparticles on the microstructure and properties of Al-Si9 Cu3 alloys for high pressure die casting applications.

CHAPTER 3:   EXPERIMENTAL PROCEDURE

We can observe in Fig. 3.2. how the SHS reaction provides the formation of an Aluminium matrix with TiB_2 particles and porosity from the cold press Ti, Al and B particles. The reaction is self propagated in along the master alloy. In our case, it doesn't matters porosity inside the matrix, because we use the obtained product to produce ceramic particles by ball milling.
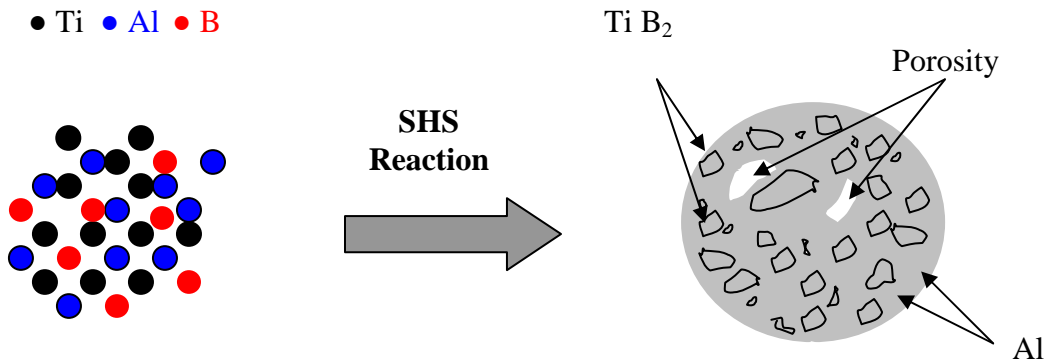

Figure 3.2.- Schematic SHS Reaction with initial reactive powders and obtained phase products

Several trials have been developed in order to obtain the master alloy with good characteristics but at a better price. 1) Commercial Titanium with a size up to 1 mm and 96.06% commercial Boron with and average particle size of 0.6 µm has been tried in order to decrease the raw material price; 2) Reaction without reactor in air or with argon supply in order to eliminate the reactor and high vacuum process; 3) The introduction of Na Cl/ K Cl to improve homogeneous dissolution and the introduction of KBF4 and Na2B4O7 as an economical boron source. The main reactions involved in the SHS process are[Nik 00],[Li 03]:

$$3\ Al + Ti \rightarrow Al_3Ti$$

$$Ti + B \rightarrow TiB_2$$

Or:

$$3\ Al + 2Ti + 2B \rightarrow Al_3Ti + TiB_2$$
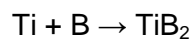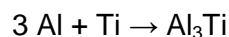
In the Table 3.1. we can observe how there is a maximum limit about the 30 wt.% of aluminium to react, how it's possible to make the reaction without reactor and in Table 3.2. what are the products obtained by the reactions. In order to characterize the raw materials and the obtained products we have employed different equipments. First we have study the raw particles and reactions with the EDS and SEM. In order to determinate the composition and structures we have employ the XRD, obtaining the product composition.

CHAPTER 3: EXPERIMENTAL PROCEDURE

Reference	Composition (%Wt)							d (mm)	P (ton)	Gas P (bar)	Result	Milling
	Ti	B	Al	Mo	NaCl/KCl	KBF$_4$	Na$_2$B$_4$O$_7$					
Ti B with reactor	69	31						25	10	2	Reaction	8h
Ti fine B 30% Al without reactor	48,2	21,8	30								Reaction	
Ti gross B 30% Al without reactor	48,2	21,8	30								Reaction	
Ti B fine without reactor	69	31									Reaction	
Ti B fine without reactor with Argon	69	31									Reaction	
Ti B gross without reactor	69	31									Reaction	
Ti B fine Al 50% without reactor	34,5	15,5	50					25	10	2	No reaction	
TiB-1 with gross Ti	48,2	21,8	30					25	10	2	Reaction	8 h
TiB-2 with gross Ti	44,8	20,3	27,9	7				25	10	2	Reaction	8 h
TiB-3 with gross Ti	47,7	21,6	29,7		1			25	10	2	Reaction	8 h
TiB-4 Ti fine	47,7	21,6	29,7		1			25	10	2	Reaction	8 h
TiB-5 Ti fine	18,2	4,1	30			47,7		25	10	2	Reaction forming white crystals	
TiB-6 Ti fine	34,5	15,5	50					25	10	2	Reaction	
TiB-7 Ti fine	20,7	9,3	70					25	10	2	No reaction	
TiB-8 Ti fine	22,4	5	30				42,6	25	10	2	No reaction	
TiB-9 Ti fine	28,5	6,4	38,1				27	25	10	2	No reaction	

Table 3.1.: SHS processed materials and reaction results.

CHAPTER 3: EXPERIMENTAL PROCEDURE

Material composition	Results
Al 30% wt. with fine Ti + boron without reactor	We can observe the formation of Al_2TiO_5, Gibbsite Al_2O_3. $3H_2O$, Ti_5O_5 and TiB_2, but lot of the Titanium combines with the Oxygen. Aluminium is dispersed in the matrix.
Al 30% wt. with gross Ti + boron without reactor	We can observe Rutile (Ti $_{0.992O2}$, Al_2TiO_5) and TiB_2. There is not a pure aluminium matrix.
Ti fine + B without reactor	A ceramic matrix of TiB_2 and TiB is formed, with particles size of about 5 microns.
Ti fine + Boron with argon and without reactor	A TiB_2 matrix is observed, with same Rutile TiO_2 and TiB. Particle size is quite inhomogeneous, but with a media of 10 microns approximately.
Ti gross + Boron without reactor	A TiB_2 matrix can be observed, and also free boron and rutile (TiO_2). Particle size is about 10 microns.
Ti + B +KBF_4	In the XRD, $KAlF_4$ is analyzed and apart also Aluminium and TiB_2. Not TiB or KBF_4 are observed. The structure is the fused matrix. When the salt melts, it covers everything, also formed TiB_2 particles, with a particle measure less than 5 microns. The main size of particles is smaller than 1 micron, with agglomerations.
Al 30% wt. +Ti + B +Mo 7%	We can observe by XRD TiB_2, Aluminium, metallic Mo, Al_3Ti and Al_6MoTi phases. Some aluminium particles covers with fine ceramic particles are also observed. The ceramic particles have a measure minor than 5 microns.
Al 30% wt. +Ti + B	Particle size smaller than 2 microns. It contains TiB_2, Al and Al_3Ti. Quite big aluminium particles covered with ceramics are observed.
Al 30% wt. +Ti fine+ B + Na Cl / K Cl 1%	We can observe that we obtain Ti B_2, Al, and Al_3Ti covered aluminium with particles size smaller than 5 microns of TiB_2, and same areas with fused salts. Not salt compounds are detected in the RX diffraction analysis.
Al 50% wt. +Ti+ B	Aluminium and TiB_2 are observed. No Al_3Ti is detected. Aluminium matrix with TiB_2 particles size smaller than 0,5 microns. Some plate like structures are detected, probably deformed aluminium.

Table 3.2: SHS Results of TiB_2 reinforcement reactions.

We can resume that TiB_2 and master alloys can be produced from gross industrial materials, and for some applications, no reactor is necessary. Some Ti oxides are formed when the reaction is made out of the reactor, but those particles in reaction with molten aluminium they can act also as reinforcements. The quantity of oxides is relatively low and is concentrated in the external surface of samples. Near all the Ti and B reacts to produce TiB_2, and in the cases where there are supplementary Ti, this Ti reacts with aluminium to give $TiAl_3$, with not free boron detected.

Influence of Alumina (Al$_2$O$_3$) and Titanium Diboride (TiB$_2$) nanoparticles on the microstructure and properties of Al-Si9 Cu3 alloys for high pressure die casting applications.

CHAPTER 3:   EXPERIMENTAL PROCEDURE

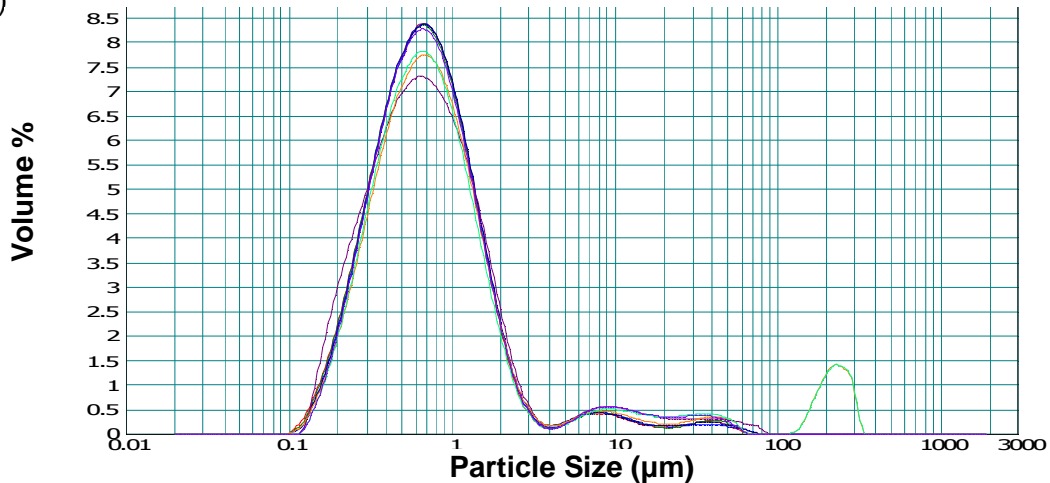## Industrial (Gross) Ti + B with reactor:

When we made the SHS reaction under vacuum with commercial Ti and B, we can observe in our experiment that only TiB$_2$ has formed, with a grain size smaller than 10 microns, and an average size of about 5 microns. In comparison with SHS reaction with fine Ti and B, created particles are bigger, because with fine particles TiB$_2$ grains produce smaller TiB$_2$ grains of about 1-2 microns. We can observe that particles are brittle, with sharp edges with porosity in the created structure. Also very fine particles, in the nanoscale around the formed particles are observed. In Fig. 3.3 we can observe how the broken area shows a brittle fracture in two different areas.
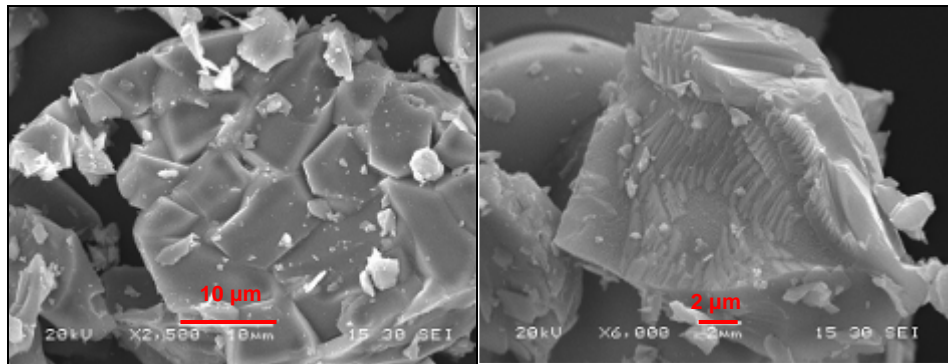
Figures 3.3: SEM images of TiB$_2$ obtained by SHS with reactor.

SHS Ti B$_2$ wet high energy ball milling

After the SHS process, ceramic SHS performs must be broken, which will induce particle size decrease. As the ceramic particles are reduced, particles have a rounder shape, increasing the possibilities to increase wettability and properties of the reinforced alloy. After 6 hours of high energy ball milling, TiB$_2$ particles are smaller, with an average size about 500 microns, but with lot of particles under 400 microns (Fig. 3.4)

Figures 3.4: Particle size distribution of TiB$_2$ obtained by SHS with reactor.

Influence of Alumina (Al$_2$O$_3$) and Titanium Diboride (TiB$_2$) nanoparticles on the microstructure and properties of Al-Si9 Cu3 alloys for high pressure die casting applications.

CHAPTER 3:   EXPERIMENTAL PROCEDURE

Lot of particles are formed by agglomeration of lot of particles, having a structure similar to black berry structures. As we can see in the size determination there are same particles that still remains with a size of about 8 µm, but it volume percentage is very small (<0.5%), as we can see in Fig. 3.4. In Fig. 3.5. we can observe how very fine particles cover the biggest particles.
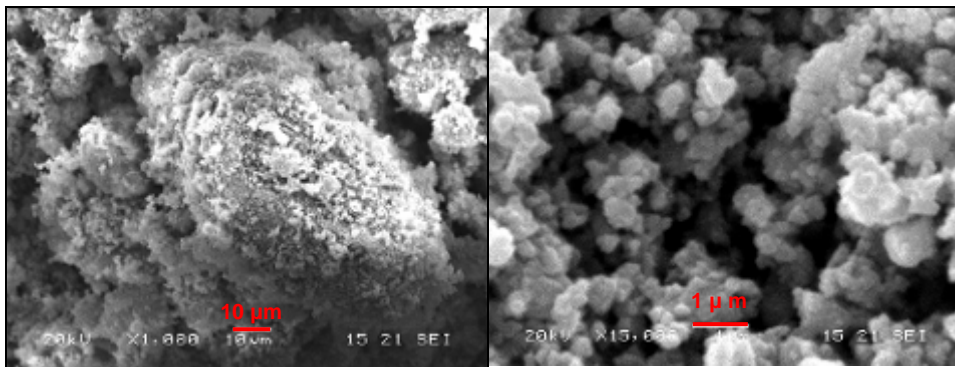
Figures 3.5: SEM images of SHS milled materials.

Very similar results are got with commercial TiB$_2$ after 6 hours of wet high energy ball milling in comparison with the SHS produced particles, as we can observe in Figures 3.6. We can notice how again particles are much rounded, because of milling, and are also agglomerates.
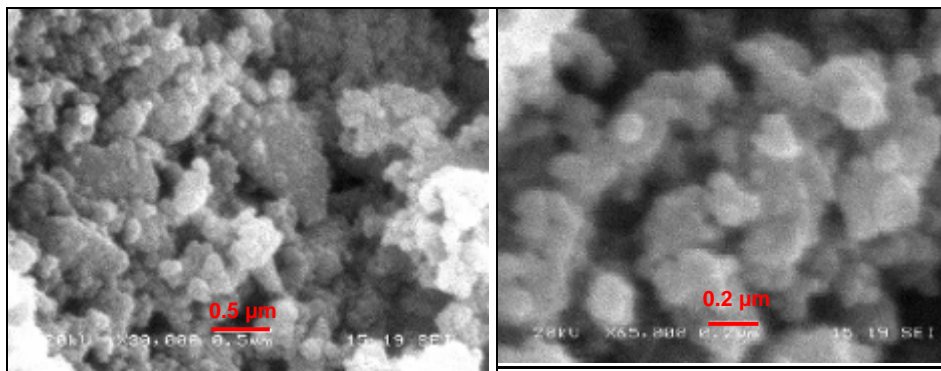
Figures 3.6.: SEM images of commercial milled materials.

<u>Nanosize Ti B$_2$ milled with aluminium with steel balls and container:</u>

In order to have a better dissolution and distribution of TiB$_2$ particles in the molten aluminium, the ceramic particles were milled with pure aluminium with steel bars in a steel container connected to land. That process was made with the idea of breaking the agglomerates and distributing them over the aluminium surface homogeneously. We can observe in Figures 3.7. how aluminium particles get covered with TiB$_2$ uniformly, with incrusted TiB$_2$ particles in the aluminium grains. Aluminium particles got a rounded shape, due to the plastic deformations in the ball milling process.

Influence of Alumina (Al$_2$O$_3$) and Titanium Diboride (TiB$_2$) nanoparticles on the microstructure and properties of Al-Si9 Cu3 alloys for high pressure die casting applications.

CHAPTER 3:   EXPERIMENTAL PROCEDURE
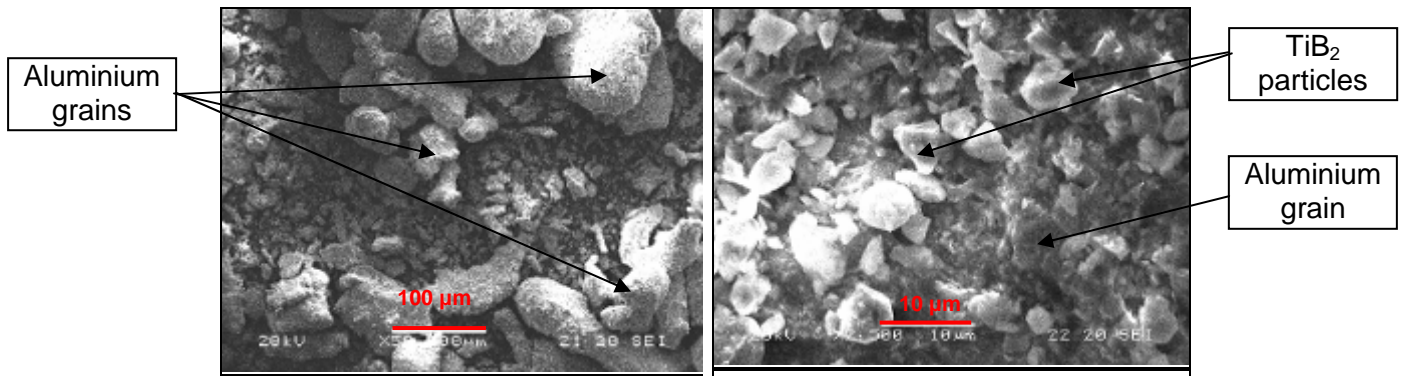
Figures 3.7.: SEM images of Nano commercial TiB$_2$ milled with aluminium.

3.2.1.2 Al$_2$O$_3$

Knano (Divn. Of K Impex – Canada) nano-Al$_2$O$_3$ are commercially available, with the reference MKN-Al2O3-AO40 for α- Al$_2$O$_3$ 99.5% pure, with and APS: 40nm and MKN-AL2O-Go15 reference is γ-Al2O3 99.5% pure, with an APS: 15 nm. Pure α and γ-Alumina with a size of 40 nm and 15 nm has been chosen because they cover the most used nanoparticles and the average size is near the ideal for getting the best performance. α alumina is a stable phase and γ-Alumina is metastable, but it's the most stable between the different alumina phases. It's not expected any change of phase of γ-Alumina. Difference in behavior can be observed between α and γ nanostructures.

3.2.1.3 Al Si9 Cu3 Fe1

The Al Si9 Cu3 Fe1 alloy is the most popular aluminium alloys in HPDC (70%), because of the excellent combination of properties that it presents. It is also known as A380 or EN AC-46.000. Its castability is very good thanks mainly to its silicon content and its small solidification interval. It is heat treatable, even though it ´s normally used in the as cast condition. It is one of the casting aluminium alloys for which more experimental data is known and it is extensively used in the HPDC foundries. The table 3.1. shows the composition range for this alloy, and the figure 3.3. the phase diagram [Zol 07]:

Element	Si	Cu	Fe	Mn	Mg	Zn	Ti	Al
wt. %	8 – 11	2 – 3.5	Max. 1.2	0.1–0.5	0.1-0.5	Max. 1.2	Max. 0.15	Balance

Table 3.3.: Typical composition ranges of the Al-Si9Cu3 alloy [Din 10].

Influence of Alumina (Al$_2$O$_3$) and Titanium Diboride (TiB$_2$) nanoparticles on the microstructure and properties of Al-Si9 Cu3 alloys for high pressure die casting applications.

CHAPTER 3:   EXPERIMENTAL PROCEDURE

The Al-Si phase diagram presents several specific features, as we can see in Fig. 3.8. The eutectics formed by Si and α- aluminium are one of the main distinct aspects. The eutectic composition is around 12.6% of Si and its formation takes place at 577°C. Furthermore the presence of silicon particles has a great influence on the properties and behaviour of the material as it controls the fluidity of the alloys as well as their mechanical properties.
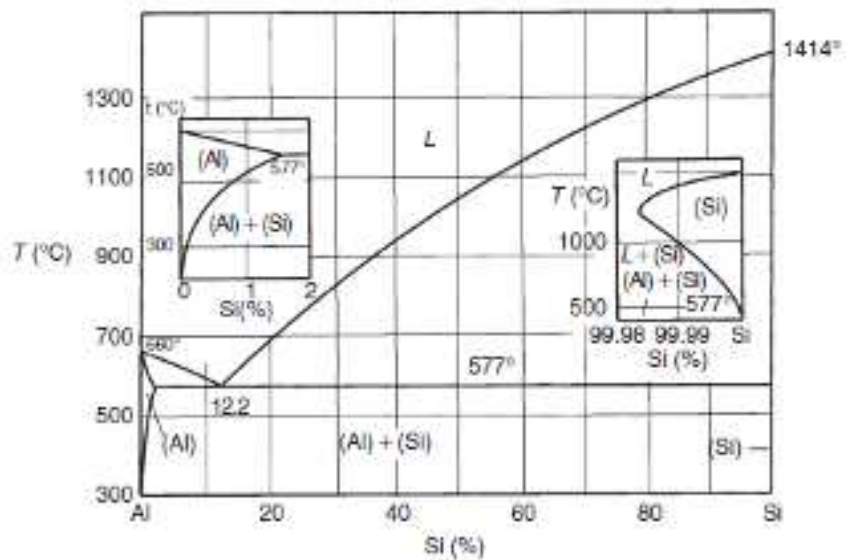
Fig. 3.8: Al-Si phase diagram [Zol 07]

The solidification and microstructure of the Al Si alloys have been deeply studied. The microstructure is characterized by α-aluminium solid solution dendrites and the needle shaped eutectic network formed by α-Al-Si. There are, depending on the alloy, also black dispersed Mg$_2$Si phases as well as α (AlFeMnSi) phases. Other shapes that can also appear are the β-Al$_5$FeSi dark needles and AlFeMnSi more light Chinese / skeleton type structures, as we can observe in Fig. 3.9.

Fig. 3.9: Fe phases determination

Influence of Alumina (Al$_2$O$_3$) and Titanium Diboride (TiB$_2$) nanoparticles on the microstructure and properties of Al-Si9 Cu3 alloys for high pressure die casting applications.

CHAPTER 3:   EXPERIMENTAL PROCEDURE

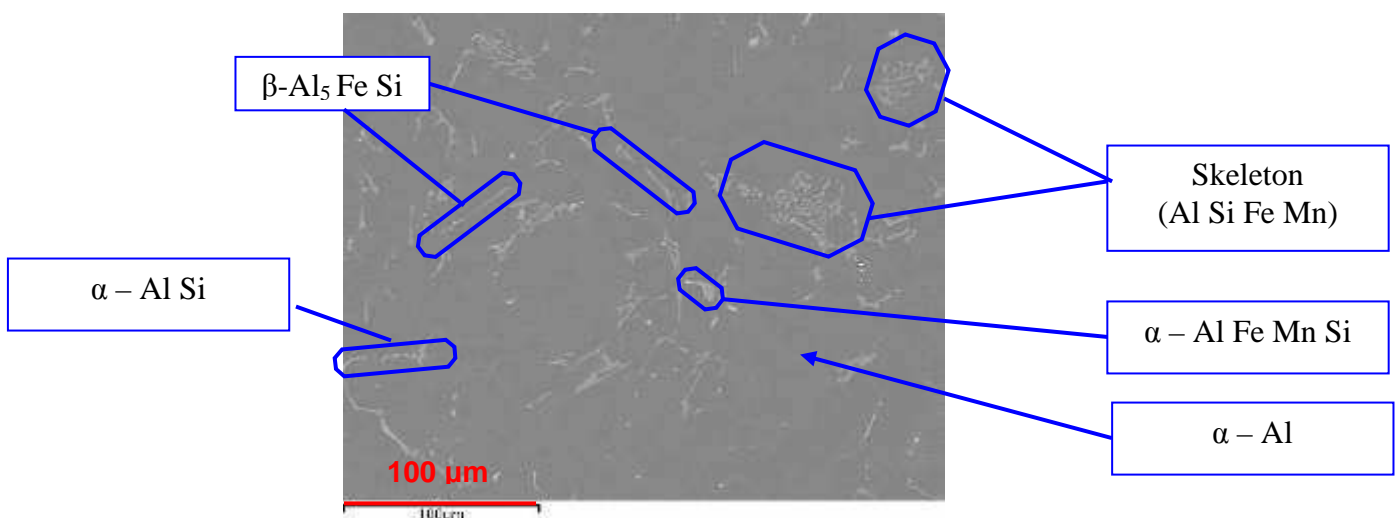The mechanical properties of the Al-Si9Cu3 alloy depend on multiple variables such as foundry process and parameters used, composition, use of silicon grain modifiers and α-aluminium dendrite refiners, purity of the alloy, porosity levels and thermal treatment (Normally not used). The standard properties for Al-Si9Cu3 alloy in the DIN 1706 standard are as follows (Minimum values of standards):

As cast HPDC: UTS:240 MPa   YS: 140 Mpa   Elongation: <1%

There are different possible thermal treatments that have been applied to this alloy. The T6 treatment is the most commonly used and has not been selected in the present work because it causes to appear the porosity in the surface of the parts (Blistering). In this case, the hardening effect is attained through the solid solution and quenching treatment followed by an artificial ageing. There is not information on Al-Si9Cu3 reinforced with nano-Ti B$_2$. There is also no information about Al-SI9Cu3 with nano-Al$_2$O$_3$ fabricated by the liquid metallurgical process.

Acquisition of the alloys

The alloys were produced by Tecnalia, with Al Si9 Cu3 commercial Befesa aluminium alloy as matrix. Their composition is based on the Al Si9 Cu3. The nanoparticles have been created *ex-situ* and pulled into the alloy. The Table 3.4. presents the composition of the alloy as supplied by Befesa Aluminio, that it's the real composition before the addition of nanoparticles.

Element	Si	Cu	Fe	Mn	Mg	Cr	Ni	Zn	Ti	Pb	Sn	Sr	Al
wt.%	8.4	1.56	0.7	0.13	0.03	0.03	0.047	0.94	0.04	0.05	0.01	0	88.063

Table 3.4: Composition of the Al-Si9Cu3 alloy employed base alloy

3.3 Production of reinforced alloys and setting up of the casting processes

Because the price of HPDC trials is high, in order to test the behavior of materials, those are measured first in a metal die casting die and after adjusting the composition to the most suitable, parts have been made in the testing HPDC die of Tecnalia, to produce different test bars, in order to cover the necessary trials to get the characterization of materials. The DC process provides also better metallographic samples in order to study the phases and structures of the alloy.

Influence of Alumina (Al$_2$O$_3$) and Titanium Diboride (TiB$_2$) nanoparticles on the microstructure and properties of Al-Si9 Cu3 alloys for high pressure die casting applications.

CHAPTER 3:   EXPERIMENTAL PROCEDURE

3.3.1   Production of components and samples

First trials were made by melting the aluminium alloy in a 3 Kg induction furnace, stirring and pouring of "*Ex-Situ*" prepared nanoparticles. In order to get the TiB$_2$ nanoparticles in a size below 0.5 µm, 3 different systems has been probed:

1) "Momentive" bought particles + ball milling; 2) SHS TiB$_2$ produced at Tecnalia + ball milling and 3) SHS TiB$_2$ (70%) produced at Tecnalia + Al (30%) (As master alloy).

The particles with the nanosizes have been alloyed to the molten aluminium by gravity and stirring, in a induction furnace with a vessel of 3.5 Kg and a stirring device with a regulation control up to 2.000 r.p.m. (Mixing rotation speed: 250 r.p.m.).

For the final trials, different compositions and addition routes were tested. Briquettes made at Tecnalia have a 500 MPa briquetting force, with the aluminium and the ceramic particles mixed and milled in a steel mill with steel balls connected to land. Some of them where sinterized by Spark Plasma Synthesis (SPS). Other briquettes that contain also a 10% of iron powder are briquetted with 5 ton force. Prepared powders were introduced by stirring in the molten metal, and commercial AlTi5B1 rod was used as standard refining agent. Protection fluxes were used to protect the liquid metal from oxidation, leaving up the dross before adding the briquettes. Briquette dissolution temperature was 720ºC, in order to simulate the working temperatures of HPDC. The briquettes were submerged during 2 minutes in the melt before stirring. Approximately in 1 minute, the briquettes were dissolved into the melt. After stirring 10 minutes, composition, TP1 and DTA samples were obtained, to establish the composition, grain size and solidification curve. Prepared material was poured in the HPDC machine and injected, in order to obtain the test bars for the definition of the mechanical properties.

The first DC trials have consisted in the study of 18 different TiB$_2$ reinforced alloys with commercial and Tecnalia´s developed SHS-TiB$_2$ (Table 3.5). The first 8 samples were made by introducing the TiB$_2$ powders into the liquid aluminium by stirring, with reinforce percentages from 0.01 to 0.2 wt. %. The second trials were made with of aluminium reinforced with TiB$_2$ particles made from SHS process briquettes. The best results were obtained with briquettes, that were the elected format for the second DC trials.

Influence of Alumina (Al$_2$O$_3$) and Titanium Diboride (TiB$_2$) nanoparticles on the microstructure and properties of Al-Si9 Cu3 alloys for high pressure die casting applications.

CHAPTER 3:   EXPERIMENTAL PROCEDURE

The developed <u>trials in die casting (DC)</u> are:

Denomination	Material	Format	wt.% of addition
AlSi9Cu3Fe1 Sample 1			
0.01 wt.% SHS-TiB$_2$	SHS	Powder	0.01
0.05 wt.% SHS-TiB$_2$	SHS	Powder	0.05
0.1 wt.% SHS-TiB$_2$	SHS	Powder	0.1
0.2 wt.% SHS-TiB$_2$	SHS	Powder	0.2
0.01 wt.% Commercial TiB$_2$	Commercial	Powder	0.01
0.05 wt.% Commercial TiB$_2$	Commercial	Powder	0.05
0.1 wt.% Commercial TiB$_2$	Commercial	Powder	0.1
0.2 wt.% Commercial TiB$_2$	Commercial	Powder	0.2
0.01 wt.% SHS-TiB$_2$	SHS	Briquette	0.01
0.05 wt.% SHS-TiB$_2$	SHS	Briquette	0.05
0.1 wt.% SHS-TiB$_2$	SHS	Briquette	0.1
0.2 wt.% SHS-TiB$_2$	SHS	Briquette	0.2
0.1% AlTi5B1 (AlSi9Cu3Fe1)	Commercial	Rod	0.1
AlSi9Cu3Fe1 Sample 2			
0.01 wt.% Commercial TiB$_2$	Commercial	Briquette	0.01
0.05 wt.% Commercial TiB$_2$	Commercial	Briquette	0.05
0.1 wt.% Commercial TiB$_2$	Commercial	Briquette	0.1
0.01 wt.% SHS-TiB$_2$	SHS	Briquette	0.01
0.05 wt.% SHS-TiB$_2$	SHS	Briquette	0.05
0.1 wt.% SHS-TiB$_2$	SHS	Briquette	0.1

Table 3.5.: Die Casting TiB$_2$ reinforced samples

The samples of grey and blue cells were ball milled with iron balls in an iron container conneted to ground before cold press, and rose briquettes were cold pressed after mixing without ball milling.

In the second DC trials, 6 alloys were made with briquettes reinforced with commercial and SHS processed particles, and they were also tested and compared with commercial AlTi5B1 refining rods, with a percentage from 0.01 to 0.1 wt. % (see Table 3.6.). Also in the second trials aluminium powders and TiB$_2$ particles were ball milled with iron balls in an iron container connected to ground before cold press.

CHAPTER 3:   EXPERIMENTAL PROCEDURE

Denomination	Material	Format	wt.% of addition
AlSi9Cu3Fe1 Sample 1			
0.01 wt.% α - Al_2O_3	Alpha alumina	Powder	0.01
0.03 wt.% α - Al_2O_3	Alpha alumina	Powder	0.03
0.05 wt.% α - Al_2O_3	Alpha alumina	Powder	0.05
0.01 wt.% γ - Al_2O_3	Gamma alumina	Powder	0.01
0.03 wt.% γ - Al_2O_3	Gamma alumina	Powder	0.03
0.05 wt.% γ - Al_2O_3	Gamma alumina	Powder	0.05
1 wt.% γ - Al_2O_3	Gamma alumina	Powder	1
AlSi9Cu3Fe1 Sample 2			
0.01 wt.% α - Al_2O_3	Alpha alumina	Briquette	0.01
0.05 wt.% α - Al_2O_3	Alpha alumina	Briquette	0.05
0.1 wt.% α - Al_2O_3	Alpha alumina	Briquette	0.1
0.01 wt.% γ - Al_2O_3	Gamma alumina	Briquette	0.01
0.05 wt.% γ - Al_2O_3	Gamma alumina	Briquette	0.05
0.1 wt.% γ - Al_2O_3	Gamma alumina	Briquette	0.1

Table 3.6.: Die Casting Al_2O_3 reinforced samples

In the case of DC trials with Al_2O_3 reinforced alloys, 7 reinforced alloys were made with the α and γ alumina by introducing by stirring the Al_2O_3 powders into the liquid aluminium, with reinforce percentages from 0.01 to 1 wt.%. 6 reinforced alloys were made with the 2 compositions with briquettes with aluminium powders and Al_2O_3 particles were ball milled with iron balls in an iron container connected to ground before cold press, with a percentage of reinforcing particles from 0.01 to 0.1 wt.%.

From those trials, at least 3 samples have being taken in order to make the mechanical characterization, and for the HPDC trials, the most suitable composition and percentages have been applied. Mechanical, thermal and microstructural analyses have been taken in order to study the properties and the causes. For the HPDC trials the table 3.6. resumes the materials, formats and percentajes of reinforcements:

CHAPTER 3:   EXPERIMENTAL PROCEDURE

Denomination	Material	Format	wt.% of addition
Sample alloy	Al Si9 Cu3	Ingot	0%
Al Ti5 B1 estandar rod	Al Ti5 B1	Rot	0,3%
TiB$_2$ commercial with 94% Al, Ti:B 2,2:1 relation	Commercial TiB$_2$	SPS Briquette	0,3%
TiB$_2$ commercial with 94% Al, Ti:B 2,2:1 relation and free Ti and B.	Commercial TiB$_2$	SPS Briquette	0,2%
TiB$_2$ commercial with 96% Al, Ti:B 2,2:1 relation	Commercial TiB$_2$	SPS Briquette	0,2%
TiB$_2$ commercial with 90% Al, Ti 69% B 31% relation	Commercial TiB$_2$	SPS Briquette	0,2%
TiB$_2$ commercial with 90% Al, Ti 69% B 31% relation	Commercial TiB$_2$	SPS Briquette	0,1%
TiB$_2$ SHS with 90% Al, Ti 69% B 31% relation	Commercial TiB$_2$	SPS Briquette	0,2%
TiB$_2$ SHS with 90% Al, Ti 69% B 31% relation	Commercial TiB$_2$	SPS Briquette	0,1%
TiB$_2$ SHS with 94% Al, Ti 69% B 31% relation	Nano TiB2	SPS Briquette	0,3%
TiB$_2$ SHS with 94% Al, Ti 69% B 31% relation	Nano TiB2	SPS Briquette	0,15%
80% Al+10% Fe+10% Commercial TiB$_2$	Commercial TiB$_2$	Briquette	0,2%
80% Al+10% Fe+10% Commercial TiB$_2$	Commercial TiB$_2$	Briquette	0,1%
TiB$_2$ commercial (AlSi9Cu3Fe1)	Commercial TiB$_2$	Powder	0,01%
TiB$_2$ commercial (AlSi9Cu3Fe1)	Commercial TiB$_2$	Powder	0,05%
TiB$_2$ commercial (AlSi9Cu3Fe1)	Commercial TiB$_2$	Powder	0,1%
TiB$_2$ commercial (AlSi9Cu3Fe1)	Commercial TiB$_2$	Powder	1%
TiB$_2$ SHS (AlSi9Cu3Fe1)	Nano TiB$_2$	Powder	0,01%
TiB$_2$ SHS (AlSi9Cu3Fe1)	Nano TiB$_2$	Powder	0,05%
TiB$_2$ SHS (AlSi9Cu3Fe1)	Nano TiB$_2$	Powder	0,1%
10% TiB$_2$ commercial+90%Al	Commercial TiB$_2$	Briquette	0,2%
10% TiB$_2$ commercial+90%Al	Commercial TiB$_2$	Briquette	0,1%
10% TiB$_2$ SHS+90%Al	Nano TiB$_2$	Briquette	0,2%
10% TiB$_2$ SHS+90%Al	Nano TiB$_2$	Briquette	0,1%
0.01 wt.% α Al$_2$O$_3$	Alfa	Powder	0.01
0.01 wt.% α Al$_2$O$_3$	Alfa	Powder	0.01
0.05 wt.% α Al$_2$O$_3$	Alfa	Powder	0.05
0.1 wt.% α Al$_2$O$_3$	Alfa	Powder	0.1
0.1 wt.% α Al$_2$O$_3$	Alfa	Powder	0.1
1 wt.% α Al$_2$O$_3$	Alfa	Powder	1
0.01 wt.% γ Al$_2$O$_3$	Gamma	Powder	0.01
0.05 wt.% γ Al$_2$O$_3$	Gamma	Powder	0.05
0.1 wt.% γ Al$_2$O$_3$	Gamma	Powder	0.1
1 wt.% γ Al$_2$O$_3$	Gamma	Powder	1
0.2 wt.% γ Al$_2$O$_3$	Gamma	Briquette	0.2
0.1 wt.% γ Al$_2$O$_3$	Gamma	Briquette	0.1
0.17 wt.% α Al$_2$O$_3$	Alfa	Briquette	0.17

Table 3.7.: Composition of the Al-Si9Cu3 alloy employed base alloy

Influence of Alumina (Al$_2$O$_3$) and Titanium Diboride (TiB$_2$) nanoparticles on the microstructure and properties of Al-Si9 Cu3 alloys for high pressure die casting applications.

CHAPTER 3:   EXPERIMENTAL PROCEDURE

We can observe in Fig. 3.10. the process employed to make the study of reinforcing the Al Si9 Cu3 alloy, from the mixing of the particles to the final test to determinate all the properties to study.
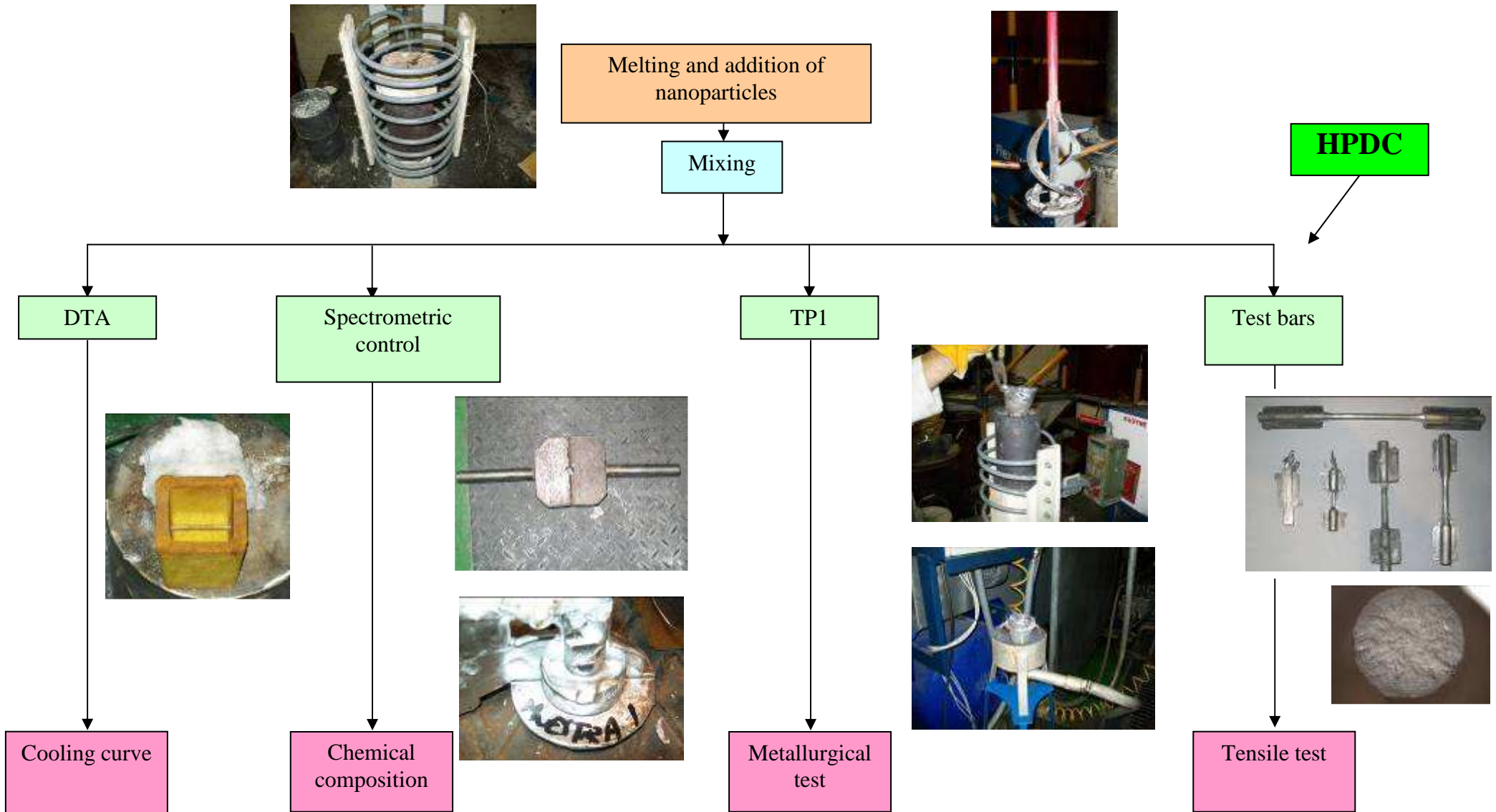

Fig. 3.10 : Test procedure

Influence of Alumina (Al_2O_3) and Titanium Diboride (TiB_2) nanoparticles on the microstructure and properties of Al-Si9 Cu3 alloys for high pressure die casting applications.

CHAPTER 3:   EXPERIMENTAL PROCEDURE.

3.4 Experimental techniques used for the analysis of the results

The different materials (A380, A380 +%TiB_2 and A380 +% Al_2O_3) were cast following the procedure explained in the previous section, with the same working and temperatures parameters. Specimens were machined from them for tensile tests at room temperature and 200ºC. The equipments and test bar employed are signalled in Fig. 3.11., including tensile test bars for room and 200ºC temperatures, resilience and dynamic test bars.
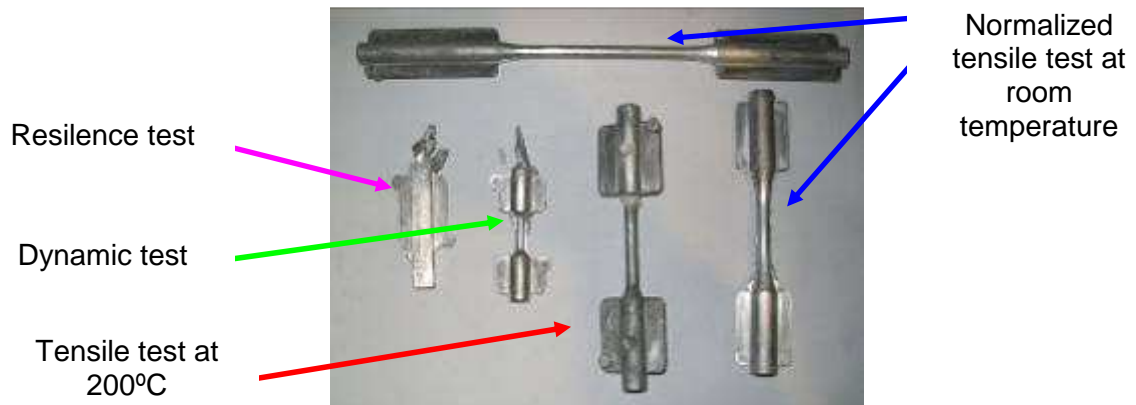

Figure 3.11.- HPDC Test bars.

<u>**Determination of mechanical properties:**</u>

In order to determinate the mechanical properties of the reinforced alloys we have employed the specimens obtained from the DC and HPDC, employing the Tensile tests at room temperature and 200ºC,

Influence of Alumina (Al_2O_3) and Titanium Diboride (TiB_2) nanoparticles on the microstructure and properties of Al-Si9 Cu3 alloys for high pressure die casting applications.

CHAPTER 3:   EXPERIMENTAL PROCEDURE.

Determination of microstructure and composition of the components of the alloys

In order to determinate the microstructure and composition of the different elements, phases and products we have employ different techniques: AWD analysis (together with line profile analysis), AFM analysis, SEM analysis, TEM analysis, OM analysis, Measurement of density and porosity (Water displacement and geometrical measurement, i.e. volume and weight relation), Chemical analysis, XRD, CTE measurements, TP1 grain size normalized essay.

The solidification curves of the materials were obtained through a time-temperature recording system based on the use of commercial sand cups which incorporate a thermocouple protected by a glass tube. The control system is based on a high speed signal capturing system connected to a computer, were the signals are processed by a specific programme developed at Tecnalia. In order to determinate the solidification curve, a commercial sand cup with a centerd thermocouple was connected to the control system. The pouring temperature, 710ºC, was controlled by a thermocouple connected to the furnace automatic temperature control system. Signals were registered every 1 second, obtaining the T/t curve. Curves were studied in combination with their first 5th derivatives curves, with a proper escalation ad smoothening of curves. Solidification curves gives very interesting information, as the solidification rate, grain and SDAS size, kind and temperature precipitation of metallic precipitations, and of course the correct or not nucleation and modification of the alloy. In order to determinate the nucleation and modification effect, solidification and their derivative curves gives very interesting parameters, as nucleation temperature, undercooling and solidification time.

DTA has been employed normally for alloys employed in others process different from HPDC, and in the case of castings especially in the study of A356 alloy and the A356 reinforced alloys. Those studies show a reduction of the latent heat and solidification time, with a better nucleation [Egi 07].

Solidification of the SHS- TIB_2 and nano-Al_2O_3 reinforced alloys

The aluminium alloy solidification curves obtained with the Al-Si9Cu3 base and reinforced alloys together with their derivative curves will be analyzed in order to determinate their differences. All the materials have been cast in the same conditions, sand mould temperature at 20ºC and casting temperature 710ºC. The casting step has been controlled so that there were no differences in the casting parameters and procedure. The repetitively of the test has being checked in order to validate the process. We can observe in Fig. 3.12. the sand cup with the thermocouple and connection wire.

Influence of Alumina (Al$_2$O$_3$) and Titanium Diboride (TiB$_2$) nanoparticles on the microstructure and properties of Al-Si9 Cu3 alloys for high pressure die casting applications.

CHAPTER 3:   EXPERIMENTAL PROCEDURE.

Figure 3.12.- Commercial sand cup for DTA determination

Determination of microstructures and compositions.

In order to determinate the microstructures and phases we have employed different equipments. OM gives us the microstructure, grain size and determination of main phases, SEM+EDS gives as the same information, but also the composition of the different phases and structures. TEM+EDS has been employed to the determination of the differences between the peripheral and central area. TEM samples were prepared through conventional thin film preparation: cutting, mechanical grinding and ion milling. After ion milling, the observable regions for TEM have thickness smaller than 50 nm. It has to be mentioned that the TEM observable areas are very small in compare with SEM areas. Having this in memory 2 things can be mentioned:

1.   The microstructure analyzed by TEM are not easily directly correlated with global microstructure of the composite materials
2.   Due to the very small volume concentration of both reinforcement (TiB$_2$ and Al$_2$O$_3$), to the hardness difference and therefore ion milling rate between matrix and reinforcement the analysis of area with both matrix and reinforcement is very difficult. Indeed, we have not been able to analyze any of this area for both samples. Therefore, all of the analyses are strictly associated with the microstructure of the aluminium-alloyed matrix.

Energy Dispersive Analysis (EDS) analysis has been associated with TEM analysis in order to map the distribution of the elements presents in the analysis zones (Oxygen, Aluminium, Silicon, Iron and Copper). Diameter of the EDS spot is close to 2 nm and analysis step on X and Y close to 4 nm.

Influence of Alumina (Al$_2$O$_3$) and Titanium Diboride (TiB$_2$) nanoparticles on the microstructure and properties of Al-Si9 Cu3 alloys for high pressure die casting applications.

CHAPTER 3:   EXPERIMENTAL PROCEDURE.

Determination of TiB$_2$ nanoparticle size distribution:

In order to determinate the particle size distribution, laser (Also MALS and AFM) measures have been determinate. The average measure of the particle with the laser is 690 nm, but there is an agglomeration of the particles that don't let to define exactly the real size of the particles. Also a big percentage of particles (About a 30% of total particles) are below 200 nm.

Density

The density of the composite materials have been measured with a Mettler AE240 precision balance, with the measure of the samples in air and in water (Archimedes determination). Samples were taken from TP1 obtained samples, similar to a die casting with a high cooling rate.

Electrical conductivity

The electrical conductivity has been tested with an Autosigma 3000 electrical conductivity meter of GE Inspection technologies. The equipment is posed over the sample and it automatically gives a value in %IACS (International Annealed Copper Standard). The %IACS value is %100 for copper, so the higher %IACS in the sample, the more conductive the material is.

Influence of Alumina (Al_2O_3) and Titanium Diboride (TiB_2) nanoparticles on the microstructure and properties of Al-Si9 Cu3 alloys for high pressure die casting applications.

CHAPTER 4:   SOLIDIFICATION & MICROSTRUCTURE

CHAPTER 4: SOLIDIFICATION & MICROSTRUCTURE

Influence of Alumina (Al$_2$O$_3$) and Titanium Diboride (TiB$_2$) nanoparticles on the microstructure and properties of Al-Si9 Cu3 alloys for high pressure die casting applications.

CHAPTER 4:   SOLIDIFICATION & MICROSTRUCTURE

4.1 Introduction

The study of the solidification and the microstructures of the alloys with and without ceramic particles as reinforcement should provide the necessary information to determinate the influence of nano TiB$_2$ and nano Al$_2$O$_3$ particles. Indeed, the direct relation between the microstructure and the alloys properties, give the clues to understand the differences in the mechanical, electrical and thermal properties of nano-reinforced alloys in comparison with the unreinforced alloys, which will be developed in chapter 5.

The HPDC casting process used to produce the different samples is characterized by a high solidification rate due to the high thermal conductivity of the metal that is used to build the moulds, in comparison with the thermal conductivity of sand or ceramic moulds. Ceramic particles such as TiB$_2$ and Al$_2$O$_3$ have a strong influence on the solidification and final microstructure of the alloys, as they creates nucleus , nucleating and modifying the solidification parameters, variating the temperatures and composition of the formed intermetallic phases. When they are added externally, in the form of ceramic particles, they tend to agglomerate, in order to reduce the free energy of particles. They can be detected in the nucleus of the grains, when acting as nucleus, but normally they are pushed toward the grain boundaries, during the solidification process. We should expect to have the same behavior by addicting the ceramic particle, but as much as they are in the nano-scale, different properties are expected, including the decrease of grain size and SDAS. [58-60, 65]

The first study is related with the **solidification**, and has been done employing the Differential Thermal Analysis (DTA), with the aid of a computer controlled acquisition device that provides Temperature / time registration. The equipment takes the information from the thermocouple placed in the center of a commercial sand cup employed for DTA determination. Temperature is controlled from the pouring temperature to the finish of solidification and intermetallic precipitation, having a frequency of measuring of 1 measurement per second. The T-t curves are registered, and scale and softening of curves are adjusted to permit to detect clearly the different points in the curves. The derivatives of the solidification curves are employed to determinate the parameters in relation with the nucleation, modification and intermetallic precipitation. The derivative of each point in the curve corresponds to the cooling rate of the material. An increase in the derivative is a decrease in the solidification rate, so a new phase releases latent heat.

The study of solidification curves provides the information to determinate the influence of TiB$_2$ and Al$_2$O$_3$ reinforcement particles on solidification, modification and precipitation. The second part is the **analysis of the microstructure and chemistry** of the reinforced alloys, and the comparison with the unreinforced materials. Optical Microscopy (OM), Scanning Electron Microscopy (SEM), Wavelength Dispersive Spectroscopy (WDS) and Transmission Electron Microscopy (TEM) techniques have been used to analyze the microstructure and the chemistry of the composite materials. The analysis of the information collected from the obtained micrographs and the comparison with the microstructure of the corresponding unreinforced alloy provide the necessary information to explain the behaviour and properties of the reinforced materials.

Influence of Alumina (Al$_2$O$_3$) and Titanium Diboride (TiB$_2$) nanoparticles on the microstructure and properties of Al-Si9 Cu3 alloys for high pressure die casting applications.

CHAPTER 4:   SOLIDIFICATION & MICROSTRUCTURE

4.2 Influence of TiB$_2$ and Al$_2$O$_3$ particles on solidification

4.2.1   Introduction. Solidification curves

The study of the solidification curves shows the effect on grain refining and alloy modification. When there are not heterogeneous nucleation sites, the metal solidification curve shows an undercooling area (ΔT_{R-U}). Instead, where impurities or homogeneous nucleation is activated, as shown in Fig.4.1. If the grain refining provides enough nucleation sites, solidifications goes with low or not undercooling [Kas 01], providing a fine grain size.
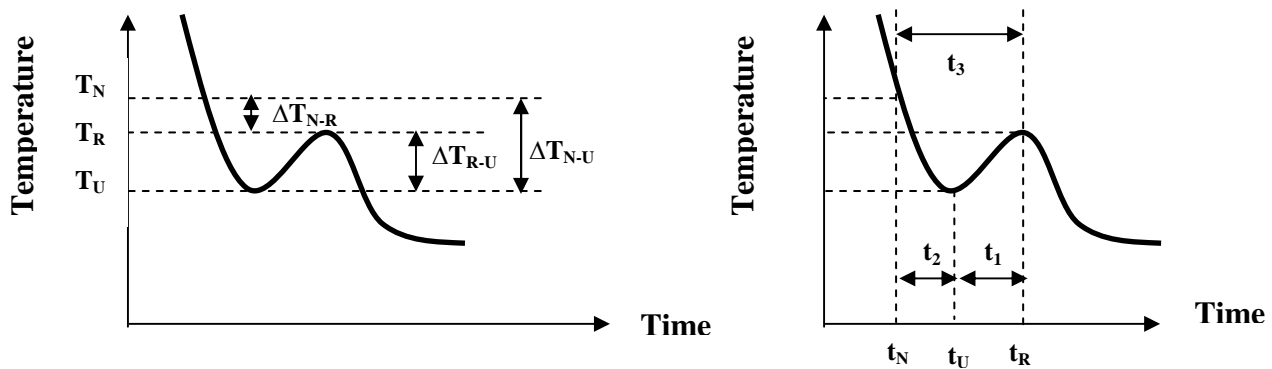

Figure 4.1.- T=f(t) curve aspects and key parameters in nucleating zone.

The parameters represented in Fig. 4.2 are explained in Table 4.1. and Table 4.2.:

Nomencl.	Parameter	Effect
T_N	Nucleation temperature (ºC)	Start of primary α -Al dendrites nucleation temperature. Beginning temperature of a series of nucleation events. There is a correlation with grain size only at high cooling rates. If the value increases, the grain size decreases [Iba 99].
T_U	Maximum undercooling temperature (ºC)	Unsteady state growth temperature. The temperature beyond which the newly nucleated crystals grow to such extent that the latent heat liberated surpasses the heat extracted from the sample. One of the best correlations with grain sizes. The maximum density of heterogeneous nucleation is reached. Increasing the value, reducing the grain size.
T_R	Maximum recalescence temperature (ºC)	Recalescence of steady state growth due to release primary α-Al dendrites.
ΔT_{R-U}	Temperature variation $T_R - T_U$ (ºC)	If this value (undercooling) tends to zero, they are sufficient favorable sites for nucleation. The grain size decrease if the undercooling value decreases.
ΔT_{N-U}	Temperature variation $T_N - T_U$ (ºC)	Not as good correlation as ΔT_{R-U}
ΔT_{N-R}	Temperature variation $T_N - T_R$ (ºC)	Not as good correlation as ΔT_{R-U}

Table 4.1.- Temperature key parameters signification in nucleating zone.

Influence of Alumina (Al_2O_3) and Titanium Diboride (TiB_2) nanoparticles on the microstructure and properties of Al-Si9 Cu3 alloys for high pressure die casting applications.

CHAPTER 4:   SOLIDIFICATION & MICROSTRUCTURE

Nomencl.	Parameter	Effect
t_1	Recalescence duration (sec.)	Liquidus undercooling duration. Good correlation with grain size. The grain size decreases if the value decreases. Related to grain growth. Not affected by thermocouple calibration.
t_2	Time between nucleation and beginning of recalescence (sec.)	Indicate the beginning of several nucleation events. Correlation problems with grain size. The grain size decreases if the value decreases.
t_3	Time between nucleation and end of recalescence (sec.)	Determinates the duration of recalescence, and has only good correlation at fast cooling rates. The grain size decreases if the value decreases.
t_N, t_U, t_R	Nucleation, recalescence starting and recalescence end times (sec.)	Correspondent times of Nucleation, maximum undercooling and maximum recalescence temperatures.

Table 4.2.- Time key parameters signification in nucleating zone.

We can observe the different structures that we can get from the cooling curve in Fig. 4.2, with two different areas, the Area 1 (nucleation zone) and Area 2 (modification zone). In function of the solidification curves the grain size is fine or coarse in Area 1 and the eutectic has an acicular, laminate, modified or overmodified structure.

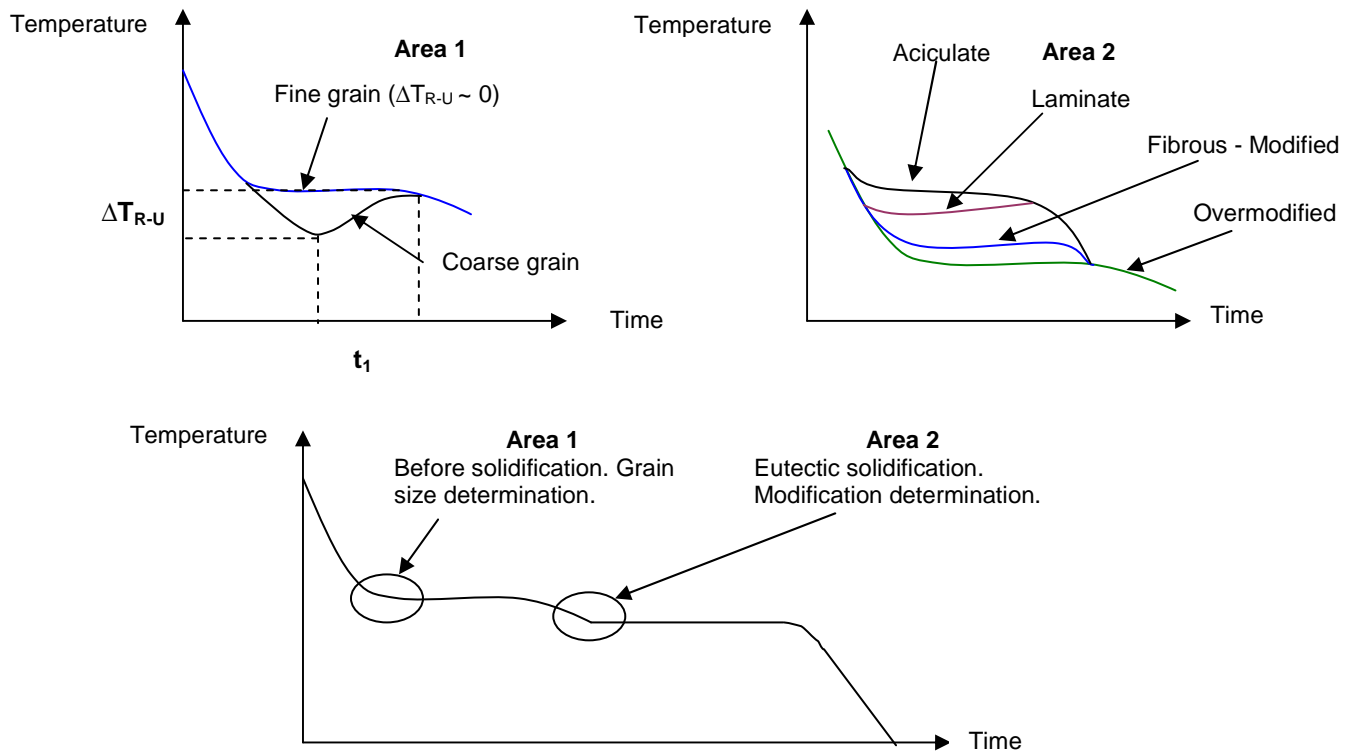**Figure 4.2.- Nucleation (Area 1) and Modification (Area 2) curves and arrests.**

Influence of Alumina (Al$_2$O$_3$) and Titanium Diboride (TiB$_2$) nanoparticles on the microstructure and properties of Al-Si9 Cu3 alloys for high pressure die casting applications.

CHAPTER 4:   SOLIDIFICATION & MICROSTRUCTURE

In order to determinate the parameters related to the nucleation temperature, first, second and fifth derivatives of temperature versus time are used [Spa 10]. Indeed to the small amounts of heat involved by certain phase transformations, emphasized small heat effects. The **times of beginning and end of recalescence** are the minimum and maximum on the cooling curve, and can be detected as zeros on the first derivative curve (dT/dt=0). If we represents (-dT/dt), exothermic reactions move the curve (-dT/dt) up and endothermic down. The exothermic reactions are caused when the atoms become more ordered, increasing the entropy, giving heat on cooling. We can observe in Fig. 4.3. the main reactions with the solidification curve and its first derivative.
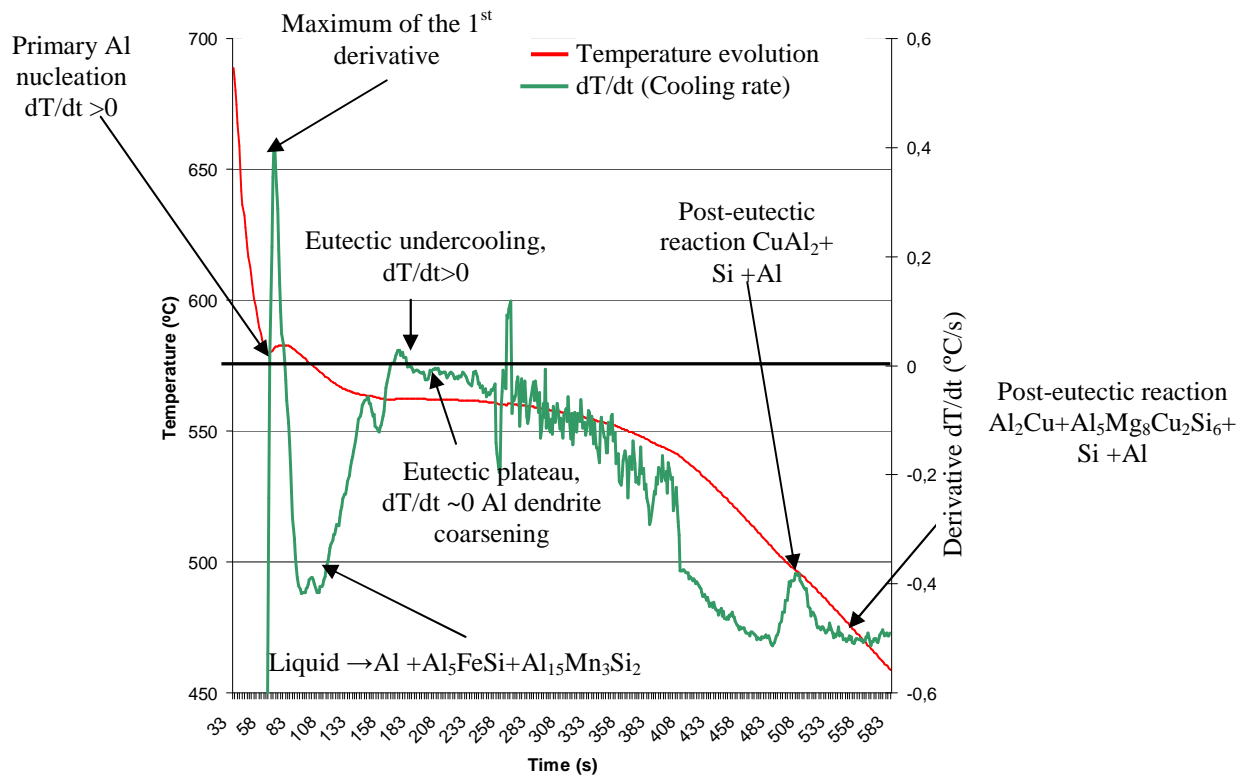

Figure 4.3.- T=f(t) and dT/dt curves with main identified reactions

Influence of Alumina (Al$_2$O$_3$) and Titanium Diboride (TiB$_2$) nanoparticles on the microstructure and properties of Al-Si9 Cu3 alloys for high pressure die casting applications.

CHAPTER 4:   SOLIDIFICATION & MICROSTRUCTURE

The **solidification rate** (ºc/s) is determinate by the first derivative (dT/dt) in the area before the first arrest, as we can observe in Fig. 4.4. First derivative and successive derivatives has been calculated as:

$$\frac{dT}{dt} = \frac{T_2 - T_1}{t_1 - t_2}$$

Where T is temperature and t is time. It depends on the material, size and form of the cup the quantity of heat that can be extracted per second. The solidification rate is expected to be increased by ceramic particle additions [Egi 07]. In our case, the solidification rate is approximately 0.16 ºC/s.
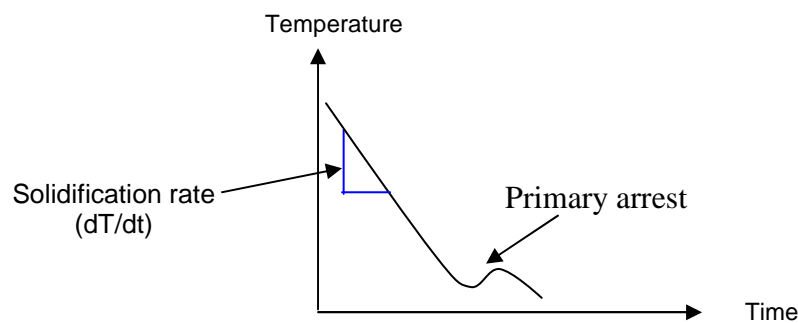

Figure 4.4.- T=f(t) and dT/dt curves with main identified reactions

The second derivative is used as a precise indicator of the **Nucleation temperature** T$_N$, with a minimum peak that shows the precise moment when the cooling rate (dT/dt)cc goes upwards, indicating the start of latent heat evolution, as we can see in the blue line in Fig. 4.5. The second derivative passes through zero in a positive direction (going up) at the strongest part of the exothermic (going down) arrest. The **nucleation time** is defined from the maximum peak on the second derivative. It's used also to determinate minor reactions, as the formation of iron-rich intermetallics, Al$_5$FeSi, Aluminium-Silicon eutectic, Mg$_2$Si-Al eutectic and Al$_2$Cu-Al eutectics [Spa 10]. It's expected to have an increase in T$_n$ and a decrease of t$_n$, because the addition of ceramic particles [Egi 07].
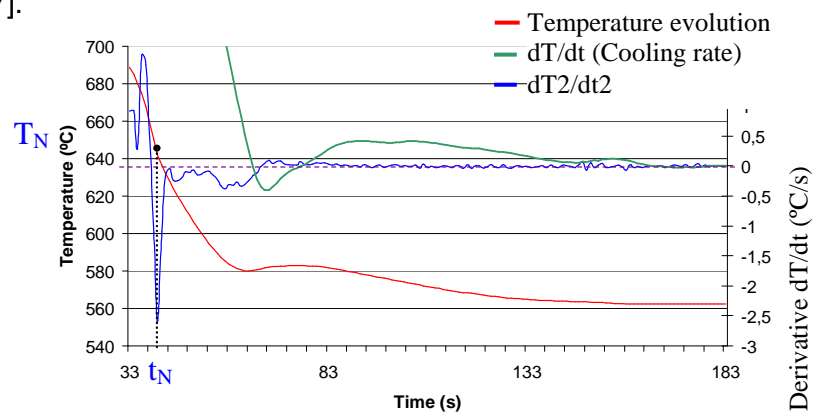

Figure 4.5.- Nucleation temperature (T$_n$) and time (t$_n$) determination.

Influence of Alumina (Al_2O_3) and Titanium Diboride (TiB_2) nanoparticles on the microstructure and properties of Al-Si9 Cu3 alloys for high pressure die casting applications.

CHAPTER 4: SOLIDIFICATION & MICROSTRUCTURE

If we want to determinate the points in the liquidus arrest, we employ 4th and 5th derivatives [Spa 10]. The point of **stars of liquidus** (N) is given by the intersection of the 5th derivative with zero, as in Fig.4.6.
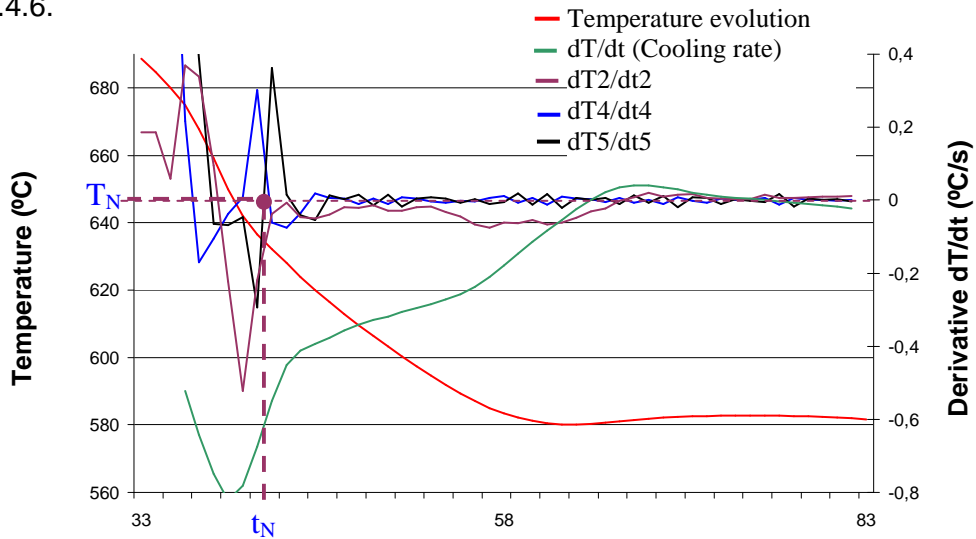

Figure 4.6.- Point of start of liquidus (N) determination with 5th derivative

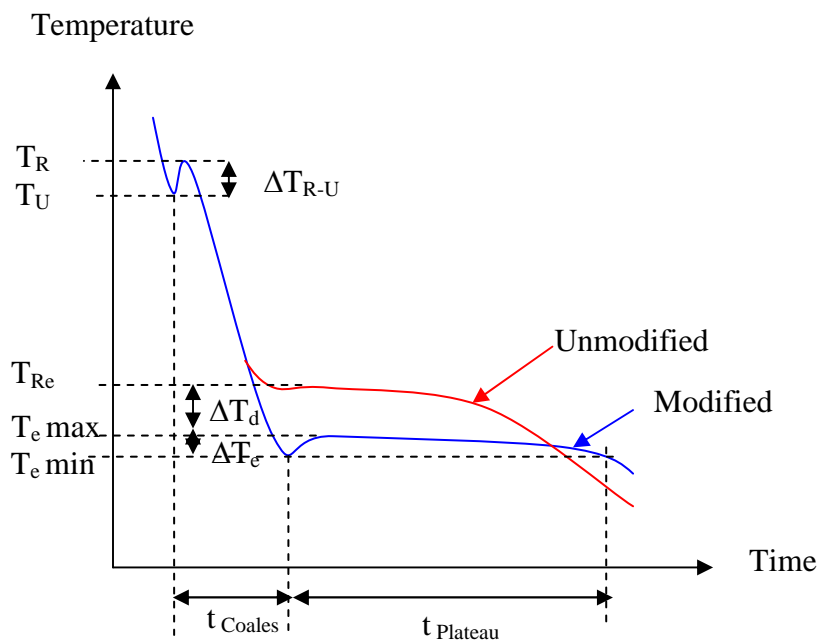In order to determinate the eutectic reaction, we can see in Fig 4.7. what are the employed characteristic parameters:

Figure 4.7.- Eutectic reaction characteristic parameters

Influence of Alumina (Al$_2$O$_3$) and Titanium Diboride (TiB$_2$) nanoparticles on the microstructure and properties of Al-Si9 Cu3 alloys for high pressure die casting applications.

CHAPTER 4:   SOLIDIFICATION & MICROSTRUCTURE

As the temperature of main eutectic reaction in the sample has a higher value, a more acicular structure is created by the aggregation of nano-particles. Lower eutectic temperature and times imply better modification [Nik 11].

If we study the second derivative, we can also determinate very interesting points [Mac 96].

- ⊕ The first maximum of the second derivative occurs before the **β-phase** thermal anomaly. The second maximum occurs before the eutectic growth. If we want to determinate the time and temperature of β-phase, we employ the first two maximums of second derivative.

- ⊕ In order to determinate the **time and eutectic temperature**, that corresponds to the time between the start of beginning of eutectic growth and the beginning of the post-eutectic reaction, we use the second maximum and the maximum of second derivative. The end of the eutectic reaction is the minimum in the second derivative.

The main **reactions during the solidification** of the Al-Si9Cu3 alloys have been already previously studied by different researchers [Bac 90],[Zol 07]. The temperature at which the reactions take place may vary according to the exact alloy composition and process conditions but the main features of the solidification of these types of alloys have been identified as follows:
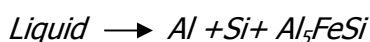
1) *Preliquidus area with Al$_{15}$(Fe,Mn)$_3$Si$_2$ formation at around 605ºC.*

2) *Development of the α-aluminium dendrites at around 600ºC.*

3) *Precipitation of rich Al Mn Fe based intermetallics around 578-575ºC*

   Liquid $\longrightarrow$ Al + Al$_{15}$(Fe,Mn)$_3$Si$_2$ and Liquid
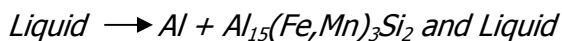
4) *Main eutectic reaction with rich Si and Mn-Fe phases at around 562ºC*

   Liquid $\longrightarrow$ Al +Si+ Al$_5$FeSi

5) *Precipitation of the Mg$_2$Si at around 512-509ºC (Only for high Mg percentages)*

   Solid $\longrightarrow$ Al + Mg$_2$Si

6) *Precipitation of the Al$_2$Cu at around 494-476ºC*

   Solid $\longrightarrow$ Al + Al$_2$Cu

7) *Precipitation of complex eutectics rich in Al$_2$Cu and Al$_5$Mg$_8$Si$_6$Cu$_2$ at around 494-476ºC*

   Solid $\longrightarrow$ Al + Si + Al$_2$Cu + Al$_5$Mg$_8$Si$_6$Cu$_2$
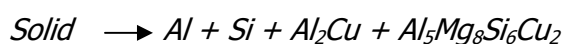
CHAPTER 4: SOLIDIFICATION & MICROSTRUCTURE

As we are going to see in the solidification curves in Fig.4.10 to 4.15 , obtained values are near the calculated interval. With Thermo-calc we can determinate the **precipitations** of the alloy. In our case, we show the results for the Silicon and Copper, which are the two main allowing elements. We can observe in Fig. 4.8. A and B that for our composition, the liquidus temperature about 550ºC and the development of alpha dendrites about 600ºC, the eutectic point about 570ºC and the Al Fe Si in the Beta structure at 585ºC.
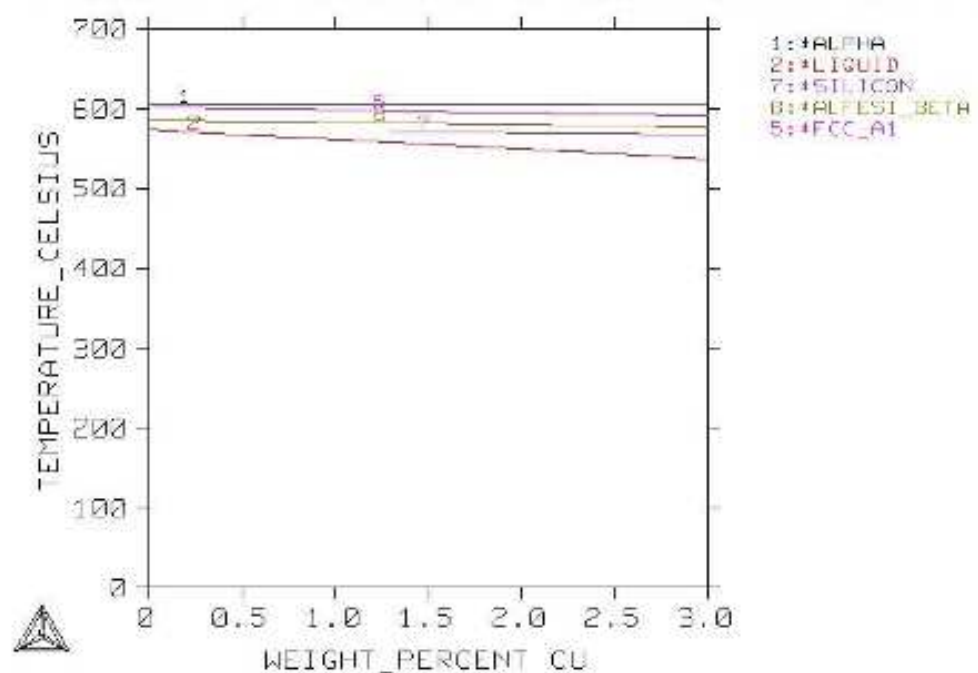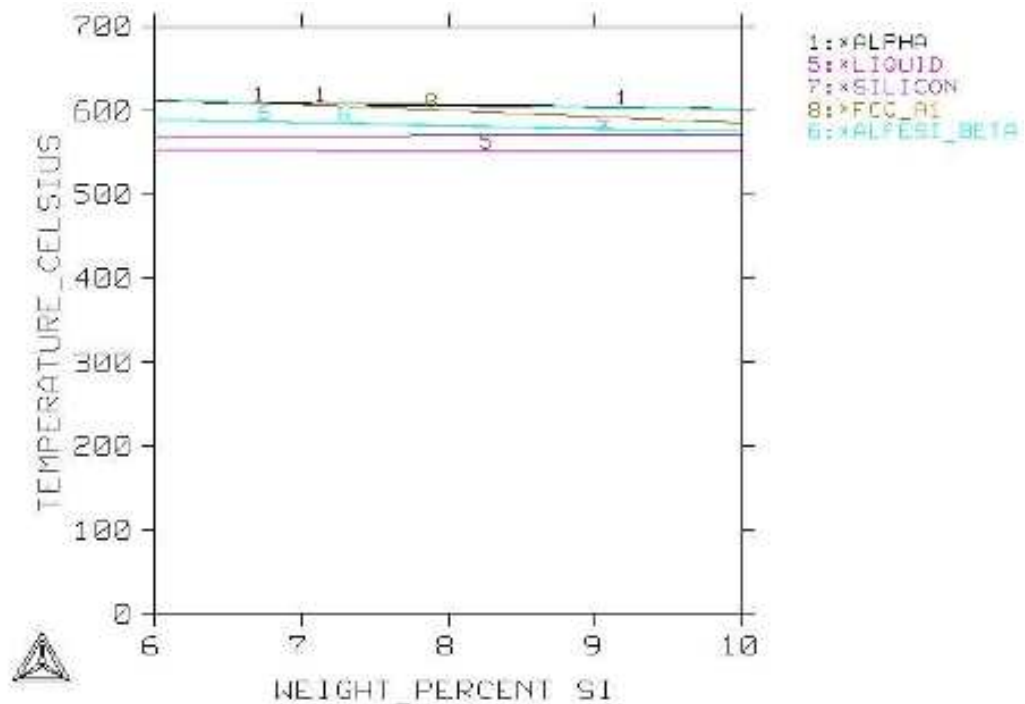
Figures 4.8. A and B- Determination of liquidus temperature and precipitations with Thermo-calc

Influence of Alumina (Al$_2$O$_3$) and Titanium Diboride (TiB$_2$) nanoparticles on the microstructure and properties of Al-Si9 Cu3 alloys for high pressure die casting applications.

CHAPTER 4: SOLIDIFICATION & MICROSTRUCTURE

The point of starting of **Al$_2$Cu precipitation** (A) is determinate by the intersection with zero of 4th and 5th derivative, using the 5th derivative to filter out the zero crossovers due to background noises. The point of starting of **Al$_5$Mg$_8$Cu$_2$Si$_6$ precipitation** (B) is determined also as the point (A), as they are signalled in Fig. 4.9. Another way to determinate the beginning of the post-eutectic reaction is obtaining the maxima of the second derivative [Mac 96].
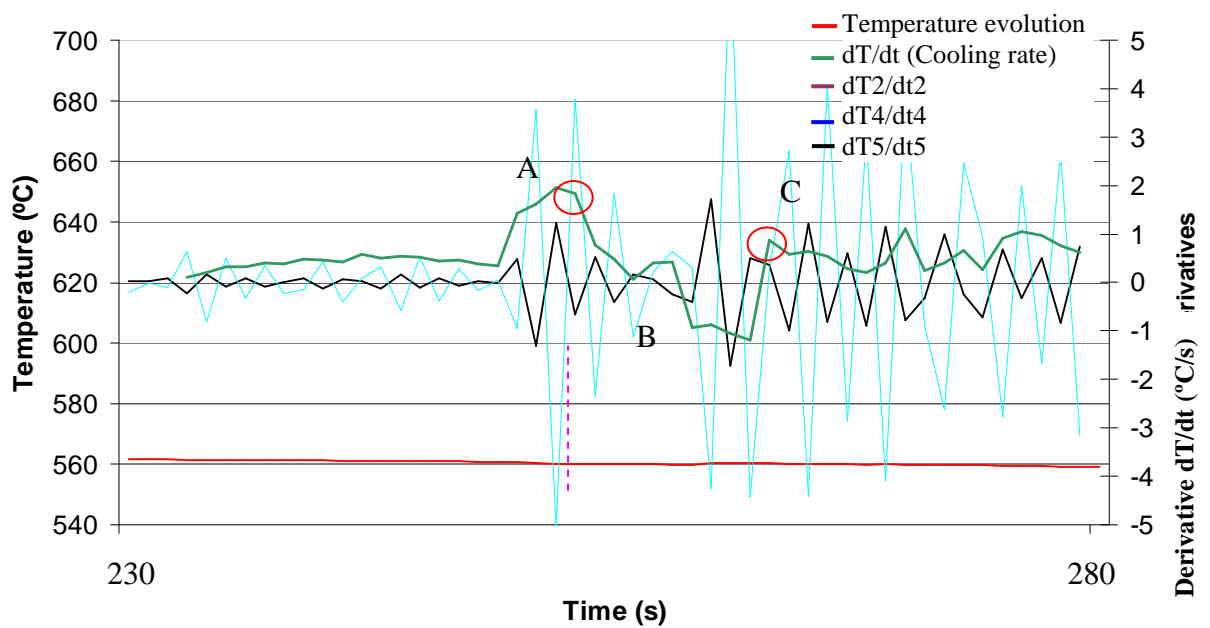

Figure 4.9.- Determination of Al$_2$Cu and Al$_5$Mg$_8$Cu$_2$Si$_6$ start point and area

We are going to analyse the unreinforced and reinforced alloys in order to compare the solidification curves. As the percentage of reinforcement in the alloys is low (< of 0.2 wt.%) we want to determinate the influence over the microstructures and phases formation, what can give to us the necessary information to interpret why there are the differences in the properties of the reinforced alloys. As we have mentioned before, the changes on the curves indicates what will be the internal microstructure of alloys, and also the refining and modifying effect.

Influence of Alumina (Al$_2$O$_3$) and Titanium Diboride (TiB$_2$) nanoparticles on the microstructure and properties of Al-Si9 Cu3 alloys for high pressure die casting applications.

CHAPTER 4:   SOLIDIFICATION & MICROSTRUCTURE

In Fig.4.10. we can determinate the **solidification reactions and their temperatures** (Second derivative eliminated to simplify). We can observe differences with the predicted temperatures for reactions during solidification, due to the reinforcement. The differences between the solidification curves can be observed on Fig. 4.11 to 4.15. The red circle numbers (From 1 to 7) correlates with the explained reactions during solidification of page 74.
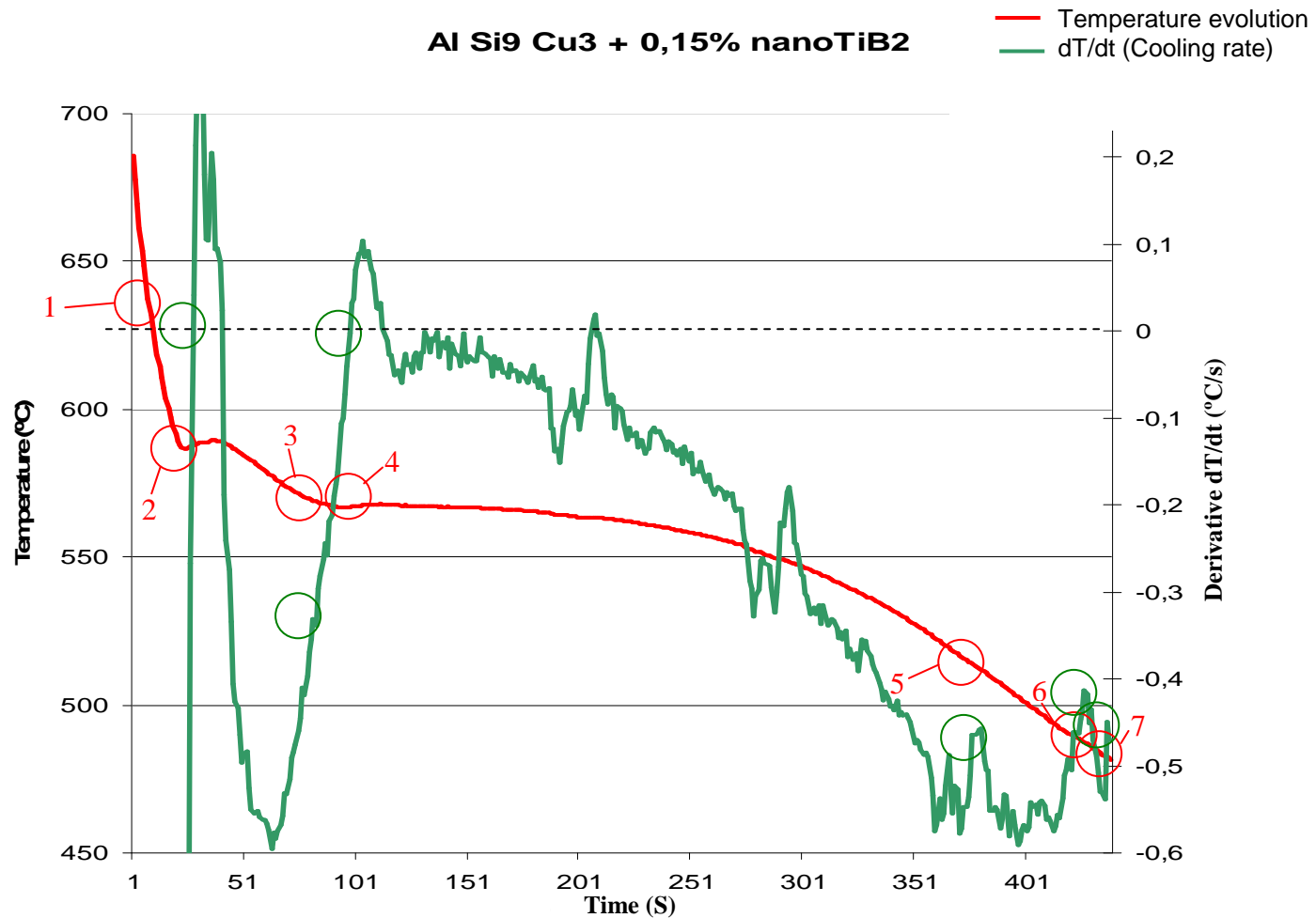

Figure 4.10.- DTA solidification of Al Si9 Cu3 + 0.15% nano TiB$_2$ sample.

CHAPTER 4: SOLIDIFICATION & MICROSTRUCTURE

In Fig. 4.11. we can observe the solidification curve with the temperature evolution y the 1st,2nd, 4th and 5th derivatives for the base Al SI9 Cu3 alloy. As we have seen before, the analysis of the derivatives give us the main solidification parameters and precipitation phases. The obtained results match the results of the previous literature review for the solidification parameters and precipitation phases. The red circle numbers (From 1 to 7) correlates with the explained reactions during solidification of page 74.
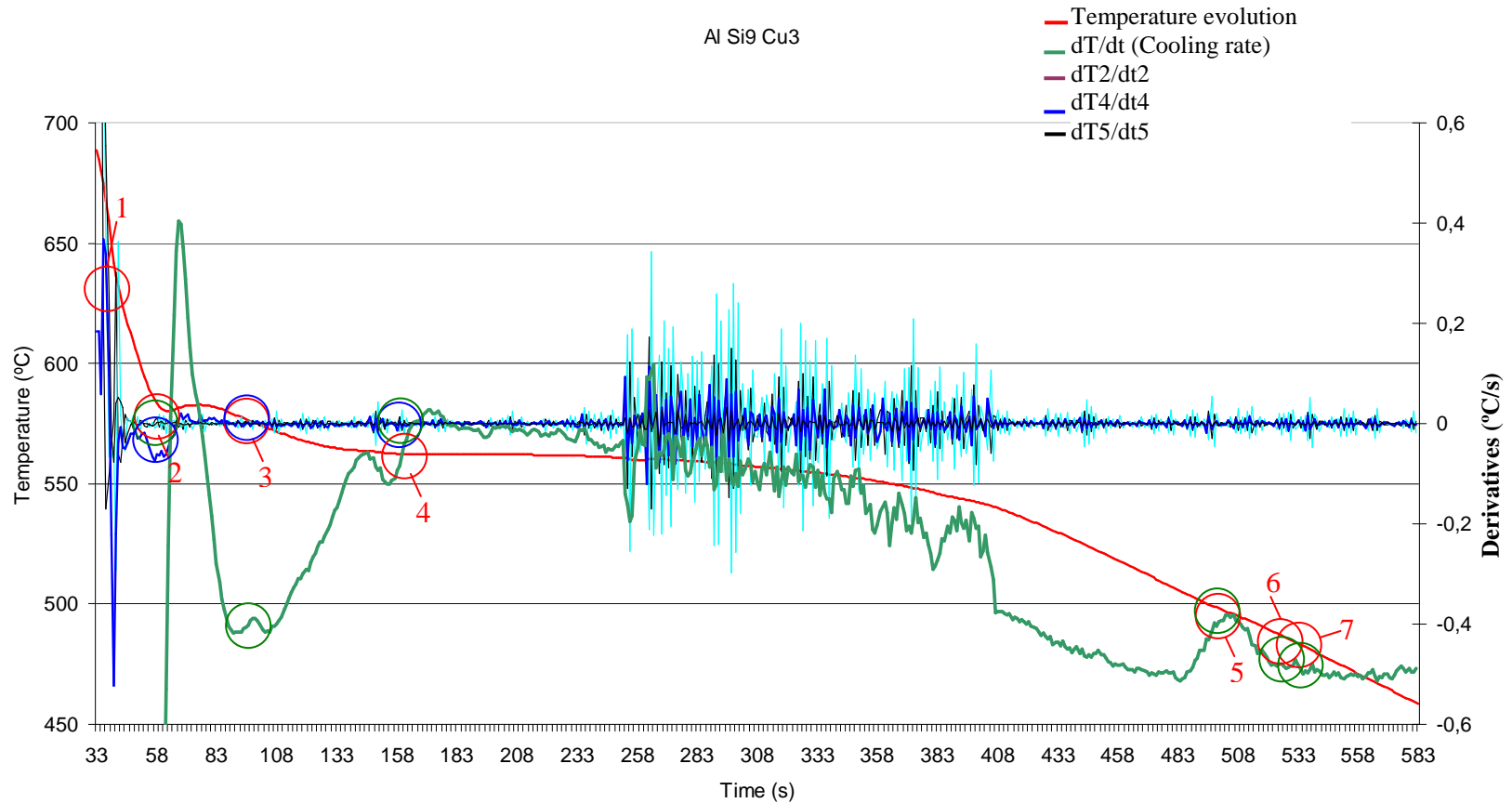

Figure 4.11.- DTA solidification of Al Si9 sample.

Influence of Alumina (Al$_2$O$_3$) and Titanium Diboride (TiB$_2$) nanoparticles on the microstructure and properties of Al-Si9 Cu3 alloys for high pressure die casting applications.

CHAPTER 4: SOLIDIFICATION & MICROSTRUCTURE

TiB$_2$ reinforced alloys

In Fig. 4.12. and 4.13. we can observe the solidification curves of TiB$_2$ reinforced alloys, with the temperature evolution and 1st and 2nd derivatives. We are going to study the variations in the solidification parameters to determinate the refining effect of TiB$_2$ particles, the eutectic modification, the aluminium grain size, the microstructure and the precipitation phases with their temperatures. The red circle numbers (From 1 to 4) correlates with the explained reactions during solidification of page 74.
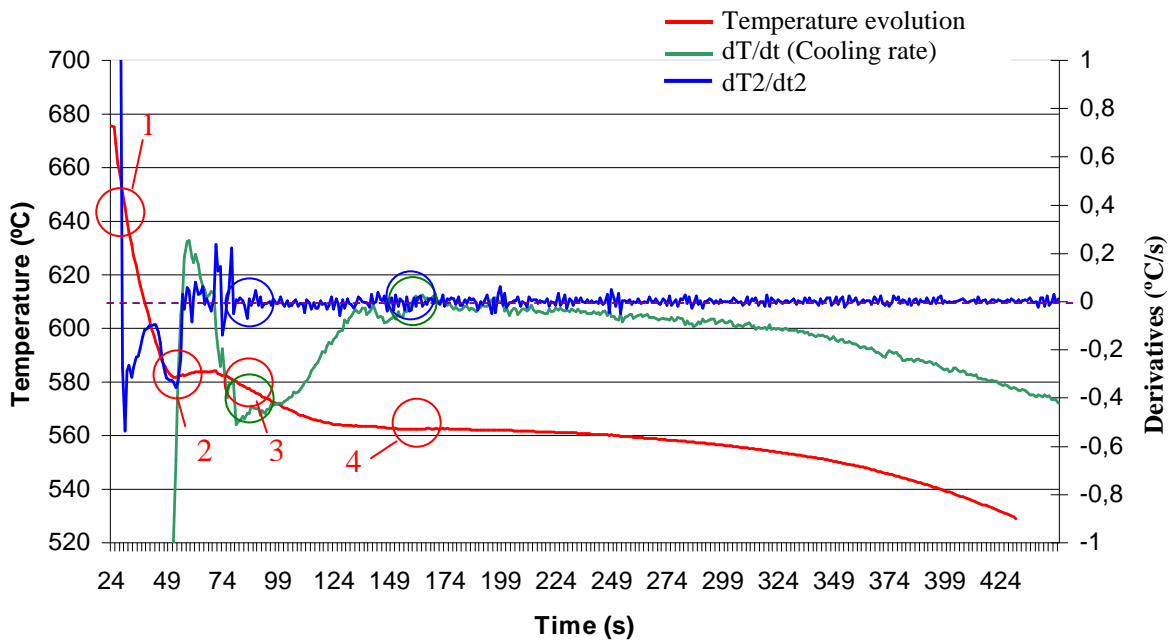

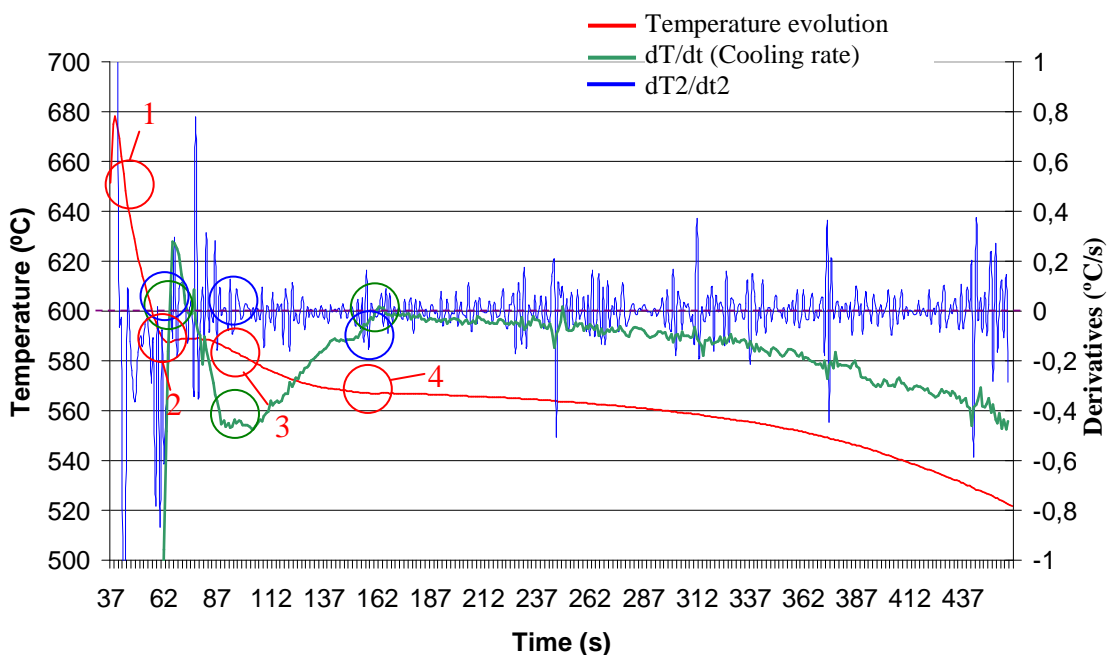**Figure 4.12.- DTA solidification of 0.2% SHS-TiB$_2$**

Figure 4.13.- DTA solidification of 0.2% commercialTiB$_2$ briquette

Influence of Alumina (Al_2O_3) and Titanium Diboride (TiB_2) nanoparticles on the microstructure and properties of Al-Si9 Cu3 alloys for high pressure die casting applications.

CHAPTER 4: SOLIDIFICATION & MICROSTRUCTURE

The **main solidification characteristics**, analysed during this study of the TiB_2 reinforced curves are listed in Table 4.3, with an accuracy in the temperature measure of 0.1 ºC. We can observe:

- An increase of temperature in the **$Al_{15}(Fe,Mn)_3Si_2$** formation of about 10ºC. This increase is related with the incorporation of TiB_2 to the melt, as explained in the literature review section, in page 3.
- An increase in the **α – aluminium dendrites** development temperature, due to the refining effect of TiB_2, that tends to increase the nucleation temperature an to decrease the undercooling temperature. The difference in the undercooling temperature is about 1.5 ºC.
- The **temperature of precipitation of Al Mn Fe based intermetallics** is also higher in the reinforced alloys, because the effect of introducing ceramic particles as reinforcements. The difference variates from 2 to 8 ºC.
- The **eutectic reaction temperature** is higher also, promoting a more pronounced acicular structure for TiB_2 reinforced alloys than the Al Si9 Cu3 sample, with a variation of 4ºC maximum for commercial TiB_2.

Solidification crystal structures	Al Si9 Cu3 (ºC)	0.2% SHS-TiB_2 (ºC)	0.2% commercial TiB_2 (ºC)
Preliquidus area with $Al_{15}(Fe,Mn)_3Si_2$ formation. Point 1 in the graphics.	641.9	650.6	648.1
Development of the α-aluminium dendrites. Point 2 in the graphics.	582.8	584.1	584.1
Precipitation of rich Al Mn Fe based intermetallics (point 3 in the graphics): Liquid ⟶ Al + $Al_{15}(Fe,Mn)_3Si_2$ + Liquid	574.9	576.5	582.8
Main eutectic reaction with rich Si and Mn-Fe phases (point 4 in the graphics). Liquid ⟶ Al +Si+ Al_5FeSi	562.2	562.4	566.9

Table 4.3: Main solidification crystal structures of the Al Si9 Cu3 TiB_2 reinforced alloys obtained from the experimental castings.

Influence of Alumina (Al$_2$O$_3$) and Titanium Diboride (TiB$_2$) nanoparticles on the microstructure and properties of Al-Si9 Cu3 alloys for high pressure die casting applications.

CHAPTER 4: SOLIDIFICATION & MICROSTRUCTURE

Other main parameters obtained from the experimental curves and their derivatives have been summarized in the Table 4.4 with an accuracy in the temperature measure of 0.1 ºC. We can observe that:

- The nucleation (Tn), maximum undercooling (Tu) and maximum recalescence temperature (Tr) are increased with the TiB$_2$ addition. The explanation is that introducing TiB$_2$ as ceramic reinforcement increases these values as seen in the literature review.

- The undercooling ΔT_{R-U} is lower after the TiB$_2$ addition. TiB$_2$ particles act as a grain refiner and the undercooling decreases with the refining of the structure,

- Comparing the two alloys containing TiB$_2$, commercial TiB$_2$ has a better refining effect.

- The liquidus undercooling time is higher in TiB$_2$ reinforced alloys. That could suppose a higher grain size. As in the rest of parameters the nucleation is better, we could expect fine acicular dendrites in the microstructure of the reinforced alloys.

Reference	T_N (ºC)	T_U (ºC)	T_R ºC)	ΔT_{R-U} (ºC)	ΔT_{N-U} (ºC)	ΔT_{N-R} (ºC)	t_1 (s)	t_2 (s)	t_3 (s)
Al Si9 Cu3 Sample	649.9	582.8	580.1	2.8	67.0	69.8	13	24	37
0.2 wt.% SHS-TiB$_2$	650.6	584.1	581.6	2.4	66.5	68.9	17	24	41
0.2 wt.% CommercialTiB$_2$	655.1	589.3	587.3	1.9	65.8	67.8	14	21	35

Table 4.4: Main parameters obtained of TiB$_2$ reinforced alloys.

We can see in Table 4.5. what are the controlled parameters in the zone eutectic as explained in Fig.4.9 with an accuracy in the temperature measure of 0.1 ºC. The eutectic temperature is increased, also the coalescence time is increased but the plateau time is decreased.

Modification	T_{Re} (ºC)	Te, max (ºC)	Te, min (ºC)	ΔT_e (ºC)	ΔT_d (ºC)	$t_{coalesc.}$ (ºC)	$t_{e.plat}$ (ºC)
Al Si9 Cu3 Sample	566.4	562.4	562.2	0,23	4,0	100	90
0.2 wt.% SHS-TiB$_2$	566.4	562.6	562.4	0,24	3,8	105	67
0.2 wt.% CommercialTiB$_2$	566.2	567.0	566.9	0,08	-0,8	116	86

Table 4.5: Eutectic temperatures and times

Influence of Alumina (Al_2O_3) and Titanium Diboride (TiB_2) nanoparticles on the microstructure and properties of Al-Si9 Cu3 alloys for high pressure die casting applications.

CHAPTER 4: SOLIDIFICATION & MICROSTRUCTURE

As a conclusion, TiB_2 ceramic particles acts as grain refiners without an excess of titanium (About a 0.15% wt.% in the alloy), with an increase in the temperatures of the different phases and transformations, reducing the undercooling . Very fine acicular structures are expected in the reinforced samples. A better grain refining effect is expected for commercial TiB_2 than SHS-TiB_2, but in both cases the SDAS should be smaller.

Al_2O_3 reinforced alloys

In Fig. 4.14 and 4.15 we can observe the solidification curves of Al_2O_3 reinforced alloys, with the temperature evolution and 1st and 2nd derivatives. We are going to study the variations in the solidification parameters to determinate the possible refining effect of Al_2O_3 particles, the eutectic modification, the aluminium grain size, the microstructure and the precipitation phases with their temperatures. The red circle numbers (From 1 to 6) correlates with the explained reactions during solidification of page 74.
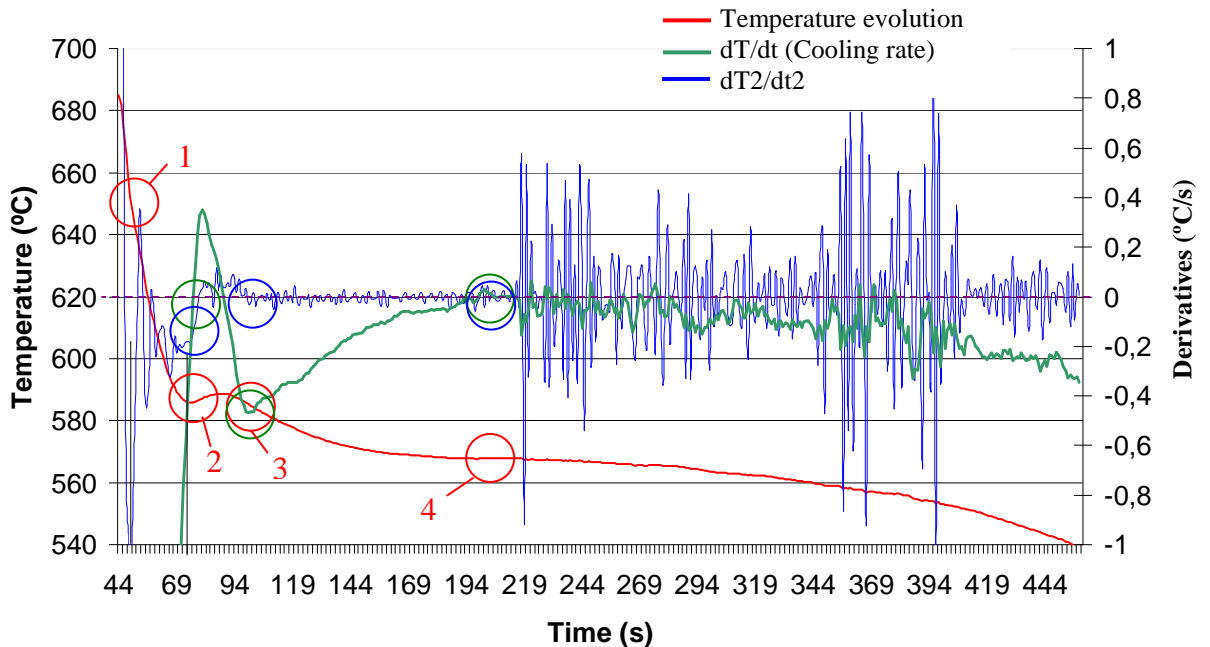

Figure 4.14.- DTA solidification of 0.1% of gamma Al_2O_3 briquette

Influence of Alumina (Al$_2$O$_3$) and Titanium Diboride (TiB$_2$) nanoparticles on the microstructure and properties of Al-Si9 Cu3 alloys for high pressure die casting applications.

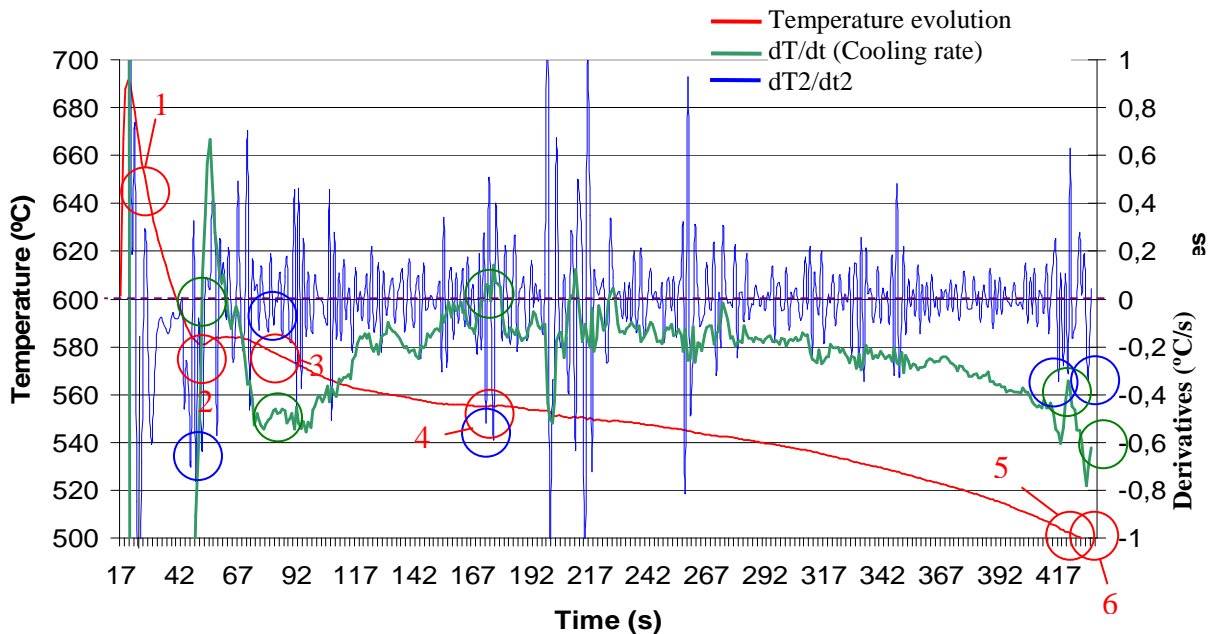CHAPTER 4: SOLIDIFICATION & MICROSTRUCTURE

Figure 4.15.- DTA solidification of 0.17% of alpha Al$_2$O$_3$ briquette

The main solidification characteristics of the Al$_2$O$_3$ reinforced curves are in Table 4.6 with an accuracy in the temperature measure of 0.1 ºC. We can observe:

- An increase of temperature in the Al15(Fe,Mn)3Si2 formation of about 10ºC. This increase is related with the incorporation of Al$_2$O$_3$ to the melt, as explained in the literature review section.

- An increase in the α – aluminium dendrites development temperature, due to the refining effect of Al$_2$O$_3$, that tends to increase the nucleation temperature and to decrease the undercooling temperature. The difference is about 6 ºC.

- The temperature of precipitation of Al Mn Fe based intermetallics is also higher in the reinforced alloys, because the effect of introducing ceramic particles as reinforcements. The difference variates from 2 to 10 ºC.

- The eutectic reaction is higher in γ-Al$_2$O$_3$, promoting a more acicular structure than in the Al Si9 Cu3 sample. However, in the gamma alumina reinforced alloy this value is smaller than the non reinforced sample and the structure should be a modified structure. In the 0.2 wt.% γ-Al$_2$O$_3$ sample the solidification curve has practically not a plateau zone with many intermediate reactions, so the determination of the eutectic point is quite confusing.

Influence of Alumina (Al$_2$O$_3$) and Titanium Diboride (TiB$_2$) nanoparticles on the microstructure and properties of Al-Si9 Cu3 alloys for high pressure die casting applications.

CHAPTER 4: SOLIDIFICATION & MICROSTRUCTURE

Solidification crystal structures	Al Si9 Cu3 (ºC)	0.17 wt.% α Al$_2$O$_3$ (ºC)	0.1 wt.% γ Al$_2$O$_3$ (ºC)
Preliquidus area with Al$_{15}$(Fe,Mn)$_3$Si$_2$ formation. Point 1 in the graphics.	641.9	652.0	651.7
Development of the α-aluminium dendrites. Point 2 in the graphics.	582.8	589.3	588.7
Precipitation of rich Al Mn Fe based intermetallics (point 3 in the graphics): Liquid ⟶ Al + Al$_{15}$(Fe,Mn)$_3$Si$_2$ + Liquid	574.9	584.8	577.2
Main eutectic reaction with rich Si and Mn-Fe phases (point 4 in the graphics). Liquid ⟶ Al +Si+ Al$_5$FeSi	562.2	567.7	555.0

Table 4.6.: Main solidification crystal structures of the Al Si9 Cu3 based materials obtained from the experimental castings.

Other main parameters obtained from the curves have been summarized in the Table 4.7. with an accuracy in the temperature measure of 0.1 ºC. We can observe that:

- The nucleation (Tn), maximum undercooling (Tu) and maximum recalescence temperature (Tr) are increased with the Al$_2$O$_3$ addition. The explanation is that introducing Al$_2$O$_3$ as ceramic reinforcement, more nuclei are activated, acting as a nucleation points.

- The undercooling ΔT_{R-U} is higher after the Al$_2$O$_3$ addition. In the case of acicular grains, grains are large in one direction, and could modify the undercooling $\Delta TR-U$ parameter. Comparing the two alloys containing Al$_2$O$_3$, gamma Al$_2$O$_3$ has a lower undercooling, but difference between the two alloys is small.

- The liquidus undercooling time is smaller or equal in Al$_2$O$_3$ reinforced alloys than in sample alloy. That should suppose a smaller grain size. As in the rest of parameters the nucleation is better unless the undercooling, we can expect also fine acicular dendrites in the microstructure of the reinforced alloys.

Influence of Alumina (Al$_2$O$_3$) and Titanium Diboride (TiB$_2$) nanoparticles on the microstructure and properties of Al-Si9 Cu3 alloys for high pressure die casting applications.

CHAPTER 4: SOLIDIFICATION & MICROSTRUCTURE

Reference	T$_N$ (ºC)	T$_U$ (ºC)	T$_R$ ºC)	ΔT$_{R-U}$ (ºC)	ΔT$_{N-U}$ (ºC)	ΔT$_{N-R}$ (ºC)	t$_1$ (s)	t$_2$ (s)	t$_3$ (s)
Al Si9 Cu3 Sample	649.9	582.8	580.1	2.78	67.1	69.8	13	24	37
0.1% of gamma Al$_2$O$_3$	658.6	588.7	585.9	2.88	69.9	72.8	13	27	40
0.17% of alpha Al$_2$O$_3$	663.8	584.1	580.9	3.28	79.7	82.9	10	27	37

Table 4.7.: Main parameters obtained

We can see in Table 4.8. what are the controlled parameters in the zone eutectic as explained in Fig.4.9 with an accuracy in the temperature measure of 0.1 ºC. The eutectic temperature is increased except the 0.17 wt.% of alpha Al$_2$O$_3$, how the coalescence time is increased and the plateau time is decreased.

Modification	T$_{Re}$ (ºC)	Te, max (ºC)	Te, min (ºC)	ΔT$_e$ (ºC)	ΔT$_d$ (ºC)	t$_{coalesc.}$ (ºC)	t$_{e.plat}$ (ºC)
Al Si9 Cu3 Sample	566.4	562.4	562.2	0.23	4.0	100	90
0.1% of gamma Al$_2$O$_3$	566.4	567.8	567.7	0.15	-1.4	150	21
0.17% of alpha Al$_2$O$_3$	566.4	555.6	555.0	0.62	10.8	145	29

Table 4.8.: Eutectic temperatures and times

As a conclusion, Al$_2$O$_3$ ceramic particles act as **grain refiners**, with an increase in the temperatures of the different phases and transformations, but without reducing the undercooling. **Very fine acicular structures** are expected also in the Al$_2$O$_3$ reinforced samples. We can explain why is so difficult to **automate the DTA´s** analysis for aluminium, as big changes are detected in the solidification curves with very few percentages of in situ or "*ex-situ*" produced reinforcing ceramic particles.

4.2.1.1 Determination of solidification parameters in function of the composition of the alloys

It's very interesting to determinate the main solidification parameters without employing DTA analysis. If we can employ only a mass spectrometer to determinate the alloy composition, and use the alloy composition to determinate the nucleation time, the Silicon eutectic temperature and the eutectic Al Si Cu eutectic temperature it would give us a non expensive method to compare how variations in composition modify the solidification parameters.

Influence of Alumina (Al$_2$O$_3$) and Titanium Diboride (TiB$_2$) nanoparticles on the microstructure and properties of Al-Si9 Cu3 alloys for high pressure die casting applications.

CHAPTER 4: SOLIDIFICATION & MICROSTRUCTURE

The **liquidus temperature** is important to study in order to determinate physical and metallurgical parameters of the solidifying alloy, as the solid fraction, the microstructure and chemical composition of the alloy at the solid/liquid interface, the solute super saturation point, the degree of undercooling... In order to determinate the liquidus temperature of hypoeutectic alloys they are 3 different formulas [Dju 04]. As the composition is near the limits of **Drossel formula** (only the Zn is over the <0.63% limit), we employ its formula:

$$T_{LIQ} = 661 - 4.97\,Si - 0.15\,(Si)^2 - 6.13\,Cu - 17.4\,Mg + 2.72\,Zn + 5.08\,CuMg\ (^{\circ}C)$$

If we employ the **Vijayaraghavan formula** based on the aluminium-silicon-copper ternary phase, we must evaluate that the formula has not into account of the potential influence of other elements, so its accuracy is not so good:

$$T_{LIQ} = 664 - 6.9\,Si - 2.5\,Cu\ (^{\circ}C)$$

If we employ the second degree polynomial equations, we can obtain the Liquidus temperature in function of the **silicon equivalent**:

$$T_{LIQ}^{Al-Si\sum X_i} = 660.452 - 6.110 \sum Si_{EQ}^{Xi} - 0.057 \sum Si_{EQ}^{Xi\ 2}\ (^{\circ}C)$$

Where:

$$Si_{EQ} = Si + \sum Si_{EQ}^{Xi}\ (wt.\%)$$

And we obtain the values registered in Table 4.9. in ºC with an accuracy in the temperature measure of 0.1 ºC:

Sample	Drossel Liquidus temperature (ºC)	Vijayaraghavan Liquidus temperature (ºC)	Si$_{EQ}$ Calculated Liquidus temperature (ºC)	Experimental Liquidus temperature (ºC)
Al Si9 Cu3 Sample	598.7	600.3	593.1	591.8
0.2 wt.% SHS-TiB$_2$	598.3	600.1	592.9	592.2
0.2 wt.% Commercial TiB$_2$	599.8	601.3	593.9	604.3
0.1 wt.% of γ Al$_2$O$_3$	599.6	601.1	593.8	595.9
0.17 wt.% of α Al$_2$O$_3$	599.9	601.3	593.9	592.8

Table 4.9.: Liquidus temperature from the Silicon equivalent formula

Influence of Alumina (Al$_2$O$_3$) and Titanium Diboride (TiB$_2$) nanoparticles on the microstructure and properties of Al-Si9 Cu3 alloys for high pressure die casting applications.

CHAPTER 4: SOLIDIFICATION & MICROSTRUCTURE

We can observe that there are differences between the calculated liquidus temperatures and the experimental liquidus temperatures, but the most exact formula is the silicon equivalent, with values very similar to values estimated in this study. So we can employ this formula for the calculation of Liquidus temperature of non-reinforced alloys, but when we add TiB$_2$ ceramic particles the formulations are not capable of predicting the changes produced by ceramic particles. We can adjust the Si$_{EQ}$ formula to determinate the Liquidus temperature in order to introduce a coefficient to evaluate the effect of 0.02 wt.% of TiB$_2$ particle additions with the values obtained in table 4.9.:

$$T_{LIQ}^{Al-Si \sum X_i}{}_{TiB2} = 660.452 - 6.110 \sum Si_{EQ}^{Xi} - 0.057 \sum Si_{EQ}^{Xi\,2} \quad \mathbf{\underline{+ 4.85\ (^oC)}}$$

The calculated **maximum eutectic temperature** for an unmodified alloy (T$_R$) is calculated by the equation suggested by Mondolfo [Mon 79]:

$$T_{Re} = 577 - \frac{12.5}{W_{Si}}.(4.43 \cdot w_{Mg} + 1.43 \cdot .W_{Fe} + 1.93 \cdot W_{Cu} + 1.7 \cdot W_{Zn} + 3.0 \cdot W_{Mn} + 4.0 \cdot W_{Ni})\,(^oC)$$

Another way to make the calculation is with the formula proposed by Gruzleski et al [Gru 95]

$$T_{AlSi,E} = 660.452 - (6.11\ Si + 0.057\ Si^2)\,(12.6/Si) - (3.4\ Cu + 1.34\ Fe + 6.3$$
$$Mg + 1218.9\ Sr - 32965\ Sr^2 - 4.293\ Sb + 186.3\ Sb^2 - 495.5\ Sb^2)\,(^oC)$$

If we employ the second degree polynomial equations, we can obtain the eutectic nucleation temperature function of the silicon equivalent proposed by Djurdjevic [Dju 11]:

$$T_{EAlSiNUC} = 660.452 - [(6.11\ Si_{EQ} + 0.057\ Si_{EQ}^2) * (\ Si_{AL-Si\ EU}/Si_{ACTUAL})]\,(^oC)$$

The obtained results are show in Table 4.10 with an accuracy in the temperature measure of 0.1 ^oC.

Sample	Mondolfo Eutectic nucleating temperature (^oC)	Gruzleski Eutectic nucleating temperature (^oC)	Si$_{EQ}$ Calculated Eutectic nucleating temperature (^oC)	Experimental Eutectic nucleating temperature (^oC)
Al Si9 Cu3 Sample	566.4	569.8	561.5	562.8
0.2 wt.% SHS-TiB$_2$	566.4	569.7	561.5	563.0
0.2 wt.% Commercial TiB$_2$	566.4	570.0	561.4	567.6
0.1 wt.% of γ Al$_2$O$_3$	566.4	570.0	561.4	567.9
0.17 wt.% of α Al$_2$O$_3$	566.2	569.9	561.4	563.8

Table 4.10.: Maximum eutectic temperature calculation

Influence of Alumina (Al$_2$O$_3$) and Titanium Diboride (TiB$_2$) nanoparticles on the microstructure and properties of Al-Si9 Cu3 alloys for high pressure die casting applications.

CHAPTER 4: SOLIDIFICATION & MICROSTRUCTURE

We notice that the most accurate calculation is made with the Si$_{EQ}$ method for the unreinforced alloy. So we can employ this formula for the calculation of Liquidus temperature of non-reinforced alloys, but when we add ceramic particles the formulations are not capable of predicting the changes produced by ceramic particles. However in this case the temperature variation is smaller than in the nucleation temperature (Maximum 5ºC).

We can adjust the Si$_{EQ}$ formule to determinate the eutectic nucleation temperature in order to introduce a coefficient to evaluate the effect of 0.02 wt.% of TiB$_2$ or Al$_2$O$_3$ particle additions:

$$T_{EAlSiNUC} = 660.452 - [(6.11\ Si_{EQ} + 0.057\ Si_{EQ}^2) * (Si_{AL\text{-}Si\ EU}/Si_{ACTUAL})] + \textbf{4.15\ (ºC)}$$

The higher the coalescence time, the longer the primary dendrites, with a smaller grain size in the longitudinal direction of base alloy. The diminution of plateau time denotes that the interdendritic liquid is less than in the sample, with smaller secondary arm dendritic spacing (SDAS). In the case of 0.17 wt.% alpha Al$_2$O$_3$ alloy, the eutectic temperature is much lower than in the sample, and a better modification is expected in this sample, and worse in 0.1% of gamma Al$_2$O$_3$ briquette and 0,2% commercial TiB$_2$ briquette with 90%Al and 10% TiB$_2$.

4.2.2 Discussion and conclusions of the solidification study

Solidification curves of both the reinforced and unreinforced materials have been obtained by casting the materials into normalized sand cups containing thermocouples linked to a data acquisition system. The T-t curves and their corresponding dT/dt curves provide valuable information on the solidification and precipitation of intermetallic phases. We can observe the comparison of the curves in Fig. 4.16.
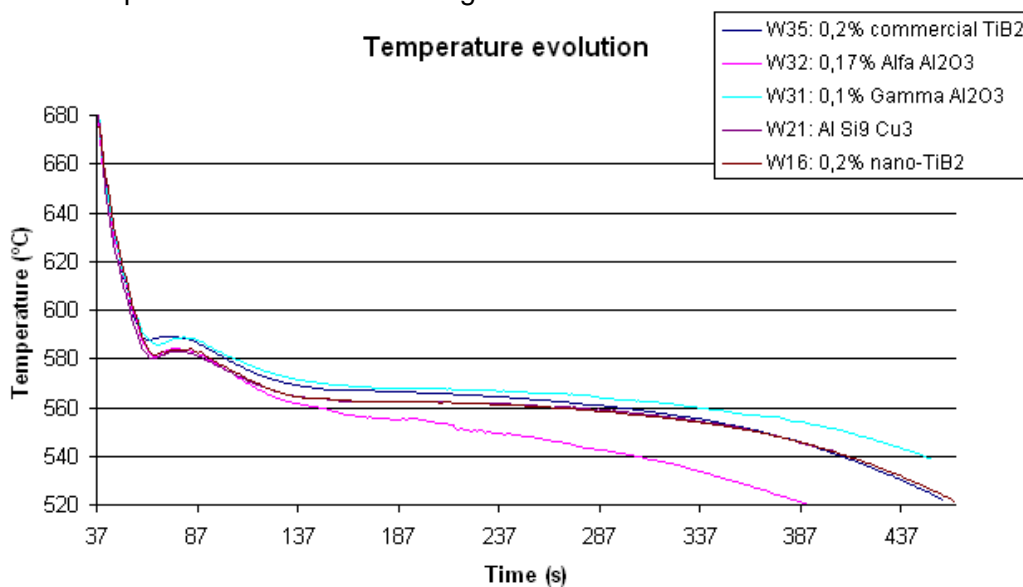

Figure 4.16.- Temperature evolution graphic

CHAPTER 4: SOLIDIFICATION & MICROSTRUCTURE

The **addition of ceramic particles made a modification of the solidification curve**, leading to:

- An increase of the recalescence temperature and a decrease in the temperature variation in the recalescence area. Only with the 0.17 wt.% of α-alumina, the results are very similar to the results obtained with the alloy sample. An increase of the temperature of α-aluminium dendrites is also detected.

- An increase of temperature of intermetallics precipitation (Al Mn Fe, Mg_2 Si, Al_2 Cu, Al_5 Mg_8 Si_6 Cu_2).

- Liquidus temperature calculation by drossel / Vijayaraghavan and Silicon equivalent, give an approximate value of liquidus temperature, with a narrowest result for silicon equivalent technique. However, this formula is not prepared to determinate the variation in the liquidus temperature induced by the TiB_2 and Al_2O_3 reinforcements. There is an increase between 2 and 8 °C approximately.

With this results, in the **first area (Nucleation)**, we can deduce, due to the increase of the temperature and the decrease of the recalescence area and recalescence time, 1) that there is a better nucleation, and 2) the effect of the nanoparticles gets a better nucleated DTA profile for the TiB_2 particles, and something intermediate for Al_2O_3 particles. These results can be observed in Fig. 4.17., where the Al-Si9Cu3 has the smaller recalescence temperature and the biggest undercooling.
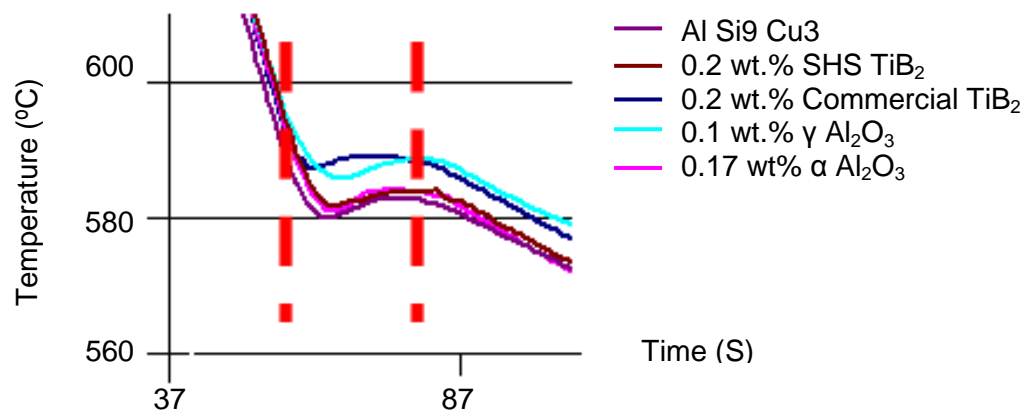

Figure 4.17.- Recalescence comparison between samples

Influence of Alumina (Al$_2$O$_3$) and Titanium Diboride (TiB$_2$) nanoparticles on the microstructure and properties of Al-Si9 Cu3 alloys for high pressure die casting applications.

CHAPTER 4: SOLIDIFICATION & MICROSTRUCTURE

In the **second area (Modification),** we can observe in Fig 4.18. that the 0.1 wt.% γ-alumina and 0.2 wt.% commercial TiB$_2$ have a more acicular characteristic curve because they are the ones with higher temperatures, the Al Si9 Cu3 sample and the 0.2 wt.% SHS TiB$_2$ are very similar with a fibrous structure and the 0.17 wt.% of α-alumina has a more laminate characteristic curve, because it has the smallest temperature in the eutectic area.
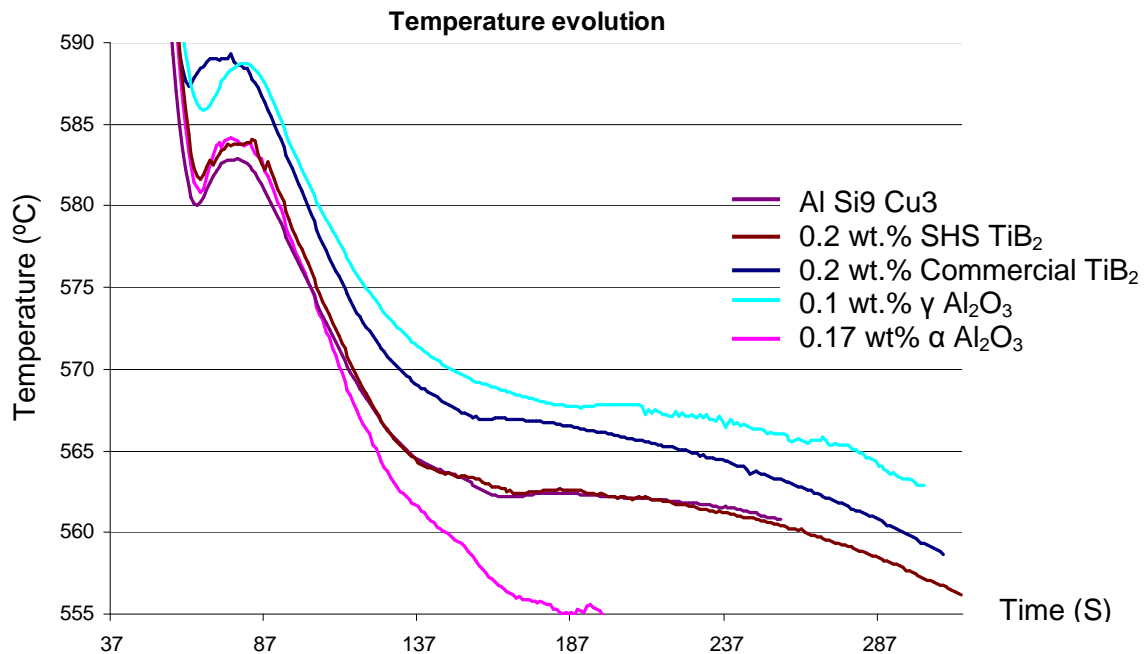

Figure 4.18.- Modification comparison between samples

Conclusions of the study of the comparison between samples

- An increase of eutectic main reaction temperature with Si and Mn-Fe phases, except the 0.17 wt.% of α-alumina, but in the rest of the different concentration essays studied in the project (10 samples of γ and α Al$_2$O$_3$ nano-reinforced alloys with concentrations between wt. 0.01% to 1%), the eutectic temperature is higher (The media is about 5 ºC higher). This difference in 0.1 wt.% γ-alumina can be explained by variations during the DTA essay.

- The coalescence time is bigger in all the reinforced alloys. That corresponds with larger dendrites. A higher value can be also related with the directional dendrites, because they have more time to grow.

Influence of Alumina (Al$_2$O$_3$) and Titanium Diboride (TiB$_2$) nanoparticles on the microstructure and properties of Al-Si9 Cu3 alloys for high pressure die casting applications.

CHAPTER 4: SOLIDIFICATION & MICROSTRUCTURE

- The plateau time is smaller in all the reinforced alloys, corresponding with smaller secondary dendrites arm spacing.

- The comparison between the TiB$_2$ and Al$_2$O$_3$ particles shows that TiB$_2$ particles have a lower coalescence time than Al$_2$O$_3$ particles, but they have a bigger plateau time. That difference should give a larger and with a bigger SDAS in the case of TiB$_2$ particles.

- Calculation of eutectic temperature by Mondolfo´s, Gruzleski and Djurdjevic gives a very good estimation, especially with Djurdjevic formula (Within 1ºC). However, is not capable of determinate the variation promoted by the reinforcement particles, with differences of about 5-10ºC.

- Very small concentrations of in situ or ex situ produced ceramic particles modify the DTA´s curves, making difficult to automate the control process.

4.3 Influence of TiB$_2$ and nano-Al$_2$O$_3$ particles on the microstructure

The microstructure of the TiB$_2$ and Al$_2$O$_3$ reinforced alloys has been analysed with OM, SEM and TEM. These studies have been completed with WDS analysis. Samples have been studied and their microstructures have been compared with the unreinforced alloys cast in the same conditions.

The main objective was to analyse the chemical interactions between the particles and the aluminium alloy matrix components that helped understanding the measured change of thermal and mechanical properties of the reinforced material. It is known that the TiB$_2$ particles have a grain size decreasing effect, following mechanisms already researched and used by the aluminium grain refining industry. The role and mechanisms of the Al-Ti-B grain refiners, that contain such particles, have been thoroughly studied but the main interest of the microstructural analysis was to check any other possible interactions that may appear with higher TiB$_2$ contents and smaller particles. In the case of the Al$_2$O$_3$, many studies have been carried out to make AMCs reinforced with alumina, and the study of the shape, quantity and surface treatments in order to increase the wettability between the matrix and the alumina. We are going to study Al$_2$O$_3$ and TiB$_2$ particles because they don't react with molten aluminium, and they can have a relative good wettability. Small particle size and narrow size distribution, large surface area, spherical morphology are qualities that have the elected particles, in order to obtain the best microstructures and properties with rounded nano-particles of 40 and 15 nm in the stable and metastable α and γ Al$_2$O$_3$, and TiB$_2$ particles with round faces by the decrease from 5 microns to about 500 nm after milling.

Influence of Alumina (Al$_2$O$_3$) and Titanium Diboride (TiB$_2$) nanoparticles on the microstructure and properties of Al-Si9 Cu3 alloys for high pressure die casting applications.

CHAPTER 4: SOLIDIFICATION & MICROSTRUCTURE

4.3.1 Microstructure of the Al-Si based materials reinforced with nano-TiB$_2$ and nano-Al$_2$O$_3$

The Al-Si alloys have been one of the most studied alloys for sand, die casting and LPDC, but no so much the Al Si9 Cu3 Fe1 that it's employed in aluminium HPDC. Due to the excellent combination of properties it shows, Al Si9 Cu3 is employed with good castability and mechanical properties. The number of works related to the study of the microstructure of the alloy reinforced with nano-TiB$_2$ is very low and not any reference has been found where the Al-Si9Cu3 + nano-TiB$_2$ alloys have been fabricated by HPDC. The analysis of those previous works suggests that the presence of TiB$_2$ particles has an influence on the grain size and morphology of α phase of the composite materials [Mis 04]. In some studies [Sch 07] [Kum 09], TiB$_2$ particles are observed at the grain boundaries, suggesting that they are pushed out during solidification, but a small proportion are also retained within the α-Al grains due to engulfment.

The number of works related to the study of the microstructure of the Al SI9 Cu3 alloy reinforced with nano-Al$_2$O$_3$ is very low, though some references has been found where the Al-Si + Al$_2$ O$_3$. The analysis of those previous works suggests that the increase of surface roughness of Al$_2$O$_3$ particles increase the wetting contact angle, reducing wetting [Agu 10] .The presence of Al$_2$O$_3$ particles has an influence on the grain size and morphology of the α phase of the composite materials because Al$_2$O$_3$ particles are pushed by the aluminium dendrites into the last freezing eutectic liquid. Thus, Al$_2$O$_3$ particles are surrounded by the eutectic silicon, with a good interfacial bonding, and some of the particles within the grains [El- 10]. Aluminium dendrites became smaller and a more fine eutectic area is obtained [Hüs06]. In the case of Al-Si hypereutectic alloys reinforced with γ -Al$_2$O$_3$ and TiO$_2$, they have a refinement of microstructure, of the dendritic arm length, the SDAS, the interlamellar spacing in the eutectic silicon phase and the primary silicon particles [El- 11].

Influence of Alumina (Al$_2$O$_3$) and Titanium Diboride (TiB$_2$) nanoparticles on the microstructure and properties of Al-Si9 Cu3 alloys for high pressure die casting applications.

CHAPTER 4: SOLIDIFICATION & MICROSTRUCTURE

4.3.1.1 Optical and SEM microscopy analysis

The comparison of the microstructure between the Al Si9 Cu3 and reinforced alloys provides clear indications of the effect of the TiB$_2$ and Al$_2$O$_3$ particles. TiB$_2$ particles cannot be discerned at low magnifications due to their small size (0.5-2.5 microns) but their influence can be indirectly appreciated. The reinforcing particles modify the microstructure of the samples, giving two different areas, one granular in the periphery and another acicular in the center. In this acicular area, the grains are orientated, and the subgrains are much smaller, with a best distributed eutectic. If the percentage of solute is increased, they are more heterogeneous nuclei, promoting an equiaxial dendrite structure. Also if we increase the cooling rate, the structure tends to an equiaxial dendrite structure. If the cooling is very slow and the solute concentration is low, cellular dendrites are formed.

The reinforced alloys were also analysed with the SEM technique. The main objective was to identify the different phases and to observe the possible interaction and influence of the TiB$_2$ and Al$_2$O$_3$ particles.

a) Al Si 9 Cu3 Sample:

We are going to study first the Al Si9 Cu3 base alloy, in order to establish a point to make a comparison with the reinforced alloys. As we can see in the micrograph of Fig. 4.19., there is homogeneous grain dispersion in all the areas, with equiaxial dendrites in the periphery and in the center.
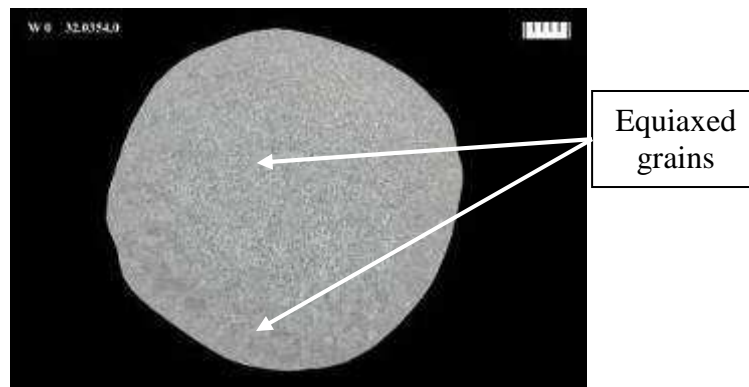

Figure 4.19.- Al Si9 Cu3 alloy TP1 essay OM macrograph analysis

Influence of Alumina (Al$_2$O$_3$) and Titanium Diboride (TiB$_2$) nanoparticles on the microstructure and properties of Al-Si9 Cu3 alloys for high pressure die casting applications.

CHAPTER 4: SOLIDIFICATION & MICROSTRUCTURE

We can observe in Fig. 4.20 that they are some little microshrinkages. The grains are equiaxial and the structure is quite modified with rounded dendrites. Solute percentage is higher in the center than in the periphery.
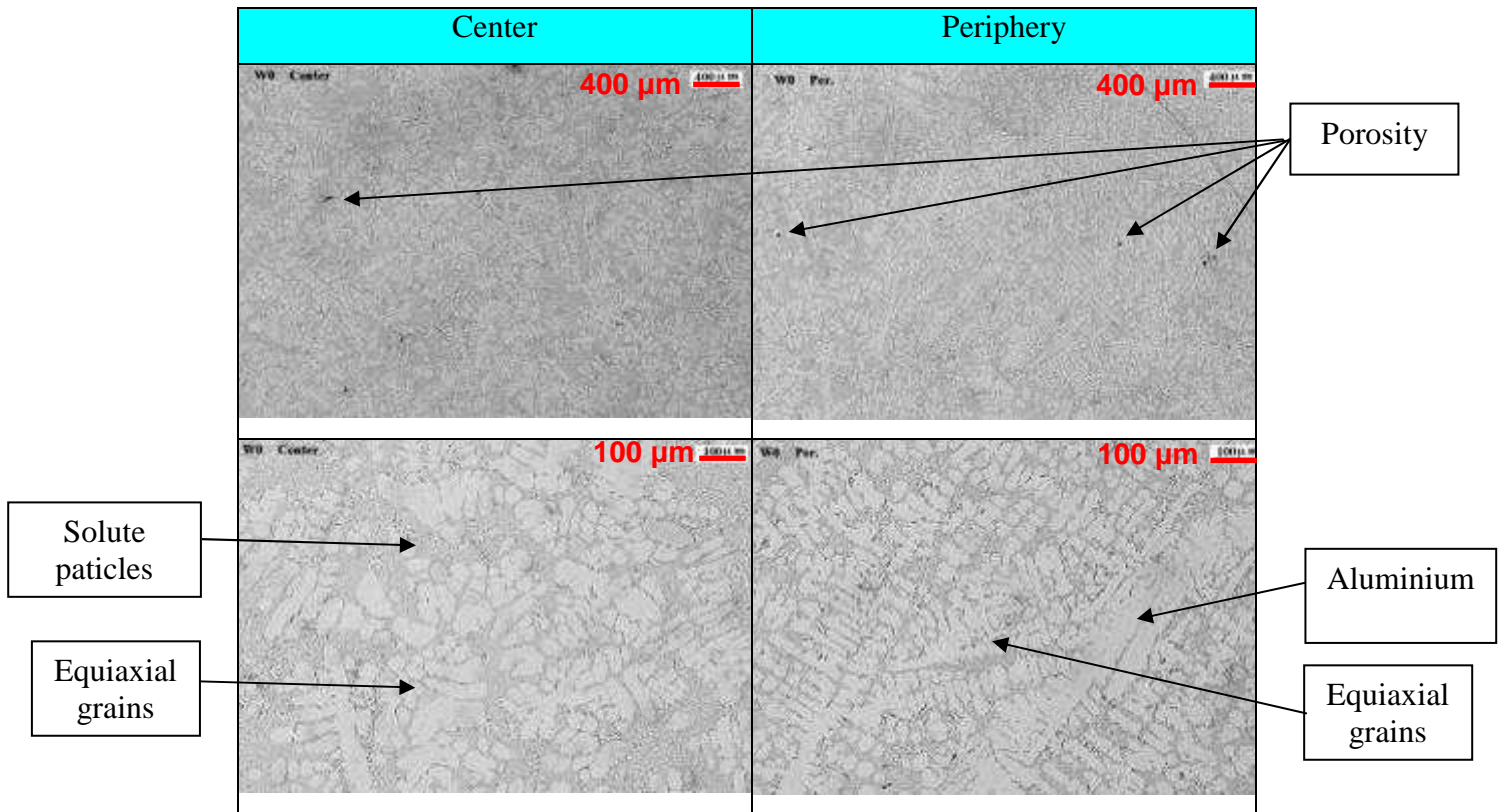

Fig. 4.20.: Al Si 9 Cu3 OM micrographs

As we can see in Fig. 4.21., the aluminium dendrites (dark structures) are surrounded by eutectic aluminium silicon (grey) and intermetallics (white rounded particles). The grains have an equiaxial form. As we can see, the aluminium dendrites are surrounded by eutectic silicon and intermetallics. The grains have and equiaxial form. We can conclude that it's a typical structure of an Al Si9 Cu3 alloy.
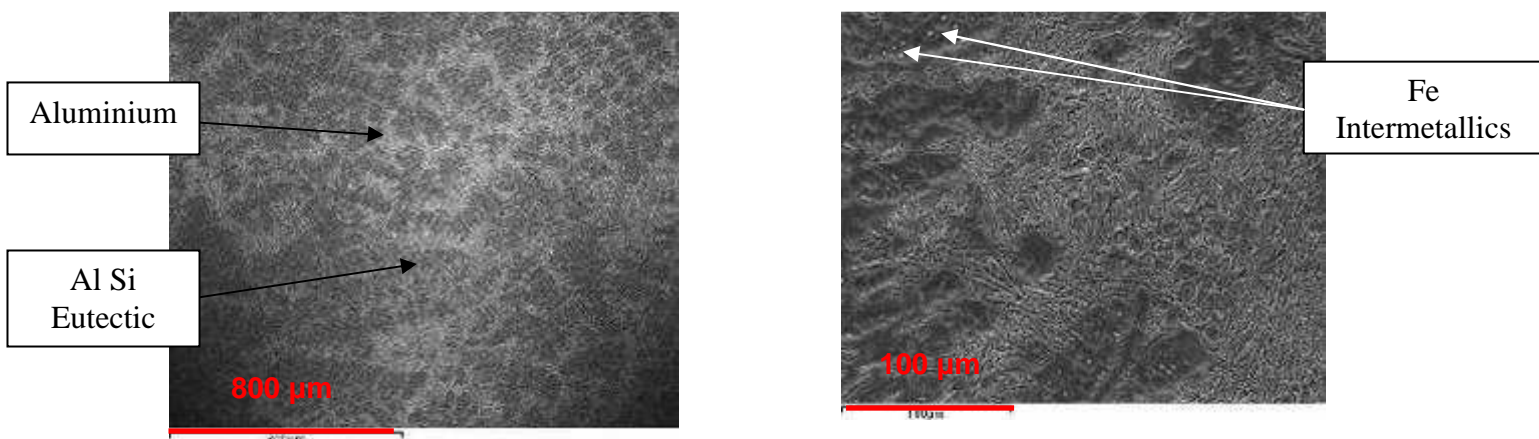

Figure 4.21.- Al Si9 Cu3 typical SEM micrographs

Influence of Alumina (Al$_2$O$_3$) and Titanium Diboride (TiB$_2$) nanoparticles on the microstructure and properties of Al-Si9 Cu3 alloys for high pressure die casting applications.

CHAPTER 4: SOLIDIFICATION & MICROSTRUCTURE

b) 0.2 wt.% SHS-TiB$_2$ and 0.2 Commercial TiB$_2$

The study of the microstructure of SHS and comercial TiB$_2$ reinforced alloys can give us an idea of how the nano-particles modify the structure and properties of reinforced alloys, due to the very difficult particle detection when we employ only a 0.2% of TiB$_2$ reinforcement. After the analysis of the different samples, we have conclude that micrograph structures are near the same in both TiB$_2$ reinforced alloys. Because of that, we are going to show the results of the study of one of the alloys, in this case the SHS-TiB$_2$ reinforced alloy. We can observe in Fig. 4.22. that there is a non-homogeneous grain, with equiaxial dendrites in the periphery and columnar dendrites in the center. Very little microshrinkages are observed.
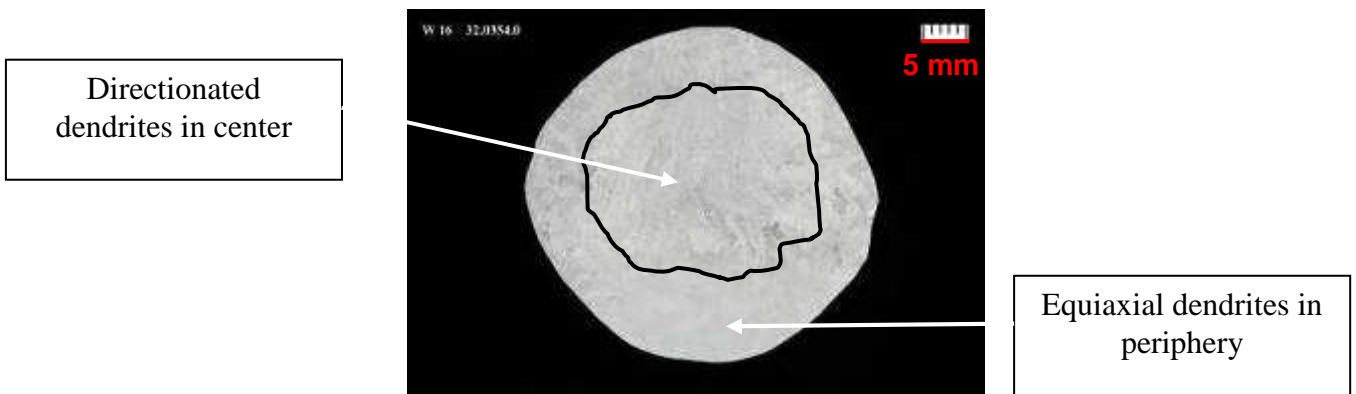

Figure 4.22.- SHS-TiB$_2$ reinforced alloy TP1 essay OM macrograph analysis

It's very important to know how good the recovery of TiB$_2$ particles is after the dissolution in the molten aluminium. Ti recovery percentage is estimated (by the base alloy composition, the percentaje of added reinforcement and the obtained alloy composition) of 78.3% in the SHS TiB$_2$ reinforced alloy and 76.2% in the commercial TiB$_2$ reinforced alloy. It's not a very good recovery rate, because if we compare with Al Ti5 B1 standard row, the percentage is about the 98%.

Influence of Alumina (Al$_2$O$_3$) and Titanium Diboride (TiB$_2$) nanoparticles on the microstructure and properties of Al-Si9 Cu3 alloys for high pressure die casting applications.

CHAPTER 4: SOLIDIFICATION & MICROSTRUCTURE

As we can see in the micrographs in table 4.23, there is a non-homogeneous grain, with equiaxial dendrites in the periphery and columnar dendrites in the center. Very little microshrinkages are observed.
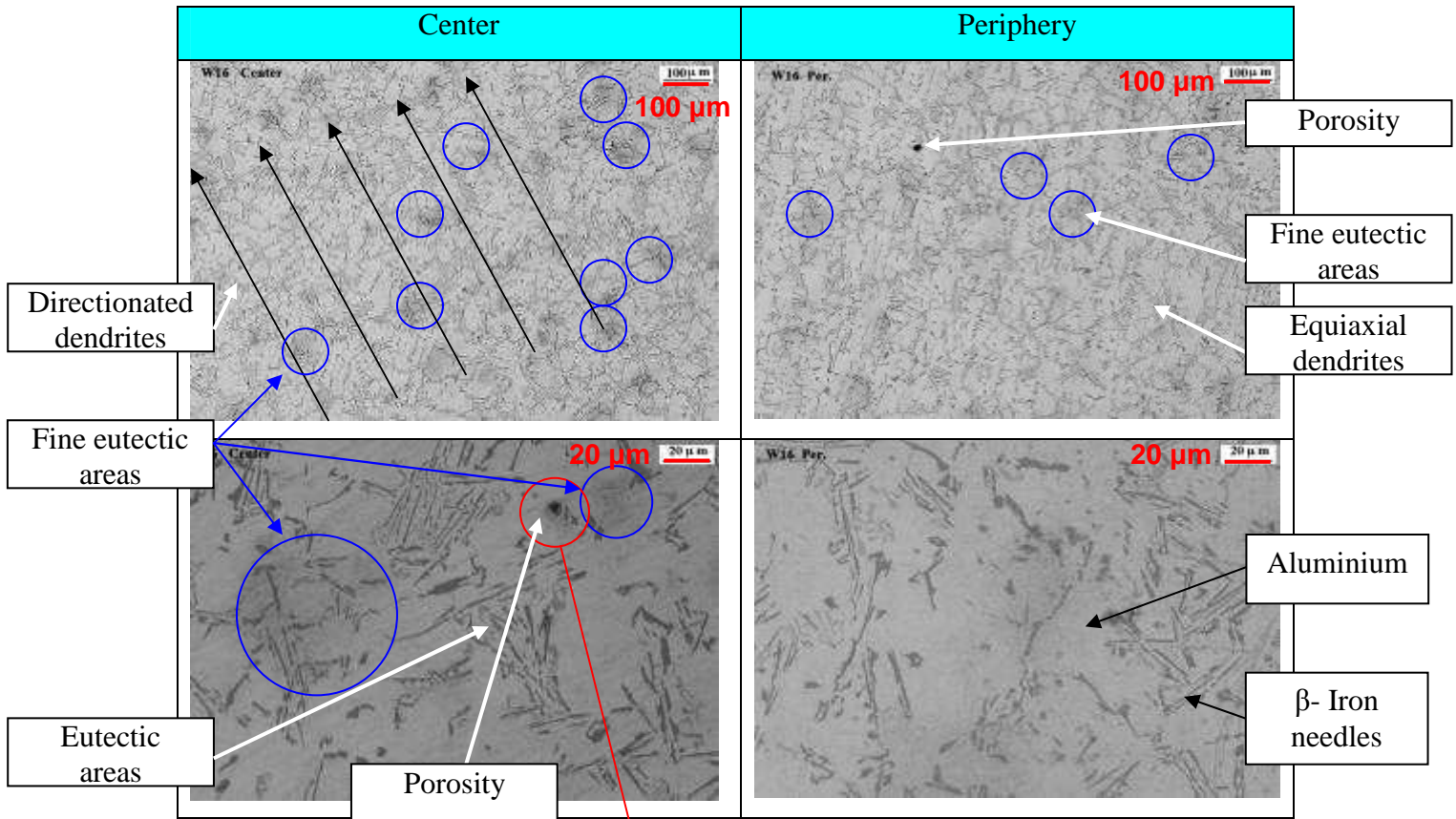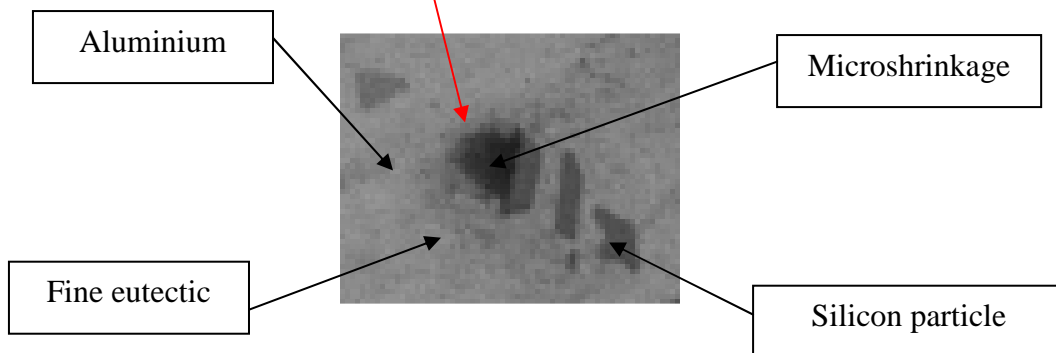

Fig. 4.23: OM Study of grain and precipitates in the central and peripheral areas

The porosity decreases in the center, being stabilized by eutectic silicon particles.

Influence of Alumina (Al$_2$O$_3$) and Titanium Diboride (TiB$_2$) nanoparticles on the microstructure and properties of Al-Si9 Cu3 alloys for high pressure die casting applications.

CHAPTER 4: SOLIDIFICATION & MICROSTRUCTURE

With the combination of EDS and SEM we determinate the different elements that constitute the alloy, as we can observe in Fig. 4.24 and Fig. 4.25. We can't see in the pictures the composition and the presence of TiB$_2$ particles in the center or in the border of grain. There is a different structure in the periphery and the center of the sample, as we have seen in the optical microscopy. TiB$_2$ particles modify the microstructure of the samples, giving two different areas, one granular in the periphery and another acicular in the center. In this acicular area, the grains are orientated, and the sub grains are much smaller, with a best distributed eutectic. We can see that the aluminium dendrites are surrounded by very fine eutectic silicon and intermetallics, with a higher concentration of solute in the center, and the only difference between the two TiB$_2$ reinforced alloys is that in the case of commercial TiB$_2$ reinforced alloy are less fine eutectic areas than in the case of reinforcing with SHS-TiB$_2$. The EDS and SEM observed Fe intermetallics are formed as skeleton structures in the center, but small β-iron rich needles are detected in the periphery. Not β-iron needles are detected. There is a higher solute concentration in the center, with narrowest dendrites. Same porosity is detected associated to the eutectic precipitations. There has been not possible to detect any TiB$_2$ particle in the sample. We suppose that the TiB$_2$ is well dissolved in the aluminium matrix or in the grain boundary, and in this case, the titanium concentration is so low that it's very difficult to detect by EDS.
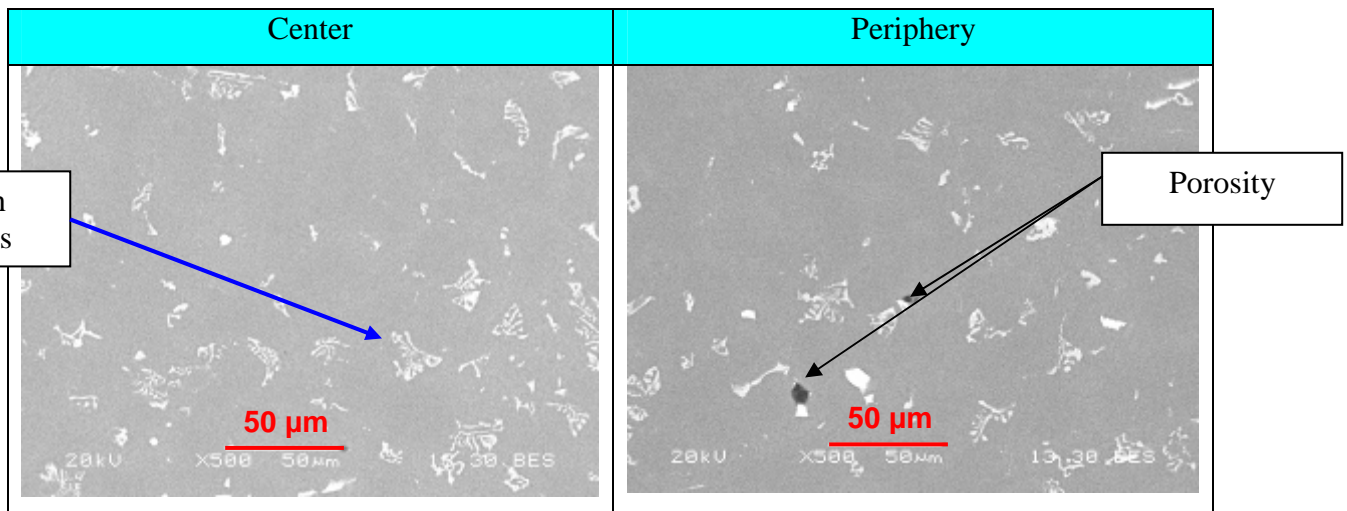

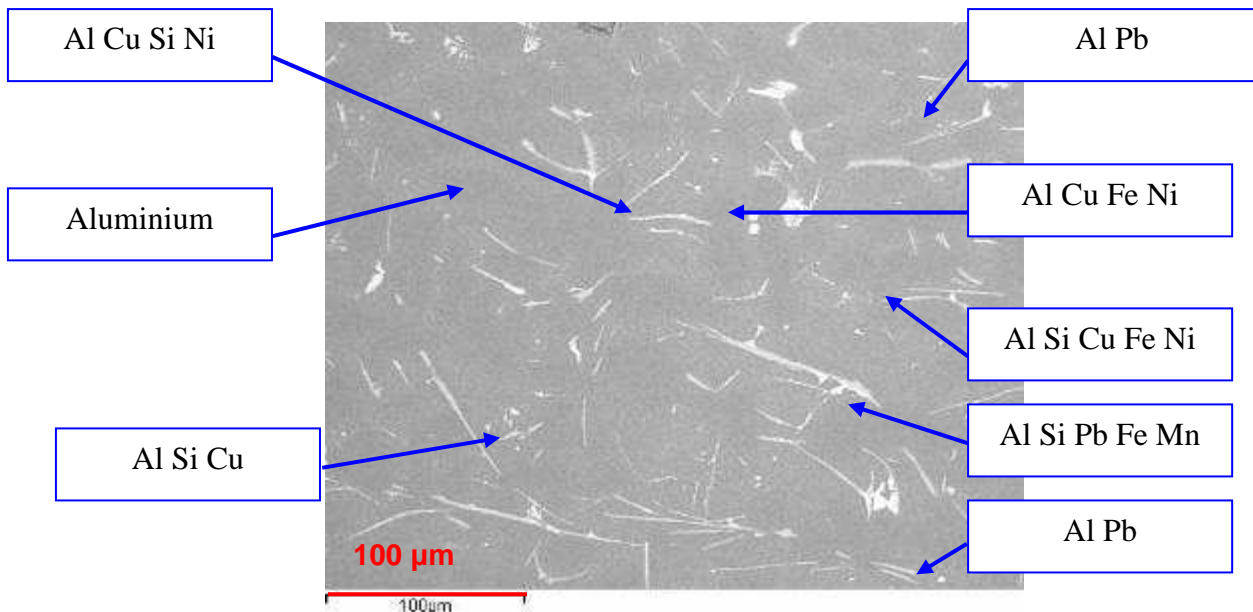**Fig. 4.24.: SEM study of SHS-TiB$_2$ reinforced alloy**

Influence of Alumina (Al$_2$O$_3$) and Titanium Diboride (TiB$_2$) nanoparticles on the microstructure and properties of Al-Si9 Cu3 alloys for high pressure die casting applications.

CHAPTER 4: SOLIDIFICATION & MICROSTRUCTURE

Al Cu Si Ni

Al Pb

Aluminium

Al Cu Fe Ni

Al Si Cu Fe Ni

Al Si Pb Fe Mn

Al Si Cu

Al Pb

100 µm

100µm

Figure 4.25.- Phase determination in SHS-TiB$_2$ reinforced alloy by EDS and SEM

We can obtain the next conclusions after the analysis of the differences between the center and the periphery:

- Equiaxial dendrites in the periphery, and Equiaxial - Columnar in the center.

- Higher solute concentration in the center.

- Narrowest and directional / oriented dendrites in the center.

- More areas with the very fine eutectic structure in the central area (Blue circles in Fig. 4.23).

- The porosity decreases in the center, being stabilized by eutectic silicon particles (Fig. 4.23). Less porosity than the Al-Si9Cu3 base alloy.

- Free β-iron phases have been not detected. However lots of beneficial skeleton structures are dispersed homogeneously.

Influence of Alumina (Al$_2$O$_3$) and Titanium Diboride (TiB$_2$) nanoparticles on the microstructure and properties of Al-Si9 Cu3 alloys for high pressure die casting applications.

CHAPTER 4: SOLIDIFICATION & MICROSTRUCTURE

C) 0.1 wt.% of gamma Al$_2$O$_3$ and 0.17wt. % of alfa Al$_2$O$_3$:

The study of the microstructure of Al$_2$O$_3$ reinforced alloy is important to determinate the structure and properties of the reinforced alloys, and also can give us the distribution, size and function of Al$_2$O$_3$ particles in the grains and grain boundaries. After the analysis of the different samples, we have concluded that micrograph structures are near the same in both Al$_2$O$_3$ reinforced alloys. Because of that, we are going to show the results of the study of one of the alloys, in this case the 0.1 wt.% γ-Al$_2$O$_3$ reinforced alloy. We can observe in Fig.4.26. that there are equiaxial dendrites in the periphery and columnar dendrites in the center. No microshrinkages are observed.
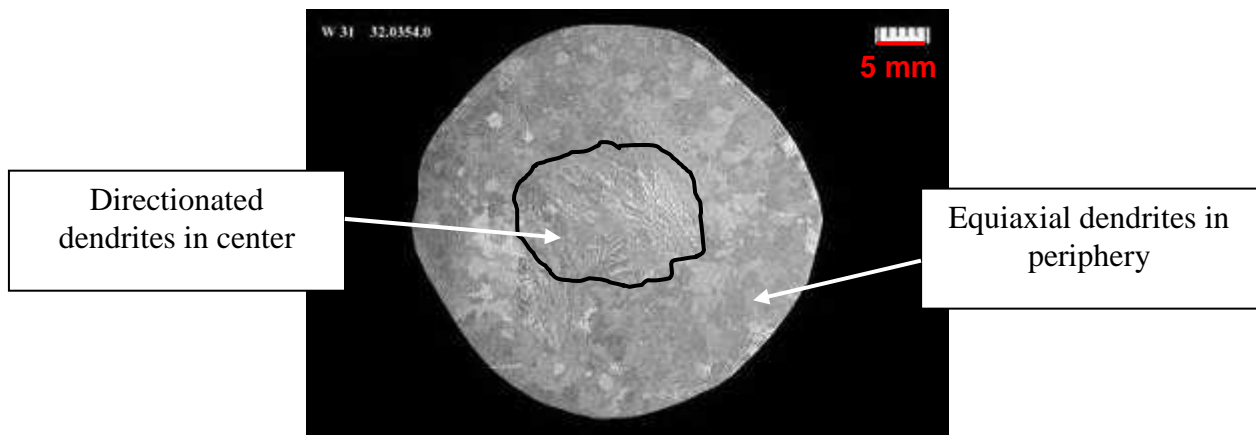

Figure 4.26.- 0.1 wt.% γ-Al$_2$O$_3$ reinforced alloy TP1 essay OM macrograph analysis

The alumina recovery percentage is estimated (by the base alloy composition, the percentaje of added reinforcement and the obtained alloy composition) in a 78.3%. It's not higher due to the low melting temperature and because we don't use magnesium to increase the dissolution of Al$_2$O$_3$.

Influence of Alumina (Al$_2$O$_3$) and Titanium Diboride (TiB$_2$) nanoparticles on the microstructure and properties of Al-Si9 Cu3 alloys for high pressure die casting applications.

CHAPTER 4: SOLIDIFICATION & MICROSTRUCTURE

As we can see in the micrographs in Fig. 4.27., there is a non-homogeneous grain, with equiaxial dendrites in the periphery and columnar dendrites in the center. Very little microshrinkages are observed.
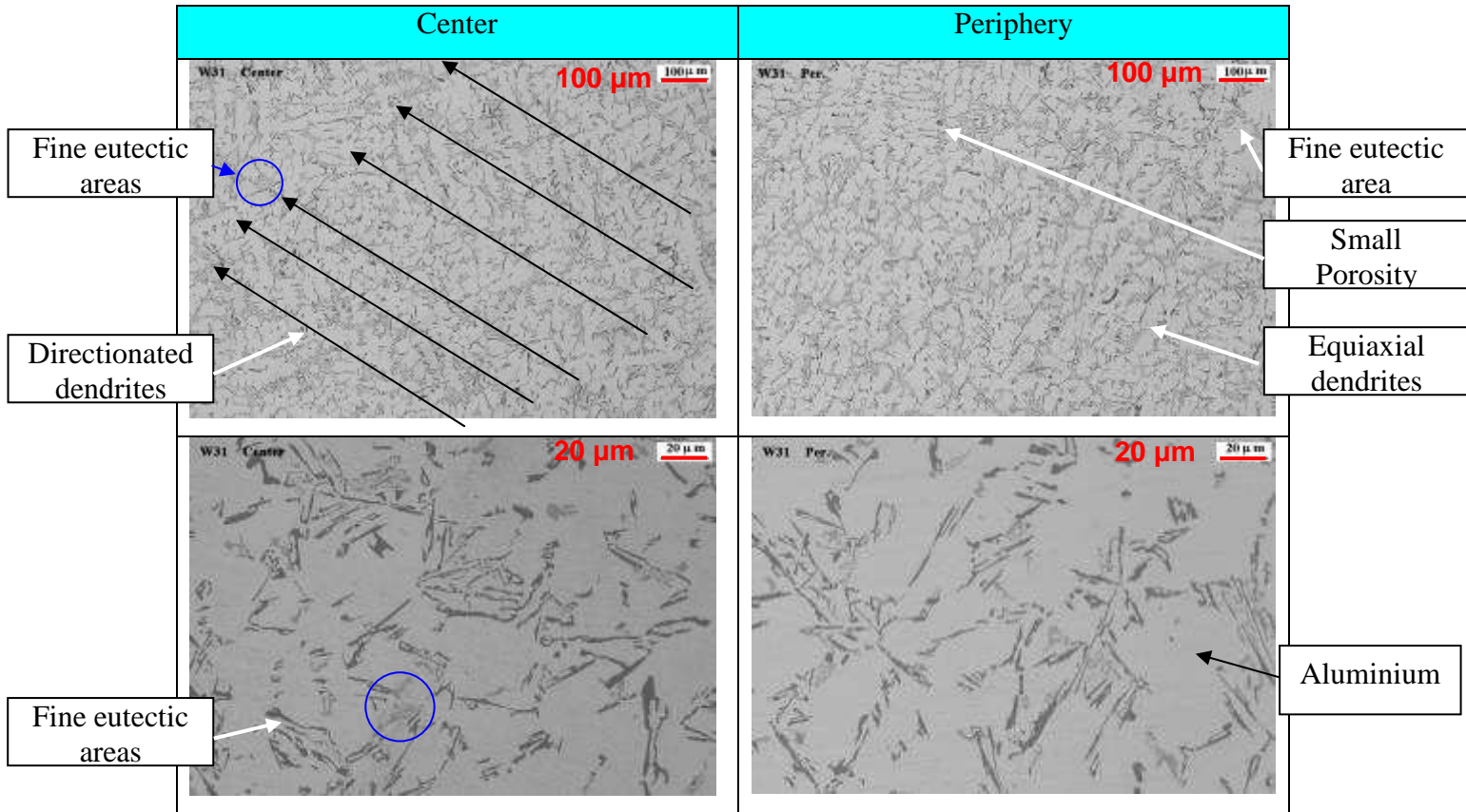
Figures 4.27.: OM Study of grain and precipitates in the central and peripheral areas

With the EDS and SEM we determinate the elements that constitutes the alloy. We can observe the composition of the phases in the Fig. 4.28.
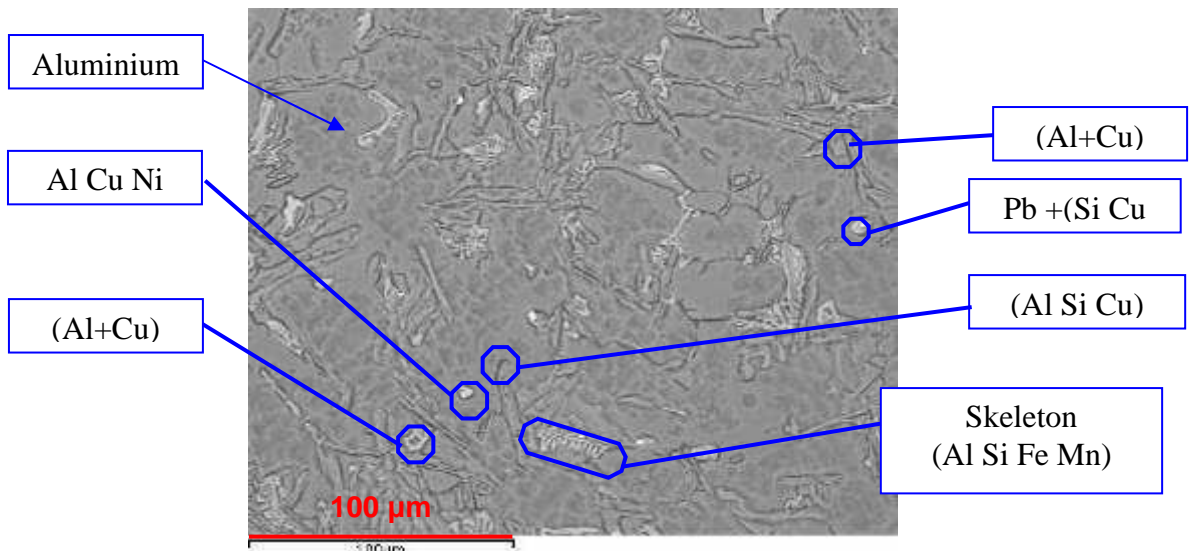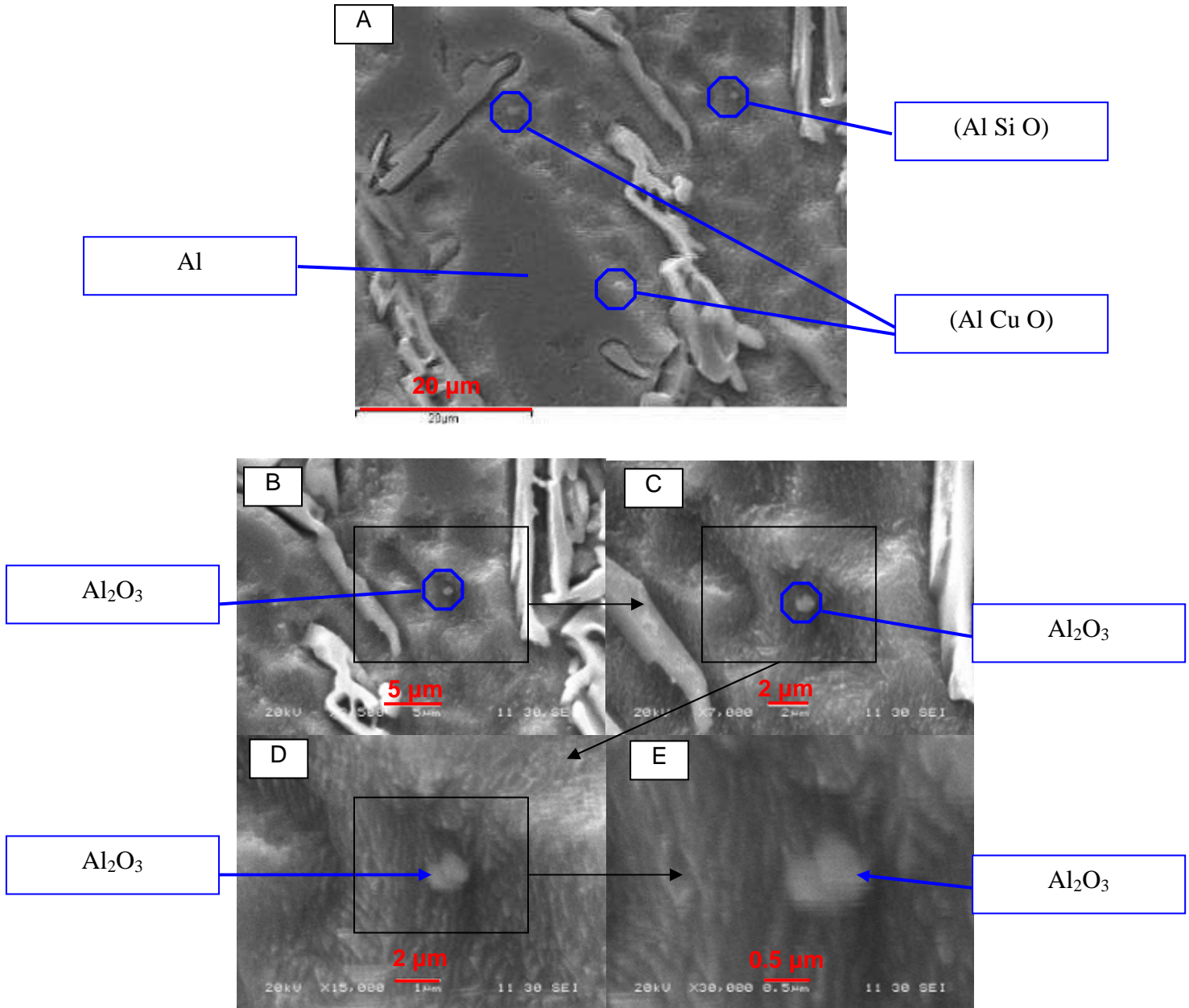

Figure 4.28.- Phase determination in γ-Al$_2$O$_3$ reinforced alloy by EDS and SEM

Influence of Alumina (Al$_2$O$_3$) and Titanium Diboride (TiB$_2$) nanoparticles on the microstructure and properties of Al-Si9 Cu3 alloys for high pressure die casting applications.

CHAPTER 4: SOLIDIFICATION & MICROSTRUCTURE

We can observe the presence of Al$_2$O$_3$ in the alloy in the center of the aluminium grains and in the grain boundary in the Fig. 4.29. A,B,C,D and E. The grains inside the aluminium grains affect the nucleation effect. The grains that are near the grain boundaries are pushed by the solidification front, but observed Al$_2$O$_3$ particles in spite of being near the grain boundaries, they seem to be also nucleating sides.

Figures 4.29. A,B,C,D and E.- Al$_2$O$_3$ particles detection by EDS and SEM

Influence of Alumina (Al$_2$O$_3$) and Titanium Diboride (TiB$_2$) nanoparticles on the microstructure and properties of Al-Si9 Cu3 alloys for high pressure die casting applications.
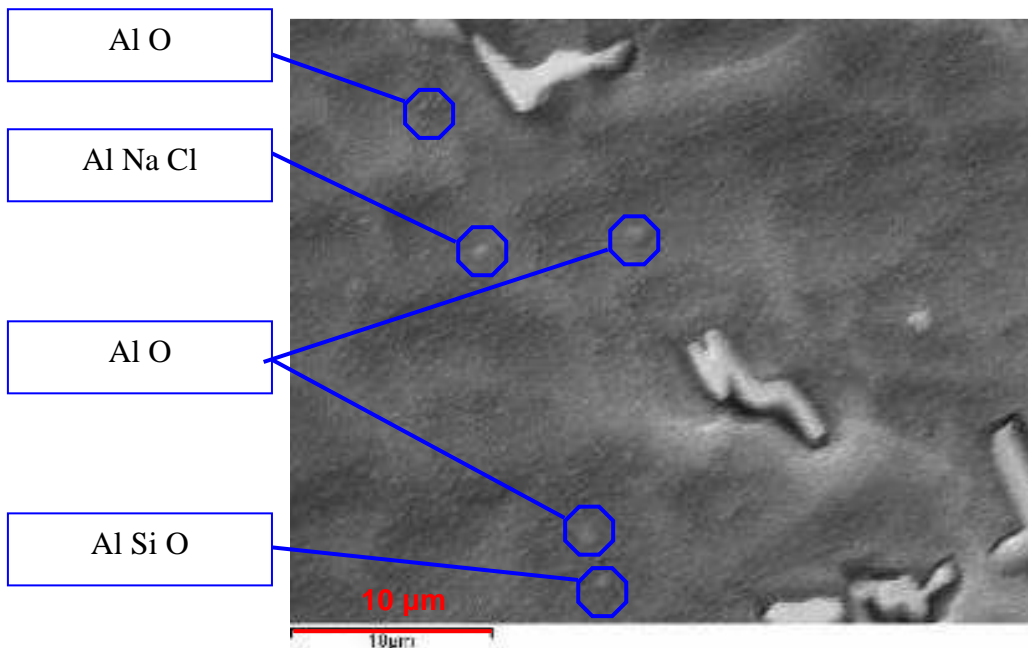
CHAPTER 4: SOLIDIFICATION & MICROSTRUCTURE

Al$_2$O$_3$ particles are presented in the center of the grains. They act as grain refiners, with an agglomerated structure of about 0.5 to 1 Microns, which corresponds to the size more adequate to act as grain refiner for TiB$_2$ nucleating particles [Que 04-02].

We can obtain the next conclusions after the analysis of the differences between the center and the periphery, and from the microstructure:
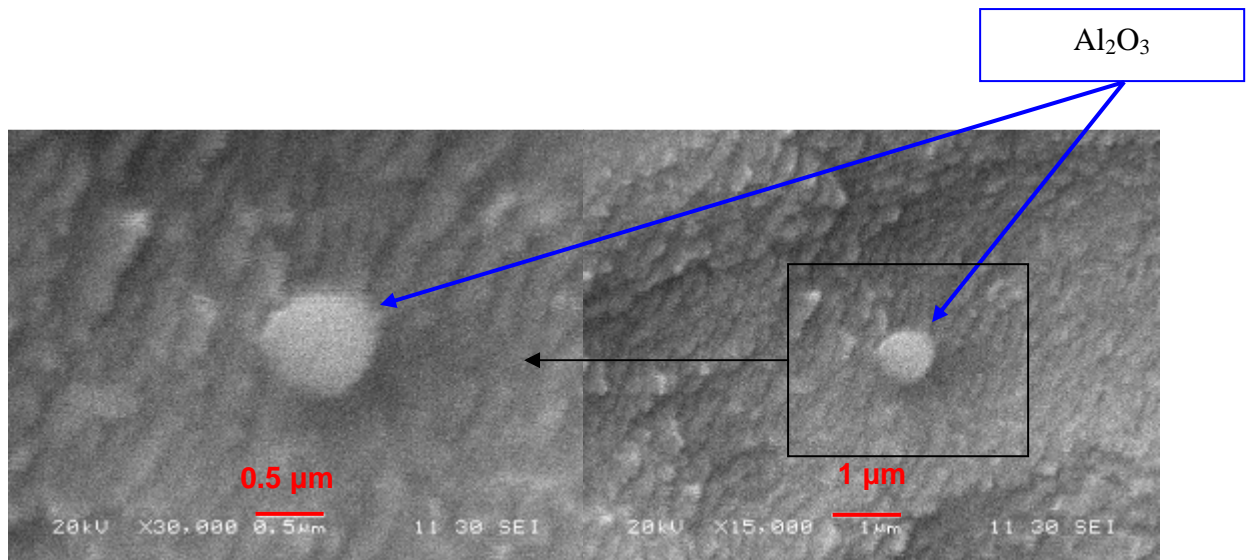
- Equiaxial dendrites in the periphery and Equiaxial - Columnar in the center.

- Near no porosity is observed and the detected porosity is very small. The porosity is mainly in the interdendritic area.

- Higher solute concentration in the center.

- More areas with the very fine eutectic structure in the center area (Blue circles in Fig. 4.27), but less than the nano-reinforced TiB$_2$ samples.

- Detected Al$_2$O$_3$ particles are in the center of the grains, acting as solidification nuclei. They show a rounded agglomerated structure of about 0.5 to 1 microns.

- Narrowest and directional / oriented dendrites in the center.

We can also observe the presence of Al$_2$O$_3$ in the alloy in the Fig. 4.30. A,B and C. The detected Al$_2$O$_3$ particles are again in the center of the grains, acting as nucleating sides.

Influence of Alumina (Al$_2$O$_3$) and Titanium Diboride (TiB$_2$) nanoparticles on the microstructure and properties of Al-Si9 Cu3 alloys for high pressure die casting applications.

CHAPTER 4: SOLIDIFICATION & MICROSTRUCTURE

Al$_2$O$_3$

**Figures 4.30. A,B and C.- Al$_2$O$_3$ particles detection by EDS and SEM**

We can obtain the next conclusions after the analysis of the differences between the center and the periphery and from the microstructure:

- Equiaxial dendrites in the periphery and Equiaxial - Columnar in the center.

- Higher solute concentration in the center.

- Very small porosity is detected. There is not big porosity, and the presented porosity is in the interdendritic area.

- Narrowest and directional / oriented dendrites in the center.

- More areas with the very fine eutectic structure in the center area (Blue circles), but less in comparison with TiB$_2$ reinforced alloys.

- Detected Al$_2$O$_3$ particles are in the center of the grains, acting as solidification nuclei. They show a rounded agglomerated structure of about 0.5 to 1 microns.

Influence of Alumina (Al$_2$O$_3$) and Titanium Diboride (TiB$_2$) nanoparticles on the microstructure and properties of Al-Si9 Cu3 alloys for high pressure die casting applications.

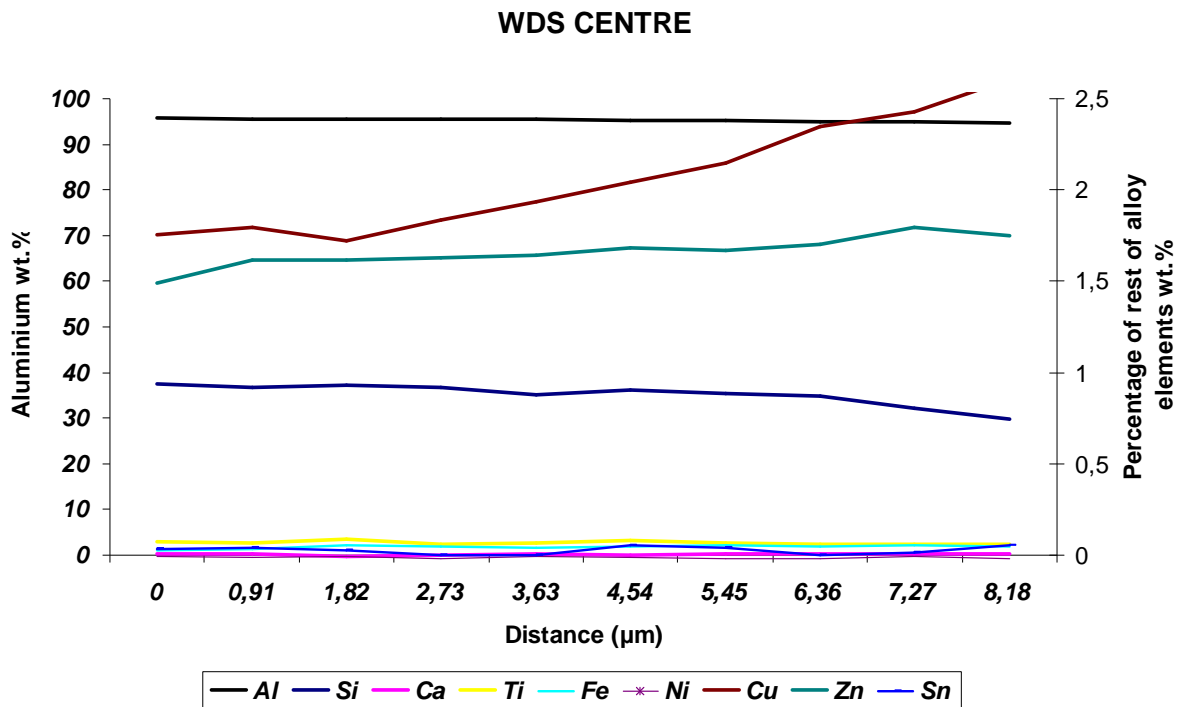CHAPTER 4: SOLIDIFICATION & MICROSTRUCTURE

4.3.1.2 WDS analysis

In order to determinate the differences between the peripheral and central area, WDS analysis has been made. Many different precipitates have been determined, but we focus on defining if the central area has a higher solute concentration. With this purpose a dendritic area has been analysed, to compare their compositions. We can see in Fig. 4.31 an example of WDS in the pheripheric area. We observe how the aluminium wt.% is approximately a 97.5 wt.%. The rest of elements remains quite stable in their values, with a Cu and Si concentration of about 0.9 wt.%.

WDS PERIPHERY
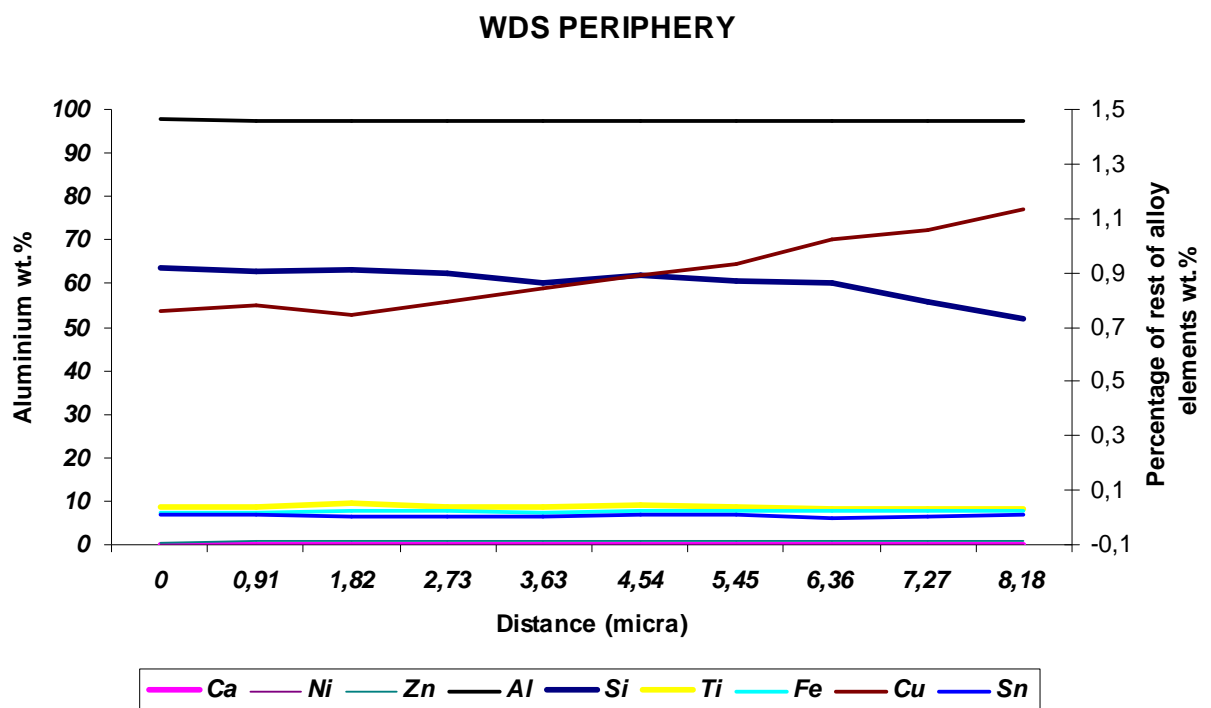
Figures 4.31.- Determination of peripheral Al dendrite composition by WDS

If we observe the Fig. 4.32. of an example of WDS in the central area, the estimated aluminium wt.% is about 95.5 wt.%. The rest of elements have a bigger concentration, with a 0.7 wt.% Si, a 1.5 wt.% of Zn and a 2 wt.% of Cu.

Influence of Alumina (Al$_2$O$_3$) and Titanium Diboride (TiB$_2$) nanoparticles on the microstructure and properties of Al-Si9 Cu3 alloys for high pressure die casting applications.

CHAPTER 4: SOLIDIFICATION & MICROSTRUCTURE

WDS CENTRE

Figures 4.32.- Determination of central Al dendrite composition by WDS

In despite of been a very punctual detection system, we see a tendency to increase the solute and to decrease the aluminium percentage between the samples in the way from the peripheral to central areas. The aluminium percentage changes from approximately the 97.5% to 95.5% in weight in from the external to the center area.

4.3.1.3 TEM and AES analysis of the reinforced material

The reinforced samples were analyzed through TEM in order to study the effect of the Al$_2$O$_3$ and TiB$_2$ particles in the generation of dislocations as well as possible reaction layers between the particles and the matrix and to determinate the role of ceramics in the precipitation of intermetallic phases.

The TEM analysis of the TiB$_2$ and nano- reinforced Al$_2$O$_3$ Al Si9 Cu3 alloys shows some common features concerning the Al-Si based alloy. TEM has been employed due to the difficulties with SEM to detect the TiB$_2$ nano-particles in the matrix and to determinate the particles that can't be detected by SEM. They are not big differences between the reinforced Al$_2$O$_3$ and TiB$_2$ materials, and that's the reason why we have focused the study in determinate the differences between the central and peripheral area.

Influence of Alumina (Al$_2$O$_3$) and Titanium Diboride (TiB$_2$) nanoparticles on the microstructure and properties of Al-Si9 Cu3 alloys for high pressure die casting applications.
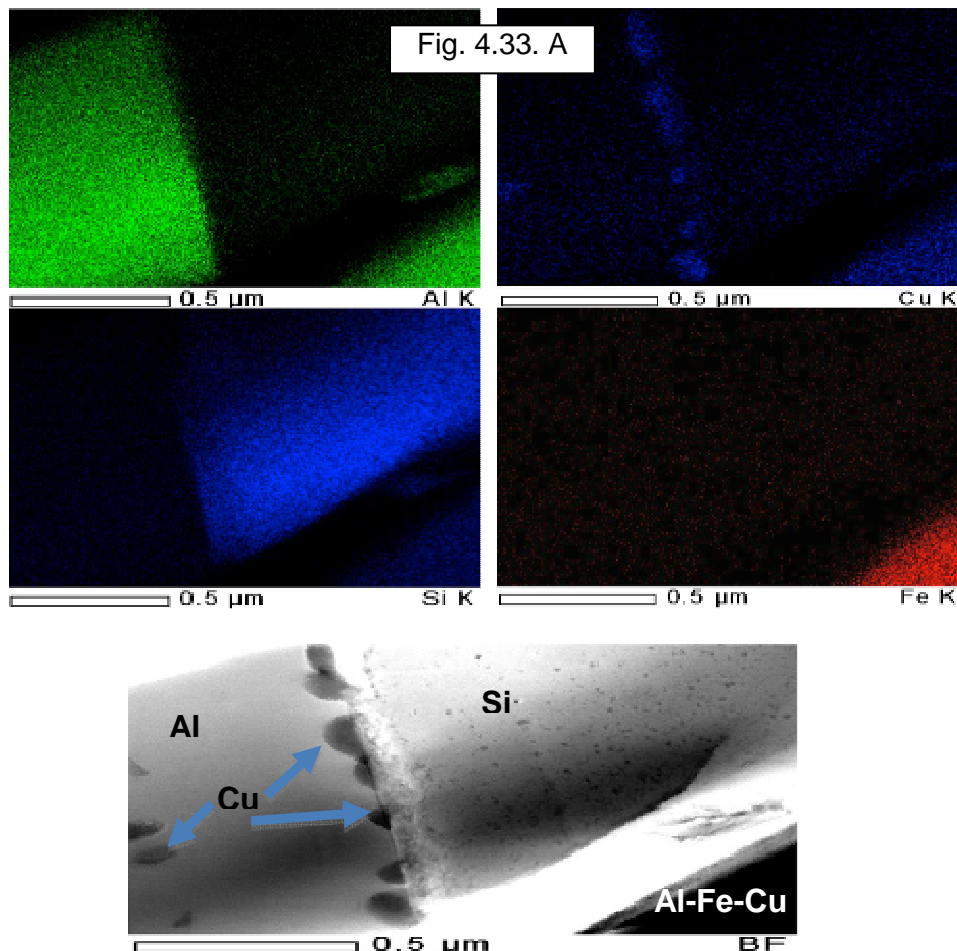
CHAPTER 4: SOLIDIFICATION & MICROSTRUCTURE

Two different samples have been employed. The first is has a 0.1% of gamma Al$_2$O$_3$ and the second has a 0.01% of commercial TiB$_2$, because the different reinforcement have same microstructure with the same reinforcement element.

The aluminium alloyed samples reinforced with TiB$_2$ and Al$_2$O$_3$ were analyzed through TEM in order to study the effect of the reinforcement particles with the microstructure and with the chemistry of the matrix/reinforcement interfacial zones. As already described, 2 areas related to the acicular grain zone (mainly in the center of the foundry samples) and to the small grain zone (mainly on the edge of the foundry sample) have been analyzed by TEM for both reinforced composite materials.

Basically we have observed difference in the microstructure for the samples analyzed in the center and samples analyzed in the edge but we do not have observed any difference on the microstructure of the matrix between sample reinforced with TiB$_2$ and sample reinforced with Al$_2$O$_3$. Therefore the discussion of this TEM part will only be associated with the localization of the TEM samples (center or edge) but not with the reinforcement type (TiB$_2$ and Al$_2$O$_3$).

Figures 4.33. A and B shows typical microstructure of the matrix taken into the **center** of the sample where acicular grains are found in two areas.

Influence of Alumina (Al$_2$O$_3$) and Titanium Diboride (TiB$_2$) nanoparticles on the microstructure and properties of Al-Si9 Cu3 alloys for high pressure die casting applications.

CHAPTER 4: SOLIDIFICATION & MICROSTRUCTURE

Figure 4.33.- A and B : TEM micrograph of typical microstructure of sample in the center of the foundry sample namely acicular grain zone. Each TEM micrograph (bright field image is associated with 4 EDS corresponding maps (Al, Cu, Si and Fe)).

Influence of Alumina (Al$_2$O$_3$) and Titanium Diboride (TiB$_2$) nanoparticles on the microstructure and properties of Al-Si9 Cu3 alloys for high pressure die casting applications.
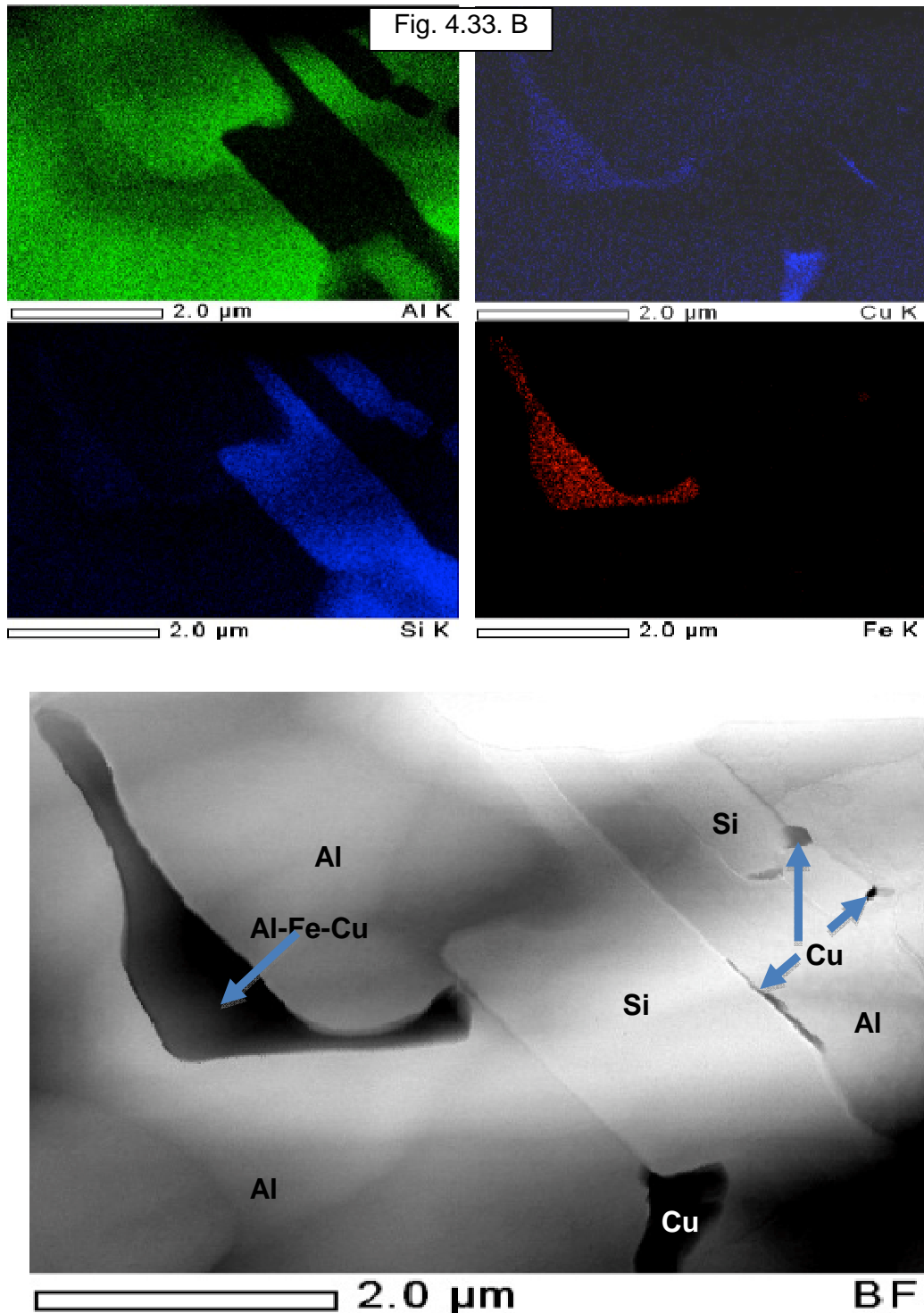
CHAPTER 4: SOLIDIFICATION & MICROSTRUCTURE

Several features can be observed:

1. Density of dislocation is negligible. No dislocations are observed on TEM pictures.
2. Large single crystal grains of pure silicon are observed. Also very small rounded silicon crystals are detected. There are normally Si crystals, but with few Cu inside, and same of the detected Cu could be attributed to the ion milling processing of samples.
3. At the boundary of the Si grain and inside the Al one, precipitation of pure Cu spot (grain size close to 150 nm) are observed.
4. Al-Fe-Cu grains are observed inside Al grains, normally relatively smalls (<5 microns) and with a no deleterious acicular shape.
5. Al grain size is in the order of few microns in diameter.

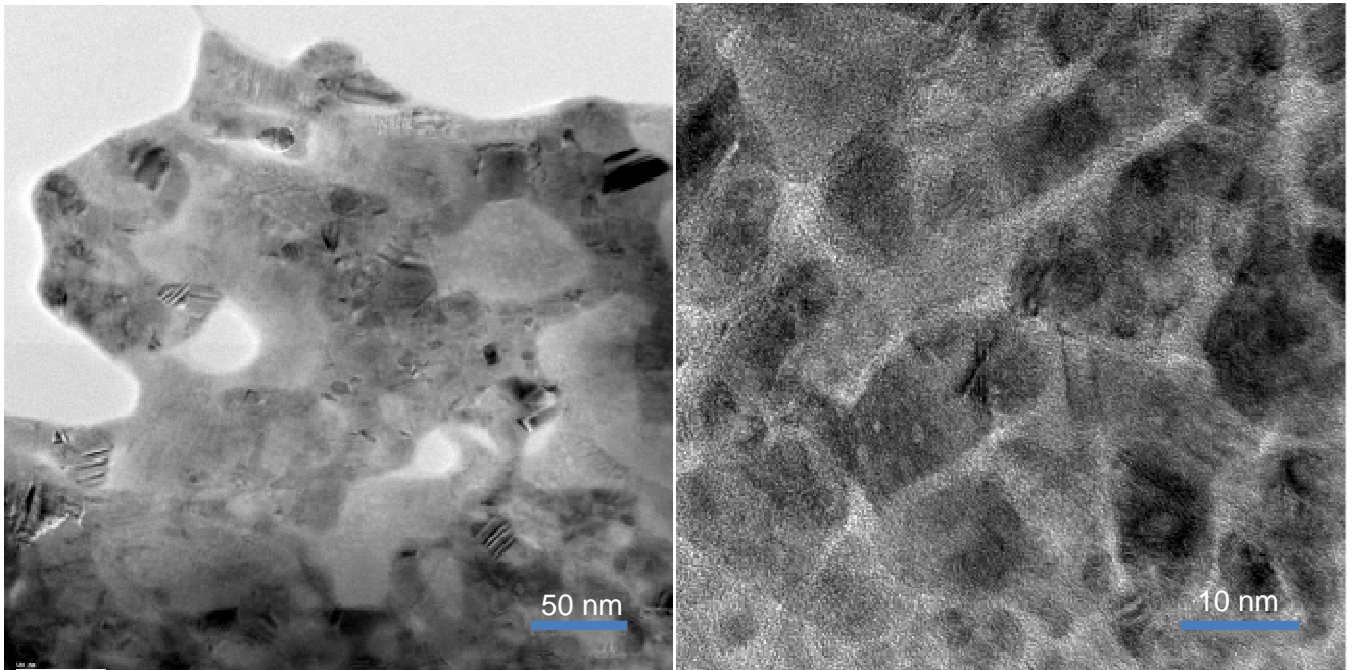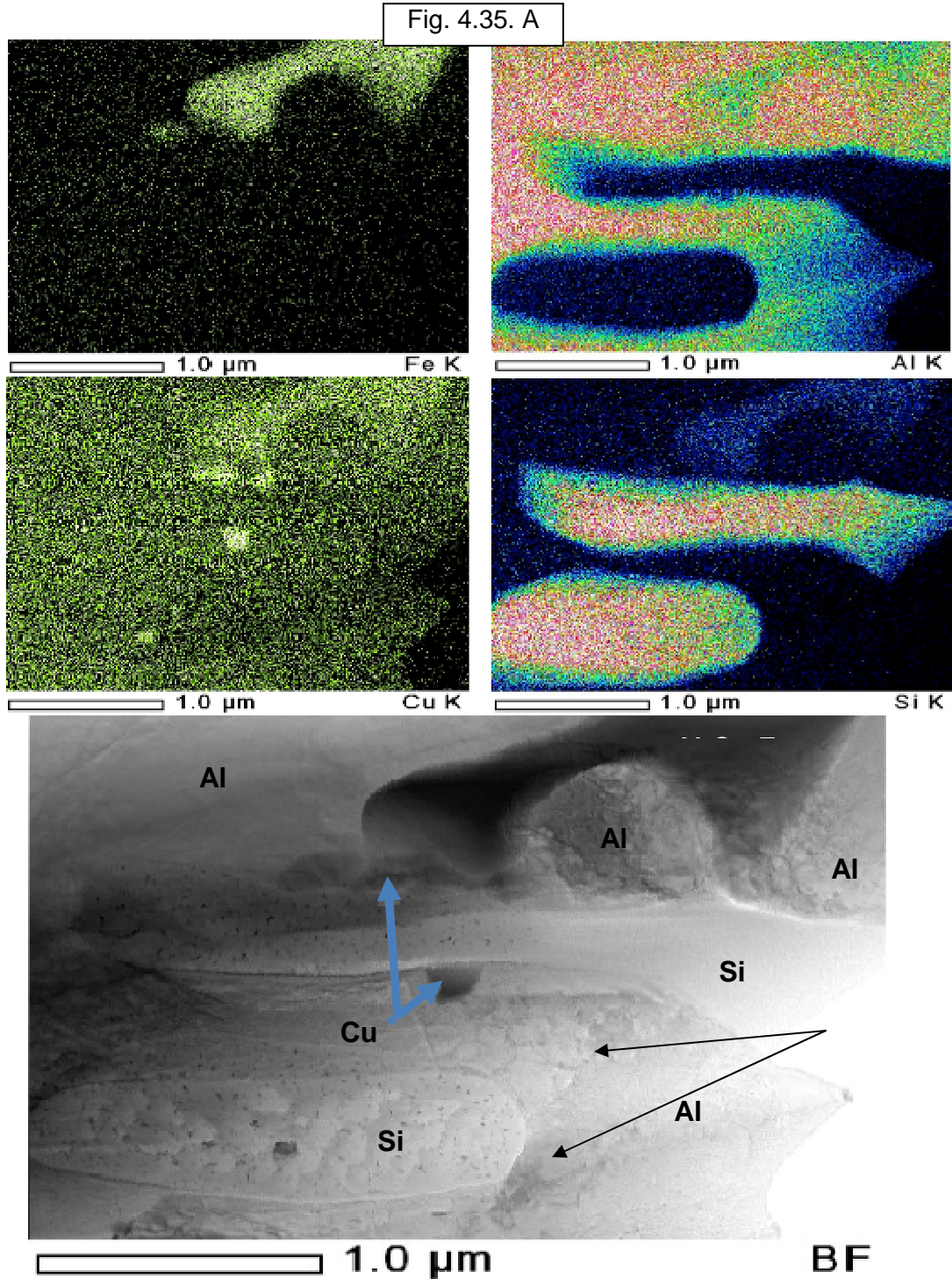Figures 4.34. show typical microstructure of the matrix taken into **the peripheral area of sample**.

Figure 4.34.- TEM micrograph of typical microstructure of sample in the edge of the foundry sample

Influence of Alumina (Al$_2$O$_3$) and Titanium Diboride (TiB$_2$) nanoparticles on the microstructure and properties of Al-Si9 Cu3 alloys for high pressure die casting applications.

CHAPTER 4: SOLIDIFICATION & MICROSTRUCTURE

Figures 4.35. A) and a B) show typical microstructure of the matrix taken into **the peripheral area of sample,** where small grain zones are found. Each of the bright field micrograph is associated with EDS maps in order to analyze the distribution of the Al, Cu, Si and Fe elements within the TEM analysis zone.

Fig. 4.35. A

Influence of Alumina (Al$_2$O$_3$) and Titanium Diboride (TiB$_2$) nanoparticles on the microstructure and properties of Al-Si9 Cu3 alloys for high pressure die casting applications.

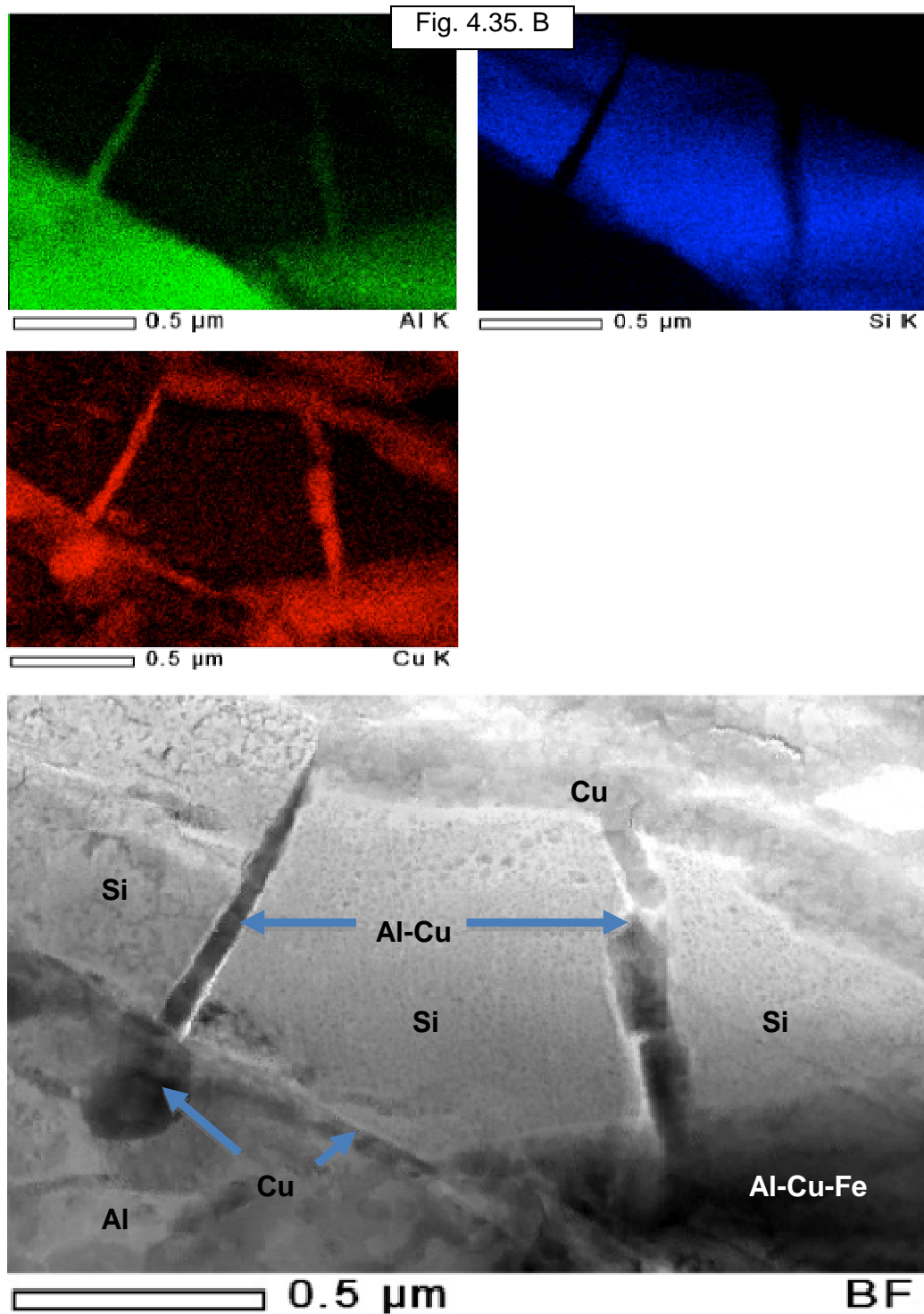CHAPTER 4: SOLIDIFICATION & MICROSTRUCTURE

Figure 4.35. A) and B).- TEM micrograph of typical microstructure of sample in the edge of the foundry sample namely small grain zone. Each TEM micrograph (bright field image is associated with 4 EDS corresponding maps (Al, Cu, Si and Fe).

Influence of Alumina (Al$_2$O$_3$) and Titanium Diboride (TiB$_2$) nanoparticles on the microstructure and properties of Al-Si9 Cu3 alloys for high pressure die casting applications.

CHAPTER 4: SOLIDIFICATION & MICROSTRUCTURE

Several features can be observed:

1. Density of dislocation is negligible. No dislocations are observed on TEM pictures.
2. Large single crystal grains of pure silicon are observed.
3. At the boundary of the Si grain and inside the Al one, precipitation of pure Cu spot (grain size close to 150 nm) are observed. In zones of fracture of Si crystals, these copper grains are observed in the space between the Si crystals with length up to 1 µm.
4. Si is normally detected in combination with Al and Cu.
5. Al-Fe-Cu grains are observed inside Al grains.
6. Two Al grain size zone can be observed: In first one, the Al grain size is in the order of few microns in diameter whereas in the second one (see Fig. 4.36.) Al grain size in the order of 10 nm in diameter can be observed.

Several differences can be observed between the central and peripheral area:

1. Density of dislocation it negible in the center and in the peripheral area. In the case of the peripheral area two different aluminium grain sizes are detected, with a size about few microns and the other are of about 10nm. In the case of the central area, Al grain size is in the order of few microns.
2. The silicon is detected as single phase grains in the center, but Al Si Cu structures are more common in the external area. This can be explained by a solute enrichment in the center, in concordance with the WDS analyses.

4.3.1.2 Aluminium grain size

The TP1 samples analysis is a normalized method to determinate the aluminium grain size. But as we are going to observe this method is not adequated to determinate the grain size of reinforced alloys. The determination of grain size is very difficult, due to the acicular structure in the center of the samples. The first measures were determinate using the ASTM E 112: 1996 E2 standard, but with the criteria of considering the acicular set of subgrain as a unique grain. The results obtained are summarized in Table 4.11., that don't match the OM observed grain sizes.

Reference	Grain Size Periph. (µm)	Grain Size Center (µm)
Al Si9 Cu3 Sample	888	888
0.2 wt.% SHS-TiB$_2$	944	3333
0.2 wt.% Commercial TiB$_2$	1059	3882
0.1 wt.% of γ Al$_2$O$_3$	1059	3705
0.17 wt.% of α Al$_2$O$_3$	1176	4588

Table 4.11.: ASTM E 112: 1996 E2 grain size determination

Influence of Alumina (Al$_2$O$_3$) and Titanium Diboride (TiB$_2$) nanoparticles on the microstructure and properties of Al-Si9 Cu3 alloys for high pressure die casting applications.

CHAPTER 4: SOLIDIFICATION & MICROSTRUCTURE

This system it's not adequate to determinate the grain size, because the dendrites are very long and very fines in the acicular zone with zones where different dendrites can cross one to the other, as we can observe in Fig. 4.36.:
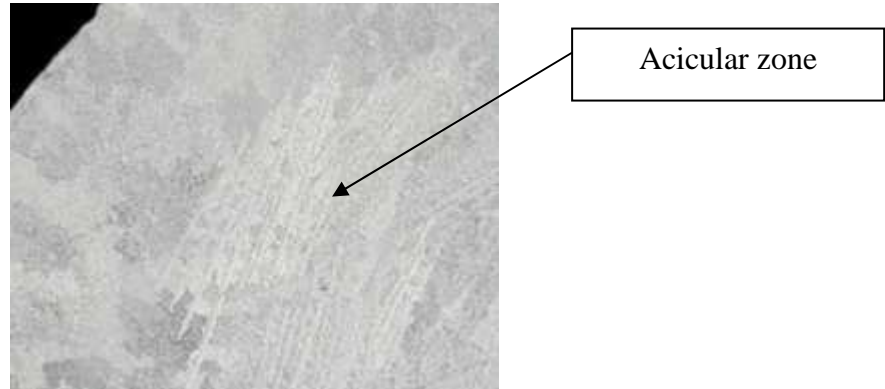

Figure 4.36.- Acicular dendrite zone detail in the center of a reinforced alloy

As much as it's very difficult to determinate the grain size of the central acicular zone we have chosen another method to determinate the real grain size. SDAS (Secondary dendrite arm spacing) determination has been done to determinate the nucleating effect of ceramic particles. When there is a reduction in the SDAS, the nucleation is better and better mechanical properties are obtained [Cac 96]. The final SDAS variates with the solidification time and the solute profile of the solidifying alloy [Eas 10-1]. We observe in Fig. 4.37. what it's the SDAS over a real dendrite.
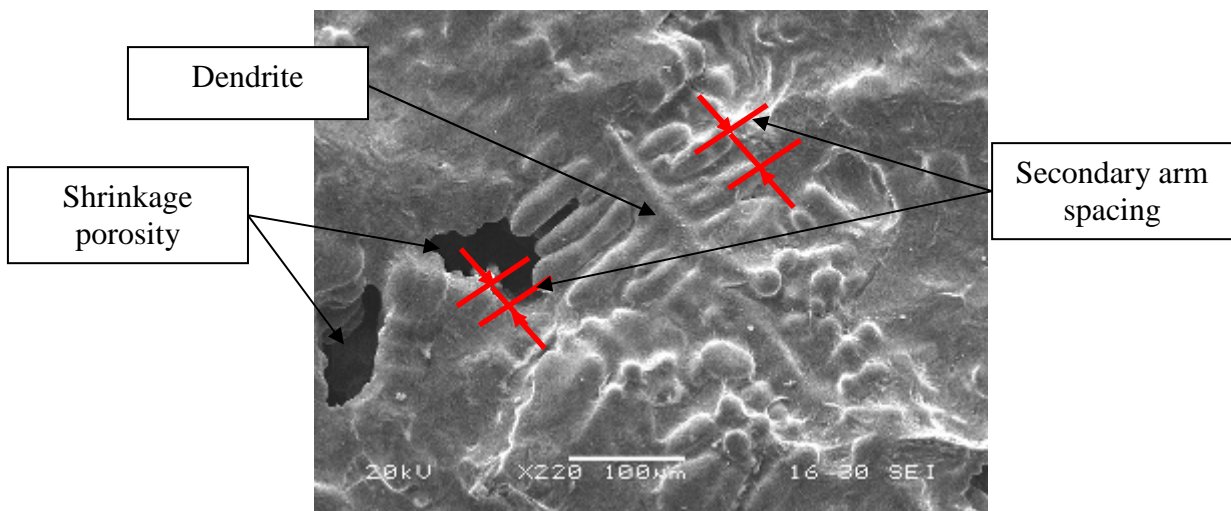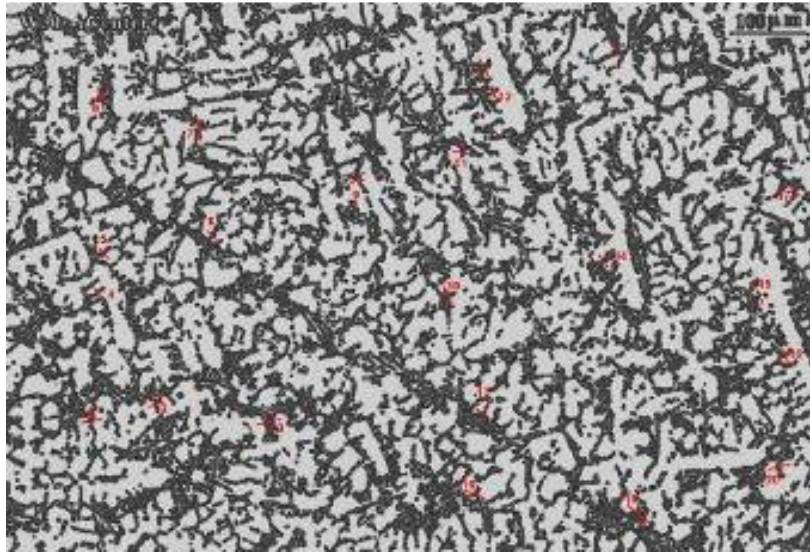

Figure 4.37.- Secondary dendrite arm spacing determination

Influence of Alumina (Al$_2$O$_3$) and Titanium Diboride (TiB$_2$) nanoparticles on the microstructure and properties of Al-Si9 Cu3 alloys for high pressure die casting applications.

CHAPTER 4: SOLIDIFICATION & MICROSTRUCTURE

In order to determinate the SDAS, as the dendrite structure is not equiaxial all over the samples, ImageJ software has been employed, 20 different measure points have been determinate for every alloy to calculate the average SDAS value, as we can see in the red marks in Fig.4.38.:

Figures 4.38.- Secondary dendrite arm spacing determination

In HPDC castings, where there are very high cooling rates the intermetallic particles are typically in the order of 10 to 50 µm [Tay 04]. In our case, the TP1 essay has high cooling rates, but smaller than HPDC, because we have employed the obtained TP1 samples to determinate the grain sizes. Results show that reinforced alloys in DC samples have a SDAS that we can even compare with HPDC values. We see the results in the Table 4.12.:

Reference	SDAS Periph.(µm)	SDAS Center (µm)	Variation (µm)
Al Si9 Cu3 Sample	26	34	+8
0.2 wt.% SHS-TiB$_2$	30	26	-4
0.2 wt.% Commercial TiB$_2$	22	18	-4
0.1 wt.% of γ Al$_2$O$_3$	28	26	-2
0.17 wt.% of α Al$_2$O$_3$	29	25	-4

Table 4.12.: SDAS peripheral and central determination

Influence of Alumina (Al$_2$O$_3$) and Titanium Diboride (TiB$_2$) nanoparticles on the microstructure and properties of Al-Si9 Cu3 alloys for high pressure die casting applications.

CHAPTER 4: SOLIDIFICATION & MICROSTRUCTURE

In the non reinforced Al Si9 Cu3 sample, the SDAS in the center is bigger than in the periphery, due to the highest cooling rate in the periphery. In all of the reinforced materials, the SDAS is smaller in the center of the sample, promoting a better nucleation. This can be explained by the increase of the solute and the presence of ceramic particles. There is an equation that relations the SDAS with the coalescence time (t$_{coales}$), that it's the time were the dendrite arms grow by coalescence between solidus and liquidus [Eas 10-2].

$$SDAS = K \cdot t_{coalesc.}^{n}$$

Where "n" is between 0.33 and 0.5 and K is a fitting factor dependent of alloy elemental concentration and constituents. The experimental obtained results are represented in Table 4.13., with the coalescence time calculated in Table 4.8., page 85.

SDAS	t$_{coalesc.}$ (S)	SDAS periph (µm)	SDAS center (µm)
Al Si9 Cu3 Sample	100	26	34
0.2 wt.% SHS-TiB$_2$	105	30	26
0.2 wt.% Commercial TiB$_2$	116	22	18
0.1 wt.% of γ Al$_2$O$_3$	150	28	26
0.17 wt.% of α Al$_2$O$_3$	145	29	25

Table 4.13.: SDAS peripheral and central relation with coalescence time

There is not a good relation between the equation and the obtained values, but it can be explained by the dendrite form, that it's not equiaxial. If we employ the "time plateau" we observe that a reduction in the plateau time promotes a decrease of the SDAS in the center SDAS, resumed in Table 4.14. with the plateau time calculated in Table 4.8.

SDAS	t$_{Plateau.}$ (S)	SDAS periph (µm)	SDAS center (µm)
Al Si9 Cu3 Sample	90	26	34
0.2 wt.% SHS-TiB$_2$	67	30	26
0.2 wt.% Commercial TiB$_2$	86	22	18
0.1 wt.% of γ Al$_2$O$_3$	21	28	26
0.17 wt.% of α Al$_2$O$_3$	29	29	25

Table 4.14.: SDAS peripheral and central relation with plateau time

Influence of Alumina (Al$_2$O$_3$) and Titanium Diboride (TiB$_2$) nanoparticles on the microstructure and properties of Al-Si9 Cu3 alloys for high pressure die casting applications.

CHAPTER 4: SOLIDIFICATION & MICROSTRUCTURE

We can detect the tendency to decrease in the SDAS in the center with decreasing plateau time, but there is not also a good relation. Solute concentration in the center of the samples has an acicular directional structure, with a lower SDAS parameter and less porosity. For the same composition, the higher the cooling rate, the smaller the SDAS and also the smaller the porosity [Sei 09], what can explain the increase in the base Al Si9 Cu3 alloy of SDAS in the center of the sample in comparison with the peripheral area.

4.3.1.3 Electrical conductivity analysis

The electrical conductivity decreases when we add the element addition [Mac 98] and when the grain size decreases. We observe the different between the different alloys and the variation in the properties in function of making the test in the periphery or in the center of the test bars, and also in the acicular and granular area, as we can see in Table 4.15 to 4.19.
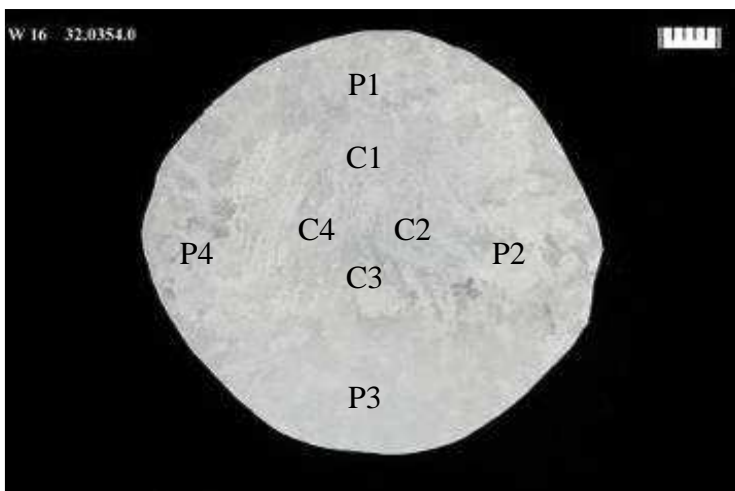
Base sample
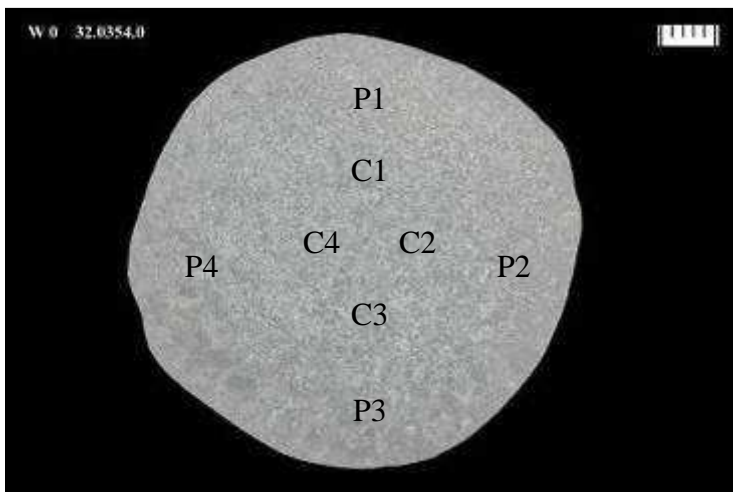
Point	Value (%IACS)	Average (%IACS)
P1	29.60	
P2	30.15	30,06
P3	30.55	
P4	29.95	
C1	30.00	
C2	30.25	30,31
C3	30.60	
C4	30.40	

Table 4.15: IACS determination

0.2% TiB$_2$ SHS

Point	Value (%IACS)	Average (%IACS)
P1	29.55	
P2	29.60	29,57
P3	29.60	
P4	29.55	
C1	29.55	
C2	29.70	29,56
C3	29.50	
C4	29.50	

Table 4.16: IACS determination

CHAPTER 4: SOLIDIFICATION & MICROSTRUCTURE

0.2% commercial TiB$_2$:
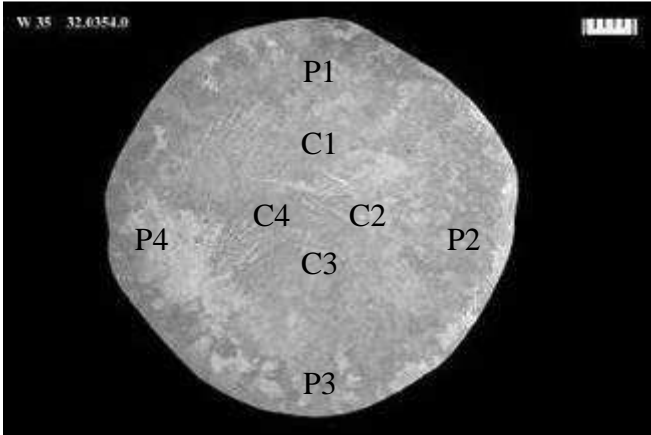
Point	Value (%IACS)	Average (%IACS)
P1	28.05	
P2	28.75	
P3	28.10	28.22
P4	28.00	
C1	28.05	
C2	28.50	
C3	28.35	28.25
C4	28.10	

Table 4.17: IACS determination

0.1% Al$_2$O$_3$ gamma alumina briquette:
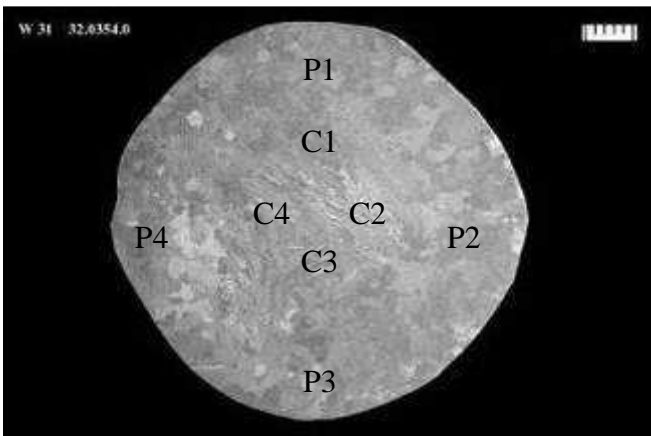
Point	Value (%IACS)	Average (%IACS)
P1	29.05	
P2	29.05	
P3	29.05	29,07
P4	29.15	
C1	29.00	
C2	29.10	
C3	29.10	29,06
C4	29.05	

Table 4.18: IACS determination

0.17% Al$_2$O$_3$ alpha alumina briquette:
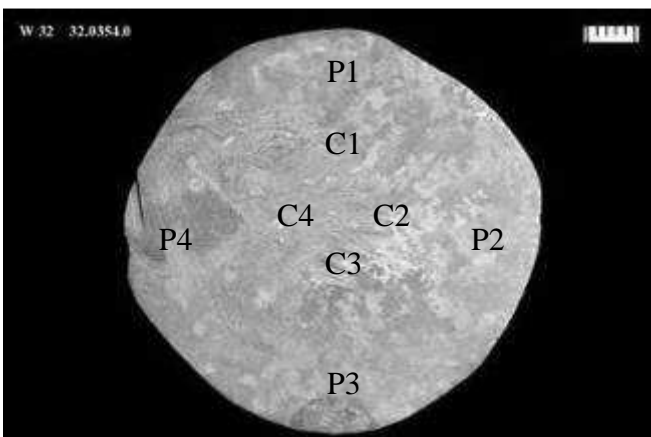
Point	Value (IACS)	Average (IACS)
P1	28.60	
P2	28.85	
P3	28.85	28,65
P4	28.30	
C1	28.70	
C2	28.80	
C3	28.85	28,76
C4	28.70	

Table 4.19: IACS determination

Influence of Alumina (Al_2O_3) and Titanium Diboride (TiB_2) nanoparticles on the microstructure and properties of Al-Si9 Cu3 alloys for high pressure die casting applications.

CHAPTER 4: SOLIDIFICATION & MICROSTRUCTURE

Values for modified samples in both areas are similar. We compare the obtained results with the expected values obtained from NADCA formula [Mac 98] for the different compositions in the Table 4.20.:

IACS% = 36.44-0.72Si-0.26Cu-0.32Fe-0.63Mg-0.08Mn+0.01Ni+0.02Cr-0.36Zn-0.27Ti+0.31Sr.

	Si	Fe	Cu	Mn	Mg	Cr	Ni	Zn	Ti	Pb	Sr	IACS% NADCA	IACS% Obtained
Al Si9 Cu3 Sample	8.580	0.860	1.780	0.181	0.033	0.049	0.073	0.940	0.045	0.053	0	29.15	30.18
0.2 wt.% SHS-TiB_2	8.610	0.850	1.780	0.186	0.046	0.051	0.073	0.930	0.046	0.053	0	29.12	29.56
0.2 wt.% Commercial TiB_2	8.460	0.950	1.740	0.189	0.029	0.054	0.072	0.930	0.045	0.051	0	29.21	28.23
0.1 wt.% of γ Al_2O_3	8.480	0.880	1.770	0.186	0.012	0.053	0.074	0.930	0.045	0.052	0	29.23	29.06
0.17 wt.% of α Al_2O_3	8.460	0.900	1.730	0.181	0.023	0.051	0.073	0.930	0.045	0.050	0	29.24	28.7

Table 4.20.: IACS determination by NADCA formula and experimental results

As we can see, the values are quite similar, and approximately they match the expected values. A conductivity decrease can be explained, because if we have more grain boundaries is more difficult to conduct the electrical energy. The difference between the center and the peripheral areas are more similar in values when adding ceramic particles, but also the SDAS values difference is smaller between the two areas. In the non inoculated sample, the conductivity in the center is higher than in the periphery, which could be correlated with a higher SDAS value is the center. We can adjust the NADCA IACS% formula to determinate IACS% value, modify to evaluate the effect of 0.02 wt.% of TiB_2 or Al_2O_3 particle additions:

IACS% = 36.44-0.72Si-0.26Cu-0.32Fe-0.63Mg-0.08Mn+0.01Ni+0.02Cr-0.36Zn-0.27Ti+0.31Sr **- 0.31**

The variation of conductivity between the center and the peripheral is also bigger in the non inoculated sample, with a correlation with a higher difference between SDAS values in both areas, as it's reflected in Table 4.21.:

Reference	SDAS Periph.(µm)	IACS% Periph.	SDAS Center (µm)	IACS% Center	SDAS Average (µm)	IACS% Average
Al Si9 Cu3 Sample	26	30.06	34	30.31	30	30.18
0.2 wt.% SHS-TiB_2	30	29.57	26	29.56	28	29.56
0.2 wt.% Commercial TiB_2	22	28.22	18	28.25	20	28.23
0.1 wt.% of γ Al_2O_3	28	29.07	26	29.06	27	29.06
0.17 wt.% of α Al_2O_3	29	28.65	25	28.76	27	28.70

Table 4.21.: IACS and SDAS relation in the peripheral and central area

Influence of Alumina (Al$_2$O$_3$) and Titanium Diboride (TiB$_2$) nanoparticles on the microstructure and properties of Al-Si9 Cu3 alloys for high pressure die casting applications.

CHAPTER 4: SOLIDIFICATION & MICROSTRUCTURE

A decrease in the electrical conductivity can be observed by adding few quantities of ceramic particles (Around a 4% of IACS electrical conductivity value by adding less than a 0.2% of nanoparticles). The tendency reflects that if the SDAS average value is increased, the IACS% also increase its value, as we can observe in Fig. 4.39.:
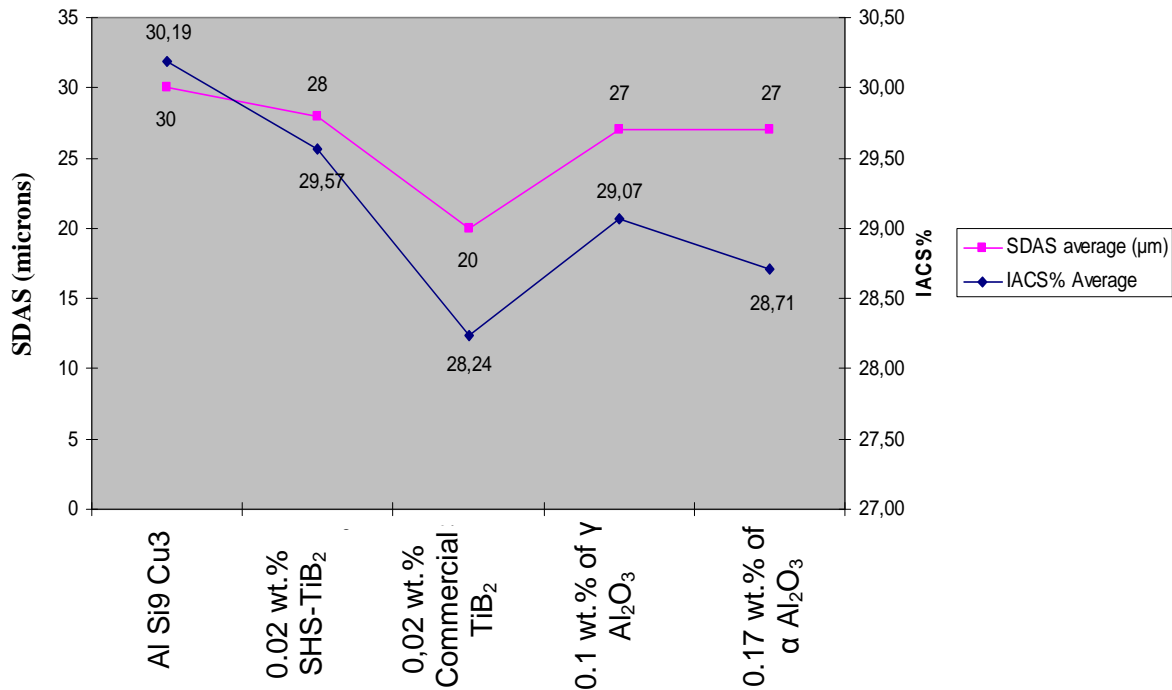

Figure 4.39.: Comparative diagram between SDAS and IACS

4.3.2 Discussion of the results

The comparison of the reinforced alloys with the corresponding <u>unreinforced alloy</u> shows that there is homogeneous grain dispersion in all the areas, with equiaxial dendrites in the periphery and in the center in the case of the non reinforced alloy. Also micro shrinkages are observed.

In the case of the reinforced alloys, there is a non-homogeneous grain, with equiaxial dendrites in the periphery and columnar dendrites in the center. Very little micro shrinkages are observed, and the central dendrites are oriented and are narrowest than the non reinforced alloy.

Very small β-iron needles are detected, of about 20 microns size. The normal size of β-needles variates from 10-50 µm in HPDC standard Al Si9 Cu3 alloys [Tay 04], but is always much smaller in comparison with DC samples employed for the metallurgical examination (Approximately 1/5 of β-needles in DC by comparison with HPDC samples). This can be related with the size and morphology of dendrites and the secondary dendrites arms, than can promote the needles to break in smaller needles.

Influence of Alumina (Al$_2$O$_3$) and Titanium Diboride (TiB$_2$) nanoparticles on the microstructure and properties of Al-Si9 Cu3 alloys for high pressure die casting applications.

CHAPTER 4: SOLIDIFICATION & MICROSTRUCTURE

Very fine eutectic structures are detected in the central area of the reinforced alloys. In the case of TiB$_2$ reinforced alloys there are more than in the case of Al$_2$O$_3$ reinforced alloys. The presence of small Si particles is attributed to Si enrichment of the remaining melt due to the formation of eutectic Al (Aluminium spikes) at the eutectic temperature. Following the nucleation of eutectic Al on the primary α-Al dendrites, fine Si particles form at the solidification front upon which the eutectic Si flakes and fibers could develop [Naf 08]. This fine eutectic is very interesting to obtain good mechanical properties.

Observing the porosity, Al$_2$O$_3$ nano-particles promote the decrease in the size and number of porous. TiB$_2$ nano-particles also have a positive effect. This can be related with the capacity of ceramic particles to stabilize porosity, and as the total surface of ceramic particles is bigger, the smaller the porosity diameter. In our case, the employed Al$_2$O$_3$ nano-particles size (15-40 nm) is much smaller than TiB$_2$ particles (690 nm aprox.), so also the total surface is higher. However as in Fig. 4.30. we can observe nano-particles agglomerations of about 0.5 µm, that reduced the total surface of ceramic particles in contact with the aluminium matrix, but they are placed at the center of the aluminium grains, and they act as grain nucleation sites. In the case of Al$_2$O$_3$ reinforced alloys near no porosity is observed in the microscopy examination. Also a smaller SDAS promotes and smaller porosity, and also SDAS is lower in reinforced alloys.

There is a higher solute concentration in the center of the samples than in the periphery. That promotes dendritic or equiaxial grains, in function of the cooling rate. Aluminium percentage variates approximately from a 97, 5 to 95, 5% Wt. in the center of the reinforced areas, determined by WDS

With the EDS and SEM we can't detect the presence of Ti B$_2$ particles in the center or in the border of grain, due to the small size of particles, but more because the very low reinforcing percentage. Al$_2$O$_3$ particles tend to get inside the grain and in the grain boundaries, with an agglomerated structure of about 0.5 - 1 micron. In the case of particles in the center of the grains, the Al$_2$O$_3$ particles act as grain refinement nucleus.

ASTM E 112: 1996 E2 standards is more adequate to determinate grain size of equiaxial grains, and with the determination of grain size applying this standard is not possible to explain the behavior of reinforced alloys.

Using the determination of SDAS, in all the reinforced alloys is smaller than in base alloy, with the smaller SDAS in the case of TiB$_2$. As much as SDAS is directly related with the UTS, its value should be increased as much as SDAS decreases. In the Al Si9 Cu3 sample, a SDAS bigger in the center than in the periphery, can be explained by the highest cooling rate in the periphery. In the rest of cases, SDAS smaller in the center of the sample, promotes a better nucleation, and can be explained by the increase of the solute and the presence of ceramic particles.

Influence of Alumina (Al$_2$O$_3$) and Titanium Diboride (TiB$_2$) nanoparticles on the microstructure and properties of Al-Si9 Cu3 alloys for high pressure die casting applications.

CHAPTER 4: SOLIDIFICATION & MICROSTRUCTURE

There is not a good relation between coalescence time (t$_{coales}$) and the obtained values, but it can be explained by the dendrite form, that it's not equiaxial. If we employ the time plateau we detect a tendency to decrease SDAS in the center with decreasing plateau time.

Values for electrical conductivity are quite similar, and approximately they match the expected values from NADCA. We can observe a conductivity decrease in comparison with the base alloy. We can explain the decrease in the conductivity because if we have more grain boundaries by a decrease in the SDAS value, is more difficult to conduct the electrical energy. In the non inoculated sample, the conductivity in the center is higher than in the periphery, in correlation with a higher SDAS value is the center.

A decrease in the electrical conductivity can be observed by adding few quantities of ceramic particles (Around a 4% of IACS electrical conductivity value by adding less than a 0.2% of nanoparticles). In our case, the higher SDAS in the non reinforced alloy is associated with an increase of the IACS%.

4.4 Conclusions

The solidification pattern of metallic materials is varied by adding nano and TiB$_2$ particles. The complete study has been determinate by the DTA, TP1 and injection test, simulating industrial parameters.

The microstructure has been determined from TP1 test and also from injected samples, employing different equipments as OM, SEM, TEM and WDS, determining the effect of Al$_2$O$_3$ and TiB$_2$ particles in the microstructure and properties of the alloys.

The analysis of the T-t curves and the corresponding derivatives curves up to the fifth derivative have confirmed the effect of particles in the solidification pattern. Main conclusions of thermal analysis of the reinforced alloys are:

1) Al$_2$O$_3$ and TiB$_2$ particles influence aluminium grains nucleation, eutectic reaction and intermetallic precipitations. The nucleation temperature is increased, as the recalescence temperature. This effect is related to the incorporation of ceramic particles as heterogeneous nuclei.

2) TiB$_2$ has more influence in the nucleation than Al$_2$O$_3$ particles. This is related to the employ of TiB$_2$ in commercial grain refiners as main refiner. Also TiB$_2$ particles are related in some studies as the most effectives for Aluminium grain refining.

3) The influence of the particles should have a positive influence on the mechanical properties of the reinforced alloys since it decrease the undercooling, promoting a better nucleation.

Influence of Alumina (Al$_2$O$_3$) and Titanium Diboride (TiB$_2$) nanoparticles on the microstructure and properties of Al-Si9 Cu3 alloys for high pressure die casting applications.

CHAPTER 4: SOLIDIFICATION & MICROSTRUCTURE

The analysis of the microstructure shows very interesting conclusions that determinate the effect of the Al$_2$O$_3$ and TiB$_2$ particles. It has been demonstrated that the presence of the ceramic nano-particles has a direct effect on the microstructure. These effects should have a corresponding effect on the electrical, mechanical and thermal properties of the reinforced materials. The most important conclusions are:

1) The employ of ceramic nano-particles reduce the porosity size and quantity. It's more remarkable in the case of Al$_2$O$_3$ than in TiB$_2$ particles.

2) Acicular oriented very fine dendrites are promoted by the nano-particle addition. The SDAS is smaller in the reinforced alloys and also the SDAS decrease in the center of the samples.

3) Al$_2$O$_3$ and TiB$_2$ particles modify the structure, with smaller detrimental β-iron needles.

4) Very fine eutectic structures are detected in the center of the reinforced alloys, especially with TiB$_2$ reinforced alloys.

5) The SEM analysis shows that Al$_2$O$_3$ particles acts as nucleating points, with agglomerate particles of about 0,5-1 micron.

6) The TEM analysis shows a very small dislocation density. Alumnimium grains have two different sizes in the peripheral area, with also very fine aluminium grains about 10 nm. The center has a solute enrichment, also detected by WDS.

7) Electrical conductivity decreases by adding few quantities of ceramic particles and is quite similar in the center and periphery of reinforced alloys and a relation between SDAS and IACS has been observed.

8) We can determinate what are the better particle for different industrial applications:

   a. Parts with improved mechanical properties: As TiB$_2$ has an smaller SDAS than Al$_2$O$_3$ particles, the YS and UTS can be improved, so it´s more interesting to add TiB$_2$ particles than Al$_2$O$_3$. The shorter distances between particles and SDAS prevent crack growth and their interconnection, increasing the elongation. So for parts with plastic deformation it would be better to add TiB$_2$ particles.

   b. Parts with internal pressure or fluids: As Al$_2$O$_3$ reinforced alloys has less porosity, they have a better behavior against leakage.

Influence of Alumina (Al$_2$O$_3$) and Titanium Diboride (TiB$_2$) nanoparticles on the microstructure and properties of Al-Si9 Cu3 alloys for high pressure die casting applications.

CHAPTER 5: MECHANICAL PROPERTIES

CHAPTER 5: MECHANICAL PROPERTIES.

Influence of Alumina (Al$_2$O$_3$) and Titanium Diboride (TiB$_2$) nanoparticles on the microstructure and properties of Al-Si9 Cu3 alloys for high pressure die casting applications.

CHAPTER 5:   MECHANICAL PROPERTIES

5.1 Introduction. Strengthening mechanisms

Introduction

Pure aluminium is a soft metal with insufficient strength for most engineering applications. In the automotive industry cast aluminium is increasing it percentage in the total weight of the car, displacing other materials with a higher density. In order to achieve the maximum decrease in weight to reduce energy consumption and emissions, the cast aluminium alloys should be employed in structural applications. New aluminium alloys have been developed to obtain better properties by a correct concentration of allowing elements.

In order to get interesting properties we can employ other strengthening process, as the employ of grain refiners and modifiers, increase of solidification rate, severe deformation, ultrasonic vibration, thermal treatments and reinforcements. In all the cases the mobility of dislocations is reduced, promoting the necessity of higher forces to move the dislocations through the aluminium alloy.

A dislocation is a defect or irregularity within a crystal structure. They have a strong influence on material properties (UTS, YS, elongation, hardness and fatigue). They are classified in two main types: edge and screw, but normally we can observe a mixture of both types in real alloys.

Employing different strengthening process we obtain the decrease of dislocation mobility, becoming the sum of the effect of the different strengthening mechanism and also of alloy composition [Mah 08]. The dislocation motion occurs by sequential bond breaking and bond reforming, so the resistance to deformation (strength) can be improved by decreasing the possibility to move, putting obstacles in the way of displacement.

In general all the strengthening mechanisms increase the UTS and YS and decrease the elongation. In all the cases, the strength is got by impeding the motion of the dislocations. We define following the different strengthening mechanisms that are involved in the reinforcement of aluminium alloys:

1) Grain and subgrain strengthening: The Aluminium alloy is strengthened by the grain and subgrain reduction. The reason is that the slip in a grain is constrained by the presence or absence of slip in neighbouring grains or subgrains. Normally a discontinuity of slip planes or a change in the slip direction is needed to get slip across the grain or subgrain boundaries. In this case, grain and subgrain boundaries acts as barriers to dislocation movement.

Influence of Alumina (Al$_2$O$_3$) and Titanium Diboride (TiB$_2$) nanoparticles on the microstructure and properties of Al-Si9 Cu3 alloys for high pressure die casting applications.

CHAPTER 5:   MECHANICAL PROPERTIES

There is a direct relation between the YS and the grain and subgrain size. This relation has the name of Hall-petch [Hal 51]. We can see how they are related:

$$\sigma_y = \sigma_0 + kd^{-1/2}$$

Where is the YS, σ_0 is the intrinsic YS, d is the grain diameter and k is a constant for a given material. So we can deduce that a decrease of grain size (d) promotes an increase of YS (σ_y). A second phase is not required.

2) Solid solution strengthening (Solute hardening):

Impurities dissolved by addition to the melt promote the strengthening [Wik 11-02]. As much as there is a distort lattice mechanism, the distort can be produced by a substitution or interstitial mechanism. This implies an increase of energy of the crystal due to the lattice increase, and also the increase of dislocations near the distorted area. If the distortion increases, the dislocation mobility is reduced.

In the case of the aluminium alloys, some alloying elements have a great influence in the solid solution strengthening, like Cu or Mg. Any alloying element is not suitable to get this type of strengthening, because there must exist an atomic misfit with the aluminium matrix and also to have high solid solubility. The strengthening effect is increase if:

- The radius of the two particles is very different.

- If we increase the quantity of dissolved particles.

Of both effects, the most important is the ratio relation. The continuous solid solutions show a maximum strength at an intermediate composition. A second phase is not required.

3) Strain Hardening (Work hardening / cold work):

The strain hardening is produced by low temperature plastic deformation [Wik 11-03]. The strengthening mechanism involves:

- Dislocation creation due to the plastic deformation.

- Multiplication of dislocation number and movement of dislocation induced by the repeated deformation than promotes that dislocations repel between them.

Influence of Alumina (Al$_2$O$_3$) and Titanium Diboride (TiB$_2$) nanoparticles on the microstructure and properties of Al-Si9 Cu3 alloys for high pressure die casting applications.

CHAPTER 5:   MECHANICAL PROPERTIES

The main effect is an increase of YS, because the rearrangement of dislocations of the structure of crystals and the phases those are in the neighbourhood. Same areas of entangled dislocations don't allow the movement of surrounding dislocations. If we continue with consecutive strain hardening process, YS tends to be similar to UTS, but with a decrease in the Elongation, promoting a brittle material. A second phase is not required. They are several processes to produce the strain hardening, involving forging, extrusion, rolling, drawing, bending and ECAP.

4) Dispersion strengthening (Orowan strengthening):

The dispersion strengthening is promoted by the addition of elements as fibres, particulates, or others, with and strengthening effect due to the dispersion of a second phase in the aluminium alloy [Lem 81], [Cly 93]. The dislocation movement is reduced across grain boundaries with different phases, and the dislocations movement is only possible bypassing the addicted elements. It this movement dislocation loops are created, and they are called Orowan loops, and the strengthening mechanism is also known as Orowan strengthening. This motion promotes an increase of YS.

The effect is more important in case of:

- Hard second phase (Less possibilities to have a plastic deformation).

- Ductile matrix as aluminium matrix (More capacity of the matrix to have plastic deformation).

- High percentage of second phase elements (More possibilities to reduce dislocation movement).

- Spherical or rounded second phase (Less stress concentration than sharp edges).

- Small second phase (Higher specific surface area per volume unit).

In order to promote a good dispersion strengthening, particle grain size range should be between 0.01 and 0.7 μm [Han 05], [Cly 93], but the most important points are the spacing between particles and their size.

5) Precipitation strengthening (Age hardening):

Is more common in aluminium alloys, and the strengthening effect is promoted by the precipitation of small particles, normally from a supersaturated solid solution (In this case is called "age hardening"). A natural or artificial ageing treatment is necessary in order to convert second phase particles from solid solution to fine precipitate structure [Lem 81], [Cly 93].

Influence of Alumina (Al_2O_3) and Titanium Diboride (TiB_2) nanoparticles on the microstructure and properties of Al-Si9 Cu3 alloys for high pressure die casting applications.

CHAPTER 5: MECHANICAL PROPERTIES

The strength is produced because dislocation movement is reduced across grain boundaries between different phases of fine dispersion of precipitates. If the process is at room temperature then is called natural aging, but if a heat treatment is needed, then is called artificial aging. The effect is similar to dispersion strengthening, because the nature of elements and strength distribution, but with an smaller precipitates size.

6) Load transfer between matrix and reinforcement:

If the matrix contains a no plastically deforming reinforcement, when a load is applied to the aluminium, it can transmit that load to the reinforcement. Normally the reinforcement must have a high aspect-ratio, in order to promote the load transference by shear stress at the matrix-reinforcement interface. A ratio of 10:1 is usually recommended as the smallest ratio to transfer the load [Aik 97].

7) CTE mismatch between the matrix and the reinforcements:

When the CTE between the matrix and the reinforcements are very different at microscopic level and can coexist, the strength is promoted by the strains produced in the cooling of the reinforced material, due to the different thermal contraction in the solidification process. Lot of new dislocations are created to absorb the CTE misfit. As much as there is an increment in the number of dislocations, the movement is reduced by the impediment to move, increasing YS [Han 05, Arp 03].

In the case of an eutectic alloy [Ask 03], more than one strengthening mechanism can be produced at the same moment:

- Solid solution strengthening: Constituent B in α or A in β.

- Dispersion strengthening: For example alternative layers of α and β constituents, similar to a composite.

- Grain size strengthening: If a rapid cooling is promoted, narrower alternative layers are created.

The maximum strength of an alloy should be get in the eutectic composition [Han 02].

Influence of Alumina (Al_2O_3) and Titanium Diboride (TiB_2) nanoparticles on the microstructure and properties of Al-Si9 Cu3 alloys for high pressure die casting applications.

CHAPTER 5:   MECHANICAL PROPERTIES

5.2 Experimental results

5.2.1   Mechanical properties at Room T

The tensile tests were carried out following the standard ASTM A-370 with cylindrical specimens produced by HPDC. The dimensions of the specimens were diameter = 6.25 ± 0.12 mm, L_0 = 25 ± 1, L_c > 32 mm, R = >5 and L =80 mm, and the elongation was measured with an extensometer at room temperature and at 200ºC.

Table 5.1 shows the average results obtained in the 3 tensile tests of every alloy and of their corresponding unreinforced Al Si9 Cu3 alloy.

TENSILE PROPERTIES AT 20ºC	State	Experimental data				
		Al Si9 Cu3 Sample	0.2% SHS-TiB_2	0.2% commercial TiB_2	0.1% of gamma Al_2O_3	0.17% of alpha Al_2O_3
UTS (20ºC) (MPa)	As Cast	277	291	304	297	296
YS (20ºC) (MPa)	As Cast	132	128	130	128	123
Elongation % (20ºC)	As Cast	5,6	6,8	7,1	5,2	5,1
TENSILE PROPERTIES AT 200ºC						
UTS (200ºC) (MPa)	As Cast	166	169	173	167	161
YS (200ºC) (Mpa)	As Cast	123	124	128	125	121
Elongation % (20ºC)	As Cast	4,0	4,0	5,5	6,0	4,0

Table 5.1: Tensile properties of the unreinforced and reinforced alloys at room temperature and 200ºC.

The first property to compare is the UTS at room temperature, which gives us the maximum value of stress that a part can support without the necking effect on the test bar (See Fig. 5.1.). It's very important for brittle materials, as a design value. In our case, we can observe an increase in the UTS of all the reinforced materials, which corresponds with the results of the literature review. This increase is high (About a 7%) in comparison with the small quantity of reinforcement particles (0.2 wt.%) if we look in the Fig. 5.1. the media it's quite similar for both reinforcement materials. In our case, it can be related with the dispersion of the nano-particles in the matrix, the small SDAS of dendrites and the decrease of the porosity.

CHAPTER 5:   MECHANICAL PROPERTIES

We resume the variation in UTS properties as:

- A general increase in the UTS of about a 7% by a 0.2% of reinforcement with TiB$_2$ and Al$_2$O$_3$.

- For an equivalent volume fraction of reinforcement the commercial TiB$_2$ has a better behavior than SHS-TiB$_2$, with double percentage of increase in UTS (+4.9% for SHS-TiB$_2$ and +9.5% in commercial TiB$_2$).

- For equivalent volume fraction of reinforcement of Al$_2$O$_3$, the values are very similar, and there is not a variation because of the type of Al$_2$O$_3$.
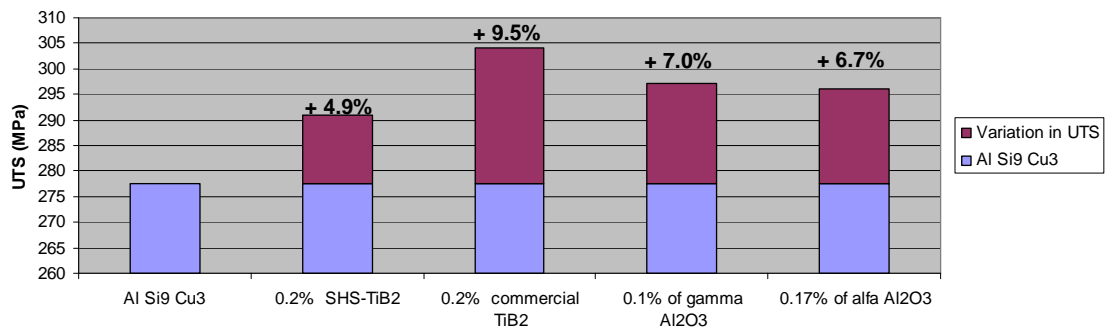
Fig. 5.1: UTS at room temperature for reinforced and base Al Si9 Cu alloys.

The YS gives us the stress at which plastic deformation becomes noticeable. This value is employed in the design of parts were permanent plastic deformations are not allowed. YS tends to decrease as we increase the reinforcement, as we can see in Fig. 5.2. This is not a common behavior if we compare with the literature review, which shows as we have seen before that YS increases it value with the reinforcing elements. The explanation could be attributed to the agglomeration of reinforcement particles. We resume the variation in YS properties as:

- For equivalent volume fraction of reinforcement (0.2% TiB2 and 0.17% Al2O3) decrease is much pronounced for the Al2O3 reinforcement type (Aprox. 2 times higher).

- For an equivalent volume fraction of reinforcement the commercial TiB$_2$ has a better behavior than SHS-TiB$_2$, with one half the decrease in YS (-3.0% for SHS-TiB$_2$ and -1.5% in commercial TiB$_2$).

- In the case of the Al$_2$O$_3$ reinforced alloys, the increase in the percentage of reinforcement of a 70% corresponds with a decrease in YS, that it's two times smaller in comparison (-3.4% in γ-Al$_2$O$_3$ and -7.2% in α-Al$_2$O$_3$).

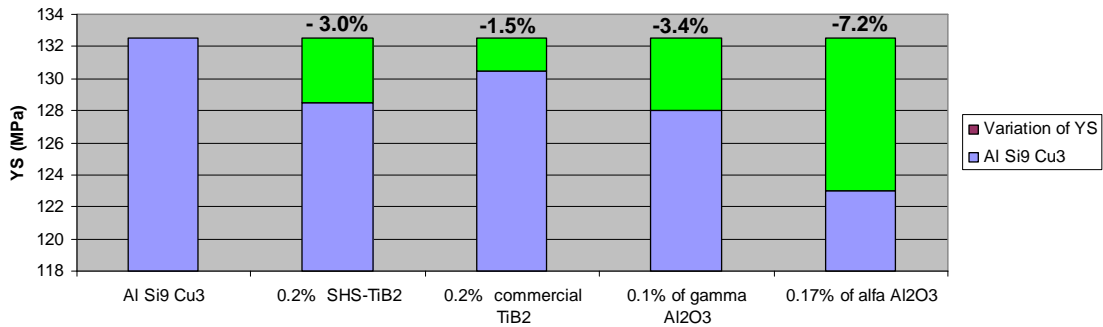**CHAPTER 5:   MECHANICAL PROPERTIES**

Fig. 5.2: YS at room temperature for reinforced and base Al Si9 Cu alloys.

The Elongation is the permanent deformation observed in the test bars after the essay. In this case the TiB$_2$ reinforced alloys shows an important increase in the elongation value, as we observe in Fig. 5.3. We know that TiB$_2$ particles have a very important refining effect with a reduction in the SDAS grain size, which can permit the increase of the elongation value. The reduction of porosity in both cases has a positive effect. In the case of the Al$_2$O$_3$, the global elongation value decreases. The explanation could be an agglomeration of Al$_2$O$_3$ nano-particles in the aluminium grains, as seen on Fig. 4.21. We resume the variation in Elongation properties as:

- TiB$_2$ reinforced alloys have an increase in the elongation (+20.4% with SHS and 25.7% with commercial TiB$_2$). It may be related with the best solidification curves in the nucleation zone, especially with commercial TiB$_2$, and also with the smallest SDAS in the commercial TiB$_2$ sample.

- Al$_2$O$_3$ reinforced materials have a decrease in the elongation in comparison with the base alloy (-8% in gamma and -9.7% in alfa Al$_2$O$_3$).

- In TiB$_2$ and Al$_2$O$_3$ reinforced materials, values are very similar for the two reinforcement types.

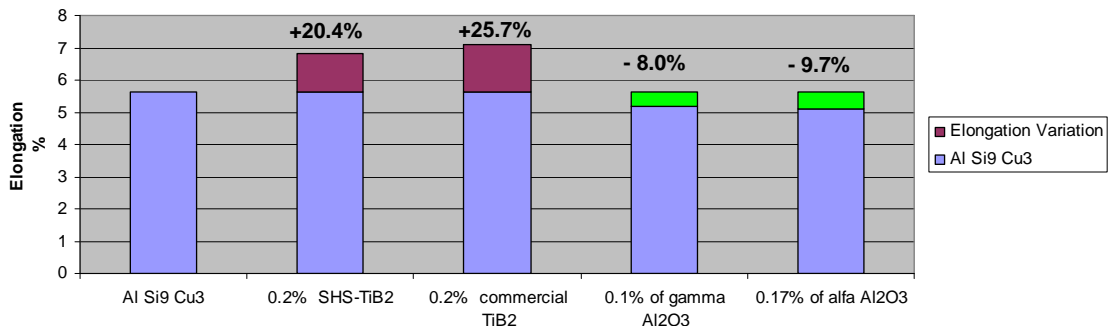- Elongation remains similar for the two different reinforcement volumes in the case of Al$_2$O$_3$.

Fig. 5.3 Elongation at room temperature for reinforced and base Al Si9 Cu alloys.

Influence of Alumina (Al$_2$O$_3$) and Titanium Diboride (TiB$_2$) nanoparticles on the microstructure and properties of Al-Si9 Cu3 alloys for high pressure die casting applications.

CHAPTER 5:   MECHANICAL PROPERTIES

All the samples were cast in the same conditions and the average of the valid values of four tensile tests were obtained for each of the data presented. The main conclusions are:

- Ultimate Tensile Strength (UTS) at 20ºC is increased by the nano-reinforcement addition.

- Yield Strength (YS) at 20ºC decreases by the reinforcement addition. The decrease is more pronounced in the Al$_2$O$_3$ reinforced materials.

- Elongation at 20ºC is increased by TiB$_2$ nano-reinforcements and decrease with the Al$_2$O$_3$ reinforced materials.

5.2.2   Mechanical properties at 200ºC

The samples were also tested at 200ºC. We can observe in Table 5.1 and 5.4. that the addition of nanoparticles increases the UTS. However, this effect is much less pronounced then for the same samples tested at room temperatures. Also 0.17 wt.% of alpha Al$_2$O$_3$ has a lower value than base material. TiB$_2$ reinforced materials have a higher value, but tendency show that increasing the temperature the UTS values tend to be more similar to the Al Si9 Cu3 base. As we increase the temperature, we may start the recovery process, with changes in the internal structure in order to decrease the energy of the system, promoting a decrease in the number of grain boundaries. However a decrease in dislocations number and also a coarsening of precipitates in the reinforced material may be also developed, with a therefore negative effect in UTS. In the case of 0.17% of Al$_2$O$_3$, we have observed a strange behaviour in the solidification curve, and may have more agglomerates and not as well dispersed Al$_2$O$_3$ particles. Also as we'll see in point 5.2.3. fracture analysis, an oxide is observed in the fracture area, which could reduce the UTS value of the essay. We resume the variation in UTS properties as:

- A general increase in the UTS of about a 3% by a 0.2% of reinforcement with TiB$_2$ and little or negative values in comparison with base alloy for the Al$_2$O$_3$ reinforced alloys.

- For an equivalent volume fraction of reinforcement the commercial TiB$_2$ has a better behavior than SHS-TiB$_2$, with double percentage of increase in UTS (+1.8% for SHS-TiB$_2$ and +4.2% in commercial TiB$_2$).

- For the reinforcement with Al$_2$O$_3$, the values are better for a 0.1% of γ- Al$_2$O$_3$ than for α- Al$_2$O$_3$ (+0.6% for γ - Al$_2$O$_3$ and -3% for α- Al$_2$O$_3$).

Influence of Alumina (Al_2O_3) and Titanium Diboride (TiB_2) nanoparticles on the microstructure and properties of Al-Si9 Cu3 alloys for high pressure die casting applications.
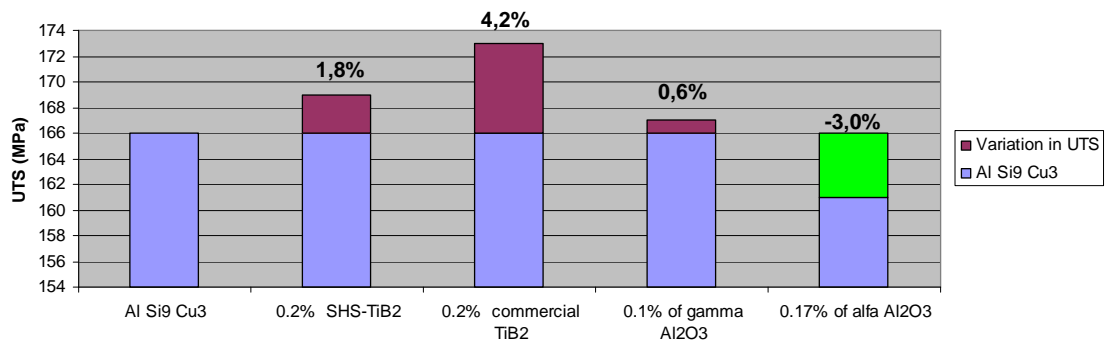
CHAPTER 5:   MECHANICAL PROPERTIES

Fig. 5.4: UTS at 200ºC for reinforced and base Al Si9 Cu alloys.

In the case of the YS at 200ºC, we can observe in the Fig. 5.5 an increase of the value, which we can explain by changes in the internal structure in order to decrease the energy of the system, promoting a decrease in the number of grain boundaries. However the increase of temperature permits more movements and the appearance of plasticity, and YS is reduced by this action. In the case of 0.17% of Al_2O_3, we have observed a strange behaviour in the solidification curve, and may have more agglomerates and not as well dispersed Al_2O_3 particles. Also as we said before, we'll see in point 5.2.3 fracture analysis that an oxide is observed in the fracture area, which could reduce the YS value of the essay. The general behaviour is very similar to the tendency on UTS. We resume the variation in YS properties as:

- A general increase in the YS of about a 2.5% by a 0.2% of reinforcement with TiB_2 and little or negative values in comparison with base alloy for the Al_2O_3 reinforced alloys.

- For an equivalent volume fraction of reinforcement the commercial TiB_2 has a better behavior than SHS-TiB_2, with 3 times the percentage of increase in YS (+0.8% for SHS-TiB_2 and +4.1% in commercial TiB_2).

- For the reinforcement with Al_2O_3, the values are better for a 0.1% of γ- Al_2O_3 than for α- Al_2O_3 (+1.6% for γ - Al_2O_3 and -1.6% for α- Al_2O_3).
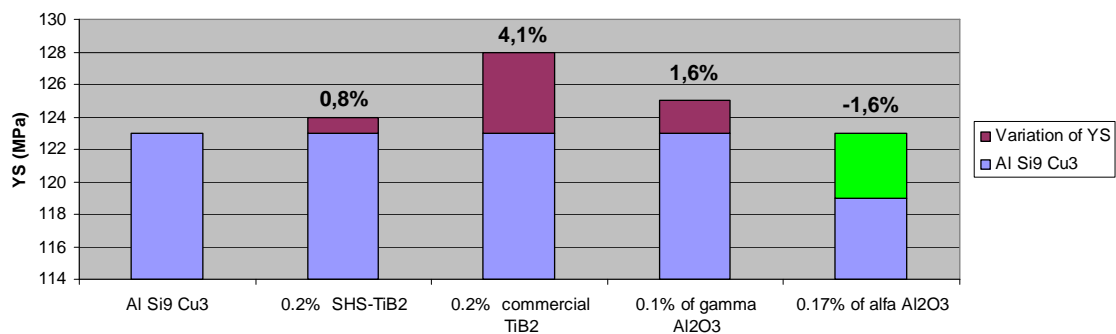

Fig. 5.5: YS at 200ºC for reinforced and base Al Si9 Cu alloys.

Influence of Alumina (Al$_2$O$_3$) and Titanium Diboride (TiB$_2$) nanoparticles on the microstructure and properties of Al-Si9 Cu3 alloys for high pressure die casting applications.

CHAPTER 5:   MECHANICAL PROPERTIES

In the case of the Elongation at 200ºC, we can observe in Table 5.6 how the values remains the same or better than the sample, but there is an increment in the Al$_2$O$_3$ alloys in comparison with the results at room temperature. In this case the change in the properties can be explained by the reduction of the total energy of the system, the grain boundaries total area reduction, the decrease in porosity. Also the presence of a ductile phase of Cu between the Si and Aluminium dendrites could improve the ductility. The difference between 0.2% SHS and 0.2% commercial TiB$_2$ reinforced alloys can be explained by the higher porosity in the first one, that we can also detect by the lower density and the presence of porosity in the tensile test bar.

- Elongation values are smaller at 200ºC than at room temperature, except for gamma Al$_2$O$_3$. The increase in the volume of the trapped porosity decreases the fracture area, and could decrease also the elongation.
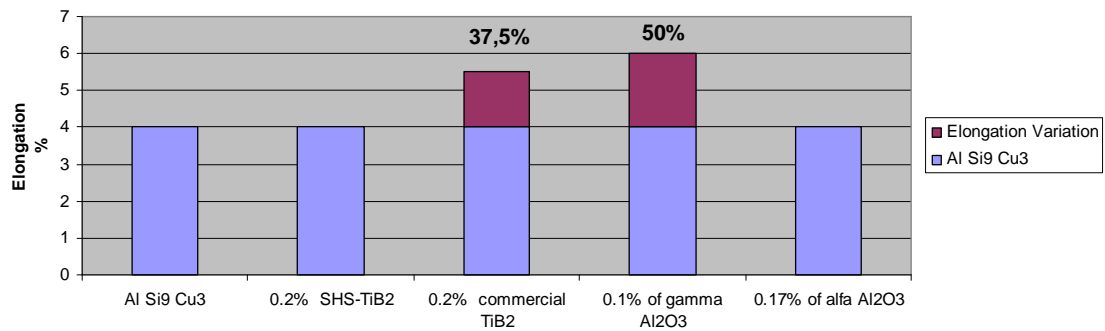

Fig. 5.6 Elongation at 200ºC for reinforced and base Al Si9 Cu alloys.

The main conclusions are:

- Ultimate Tensile Strength (UTS) at 200ºC is increased by the TiB$_2$ nano-reinforcement addition.

- Yield Strength (YS) at 200ºC is increased by the TiB$_2$ nano-reinforcement addition.

- Elongation at 200ºC is increased in some concentrations and remains stable by TiB$_2$ and Al$_2$O$_3$ reinforced materials.

5.2.2. Measurement of physical properties

Physical properties of the materials have a direct influence in their eventual mechanical properties. Therefore the measurement of density and porosity was carried out in order to draw data to complete the analysis of the mechanical properties obtained. The obtained values are resumed in Table 5.2.:

Influence of Alumina (Al$_2$O$_3$) and Titanium Diboride (TiB$_2$) nanoparticles on the microstructure and properties of Al-Si9 Cu3 alloys for high pressure die casting applications.

CHAPTER 5:   MECHANICAL PROPERTIES

Reference	S (Suspended mass into water gr.)	D (Dry mass gr.)	V = D-S	B = bulk density (g/cc) = D/V	Theoretical density (g/cc)	Porosity (%)
Al Si9 Cu3 Sample	1.55	2.62	1.07	2.49	2.84	**12.3%**
0.2 wt.% SHS-TiB$_2$	1.73	2.87	1.14	2.53	2.86	**11.6%**
0.2 wt.% Commercial TiB$_2$	1.44	2.30	0.86	2.67	2.86	**6.6%**
0.1 wt.% of γ Al$_2$O$_3$	1.24	1.96	0.72	2.73	2.86	**4.6%**
0.17 wt.% of α Al$_2$O$_3$	2.29	3.62	1.33	2.71	2.86	**5.0%**

Table 5.2: Density for reinforced and base Al Si9 Cu alloys.

Porosity decrease with the addition of ceramic nanoparticles. Al$_2$O$_3$ has a greater effect in porosity diminution than TiB$_2$ particles, but in both cases the total porosity is decreased by adding ceramic particles. The measures are in good relation with the observed less porosity in reinforced samples in the microscopy examination.

5.2.3   Fracture analysis

Fracture analysis of specimens of samples in each of the conditions studied in the work was determined with the optical microscopy. The main objective was the determination of the differences between the reinforced and non reinforced sample.

In metals brittle fractures are very dangerous and engineers try to avoid the use of brittle aluminium alloys, employing ductile alloys. Brittle fractures are characterized by a bright and granular flat cracking area, with near no plastic deformation. In the case of ductile fractures, a plastic deformation is observed, with a fibrous aspect and it can content also flat or shear face areas. The color is not so bright, having a grey color.

5.2.3.1 Fracture analysis of the Al Si9 Cu3 and Al Si9 Cu3 SHS-TiB$_2$ tensile specimens

Base alloy sample:

Large porous are observed in Fig. 5.7. due to the increase of porosity volume (As see in page. 12) by the test temperature in the 200ºC tensile sample, and in comparison with the reinforced alloys his much higher, as we detect in the density essay and in the microstructure observation. Some little oxides (Defects) also are detected. Fracture is ductile in all the samples.

Influence of Alumina (Al$_2$O$_3$) and Titanium Diboride (TiB$_2$) nanoparticles on the microstructure and properties of Al-Si9 Cu3 alloys for high pressure die casting applications.

CHAPTER 5:   MECHANICAL PROPERTIES

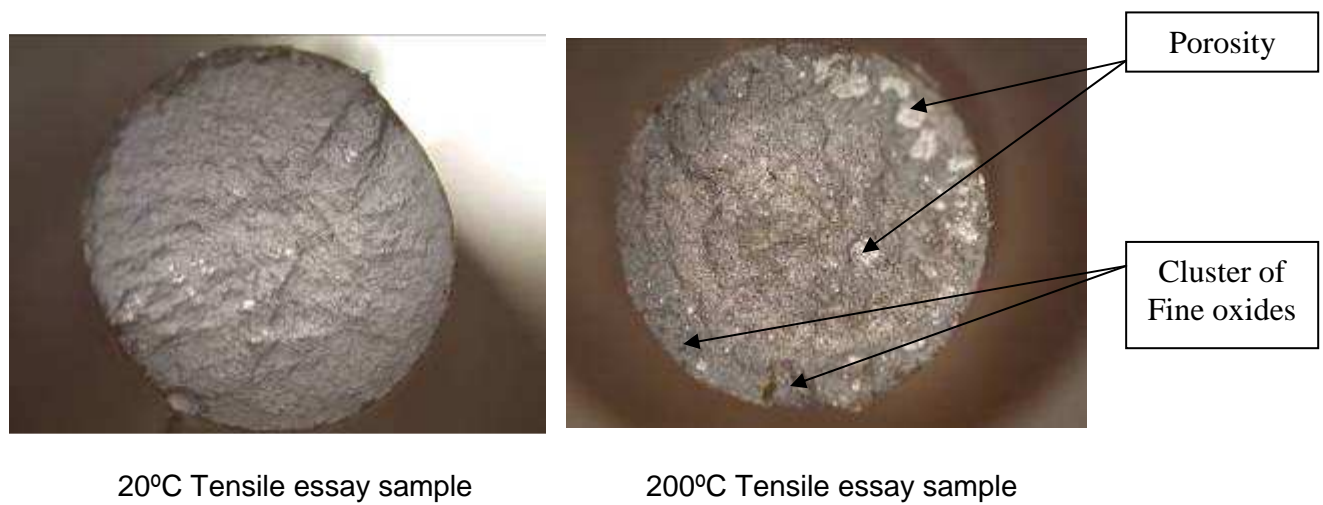20ºC Tensile essay sample   200ºC Tensile essay sample

Figure 5.7: Fracture analysis of base alloy

0.2% SHS TiB$_2$

The fracture analysis of the reinforced TiB$_2$ alloys has a very similar behaviour. Only little porosity in the 200 ºC test bar is observed in Fig.5.8., due to the liberation of same of the gas porosity by the temperature. Some little oxides at 20 ºC are also detected. Fracture is ductile in all the samples. No porosity or oxides are observed in the samples. Fracture is ductile in all the samples. This material has the better results in all the mechanical properties, and we can deduce that the internal soundness of the test bars has influence in the final mechanical properties, because it has the fewer defects in the fracture structure.
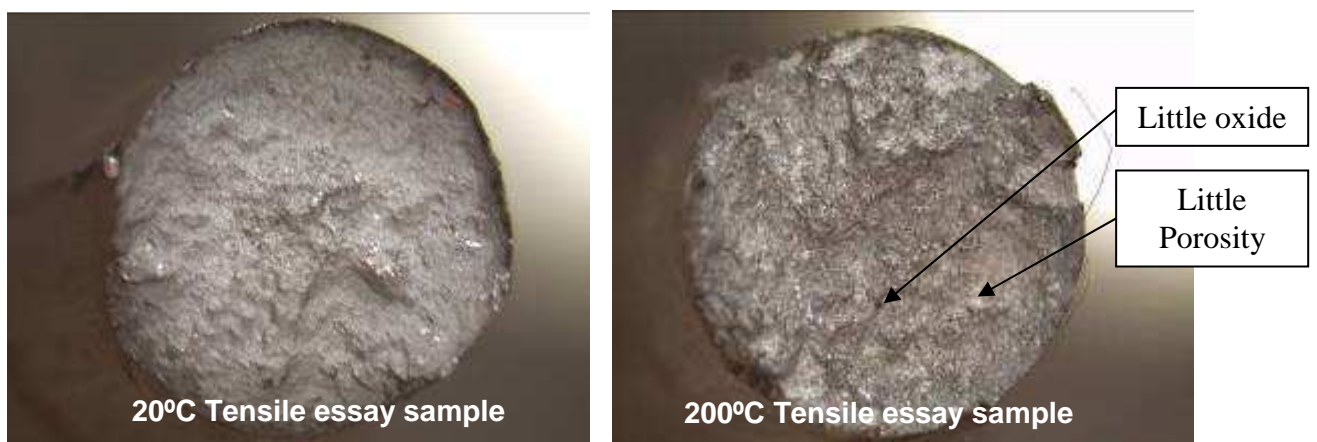

Figure 5.8: Fracture analysis of 0.02% SHS TiB$_2$ reinforced alloy

Influence of Alumina (Al$_2$O$_3$) and Titanium Diboride (TiB$_2$) nanoparticles on the microstructure and properties of Al-Si9 Cu3 alloys for high pressure die casting applications.

CHAPTER 5:   MECHANICAL PROPERTIES

0.1% Al$_2$O$_3$ gamma alumina:

The fracture analysis of the reinforced Al$_2$O$_3$ alloys has also a very similar behaviour. Only little porosity is observed in Fig 5.9. due to the liberation of same of the gas porosity by the temperature in the 200 ºC test bar. A big cluster of oxides also is detected. The clusters of oxides are brittle and they act as a defect and as starting point for the fracture. This is the reason why we should try to have good nano-oxide dispersion, avoiding oxide clustering. Fracture is ductile in all the samples.

Figure 5.9: Fracture analysis of 0.1% Al$_2$O$_3$ gamma alumina reinforced alloy

5.2.4   Analysis of the experimental results

In order to determinate the tensile properties of the reinforced materials at room temperature and high temperature (200ºC) test were carry out, including internal porosity determination and fracture analysis, in order to complement the test developed and studied in the chapter 4.

It's remarkable that with a very little quantity of reinforcement, the mechanical properties have a great variation. At **room temperature** there is an increase of UTS of about a media of 7% by the reinforcement addition. That is directly related with the decrease in the SDAS decrease in the reinforced alloys. But in the other hand, as it occurs in MMCs, the YS is reduced. This reduction is much more important in the case of Al$_2$O$_3$, with an average reduction of a 5%.

In the case of Elongation, the TiB$_2$ has a very beneficial impact of more than a 20%, related with the better nucleation solidification curve. In the case of Al$_2$O$_3$ reinforced alloys, Elongation is reduced in a 9%.

Influence of Alumina (Al$_2$O$_3$) and Titanium Diboride (TiB$_2$) nanoparticles on the microstructure and properties of Al-Si9 Cu3 alloys for high pressure die casting applications.

CHAPTER 5:   MECHANICAL PROPERTIES

At high temperatures (200ºC), in the case of 0.17 wt.% of α- Al$_2$O$_3$ we can observe a same oxide spots in the fracture area, that it can promote a slight decrease in the mechanical properties.

We observe an increase of UTS, especially for TiB$_2$ reinforced particles, of about a 3 %. The presence of the ceramic particles dispersed in the matrix and the nucleating effect can explain the increment of UTS.

We observe an increase of YS, especially for TiB$_2$ reinforced particles, of about a 2.5 %. The presence of a bigger porosity in the test sample is produced by the increase of temperature, which promotes an increment in porosity average diameter. As the no reinforced alloy has a bigger porosity, it's the more influenced, decreasing its YS.

Elongation in all the reinforced alloys is equal or superior to base alloy. This could be explained by the presence of very small ceramic particles that reduce the recovery of the material at high temperatures and stabilize porosity, and as porosity is higher in the base alloy, the elongation should decrease in comparison with the rest of alloys.

With density measures we can check how the observations made in the metallurgical analyze match well with the essays. It's very remarkable how very fine ceramic particles decrease porosity. Al$_2$O$_3$ particles has a lower porosity than TiB$_2$ particles, and in our case they are also the particles with the smallest size. In the case of γ-alumina, the porosity is lower, corresponding with a smaller particle diameter (15 nm), in comparison with α-alumina of 40 nm.

In all the studied fracture test bars the fracture is ductile. In same cases porosity and oxides are detected. Big porosity is detected in the unreinforced alloy, which correspond to the alloy with the higher porosity. In same cases, the obtained values can be directly influenced by the internal sanity. Internal defects as oxides are difficult to relate directly with the alloy, but is more sense to relation them with the process parameters.

5.2.4   Modeling of the mechanical properties

In order to determinate the mechanical properties in function of the composition of the alloy, experimental formulas has been obtained by the equip of Makhalouf, Apelian and Wang [Mac 98], employing an experiment design employing an L16 and a modified L8 Taguchi orthogonal array in the limits of concentration of the allowing elements:

<u>**Yield Strength:**</u>

P1= (9.81 + 0.49 Si + 1.44 Cu + 1.48 Fe +13.07 Mg + 1.01 Mn + 1.45 Ni + 3.84 Cr + 0.34 Zn + 5.81 Ti + 12.72 Sr)x6.89512.

CHAPTER 5:   MECHANICAL PROPERTIES

Ultimate Tensile Strength:

P2= (44.93 - 0.46 Si + 0.67 Cu - 0.18 Fe + 0.76 Mg - 0.13 Mn + 0.23 Ni + 0.16 Cr + 0.32 Zn + 0.20 Ti + 0.35 Sr)x6.89512.

Elongation:

P3 = (10.62 - 0.61 Si - 0.50 Cu - 0.46 Fe - 0.57 Mg - 0.21 Mn -0.07 Ni + 0.06 Cr + 0.25 Zn +0.08 Ti + 0.07 Sr)x6.89512.

In Table 5.3 we can observe the variation of mechanical properties with the temperature and the compositions as cast:

TENSILE PROPERTIES AT 20ºC	Experimental data				
	Al Si9 Cu3	0.2% SHS-TiB_2	0.2% commercial TiB_2	0.1% of γ Al_2O_3	0.17% of αAl_2O_3
UTS (20ºC) (MPa)	277	291	304	297	296
UTS (20ºC) (MPa) NADCA formule	292	292	292	292	292
YS (20ºC) (MPa)	132	128	130	128	123
YS (20ºC) (MPa) NADCA formule	133	134	133	131	132
Elongation % (20ºC)	5,65	6,8	7,1	5,2	5,1
Elongation % (20ºC) NADCA formule	4,28	4,26	4,33	4,35	4,36

Table 5.3: Comparison of properties obtained with NADCA formula and experimental essays [Mak 98]

We can observe that there is a little difference in the UTS and YS values, but there is much more variation with the elongation. However, the formula can not determinate the property variation due to the nano-reinforcement addition. We can modify the formulas, with adjusting coefficients in order to predict (from and industrial point of view in a very simplify way) the mechanical properties by the addition of the ceramic particles:

Yield Strength:

P1= (9.81 + 0.49 Si + 1.44 Cu + 1.48 Fe +13.07 Mg + 1.01 Mn + 1.45 Ni + 3.84 Cr + 0.34 Zn + 5.81 Ti + 12.72 Sr)x6.89512 **+ 5**

Ultimate Tensile Strength:

P2= (44.93 - 0.46 Si + 0.67 Cu - 0.18 Fe + 0.76 Mg - 0.13 Mn + 0.23 Ni + 0.16 Cr + 0.32 Zn + 0.20 Ti + 0.35 Sr)x6.89512 **– 5.2**

Elongation:

P3 = (10.62 - 0.61 Si - 0.50 Cu - 0.46 Fe - 0.57 Mg - 0.21 Mn -0.07 Ni + 0.06 Cr + 0.25 Zn +0.08 Ti + 0.07 Sr)x6.89512 **+2.6 (For TiB_2) or +0.8 (For Al_2O_3)**

Influence of Alumina (Al$_2$O$_3$) and Titanium Diboride (TiB$_2$) nanoparticles on the microstructure and properties of Al-Si9 Cu3 alloys for high pressure die casting applications.

CHAPTER 5:   MECHANICAL PROPERTIES

5.3 Conclusions

The mechanical properties of Al$_2$O$_3$ and TiB$_2$ particles reinforced aluminium alloys with have been determinate and compared with the unreinforced Al Si9 Cu3 alloy. The influence of ceramic particles has been also analyzed; porosity levels and grain sizes and morphology have been determinate to explain the main strengthening mechanisms involved. The principal conclusions of mechanical properties analysis of reinforced aluminium are:

1) The presence of very small percentages of Al$_2$O$_3$ and TiB$_2$ particles in the reinforced alloys can improve mechanical properties at room temperature. UTS is increased by the ceramic addition, but in the other hand the YS is decreased, but less in %.

2) TiB$_2$ particles increase in a very important way the Elongation, but Al$_2$O$_3$ particles has a negative effect on Elongation at room temperature.

3) At high temperatures the addition of ceramic nano-particles increase mechanical properties, but specially Elongation. The increase in UTS is less important in percentage that at room temperature.

4) Porosity quantity decrease and micro shrinkages are smaller due to the presence of ceramic particles. This effect is stronger with particles than TiB$_2$ particles, but in both cases the tendency is to decrease the internal porosity.

5) The increase in ductility with the Al$_2$O$_3$ and specially with TiB$_2$ particles is derived from the positive effect of SDAS reduction, very fine β-iron needles, very fine eutectic and fine precipitates, the smaller and less porosity, but also with a negative effect due to the non rounded shape of same of the milled particles, that can act as stress concentration points. However, the total effect is positive.

6) The Al$_2$O$_3$ and TiB$_2$ reinforced alloys have a ductile fracture. In the case of TiB$_2$ particles it can be related to the effect of nucleation sites for the precipitation of silicon and Al$_2$Cu phases, and also the decrease of solute available for the precipitation of brittle precipitates. This is observed in the metallographic analysis with the fine precipitates and phases.

7) The main strengthening mechanisms are in relation with the decrease of porosity and the grain refining effect of the Al$_2$O$_3$ and TiB$_2$ particles.

The **improvement of mechanical properties takes place in both room temperature and high temperatures**. Elongation increase can have a very important interest in industry, in order to design new parts with higher requirements, and also high temperature applications.

Influence of Alumina (Al$_2$O$_3$) and Titanium Diboride (TiB$_2$) nanoparticles on the microstructure and properties of Al-Si9 Cu3 alloys for high pressure die casting applications.

CHAPTER 6:   CONCLUSIONS

CHAPTER 6: CONCLUSIONS.

Influence of Alumina (Al$_2$O$_3$) and Titanium Diboride (TiB$_2$) nanoparticles on the microstructure and properties of Al-Si9 Cu3 alloys for high pressure die casting applications.

CHAPTER 6:   CONCLUSIONS

6.1 Conclusions

6.1.1   Introduction

The present work has been focused on studying the influence of nano- Al$_2$O$_3$ and TiB$_2$ particles on the solidification pattern, microstructure features, tensile and thermal properties of the Al-Si9 Cu3 alloys. Samples of reinforced materials have been cast by high pressure die casting in the same conditions than the unreinforced Al-Si9 Cu3 alloy. Following the main conclusions on the effect of Al$_2$O$_3$ and TiB$_2$ particles are summarized:

6.1.2   Influence of Al$_2$O$_3$ / TiB$_2$ nano-particles on microstructure

1) Al$_2$O$_3$ and TiB$_2$ particles influence aluminium grains nucleation, eutectic reaction and intermetallic precipitations. The nucleation temperature is increased, as the recalescence temperature. This effect is related to the incorporation of ceramic particles as heterogeneous nuclei.

2) TiB$_2$ has more influence in the nucleation than Al$_2$O$_3$ particles. This is related to the employ of TiB$_2$ in commercial grain refiners as main refiner. Also TiB$_2$ particles are related as the most effectives for Aluminium grain refining.

3) The influence of the particles should have a positive influence on the mechanical properties of the reinforced alloys since it decrease the undercooling, promoting a better nucleation.

4) The employ of ceramic nano-particles reduce the porosity quantity and size. It's more remarkable in the case of Al$_2$O$_3$ than in TiB$_2$ particles.

5) Acicular oriented very fine dendrites are promoted by the nano-particle addition. The SDAS is smaller in the reinforced alloys and also the SDAS decrease in the center of the samples.

6) Al$_2$O$_3$ and TiB$_2$ particles modify the structure, with smaller detrimental β-iron needles.

7) Very fine eutectic structures are detected in the center of the reinforced alloys, especially with TiB$_2$ reinforced alloys.

8) The SEM analysis shows that Al$_2$O$_3$ particles acts as nucleating points, with agglomerate particles of about 0,5-1 micron.

Influence of Alumina (Al$_2$O$_3$) and Titanium Diboride (TiB$_2$) nanoparticles on the microstructure and properties of Al-Si9 Cu3 alloys for high pressure die casting applications.

CHAPTER 6:   CONCLUSIONS

9) Electrical conductivity decreases by adding few quantities of ceramic particles and is quite similar in the center and periphery of reinforced alloys and a relation between SDAS and IACS has been observed.

6.1.3   Influence of Al$_2$O$_3$ / TiB$_2$ nano-particles on the mechanical properties

The principal conclusions of mechanical properties analysis of reinforced aluminium are:

1) The presence of very small percentages of Al$_2$O$_3$ and TiB$_2$ particles in the reinforced alloys can improve mechanical properties at room temperature. UTS is increase by the ceramic addition, but in the other hand the YS is decreased.

2) TiB$_2$ particles increase in a very important way the Elongation at room temperature, but Al$_2$O$_3$ particles has a negative effect on Elongation at room temperature.

3) At high temperatures (200 ºC) the addition of ceramic nano-particles increase mechanical properties. The increase in UTS and YS are less important in percentage that at room temperature.

4) Porosity and micro shrinkages are smaller and lower due to the presence of ceramic particles. This effect is stronger with particles than TiB$_2$ particles, but in both cases the tendency is to decrease the internal porosity.

5) The increase in ductility with the Al$_2$O$_3$ and specially with TiB$_2$ particles is derived from the positive effect of SDAS reduction, very fine β-iron needles, very fine eutectic and fine precipitates, the smaller and less porosity, but also with a negative effect due to the non rounded shape of same of the milled particles, that can act as stress concentration points. However, the total effect is positive.

6) The Al$_2$O$_3$ and TiB$_2$ particles have a ductile fracture of the aluminium. In the case of TiB$_2$ particles it can be related to the effect of nucleation sites for the precipitation of silicon and Al$_2$Cu phases, and also the decrease of solute available for the precipitation of brittle precipitates. This is observed in the metallographic analysis with the fine precipitates and phases and in the TEM with the Cu in the interstices of silicon and aluminium dendrites.

7) The main strengthening mechanisms are in relation with the decrease of porosity and the grain refining effect of the Al$_2$O$_3$ and TiB$_2$ particles.

CHAPTER 6: CONCLUSIONS

It has been demonstrated that the **Al$_2$O$_3$ and TiB$_2$ nano-particles have a direct influence on several important features of the alloys such as the microstructure, precipitating of phases during solidification, mechanical properties, decrease of the amount of defects and change of electrical and thermal properties. Al$_2$O$_3$ and TiB$_2$ particles can be used to improve properties of casting alloys,** and be very useful in the case of high mechanical and thermal requirements, also at high temperatures (200ºC).

They are also some processing conclusions that may have industrial interest:

1. A process to generate TiB$_2$ particles from commercial (gross) Ti and B has been developed employing the SHS process and by wet high energy ball milling. Also SHS reactions without reactor and the substitution of same of the raw material for cheaper salt based material can provide a cheap reinforcement material.

2. A process to introduce ceramic nano-particles in the liquid aluminium at relative low temperature and dissolution time.

3. Very small quantities of *In-situ* or *Ex-situ* impurities modify the solidification curves. That could explain the difficulties to automate the DTA´s applications for Al Si9 Cu3 alloys. True DSC should be a better way to study the reinforced alloys.

4. There is a direct relation between the internal soundness of parts and the obtained mechanical properties. The effect of specially Al$_2$O$_3$ on reducing the internal porosity provides a good way to increase the mechanical properties.

6.2 Future directions

It has been shown that addition of Al$_2$O$_3$ and TiB$_2$ nano-particles to aluminium Al Si9 Cu3 alloy has a direct effect on some important properties such as microstructure, mechanical and thermal properties. The reinforcement percentages employed in the project are quite small, giving good results. Industrial processing of nano-particle and introduction in the alloy must be improved.

Influence of Alumina (Al_2O_3) and Titanium Diboride (TiB_2) nanoparticles on the microstructure and properties of Al-Si9 Cu3 alloys for high pressure die casting applications.

CHAPTER 6: CONCLUSIONS

In order to advance in the use of nano-particles reinforced Al-Si9 Cu3 alloy for industrial applications same important aspects should be studied:

* **Industrialization of SHS and milling process.** The process must be robust and secure, without nano-particle emissions or explosion risk. Particle measure must be stable. Cheaper commercial materials must be investigated in order to decrease ceramic particle prices.

* **Optimization of particle composition, size and shape.** The particles must have the more adequate form and size in order to obtain the better results with the smallest material consume. Special care must be focus in particle degglomeration, in order to avoid losses of activity.

* **Study of the behavior of the nano-particles in other alloys.** The present study has been developed with the Al-Si9 Cu alloy, but they are similar composition alloys that can have a very similar behavior. Also pure alloys can be tested, in order to change the grain refiners by nano-particles and to increase properties. In this case, the action of the thermal treatments should be studied over the nano-particles and properties.

* **Study of cheap nano-particles compositions.** There many industrial sub products that they can be employed as nano-reinforcements for aluminium, as filter dusts, fly ashes and aluminium recycling wastes. Some of them have contaminants, but with a proper cleaning and preparation of raw materials it could be possible to decrease AMC´s prices.

* **Use of different compaction and densification systems.** If the nano-particles are embedded in a good distribution in a very dense (No porous) matrix, nano-particles have a bigger recovery. In that way processes as HIP, SPS or other should be more investigated.

* **Understanding of the hardening mechanism.** In order to improve the properties of AMC with nano-powders, in relation with the powder size and the distribution in the matrix, with the aim of optimize the process.

* **Detection of TiB_2 particles.** In order to detect TiB_2 particles, new preparing and observing methods can be employed.

Influence of Alumina (Al_2O_3) and Titanium Diboride (TiB_2) nanoparticles on the microstructure and properties of Al-Si9 Cu3 alloys for high pressure die casting applications.

REFERENCES

REFERENCES

[Agu 10] Aguilar-Santillan J. Wetting of the (0001) α-Al_2O_3 sapphire surface by molten aluminium: Effect of surface roughness. The minerals, metals & materials society and ASM international. 2010.

[Aik 97] Aikin Jr. R.M."The mechanical properties of in situ composites". JOM. 49 (8) (1997), pp. 35-39.

[All 74] United States Patent US 3.961.995. 1974. Alliot M., Beguin J.C., Moutach M., Percheron J.C. Mother Alloy of Aluminium, Titanium and Boron and process for fabrication.

[Alu 11] http://aluminium.matter.org.uk/content/html/eng/

default.asp?catid=71&pageid=2075282087

[Arp 03] Arpón R., Molina J.M., Saravanan R.A., García Cordobilla C., Louis E., Narciso j. "Thermal expansion behaviour of aluminium/SiC composites with bimodal particle distributions". Acta Materalia 51 (2003) pp. 3145-3156.

[Ask 03] The Science and Engineering of Materials, 4th ed. 2003. Brooks and Cole. Askeland D. R. –Phulé P. P.

[Bac 74] United State Patents US 3785807. 1974. Backerud S.L. Method for producing a master alloy for use in aluminium casting processes.

[Bac 90] Solidification Characteristics of Aluminium Alloys, Vol. 2. Foundry Alloys. AFS and Skanaluminium of Norway. 1990. AFS. Backerud L., Chai G., Tamminen J.

[Bac 00] United States Patents US 6.073.677. 2.000. Bäckerud L; Johnsson M; Sigworth J. Method for optimization of the grain refinement of aluminium alloys.

[Ban 88] United States Patent US 4.748.001. 1988. Banerji A., Reif W. Producing titanium carbide particles in metal matrix and method of using resulting product to grain refine.

[Boo 02] Boot D., Cooper P., StJohn D.H., Dahle A.K. A Comparison of Grain Refiner Master Alloys for the Foundry. TMS 2002.

Influence of Alumina (Al$_2$O$_3$) and Titanium Diboride (TiB$_2$) nanoparticles on the microstructure and properties of Al-Si9 Cu3 alloys for high pressure die casting applications.

REFERENCES

[Bro 99] Foseco Non-Ferrous Foundry man's Handbook.1999. Elsevier Ltd.
Brown J. R.

[Buh 11] http://www.buhlergroup.com

[Bru 87] United States patent US 4.710.348. 1987. Brupbacher J.M., Christodoulou L., Nagle D.C. Process for forming metal-ceramic composites.

[Cac 96] Cáceres C.H., Wang Q. G. "Dendrite cell size and ductility of Al-Si-Mg casting alloys: Spear and Gardner revisited". International Journal of Cast Metals Research. 1996. Vol.9, Nº 3. pp. 157-162.

[Cti 01] Aleaciones de aluminio para el moldeo. Version 1. CTIF. 2002. CTIF.

[Cly 93] Clyne T.W., Withers P.J. "An introduction to metal matrix composites". Cambridge University Press. 1993. ISBN 0-521-41808-9.

[Con 00] Conrad H, Narayan J. On the grain size softening in nanocrystalline materials. Scripta Mater 2000;42(11). pp. 1025–1030.

[Dav 07] Davis B.; Hyn J. Innovative forming and fabrication technologies: New opportunities. Final report. Argonne National Laboratory. ANL-07/31. 2007.

[Dho 11] Dhokey N. B., Rane K. K. Wear Behavior and Its Correlation withMechanical Propertiesof TiB2 Reinforced Aluminium-Based Composites. Advances in Tribology. Vol. 2011, pp. 1-8.

[Din 10] Aluminium and aluminium alloys – Castings – Chemical composition and mechanical properties. English translation of DIN EN 1706:2010-06.

[Dju 04] Djurdjevic M.B., Francis R., Sokolowski J.H. Emaldi D., Sahoo M. Comparison of different analytical methods for the calculation of latent heat of solidification of 3XX aluminium alloys. Material Science and engineering. 2004. A 386. pp. 277-283.

[Dju 11] Djurdjevic M.B. "Thermal Description of Al-Si Alloys Using Their Known Chemical Compositions". European Conference on Aluminium Alloys (ECAA 2011). 2011.

[Eas 10-1] Easton M., Davidson C., John D.S. Effect of alloy composition on the dendrite arm spacing of multi-component aluminium alloys. The minerals, Metals & materials Society and ASM international 2010.

Influence of Alumina (Al$_2$O$_3$) and Titanium Diboride (TiB$_2$) nanoparticles on the microstructure and properties of Al-Si9 Cu3 alloys for high pressure die casting applications.

REFERENCES

[Eas 10-2] Easton M., Davidson C., John D.S. Effect of alloy composition on the dendrite arm spacing of multi-component aluminium alloys. Metallurgical and materials transactions A. 2010. Nº 1528-Volume 41A.

[Egi 07] Egizabal P. Influence of Titanium Diboride (TiB$_2$) particles on the microstructure and properties of reinforced Al-Si7Mg0.3 and Al-Cu5MgTi alloys for plaster casting applications. Université Bordeaux 1. 2007.

[El- 10] El-Mahallawi I. S.; Shash Y.; Eigenfeld K.; Mahmoud, T. S.; Ragaie R. M., Shash A. Y., El Saeed M. A. Influence of nano-dispersions on strength–ductility properties of semisolid cast A356 Al alloy. Materials Science and Technology. 2010. Vol. 26, Nº 10 , pp. 1226-1231.

[El- 11] El-Mahallawi I.S., Shash Y., Ragaie R.M., Abdelaziz M.N., Mayer J., Schwedt A. Influence of nano-dispersions on microstructure features of cast Al-Si Hypereutectic Alloys. European conference on Aluminium Alloys. 2011. Poster A-134.

[Fu 07] Fu Q., Wagner T. Interaction of nano-structured metal over layers with oxide surfaces. Surface Science reports 2007. Nº 62. pp. 431-498.

[Gre 00] Greer A.L, Bunn A.M, Tronche A, Evans P.V, Bristow D.J. Modelling of inoculation of metallic melts: application to grain refinement of aluminium by Al–Ti–B. Acta Materalia, 2000, Vol. 48, Issue 11, pp. 2823-2835.

[Gro 09] Grosselle F., Timelli G., Bonollo F., Molina R. Correlation between microstructure and mechanical properties of Al-Si diecast engine blocks. Metallurgical Science and Technology. Vol 27.2. 2009.

[Gru 95] Gruzleski et.al. AFS Inc. Des Plaines, Illinois. 1995.

[Gu 02] Gu Y., Qian Y., Chen L., Zhou F. A mild solvothermal route to nanocrystalline titanium diboride. Journal of Alloys and Compounds. Volume 352, Issues 1-2. 2003. pp. 325-327.

[Guz 86] United State patent. US 4.612.073. 1986. Guzowski M.M., Sentner D.A., Sigworth. Aluminium grain refiner containing duplex crystals.

[Hal 51] Hall E.D. Proc. Phys. Soc. Serie B 64. 1951. pp. 747-765.

[Han 02] Han Y., Liu X., Bian X. "In situ TiB2 particulate reinforced near eutectic Al-Si alloy composites". Composites A 33. 2002. pp. 439-444.

Influence of Alumina (Al$_2$O$_3$) and Titanium Diboride (TiB$_2$) nanoparticles on the microstructure and properties of Al-Si9 Cu3 alloys for high pressure die casting applications.

REFERENCES

[Han 05] Han J. "Processing, microstructure evolution and properties of nano-scale aluminium alloys". PhD. University of Cincinnati. 2005. pp. 38-44.

[Hid 99] Hind A.R., Bhargava S.K., Grocott S. C. The surface chemistry of Bayer process solids: a review. Colloids and Surfaces A: Physicochemical and Engineering Aspects. Volume 146, Issues 1-3. 1999. pp. 359-374.

[Hum 91] Humphreys F.J., Basu A., Djazeb M.R. "The microstructure and strength of particulate metal-matrix composites". Metal matrix composites. Processing, microstructure and properties. 12th Riso International Symposium on materials science. 1991. pp. 51-66.

[Hüs 06] Hüseying S., Kurnaz C. Properties of alumina particulate reinforced aluminium alloy produced by pressure die casting. Materials and design. 2006. Nº 27. pp. 676-683.

[Iba 99] Ibarra D. G. Control of grain refinement of Al-Si alloys by thermal analysis. Mc Gill University. 1999.

[Iva 04] Ivar H. High Pressure Die Casting of Aluminium and Magnesium Alloys - Grain Structure and Segregation Characteristics. Norwegian University of Science and Technology (NTNU). 2004.

[Jac 77] Alumina: sintering and optical properties. 1977. Technische Hogeschool Eindhoven. Jacob J. G.

[Jia 08] Jiang Q., Lu H.M. Size dependent interphase energy and its applications. Surface Science Reports. 2008. Nº63. pp. 427– 464.

[Kau 07] Kaufmann H., Uggowitzer P.J. Metallurgy and processing of high integrity light metal pressure castings. Fachverlarg Schiele & Schön Gmbh Berlin. 2007. pp.56.

[Kas 01] Kashyap K. T., Chandrashekar T. Effects and mechanisms of grain refinement in aluminium alloys. Bull. Mater. Sci., Vol. 24, No. 4, 2001, pp. 345–353.

[Kum 09] Kumar S., Subramaniya V., Murty B.S. Functionally graded Al alloys matrix *in-situ* composites The minerals, metals & materials society and ASM international. 2009.

[Lem 81] Principles of Mechanical Metallurgy. Edward Arnold..1981. Elsevier. LeMay. pp. 155-211.

Influence of Alumina (Al_2O_3) and Titanium Diboride (TiB_2) nanoparticles on the microstructure and properties of Al-Si9 Cu3 alloys for high pressure die casting applications.

REFERENCES

[Loe 01] Loeffler J. Nano-material roadmap 2015. Overview of promising nano-materials for industrial applications. Steinbeis-Europa-Zentrum. 2005.

[Li 03] Li P., Kandalova E.G., Nikitin V.I., Luts A.R., Makarenko A.G., Zhang Y. Effect of fluxes on structure formation of SHS Al–Ti–B grain refiner. Materials Letters. 2003. Vol. 57. pp. 3694–3698.

[Ma 01] Ma Z.Y., Li J.H., Luo M., Ning X.G., Lu Y.X., Bi J., Zhang Y.Z. *In-situ* formed Al_2O_3 and TiB_2 particulates mixture-reinforced aluminium composite. Scripta Metallurgical et Materialia, 1994, Vol. 31, Issue 5, pp. 635-639

[Mac 96] Mackay R. I. Quantification of Iron in Al-Si Foundry alloys via thermal analysis. Mc Gill University. 1996.

[Mah 08] Mahboob H., Sajjadi S. A., Zebarjad S. M. Synthesis of Al-Al2O3 Nano-Composite by mechanical alloying and evaluation of the effect of ball milling time on the microstructure and mechanical properties. The International Conference on MEMS and Nanotechnology, ICMN'08.2008.

[Mak 98] Makhlouf M., Apealian D., Wang L. Microstructures and properties of aluminium die casting alloys. North American Die Casting Assoc. 1998. NADCA

[Mar 08] Martin M.I., Rabanal M.E., Gomez L.S., Torralba J.M., Milosevic O. Microstructural and morphological analysis of nanostructured alumina particles synthesized at low temperature via aerosol route. Journal of the European Ceramic Society 2008. Nº 28, pp. 2487-2494.

[Mat 07] Matsunaga T., Matsuda K.; Hatayama T., Shinozaki K., Yoshida M. Fabrication of continuous carbon fiber reinforced aluminium-magnesium alloy composite wires using ultrasonic infiltration method. Composites. 2007. Part A 38 . pp 1902-1911.

[Max 01] Maxwell I, Hellawell A. An analysis of the peritectic reaction with particular reference to Al-Ti alloys Acta Metallurgical, 1975, Vol. 23, Issue 8, pp. 901-909.

[Mil 90] Miller W.S., Humphreys F.J. "Strengthening mechanisms in metal matrix composites". Fundamental relationships between microstructure & mechanical properties of metal matrix composites. Law P.K., Gunger M.N. The Minerals, metals and materials society, 1990.

Influence of Alumina (Al$_2$O$_3$) and Titanium Diboride (TiB$_2$) nanoparticles on the microstructure and properties of Al-Si9 Cu3 alloys for high pressure die casting applications.

REFERENCES

[Mis 04] Miserez A., Muller R., Rossoll A. et al. 2004. "Particle reinforced metals of high ceramic content" Mat sci eng A-Struct 387-89: pp. 822-831.

[Mit 95] Mitra R., Mahajan Y.R. Interfases in discontinuosly reinforced metal matrix composites: An overview. Mater. Sci. 1995, Vol. 18, Nº 4, pp. 405-434.

[Miy 73] United States Patent US 3.857.705. 1973. Miyasaka Y; Masuda Y. Small grain promoting Aluminium-Titanium-Boron mother Alloy.

[Mor 01] Mortensen A. Metal Matrix Composites in industry: An overview. Ecole Politechnique Fédérale de Lausanne. 2001.

[Mon 79] Aluminium Alloys, structures and properties. London, Butherworths. 1979. Mondolfo L.F.

[Mun 97] Munro R. G. "Evaluated Material Properties for a Sintered alpha-Al$_2$O$_3$,". Journal of the American Ceramic Society. 1997. Vol. 80, pp. 1919-1928.

[MMC 01-2] http://www.ceramics.nist.gov/srd/summary/scdaos.htm

[Mun 00] Munro R. G. "Material Properties of Titanium Diboride", Journal of Research of the National Institute of Standards and Technology. 2000.Vol. 105, pp. 709-720 .

[MMC 01-1] http://www.ceramics.nist.gov/srd/summary/scdtib2.htm

[Nan 11] http://www.nanophase.com/products/details.aspx?ProductId=1

[Nik 00] Nikitin V.I., Wanqi J.I.E., Kandalova E.G., Makarenko A.G., Yong L. Preparation of al-ti-b grain refiner by shs technology. Scripta mater. 2000. Vol. 42. pp. 561–566.

[Nik 11] Niklas A., Abaunza U., Fernandez Calvo A.I., Lacaze J., Suarez R. Thermal análisis as a microstructure prediction tool for A356 aluminium parts solidified under various cooling conditions. The 69th WFC paper. 2011.

[Que 04-01] Quested T.E; Greer A.L; The effect of the size distribution of inoculant particles on as-cast grain size in aluminium alloys. Acta materalia. 2004, Vol. 52, Issue 13, pp. 3859-3868

[Que 04-02] Quested T. E., Solidification of Inoculated Aluminium Alloys. University of Cambridge. 2004.

[Ram 08] Ramachandran T.R., Sharma P.K. , Balasubramanian K. Grain Refinement of Light Alloys. 68th WFC - World Foundry Congress7th - 2008, pp. 189-193.

Influence of Alumina (Al$_2$O$_3$) and Titanium Diboride (TiB$_2$) nanoparticles on the microstructure and properties of Al-Si9 Cu3 alloys for high pressure die casting applications.

REFERENCES

[Sat 06] Sato T. Nanostructure Control for High-Strength and High-Ductility Aluminium Alloys. Nanomaterials 2006. pp. 315-346.

[Sch 98] Schumacher P, Greer A. New studies of nucleation mechanism in aluminium alloys. Implication for grain refinement practice. Mater Sci Technol. 1998;14:394.

[Sch 01] Schiøtz J. Simulations of nanocrystalline metals at the atomic scale. what can we do? what can we trust?. Science of Metastable and Nanocrystalline Alloys" A.R. Dinesen et al., 2001. A.R. Dinesen et al. pp. 127-139.

[Sch 04] Schiøtz J. Strain-induced coarsening in nanocrystalline metals under cyclic deformation. Materials Science and Engineering. 2004. A 375–377, pp. 975–979.

[Sch 07] Schaffer P.L., Miller D. N., Dahles A. K. Crystallography of engulfed and pushed TiB$_2$ particles in aluminium. Scripta Materalia. 2007. Nº57, pp.1129-1132

[Sei 09] Seifeddine S. The influence of Fe and Mn content and cooling rate on the microstructure and mechanical properties of A380-die casting alloys. Svensson. Metallurgical Science and Technology. Vol.27-1. Ed. 2009.

[She 05] Shen P., Fujii H., Matsumoto T., Nogi K. Critical Factors Affecting the Wettability of α-Alumina by Molten Aluminum. Journal of the American ceramic society. Journal of the American Ceramic Society. 2004. Vol. 87, Issue 11, pp. 2121-2159.

[Sig 86] United States Patent US 4.812.290. 1986. Sigworth G. Third element additions to Aluminium-Titanium Master Alloys.

[Sig 91] United States Patents, US 5.055.256. 1991. Sigworth G; Guzowski M. Grain refiner for aluminium containing silicon.

[Spa 10] Sparkman D. Thermal Analysis Metrics by derivatives. Meltlab. 2010. www.meltlab.com/hottopics/feb2010htopic.pdf

[Tam 05] Tam K.F. Mechanical and thermal characteristics of HIPed A1-TiB2 MMCs. City university of Hong Kong. 2005.

[Tay 04] Taylor J.A. The effect of iron in Al-Si9 casting alloys. 35th Australian Foundry Institute National Conference. 2004.

[Tee 01] Tee K.L., Lu L., Lai M.O. "In situ stir cast Al-TiB2 composite: processing and mechanical properties". Material Science and Technology. 2001. Vol. 17. pp 201-206.

Influence of Alumina (Al_2O_3) and Titanium Diboride (TiB_2) nanoparticles on the microstructure and properties of Al-Si9 Cu3 alloys for high pressure die casting applications.

REFERENCES

[Tjo 03] Tjong S.C., Tam K.F., Wu S.Q. Thermal cycling characteristics of *in-situ* Al-based composites prepared by reactive hot pressing. Composites science and technology 2003, 63, pp. 89-97.

[Tjo 05] Tjong S.C., Wang G.S., Mai Y.W. Low-cycle fatigue behaviour of Al-based composites containing in situ TiB2, Al2O3 and Al3Ti reinforcements . Materials Science and Engineering: A. 2003. Volume 358, Issues 1-2, pp. 99-106

[Tjo 06] Tjong S.C., Tam K.F. Mechanical and thermal expansion behaviour of hipped aluminium-TiB_2 composites Materials. Chemistry and physics. 2006. 97, pp. 91-97.

[Wik 11] http://en.wikipedia.org/wiki/Alumina

[Wik 11-02] http://en.wikipedia.org/wiki/Solid_solution_strengthening

[Wik 11-03] http://en.wikipedia.org/wiki/Work_hardening

[Zha 08] Guo Z., Saunders N., Miodownik P., Schillé J.P. Prediction of room temperature mechanical properties in aluminium castings. International Congress of Aluminium Alloys ICAA11. 2008.

[Zho 07] Zhong X.L., Wong W.L.E., Gupta M. Enhancing strength and ductility of magnesium by integrating it with aluminium nanoparticles. Acta materalia. 2007. Vol. 55 pp. 6338-6344.

[Zol 07] Casting aluminium alloys. Elsevier. 2007. Zolotorevsky V.S.; Belov N.A.; Glazoff M.V. pp. 359-362.